

**Investigations of the geomorphologic and pedologic system  
of sedimentary vega deposits from Lanzarote (Canary  
Islands) supported by luminescence dating – important  
steps towards their palaeoclimatic interpretation**

Dissertation  
zur Erlangung des Grades  
Doktor der Naturwissenschaften  
(Dr. rer. nat.)  
an der  
Fakultät für Biologie, Chemie und Geowissenschaften  
an der Universität Bayreuth

vorgelegt von

Hans von Suchodoletz  
(Diplom-Geograph)  
geb. am 20. 05. 1975 in Greifswald

Erstgutachter: Prof. Dr. Ludwig Zöller

Bayreuth, im August 2007

Die vorliegende Arbeit wurde in der Zeit von September 2003 bis August 2007 in Bayreuth am Lehrstuhl Geomorphologie unter der Betreuung von Herrn Prof. Dr. Ludwig Zöller, sowie am Geoforschungszentrum Potsdam unter der Betreuung von PD Dr. H. Oberhänsli angefertigt.

Vollständiger Abdruck der von der Fakultät für Biologie, Chemie und Geowissenschaften der Universität Bayreuth genehmigten Dissertation zur Erlangung des Grades eines Doktors der Naturwissenschaften (Dr. rer. nat.).

|  |                   |
|--|-------------------|
| Dissertation eingereicht               | 10.08.2007        |
| Tag des wissenschaftlichen Kolloquiums | 30.04.2008        |
| Amtierender Dekan:                     | Prof. Axel Müller |

### ***Prüfungsausschuss***

|                       |   |
|-----------------------|---|
| Erstgutachter:        | Prof. Dr. L. Zöller                     |
| Zweitgutachterin:     | PD Dr. H. Oberhänsli                    |
| Vorsitz:              | Prof. Dr. K. Hüser                      |
| Kommissionsmitglieder | PD Dr. B. Glaser<br>Prof. Dr. K. Bitzer |

# Contents

|  |           |
|--|-----------|
| Contents.....  | 3         |
| List of Tables.....  | 5         |
| List of Figures .....  | 6         |
| List of abbreviations.....   | 8         |
| Summary .....  | 9         |
| Zusammenfassung .....  | 11        |
| <b>1. Introduction .....</b>   | <b>13</b> |
| <b>2. Location and studied sites.....</b>  | <b>18</b> |
| <b>2.1. Location .....</b>   | <b>18</b> |
| 2.1.1. <i>Geology</i> .....  | 18        |
| 2.1.2. <i>Geomorphology</i> .....  | 18        |
| 2.1.3. <i>Present climate</i> .....  | 19        |
| 2.1.4. <i>Vegetation</i> .....   | 19        |
| <b>2.2. Studied sites .....</b>  | <b>20</b> |
| 2.2.1. <i>Vega of Femés</i> .....  | 20        |
| 2.2.2. <i>Vega of Guatiza</i> .....  | 21        |
| 2.2.3. <i>Vega of Teguisse</i> .....   | 21        |
| <b>3. Material and methods .....</b>   | <b>22</b> |
| <b>3.1. Material.....</b>  | <b>22</b> |
| <b>3.2. Methods.....</b>   | <b>22</b> |
| 3.2.1. <i>GIS calculations of surface areas</i> .....  | 22        |
| 3.2.2. <i>Grain size analyses</i> .....  | 22        |
| 3.2.3. <i>X-ray diffraction (XRD) analyses</i> .....   | 23        |
| 3.2.5. <i>Rock magnetism</i> .....   | 27        |
| 3.2.6. <i>Micromorphology</i> .....  | 27        |
| 3.2.7. <i>Soil analytics</i> .....   | 27        |
| <b>4. Results .....</b>  | <b>29</b> |
| <b>4.1. Stratigraphy.....</b>  | <b>29</b> |
| 4.1.1. <i>Profile of Femés</i> .....   | 29        |
| 4.1.2. <i>Profile of Guatiza III</i> .....   | 30        |
| 4.1.3. <i>Profile of Teguisse</i> .....  | 30        |
| <b>4.2. Dating Saharan dust deposits on Lanzarote (Canary Islands) by luminescence dating techniques and their implication for palaeoclimate reconstruction of NW Africa .....</b> | <b>32</b> |
| 4.2.1. <i>Introduction</i> .....   | 32        |
| 4.2.2. <i>Study area</i> .....   | 34        |
| 4.2.3. <i>Studied sites</i> .....  | 35        |
| 4.2.4. <i>Methods</i> .....  | 38        |
| 4.2.4.1. <i>Sample preparation</i> .....   | 38        |
| 4.2.4.2. <i>Measurements</i> .....   | 38        |
| 4.2.4.3. <i>Dose rate determination</i> .....  | 40        |
| 4.2.4.4. <i>Water content</i> .....  | 40        |
| 4.2.4.5. <i>Age calculation</i> .....  | 42        |
| 4.2.5. <i>Results</i> .....  | 44        |
| 4.2.5.1. <i>Dose rates</i> .....   | 44        |
| 4.2.5.2. <i>Equivalent doses</i> .....   | 45        |
| 4.2.6. <i>Discussion</i> .....   | 48        |
| 4.2.6.1. <i>Reliability of different luminescence methods</i> .....  | 48        |
| 4.2.6.2. <i>Establishing a chronostratigraphy</i> .....  | 52        |

|  |            |
|--|------------|
| 4.2.7. <i>Conclusions</i> .....  | 56         |
| 4.2.8. <i>Acknowledgements</i> .....   | 56         |
| <b>4.3. Luminescence bleaching characteristics of Saharan dust – A case study from Lanzarote, Canary Islands (Spain)</b> ..... | <b>57</b>  |
| 4.3.1. <i>Introduction</i> .....   | 57         |
| 4.3.2. <i>Regional setting</i> .....   | 58         |
| 4.3.3. <i>Material</i> .....   | 60         |
| 4.3.4. <i>Methods</i> .....  | 61         |
| 4.3.4.1. <i>Microscopy</i> .....   | 61         |
| 4.3.4.2. <i>Luminescence measurements</i> .....  | 62         |
| 4.3.5. <i>Results</i> .....  | 63         |
| 4.3.5.1. <i>Microscopy</i> .....   | 63         |
| 4.3.5.2. <i>Luminescence measurements</i> .....  | 64         |
| 4.3.6. <i>Discussion</i> .....   | 66         |
| 4.3.7. <i>Conclusions</i> .....  | 68         |
| 4.3.8. <i>Acknowledgements</i> .....   | 69         |
| 4.5.2. <i>Geographic setting</i> .....   | 93         |
| 4.5.7. <i>Conclusions</i> .....  | 122        |
| <b>5. Synthesis: Palaeoclimatic scenarios for more humid periods on Lanzarote</b> .....  | <b>124</b> |
| <b>6. Conclusion</b> .....   | <b>135</b> |
| <b>7. Outlook and perspectives</b> .....   | <b>136</b> |
| <b>8. References</b> .....   | <b>138</b> |
| <b>9. Contributions to included manuscripts</b> .....  | <b>156</b> |
| <b>10. Acknowledgements/Danksagung</b> .....   | <b>158</b> |
| <b>Declaration/Erklärung</b> .....   | <b>160</b> |

## List of Tables

|   |     |
|---|-----|
| TABLE 4.2.1. PROPERTIES OF STUDIED SITES ON LANZAROTE .....   | 36  |
| TABLE 4.2.2. KIND AND STRENGTH OF USED IRRADIATION-SOURCES .....  | 39  |
| TABLE 4.2.3. USED MEASUREMENT-PARAMETERS FOR OSL AND IRSL .....   | 40  |
| TABLE 4.2.4. LUMINESCENCE DATING: ANALYTICAL RESULTS .....  | 42  |
| TABLE 4.2.5. LUMINESCENCE DATING: EQUIVALENT DOSES AND AGES .....   | 48  |
| TABLE 4.3.1. EQUIVALENT DOSES ( $D_e$ 'S) FOR DUST AND COLLUVIAL SAMPLES FROM THE ISLANDS OF LANZAROTE (L) AND GRAN CANARIA (GC). ..... | 64  |
| TABLE 4.4.1. SEDIMENT VOLUMES STORED IN DIFFERENT STORAGES (IN $M^3$ ) IN FEMÉS. ....   | 77  |
| TABLE 4.5.1. PROPERTIES OF STUDIED SITES ON LANZAROTE. ....   | 96  |
| TABLE 4.5.2. RESULTS OF PEDOLOGIC ANALYSES, FIELD STUDIES AND ABSOLUTE CLAY CONTENTS. ....  | 107 |
| TABLE 4.5.3. ALLOPHANE ANALYSES FROM FEMÉS. ....  | 108 |
| TABLE 4.5.4. MICROMORPHOLOGICAL FEATURES OF INVESTIGATED HORIZONS IN ALL PROFILES. ....   | 111 |

## List of Figures

|   |     |
|---|-----|
| FIGURE 2.1. LOCATION OF LANZAROTE OFF NW-AFRICA AND OF STUDIED SITES ON THE ISLAND. ....  | 20  |
| FIGURE 3.1. INVESTIGATED PROFILES ON LANZAROTE WITH LUMINESCENCE (CROSSES) AND<br>MICROMORPHOLOGICAL SAMPLES (RECTANGLES) .....   | 26  |
| FIGURE 4.2.1. LOCATION MAP OF THE ISLAND OF LANZAROTE WITH THE STUDIED VEGAS OF FEMES, TEGUISE<br>AND GUATIZA III. IN ADDITION, MARINE SEDIMENT CORES FROM NEARBY LOCATIONS ARE INDICATED IN<br>THE INSET. .... | 35  |
| FIGURE 4.2.2. THE PROFILES OF FEMES, GUATIZA AND TEGUISE. GIVEN IS THE SEDIMENTARY CHARACTER OF<br>THE PROFILES AND INDICATED ARE THE SAMPLE LOCATIONS FOR LUMINESCENCE DATING WITH THEIR LAB<br>NUMBERS. ....  | 37  |
| FIGURE 4.2.3. SELECTED $D_E$ -HISTOGRAMS. LEFT: A RATHER WELL-BLEACHED SAMPLE FROM TEGUISE, RIGHT:<br>POORLY BLEACHED SAMPLE FROM FEMÉS. ....   | 44  |
| FIGURE 4.2.4. RESULTS OF THE DOSE RECOVERY TEST WITH ERROR BARS ( $2\sigma$ ). ....   | 46  |
| FIGURE 4.2.5. $D_E$ -HISTOGRAMS OF SAMPLES BT 200 AND BT 197 WITH DIFFERENT $D_E$ 'S. ....  | 50  |
| FIGURE 4.2.6. VEGA STRATIGRAPHIES WITH RELATIVE KAOLINITE CONTENTS ADJUSTED TO NUMERICAL<br>CHRONOSTRATIGRAPHY AND TO MARINE PROXIES. ....  | 53  |
| FIGURE 4.2.7. OVERVIEW OF MEASURED LUMINESCENCE AGES WITH HIATAE. ....  | 555 |
| FIGURE 4.3.1. THE CANARY ISLANDS AFFECTED BY A SAHARAN DUST STORM, 22TH OF APRIL 2002. LANZAROTE<br>AND GRAN CANARIA ARE HIGHLIGHTED. THE INSET INDICATES SAMPLING SITES ON LANZAROTE.....                      | 59  |
| FIGURE 4.3.2. SIX DAYS BACKWARD-TRAJECTORIES OF THE SAMPLED DUST PERIODS DURING 2006.....   | 61  |
| FIGURE 4.3.3. RECENT SEDIMENT SAMPLES .....   | 61  |
| FIGURE 4.3.4. MICROSCOPE IMAGES OF SAMPLES SD2 (FIGURE 4.3.4.A) AND SD3 (FIGURE 4.3.4.B).....   | 63  |
| FIGURE 4.3.5. POLYMINERAL MIDDLE/COARSE GRAIN OSL GROWTH CURVE OF SAMPLE SD3.....   | 65  |
| FIGURE 4.3.6. EQUIVALENT DOSE HISTOGRAMS OF POLYMINERAL COARSE/MIDDLE GRAIN DUST SAMPLES SD2<br>AND SD3 .....   | 65  |
| FIGURE 4.3.7. FINE GRAIN IRSL GROWTH-CURVE OF SAMPLE SD3. ....  | 66  |
| FIGURE 4.3.8. SECONDARY CONCRETIONS IN THE FRACTION $< 63\mu\text{M}$ IN A PALAEO SOL FROM LANZAROTE,<br>FORMED BY AMORPHOUS PLASMA CONSISTING OF IRON OXIDES/HYDROXIDES AND CLAY.....                          | 68  |
| FIGURE 4.4.1. HORIZONTALLY STRATIFIED LAYERS IN THE BOTTOM OF THE VEGA OF TEGUISE.....  | 72  |
| FIGURE 4.4.2. ERODED SLOPE WITH CALCRETE IN THE VEGA OF FEMÉS.....  | 72  |
| FIGURE 4.4.3. GEOGRAPHIC POSITION OF THE CANARY ISLANDS (INSET) AND INVESTIGATED SEDIMENT TRAPS ON<br>LANZAROTE (STARS). ....   | 74  |
| FIGURE 4.4.4. VEGA TRANSECTS, SURFACE OF SEDIMENT BODIES AND ALLUVIAL FANS USED FOR THE<br>CALCULATION OF STORED SEDIMENT IN FEMÉS.....   | 75  |
| FIGURE 4.4.5. VEGA TRANSECTS IN FEMÉS (LEFT SIDE: N/W-SLOPE, RIGHT SIDE: S/E-SLOPE) .....   | 75  |
| FIGURE 4.4.6. MODEL OF A HORIZONTAL CUT THROUGH A SEDIMENT BODY.....  | 76  |
| FIGURE 4.4.7. THIN SECTION OF A CARBONATIC HORIZON SHOWING A LARGE PED FRAGMENT (ARROW) WITHIN<br>THE SILTY MATRIX.....   | 81  |

|  |     |
|--|-----|
| <i>FIGURE 4.4.8. QUARTZ CONTENTS AND GRAIN SIZE FRACTIONS FROM A PROFILE IN THE CENTRE OF THE VEGA OF FEMÉS (IN %)</i> .....   | 82  |
| <i>FIGURE 4.4.9. SEDIMENTATION SCENARIOS ASSUMING A TIME SPAN OF 10 KA AND A CONSTANT SEDIMENTATION RATE OF 3.5 CM/KA</i> .....  | 85  |
| <i>FIGURE 4.4.10. SEDIMENT YIELD CORRELATED WITH ANNUAL AVERAGE PRECIPITATION AND SEDIMENTATION SCENARIOS (DASHED RECTANGLES)</i> .....  | 85  |
| <i>FIGURE 4.4.11. MIDDLE HOLOCENE LAYER DEPOSITED 8 TO 2.5 (OR 5) KA (A) BENEATH A YOUNG HOLOCENE COLLUVIUM CONSISTING OF TWO LAYERS (B<sub>I</sub> AND B<sub>II</sub>)</i> .....  | 87  |
| <i>FIGURE 4.5.1. LOCATION OF LANZAROTE AND STUDIED SITES</i> .....   | 93  |
| <i>FIGURE 4.5.2. INVESTIGATED PROFILES WITH LUMINESCENCE AGES. BLACK RECTANGLES INDICATE DEPTHS OF MICROMORPHOLOGICAL SAMPLES</i> .....  | 95  |
| <i>FIGURE 4.5.3. DARK-BROWN AGGREGATES IN THE SIEVED AND HCL-TREATED FRACTION &lt; 63 μM FROM A REDDISH/CLAYEY LAYER IN FEMÉS (230 CM)</i> .....   | 97  |
| <i>FIGURE 4.5.4. COMPARISON OF RELATIVE CLAY CONTENTS DERIVED BY LASER ANALYSES (LEFT, ARBITRARY UNITS) WITH ABSOLUTE CLAY CONTENTS DERIVED BY PIPETTE ANALYSES (RIGHT, %) FROM THE PROFILE OF FEMÉS</i> .....               | 100 |
| <i>FIGURE 4.5.5. PROXIES FROM THE VEGAS OF LANZAROTE</i> .....   | 102 |
| <i>FIGURE 4.5.6. X-RAY DIFFRACTOGRAMS FROM THE INVESTIGATED CLAY SAMPLES &lt; 2 μM FROM FEMÉS</i> .....  | 103 |
| <i>FIGURE 4.5.7. CROSS-PLOTS OF ENVIRONMENTAL MAGNETIC PARAMETERS FROM DIFFERENT VEGAS</i> .....   | 105 |
| <i>FIGURE 4.5.8. MICROMORPHOLOGIC FEATURES</i> .....   | 112 |
| <i>FIGURE 4.5.9. STRONG SHRINKING CRACKS DEVELOPED ON THE SURFACE OF RECENTLY FORMED COLLUVIAL DEPOSITS IN GUATIZA</i> .....   | 118 |
| <i>FIGURE 4.5.10. COMPILATION OF PROFILES, AGES AND PALAEOENVIRONMENTAL PROXIES</i> .....  | 121 |
| <i>FIGURE 5.1. SOIL HUMIDITY PROXIES FROM THE VEGAS OF LANZAROTE IN COMPARISON WITH PREVIOUS PALAEOCLIMATE STUDIES FROM THE EASTERN CANARY ISLANDS</i> .....   | 125 |
| <i>FIGURE 5.2. SOIL HUMIDITY PROXIES FROM LANZAROTE IN COMPARISON WITH PALAEOCLIMATE PROXIES FROM STUDIES OF THE NW AFRICAN AND MEDITERRANEAN AREA</i> .....   | 127 |
| <i>FIGURE 5.3. RECENT MAIN TRACK OF WESTERLY CYCLONES DURING NEGATIVE PHASES OF THE NORTH ATLANTIC OSCILLATION (NAO) COMPARED TO THE TRACK OF SOUTHERN CYCLONES THAT WERE PRESUMABLY MORE FREQUENT DURING GLACIALS</i> ..... | 130 |
| <i>FIGURE 5.4. THE NORTHERN LIMIT OF MONSOONAL INFLUENCE IN AFRICA AT PRESENT AND DURING THE HOLOCENE OPTIMUM, THE LATTER BOTH SHOWN AS COMPILED BY YAN AND PETIT-MAIRE (1994) AND SUPPOSED BY KUHLMANN (2003)</i> .....     | 131 |
| <i>FIGURE 5.5. RECENT SITUATION WITH (RELATIVELY) WARM SST AND AIR TEMPERATURE COMPARED TO THAT DURING GLACIAL PERIODS, WHEN SST AND AIR TEMPERATURE WERE MUCH COLDER</i> .....  | 133 |

## List of abbreviations

|                               |   |
|-------------------------------|---|
| AAS                           | Atomic Adsorption Spectrometer                                    |
| <sup>14</sup> C dating        | Radiocarbon dating  |
| $\dot{D}$                     | Dose rate   |
| D-O cycle                     | Dansgaard-Oeschger cycle  |
| D <sub>e</sub>                | Equivalent dose   |
| ESR dating                    | Electron spin resonance dating                                    |
| GC-C-IRMS                     | gas chromatography - combustion - isotope ratio mass spectrometry |
| Gy                            | Gray  |
| H <sub>2</sub> O <sub>2</sub> | Hydrogen peroxide   |
| HCl                           | Hydrochloric acid   |
| HF                            | Hydrofluoric acid   |
| ICPMS                         | Inductively Coupled Plasma Source Mass Spectrometry               |
| IPCC                          | International Panel of Climate Change                             |
| IRSL                          | Infrared stimulated luminescence                                  |
| ka                            | kiloyear (1000 years)   |
| LGM                           | Last Glacial Maximum  |
| LST                           | Lithium hetero polytungstate                                      |
| Ma                            | 1 Million years   |
| MAAD                          | Multiple aliquot additive dose protocol                           |
| MIS                           | Marine Isotope Stage based on oxygen-isotopes                     |
| NAO                           | North Atlantic Oscillation  |
| OSL                           | Optically stimulated luminescence                                 |
| SAR                           | Single aliquot regenerative protocol                              |
| SST                           | Sea surface temperature   |
| TL dating                     | Thermoluminescence dating   |
| U/Th dating                   | Uranium/Thorium dating  |
| XRD                           | X-ray diffraction   |

## Summary

On Lanzarote (Canary Islands/Spain), sequences similar to loess-palaeosol-sequences from other regions developed in dammed volcanic valleys during the Middle and Late Pleistocene. Based on former investigations, we assumed that these sequences could serve as palaeoclimate archives for the NW-African region, an area characterised by a lack of investigations from continuous terrestrial palaeoclimate archives.

The material deposited in the valleys consists of Saharan dust as well as of local volcanic material. Due to their location in valley positions and adjacent strongly eroded slopes it is obvious that these sequences do not represent classic loess-palaeosol-archives. Instead, they must consist of a mixture of in situ aeolian fallout as well as of sediments derived from colluvial input from the slopes. Consequently, prior to a correct palaeoclimatic interpretation the geomorphologic character of the archives and the properties of their sediments must be analysed. Thus, in this study we intensively investigate the geomorphologic and pedologic system, combining geomorphologic mapping and quantitative GIS-calculations with sedimentological-pedological methods (grain size, XRD, rock magnetic und pedologic analyses as well as investigation of micromorphologic properties).

Furthermore, we built up a chronostratigraphy using different luminescence-methods (quartz coarse- and fine grain-OSL, polymineral fine grain-IRSL). Fundamental investigations on the bleaching-behaviour of recent Saharan dust and colluvial sediments on Lanzarote demonstrate, that in spite of partial insufficient bleaching of the luminescence signal a dating of the valley-bottom sediments is possible. These datings were supported by a correlation of local kaolinite-contents with iron and kaolinite contents from nearby marine cores as well as a stratigraphic correlation between different profiles. Thus, we could establish a chronostratigraphy for the last 180 ka. We demonstrate that outcropped sediments were deposited almost continuously from the Middle Pleistocene until the Holocene, whereas the uppermost sections of the profiles consist of anthropogenic colluvia which can not be interpreted in a palaeoclimatic way.

The alternation of reddish-clayey and yellowish-silty layers tracks changes of soil humidity on Lanzarote rather than variations of the composition of Saharan dust. Due to the colluvial dynamics of the valleys, reddish-silty layers in the valley bottoms are not palaeosoils *sensu stricto* but mainly consist of colluvial soil sediments originating from pedogenesis on the slopes. These soils as well as unweathered material were eroded and deposited with high frequency and low amplitude. Thus, their sedimentation age in the valley bottoms is close to the primary time of aeolian deposition on the slopes and the formation of pedogenetic properties.

These findings allow a palaeoclimatic interpretation of the sediment sequences. We could demonstrate that glacial and stadial periods were characterised by higher soil moisture than interglacial and interstadial periods. When comparing our results with other palaeoclimatic studies from a broader region, we can show that the causes for periods of enhanced humidity were westerly cyclones using a more southern way than at present, as well as lowered sea and air temperatures in the area of the Canary Islands. During some periods, soil humidity was possibly occasionally amplified by a northward advance of the African summer monsoon up to the latitude of Lanzarote. Although we are not able to directly derive palaeoprecipitation values from soil moisture, we can show that maximal precipitation values must have been in the range of ca. 560 mm/a.

Our results demonstrate that during most of the investigated period of the Late Quaternary the climate of Lanzarote was influenced by northern high latitude processes. Furthermore, during most of the investigated period the recent aridity of the island was somewhat mitigated.

### Zusammenfassung

Auf Lanzarote (Kanarische Inseln/Spainien) haben sich während des Mittel- und Spätpleistozäns in abgedämmten vulkanischen Tälern Sequenzen aus lössähnlichen Sedimenten und Paläoböden entwickelt. Diese ließen aufgrund von Vorarbeiten ein Potenzial als Paläoklimaarchive für den NW-afrikanischen Raum vermuten, eine Region welche bisher durch einen Mangel an Untersuchungen kontinuierlicher terrestrischer Paläoklimaarchive gekennzeichnet ist.

Das in den Tälern sedimentierte Material besteht zum einen aus Saharastaub und zum anderen aus lokalem vulkanischen Material. Aufgrund der Talposition der Archive und der stark erodierten Talhänge ist jedoch offensichtlich, dass diese Sequenzen keineswegs klassische Löss-Paläobodenarchive darstellen. Vielmehr bestehen sie aus einer Mischung von äolisch in situ und durch kolluviale Hangprozesse abgelagerten Sedimenten. Dies bedeutet, dass vor einer korrekten paläoklimatischen Interpretation grundlegende Untersuchungen zum Charakter der Archive und Sedimente stehen müssen. Daher wurden in dieser Arbeit das geomorphologische und pedologische System intensiv untersucht, wobei geomorphologische Kartierungen und Berechnungen mit GIS mit sedimentologisch-pedologischen Methoden (Korngrößen-, XRD-, Gesteinsmagnetik- und pedogene Analysen sowie Untersuchungen mikromorphologischer Eigenschaften) verbunden wurden. Gleichzeitig wurde auf Basis von Lumineszenzdatierungen (Quarzgroß- und Feinkorn -OSL, polymineralische Feinkorn-IRSL) eine Chronostratigraphie erstellt.

Grundlegende Untersuchungen des Bleichverhaltens von rezentem Saharastaub und kolluvialen Sedimenten auf Lanzarote ergaben, dass trotz auftretender Probleme bei der Nullstellung des Lumineszenzsignals eine Datierung der Talbodensedimente möglich ist. Diese Datierungen wurden durch eine Korrelation zwischen lokalen Kaolinitgehalten und Eisen- und Kaolinitgehalten aus benachbarten marinen Kernen sowie eine stratigraphische Korrelation zwischen den verschiedenen Profilen abgesichert. Auf diese Weise konnte eine Chronostratigraphie für die letzten 180 ka erstellt werden. Es zeigt sich, dass die aufgeschlossenen Sedimente fast kontinuierlich vom Mittelpleistozän bis zum Holozän abgelagert wurden, wobei die obersten Teile der Profile aus paläoklimatisch nicht interpretierbaren anthropogen beeinflussten Kolluvien bestehen. Der Wechsel von rötlich-tonigen und gelblich-siltigen Schichten bildet Änderungen der Bodenfeuchtigkeit auf der Insel selbst ab, und wird nicht durch Änderungen der Zusammensetzung des Saharastaubeintrags beeinflusst. Aufgrund der kolluvialen Dynamik der Täler stellen die rötlich-tonigen Schichten jedoch keine Paläoböden im engeren Sinne dar, sondern bestehen

zum größten Teil aus vom Hang verlagerten Bodensedimenten, welche ebenso wie die unverwitterten Sedimente mit hoher Frequenz und geringer Magnitude in die Talböden eingetragen wurden. Daher liegt das Sedimentationsalter des Materials in den Talböden sehr nahe am Zeitpunkt seiner primären äolischen Ablagerung auf den Hängen sowie dem Zeitpunkt seiner pedogenen Überprägung.

Diese Erkenntnisse erlauben eine Interpretation der Sedimentabfolge in paläoklimatischer Hinsicht. So wird offenbar, dass Glazial- und Stadialzeiten offenbar von einer höheren Bodenfeuchtigkeit als Interglazial- und Interstadialzeiten gekennzeichnet waren. Im Vergleich mit anderen paläoklimatischen Arbeiten aus dem näheren und weiteren Umfeld können wir zeigen, dass die Ursache für Zeiten erhöhter Feuchtigkeit wahrscheinlich südlich ziehende Zyklonen der Westwindzirkulation im Zusammenspiel mit verringerten Meeres- und Lufttemperaturen im Gebiet der Kanarischen Inseln waren, evtl. gelegentlich verstärkt von einem weit nach Norden bis zu den Kanarischen Inseln vordringendem afrikanischen Sommermonsun. Obwohl von der Bodenfeuchte nicht direkt auf Paläoniederschläge geschlossen werden kann, so ist es doch möglich zu zeigen dass maximale Niederschläge in einem Bereich um ca. 560 mm/a gelegen haben müssen.

Unsere Ergebnisse belegen, dass das Klima Lanzarotes den größten Teil des untersuchten Zeitraums im Spätquartär von Prozessen der hohen nördlichen Breiten beeinflusst wurde, und dass die derzeit herrschende Aridität während langer Perioden offenbar etwas abgemildert war.

### 1. Introduction

The Fourth Assessment Report of the Intergovernmental Panel on Climate Change (IPCC) (2007) has drastically highlighted the menace of a human-triggered climate change, predicted for the coming decades. This report underlines the need for reliable datasets from key areas for understanding driving mechanisms and feedbacks in order to anticipate the future climate changes more realistically. Specifically critical are naturally instable and vulnerable environments like those of semi arid and arid regions (e.g. desert margins) (cf. Mabbutt 1989, Mountney 2003, Lioubimtseva 2004). For a buildup of future climatic scenarios, a detailed understanding of the working of the global climate system with its complex processes and feedbacks is needed. This understanding can be obtained by looking into past periods with different boundary conditions. Given the urgency of the human-triggered climate change, a growing amount of palaeoclimate studies has emerged during the last years, allowing the construction of increasingly sophisticated palaeoclimate models for different regions (e.g. Broström et al. 1998, Ganopolski et al. 1998, Kageyama et al. 1999, Siegert and Marsiat 2001, Lioubimtseva 2004). Altogether, these results form a more and more detailed jigsaw puzzle of past global climate conditions. However, this jigsaw is by far not complete yet, since climate conditions are still not understood everywhere.

One of the most interesting types of terrestrial palaeoclimate archives are loess-palaeosol sequences, where palaeosols indicate a change towards more humid conditions. Such sequences have been used in both hemispheres to derive terrestrial climatic variations during past few million years including changing wind dynamics and moisture regimes (e.g. Issar and Bruins 1983, Dodonov and Baiguzina 1995, Antoine et al. 2001, Berger et al. 2001, Schellenberger and Veit 2006, Markovic et al. 2006, Mason et al. 2007). By far most intensively studied are loess-palaeosol sequences from China, where they significantly increased our knowledge about the Quaternary palaeoclimate (e.g. Heller and Liu 1986, Kukla and An 1989, Maher and Thompson 1992). These studies proved that palaeosols developed in parallel with the marine oxygen isotope stratigraphy (MIS) during globally warmer periods since the beginning of the Quaternary. Since these palaeosols are linked to moister conditions in NW China, it was shown that they trace the dynamics of the East Asian monsoon. Furthermore, from properties of the loess the dynamics of dust transporting wind systems could be reconstructed.

In order to derive such palaeoclimatic information from loess-palaeosol sequences, different methods are used such as grain size analyses (Vandenberghé et al. 1997, Ding et al. 2000), rock magnetic analyses (Matasova et al. 2001, Maher et al. 2002), clay mineral analyses

## 1. Introduction

---

(Bronger et al. 1998, Junfeng et al. 1999), micromorphology (Bronger and Heinkele 1989, Kemp 1999) or investigations of the isotopic composition of organic matter or soil carbonates (Hatté et al. 1998, Ding and Yang 2000). Dating of these records was often attempted by luminescence dating techniques (e.g. Frechen et al. 1997, Zöller 2000, Lai et al. 2007).

The Saharan desert at the African continent close to the Canary Islands is actually the largest source of dust in the world, contributing about 50% of all mobilized mineral aeorols (Aléon et al. 2002). About 30-50% of that dust are transported towards the Atlantic Ocean, reaching even Central America (Muhs et al. 1990, Goudie and Middleton 2001, Prospero and Lamb 2003). Saharan dust forms aeolian deposits in the circum-Saharan area, which in opposite to the boreal and temperate zone are called “warm” or “desert” loess and are shown to record climate change, too (e.g. Yaalon and Bruins 1977, Coudé-Gaussen 1991, Wright 2001, Dearing et al. 2001).

The Canary Islands are located at the northern fringe of this Atlantic Saharan dust plume. Dust is mainly brought to the islands during two different synoptic situations: During the first situation, dust is entrained by so called “Calima” winds. These are low-level continental African Trade winds (Harmattan) which are deflected towards the west by Atlantic cyclones during boreal winter (cf. Criado and Dorta 2003). The second situation occurs during boreal summer, when dust is advected by the northern branch of the high altitude Saharan Air Layer. Subsequently, it sinks into the lower atmosphere north of the Canary Islands and is finally transported towards the islands via the marine Northeast Trade wind (e.g. Koopmann 1981, Bozzano et al. 2002). Dust is deposited here either during dry or wet conditions (Criado and Dorta 2003, Menéndez et al. 2007). This dust is trapped on the eastern Canary Islands where it forms deposits of different thickness (Coudé-Gaussen 1991, Grousset et al. 1998, Zöller et al. 2003, Menéndez et al. 2009).

At recent, the climate of the Canary Islands off southern Morocco is influenced by the Mediterranean climate dominated by winter precipitation and that of the hyperarid Sahara, receiving only very sparse precipitation (Jahn 1988, García-Herrera 2001). Furthermore, the local weather is also influenced by environmental changes in the arctic Atlantic which are conveyed to lower latitudes by ocean currents like the cold Canary current (e.g. Crowley 1981, Haslett and Davies 2006, Holz et al. 2007). In the past, the African monsoon was possibly another factor influencing the palaeoclimate of the islands: Kuhlmann (2003) proposed that the monsoon has reached the latitude of the Canary Islands during certain periods of the Quaternary. Thus, small changes of the NW African climate system should

## 1. Introduction

---

have had a significant influence on the Canary Islands, giving the area the character of a key region to investigate past climatic variability.

Up to now, Late Quaternary climate variations in NW-Africa and in the southwestern Mediterranean area are not well documented (e.g. Cheddadi et al. 1998). A large number of marine studies were carried out in this area which give information about dust transport and trade wind intensity changes (e.g. Moreno et al. 2001, Freudenthal et al. 2002, Moreno et al. 2002a, Nave et al. 2003, Kuhlmann et al. 2004), however it is rather difficult to extrapolate from marine records on moisture conditions in air masses and precipitation in the past (e.g. Kuhlmann 2003, Holz et al. 2007). Such information must come from terrestrial climate archives, but climate studies from the NW African continent and the Canary Islands face problems in two fields. (i) The archives are discontinuous, and dating of terrestrial sections is rather difficult and was limited to the Holocene or the latest Pleistocene (e.g. Rohdenburg 1977, Petit-Maire et al. 1986, Gasse et al. 1987, Rognon et al. 1989, Cheddadi et al. 1998, Meco et al. 2002, Lancaster et al. 2002) and (ii) Continuous sections covering the last glacial cycle are only found in the Northern Mediterranean area at least 1000 km north of the Canary Islands, e.g. the pollen-sequences of Padul in southern Spain (Pons and Reille 1998) and of Lago Grande di Monticchio in Central Italy (Allen et al. 1999). This demonstrates that there is a large gap in palaeoclimatic knowledge of the NW African region, limiting the understanding of environmental variability in this key area.

Due to the problems of discontinuity and particularly dating, the results of palaeoclimatic studies from the Eastern Canary Islands are fragmentary and must hence generally be regarded with caution. This holds especially true for those based on  $^{14}\text{C}$  dating (Meco and Pomel 1985, Petit-Maire et al. 1986, Rognon and Coudé-Gaussen 1989, Damnati et al. 1996, Meco et al. 1997, Coello et al. 1999) since this method faces strong problems here (Meco et al. 2002). These studies report a relatively wet Late Pleistocene/Early Holocene, whereas the period between 50 ka and the Last Glacial Maximum (LGM; ca. 20 ka) was characterised by several wetter periods with the occurrence of palaeosols. Studies based on thermoluminescence (TL) and U/Th dating (Pomel et al. 1985, Hillaire-Marcel et al. 1995, Rognon and Coudé-Gaussen 1996, Meco et al. 2002) are regarded as more reliable. These point to a generally wetter but instable climate between 50 ka and the Last Glacial Maximum (LGM; 20 ka), whereas the climate of the period prior to 50 ka is regarded as more humid and stable.

Earlier investigations (Zöller et al. 2003) show that sequences consisting of loess-like and palaeosol sediments are found in dammed valleys on Lanzarote. According to the authors,

## 1. Introduction

---

they continuously record the climate history of at least the last 200 ka. Thus, these sequences have the potential to fill a conspicuous gap in the palaeoclimatic knowledge of a key area in the Northern Hemisphere. Therefore, we continued the investigation of these mainly wind-transported sediments.

### Goals of the study

This study aims to pin-down information about environmental changes on Lanzarote and the adjacent NW African continent from the loess-like/palaeosol-sequences investigated by Zöller and al. (2003). However, prior to a palaeoclimatic interpretation of loess-palaeosol sequences it is crucial to investigate different aspects of the archives. (i) A robust dating and the buildup of a sound chronostratigraphy are necessary conditions for palaeoclimatic conclusions about distinct periods. Furthermore, dating is essential for a correct interpretation of pedologic processes since a prolonged time for pedogenesis has a similar effect as enhanced humidity, both resulting in an enhanced intensity of soil formation (e.g. Busacca and Cremaschi 1998, Sedov et al. 2003). (ii) It is necessary to evaluate whether investigated proxies really record palaeoclimatic changes in the studied area, or if they are inherited from aeolian or colluvial processes. This is due to the fact that sediments delivered to the archives could also show properties that were influenced by palaeoenvironmental conditions prevailing in the erosional area. (iii) An investigation of postsedimentary processes (e.g. peloturbation, carbonate dynamics) is essential since they could have mixed sediments of different age and thus have biased the chronostratigraphy of the sediments, leading to palaeoclimatic misinterpretations (e.g. Olson and Nettleton 1998, Liu et al. 2003).

Accordingly, the goals of this study are:

- Establishing a solid age model for the sediment sequences based on different luminescence techniques. Results of luminescence dating are validated using a comparison between Saharan dust proxies (kaolinite, iron) derived from marine studies from NE Atlantic cores close to the Canary Islands with a dust proxy (kaolinite) from the investigated profiles. These investigations will be discussed in chapter 4.2. (*Dating Saharan dust deposits on Lanzarote (Canary Islands) by luminescence dating techniques and their implication for palaeoclimate reconstruction of NW Africa.; Geochemistry, Geophysics, and Geosystems 2008*). Furthermore, an evaluation of the results of luminescence dating is done by investigating luminescence properties of recently deposited and recently redeposited Saharan dust. Results and discussion will

- be presented in chapter 4.3. (*Luminescence bleaching characteristics of Saharan dust – A case study from Lanzarote, Canary Islands (Spain).; submitted to Quaternary Geochronology*)
- Investigating functionality and character of the palaeoclimate archives and their sediments by analysing the geomorphological and pedological system. For the first aspect discussed in chapter 4.4. (*Geomorphological investigations of sediment traps on Lanzarote (Canary Islands) as a key for the interpretation of a palaeoclimate archive off NW Africa.; Quaternary International 2009*), we established a sediment-mass-balance using geomorphological mapping and GIS calculations and related this to the chronostratigraphy. Additionally, we developed sedimentary scenarios to estimate the approximate time resolution of the archives and the proportion of redeposited material. In chapter 4.5. (*Loess-like and palaeosol sediments from Lanzarote (Canary Islands/Spain) – indicators of palaeoenvironmental change during the Late Quaternary; in press in Palaeogeography, Palaeoclimatology, Palaeoecology*) we present investigations of the pedologic system using a multiproxy approach (granulometry, X-ray diffraction, rock magnetism, micromorphology, and soil chemistry). These investigations result in a determination of the palaeoclimatic significance of palaeosol-derived sediments, separating proxies relevant for palaeoenvironmental reconstructions from those related to post-sedimentary processes.
  - Reconstructing the temporal dynamics of palaeohumidity on Lanzarote using relevant proxies (clay content, frequency dependent susceptibility) and applying these findings to the palaeoclimatic context of the NW African region. For this purpose, in chapter 5. (*Synthesis: Palaeoclimatic scenarios for more humid periods on Lanzarote*) we first compared our palaeohumidity proxies with those derived during previous palaeoclimatic studies on the Canary Islands. Subsequently, we compared them with different palaeoclimatic proxies (for trade wind strength, Mediterranean vegetation, monsoon activity and Sea Surface Temperature) derived from investigations of the NW African/Mediterranean area, and deduced palaeoclimatic scenarios for more humid periods on Lanzarote.

## 2. Location and studied sites

### 2.1. Location

Lanzarote is the northeasternmost island of the Canary Islands (Spain) situated in the subtropical NE Atlantic, stretching northeast-southwest from 28°50' to 29°13'N (maximal length 57 km) and from 13°25' to 13° 52'W (maximal width 20 km). The minimum distance to the African continent is about 130 km (see inset of figure 2.1.).

#### 2.1.1. Geology

The Canary Islands have a completely volcanic origin and are regarded as a hot spot on a slow moving plate migrating from northeast to southwest (Carracedo et al. 1998, Geldmacher et al. 2001). Lanzarote is therefore one of the oldest islands of the Canarian archipelago. Volcanism started during the Miocene about 15.5 Ma ago and lasted until recently (last volcanic eruptions 1730-36 and 1824). Both the northern and the southern part of the island are dominated by volcanic massifs with Miocene to Pliocene ages. Volcanism is basic and basalts and pyroclastics were formed (cf. Rothe 1996). Given this basic volcanism of the island, Mizota and Matsuhisia (1995) and Jahn (1988) concluded that the quartz-rich sediments are aerosols blown off the N-African deserts.

#### 2.1.2. Geomorphology

Lanzarote and Fuerteventura are the oldest and most eroded islands of the Canarian archipelago, and peneplanation is most progressed here (cf. Höllermann 2006). Thus, the maximal altitude of Lanzarote is only 670 m. The slopes are generally smoothed and concave. The volcanic complexes are separated by the central part which shows a smoother topography, similar to most coastal areas characterised by flat abrasion terraces (Romero 2003).

The northern and southern massifs were dissected by numerous U-shaped valleys and smaller gullies (barrancos). Some of the larger valleys were dammed by volcanic material (lava flows, pyroclastica) during the Lower and Middle Pleistocene. Subsequently, the dammed valleys called “vegas” served as sediment traps for Saharan dust and local volcanic material. Sedimentation of Saharan dust and volcanic fallout occurred either in situ or later when the sediments were colluvially removed from the slopes and deposited in the vegas. These erosional events occurred quite frequently so that both kinds of material are closely interbedded with each other (see chapter 4.4.).

## **2. Location and studied sites**

---

### ***2.1.3. Present climate***

The present climate of Lanzarote is maritime-semiarid. Precipitation values range from < 100 mm at the coast up to 250 mm above 400 m a.s.l. Temperatures at sea level are quite uniform throughout the year, fluctuating only by 3.5°C around a mean value of 19.9°C. During winter, North Atlantic cyclones occasionally reach the latitude of the Canary Islands, destabilize the prevailing stable trade wind inversion layer and thus precipitation can occur. Unlike the higher western Canary Islands reaching altitudes up to 3700 m, the maximal altitude of Lanzarote (670 m) is below the condensation level of moist air and thus no precipitation from raising trade wind occurs here. The prevailing wind system throughout the year, the northeastern maritime trade wind, is only interrupted during winter by northwestern cyclonic or eastern Saharan air flow (Jahn 1988).

### ***2.1.4. Vegetation***

The vegetation of Lanzarote is very sparse, shrubby and has a disperse semi-desert character. It belongs to the Macronesian floristic association, characterised by a high proportion of endemic species. At recent it is strongly influenced by anthropogenic activity, and the natural vegetation is mostly replaced by secondary plant societies dominated by xerophytic and halophytic species (Jahn 1988, Kunkel 1993).

## 2. Location and studied sites

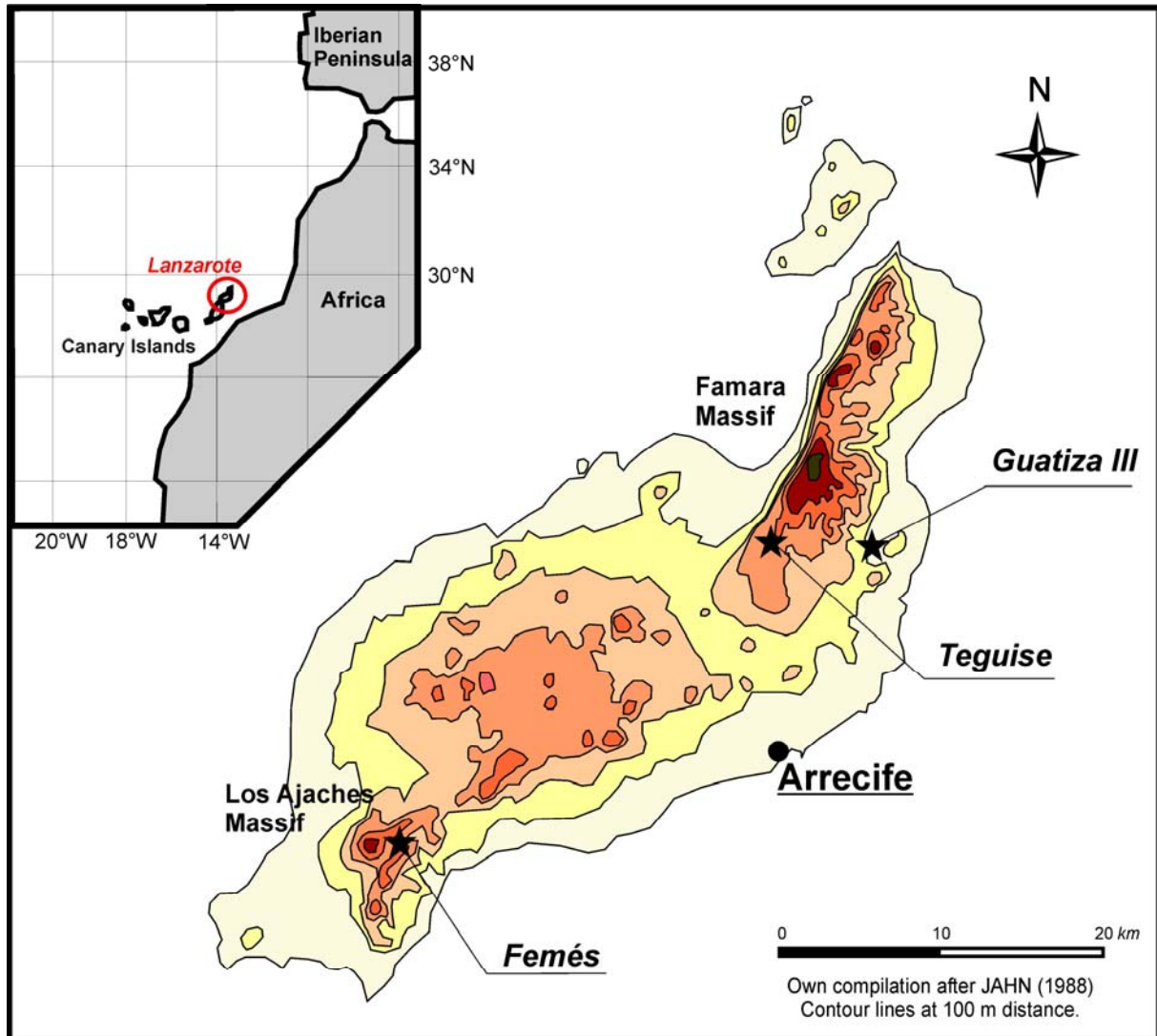


FIGURE 2.1. LOCATION OF LANZAROTE OFF NW-AFRICA AND OF STUDIED SITES ON THE ISLAND.

### 2.2. Studied sites

We studied the sediments of three vegas from the northern and the southern part of Lanzarote. (figure 2.1.)

#### 2.2.1. Vega of Femés

The vega of Femés is a SW-NE oriented valley at ca. 300 m a.s.l. in the Los Ajaches Massif in the south of Lanzarote (cf. figure 2.1.). It has a length of about three km and was completely dammed by volcanic material ca. 1.0 Ma ago, as indicated by datings of volcanites originating from the same volcanic group as those that form the damming of the vega (Coello et al. 1992, Instituto Tecnológico y Geominero de España 2005). Its catchment area has a size of ca. 5 km<sup>2</sup> whereof 18% are covered by the valley bottom (cf. figure 4.4.3.). The northwestern slopes have a relative altitude of about 200 m whereas the southeastern ones reach only ca. 100 m above the valley bottom. We resampled the profile described by Zöller

## 2. Location and studied sites

---

et al. (2003) in the southern part of the vega bottom (28°55'32''N, 13°45'19''W) since this position is far from geomorphic active slopes.

### *2.2.2. Vega of Guatiza*

The vega of Guatiza is located at the southeastern fringe of the Famara Massif in the north of Lanzarote, off the mouth of a canyon draining the highest parts of this massif reaching up to 670 m a.s.l. (cf. figure 2.1). The valley bottom has an altitude of ca. 100 m a.s.l. so that the relief difference in the catchment area is more than 500 m. To the east, volcanic damming occurred during the Middle Pleistocene about 170 ka ago (Suchodoletz et al., in preparation). Damming to the north was not complete so that the system partly remained open, making hiatae possible. The catchment area has a size of ca. 10 km<sup>2</sup> whereof 16.1% are covered by the vega bottom (cf. figure 4.4.3.). Profile Guatiza III (29°04'08''N, 13°29'22''W) was chosen since it is farther away from geomorphic active slopes than profiles Guatiza I and II described in Zöller et al. (2003).

### *2.2.3. Vega of Teguisse*

The Vega of Teguisse (also called Valle de San José) is a N-S-oriented valley at the southern fringe of the Famara Massif in the north of Lanzarote (cf. figure 2.1.). It has a length of about two km and is situated at an altitude of ca. 300 m. Volcanic material dammed the outlet of the valley in the south about 1.2 Ma ago (Instituto Tecnológico y Geominero de España 2005). However, damming was not complete so that hiatae could occur. The catchment area of the vega is about 4 km<sup>2</sup> whereof 35% are covered by the vega bottom (cf. figure 4.4.3.). Surrounding slopes have a relative altitude of ca. 100 m so that geomorphic activity is lower than in Femés and Guatiza. The investigated profile (29°04'52''N, 13°30'55''W) was chosen since it is located about 100 m from the eastern slope and 1.5 km from the damming so that neither an influence from the slopes nor hiatae are expected.

## 3. Material and methods

### 3.1. Material

Today, numerous pits give access to the bottom sediments of the vegas on Lanzarote. After studying different outcrops in the vegas, we selected profiles located distal to slopes delivering coarse colluvial material. We described stratigraphic changes recorded in the sections along the outcrops in order to document facies variability. The presence of carbonate was checked using 10% hydrochloric acid (HCl). Prior to sampling, we cleaned the profiles by removing the weathered 10 to 20 cm at the surface.

For laser-grain size and rock magnetic analyses we took 392 samples at a resolution of 5 cm. For 14 selected samples from Femés, clay contents were determined using pipette-analyses (table 4.5.2.) Sampling resolution for bulk XRD-analyses and carbonate contents (190 samples) was 10 cm, whereas XRD-analyses of the clay fraction were performed for only 6 samples from Femés (50, 170, 205, 485, 525 and 580 cm). Measurements of pH value, electric conductivity and Na-saturation were carried out in distinct layers reflecting facies changes of the profiles (50 samples). For three samples from Femés (65, 205 and 525 cm), X-ray amorphous clay was analysed. For luminescence dating, 37 samples were collected during night. The upper parts of the sections (apart from anthropogenic colluvia) we sampled at a resolution of 20 – 30 cm for luminescence dating, whereas in the lower parts sampling was restricted to a distance of 50 – 200 cm (for sampling locations in the profiles see figure 3.1.). Furthermore, we gained three samples of recent Saharan dust on Lanzarote and Gran Canaria (for dust sampling see chapter 4.4.). For micromorphology studies, we retrieved 24 oriented samples as blocks of 5\*2\*2 cm from the outcrops (for sampling locations in the profiles see figure 3.1.).

### 3.2. Methods

#### 3.2.1. GIS calculations of surface areas

Calculations of the vega catchments were performed using the GIS Arc Map 9.0 (ESRI). The digital database of elevation contour lines was provided by GRAFCAN, Cartografía de Canarias S.A. The vector data were triangulated for the calculation of a digital elevation model, where the height information is referenced per pixel.

#### 3.2.2. Grain size analyses

Aliquots of 10 g were treated with 10 and 30% hydrochloric acid (HCl) at 65°C to remove carbonate and dolomite as well as with 32% hydrogen peroxide (H<sub>2</sub>O<sub>2</sub>) to oxidize organic

### 3. Material and methods

---

carbon. In order to destroy abundant aggregates consisting of clay, ferromanganese oxides and hydroxides, we treated the sieved fraction  $< 63 \mu\text{m}$  with ultrasonic for some hours. Subsequently, 0.1 M sodium pyrophosphate was added and the sample was shook for 24 h to disperse clay. Samples were measured three times using a Malvern 2600C Analyser at GFZ Potsdam. For further analyses we used the mean of three replicate measurements.

Following Konert and Vandenberghe (1997), we used a conspicuous inflection point of the grain size distributions separating the first dominant peak from the following, and thus obtained a limit clay/silt of  $6.18 \mu\text{m}$ . In order to get the weathering signal, the ratio of clay and the fraction  $< 42 \mu\text{m}$  was taken to remove the signal of coarse silt. Coarse silt and fine sand show very similar depth functions, and due to their smaller specific surface they are believed not to contribute to weathering on the island as strong as fine/middle silt (cf. Helgeson et al. 1984).

#### 3.2.3. X-ray diffraction (XRD) analyses

For XRD of *bulk samples*, we leached the carbonate in aliquots of 5 g with 10% acetic acid at room temperature. After washing, drying and grinding we added 2% Md-IV sulfide as a reference standard, which allows a semi-quantitative estimation of the minerals contained in the sediment (Krischner 1990). Samples were measured on a Siemens D 5005 diffractometer at the University of Potsdam (2s/point,  $4 - 42^\circ 2\theta$ , Cu-tube FLCu-4KE). In order to interpret the results we used the program MacDiff 4.2.5. on a Macintosh computer (Petschick 2000). For identification of the minerals, the peaks with highest intensity of the minerals were used: For Md-IV-sulfide the molybdenite peak at  $14.39^\circ 2\theta$ , for quartz the peak at  $26.67^\circ 2\theta$ , for kaolinite the peak at  $12.34^\circ 2\theta$  and for illite the peak at  $8.84^\circ 2\theta$ . Relative amounts of kaolinite and illite were calculated using the ratio between their peaks and that of Md-IV-sulfide. To obtain absolute quartz contents, we produced a calibration-curve consisting of 11 samples with increasing amounts of quartz in an artificial mineral composite (feldspars, muscovite, olivine), spiked with 5% Md-IV-sulfide.

To analyse the *clay fraction*, aliquots of 7 g were dispersed and the fraction  $< 2 \mu\text{m}$  was separated. The suspension was dispersed on a glass slide allowing the clay minerals to orientate. Measurements were executed at a Seifert XRD C 3000 TT diffractometer (CuK $\alpha$ , 40 kV, 30 mA,  $2.5-30.01^\circ 2\theta$ ; step scan 15.0 s; step size  $0.03^\circ$ ) at Dresden University of Technology. Samples were measured three times after the following preparation steps: air drying, solvation with ethylene glycol (48 hours) and heat treatment (2 h at  $550^\circ\text{C}$ ). Interpretation was done using the programme Siemens Diffracplus BASIC 4.0#1.

### 3. Material and methods

---

XRD analyses are described in more detail in chapter 4.5.

#### 3.2.4. Luminescence dating

During luminescence dating at the University of Bayreuth, samples were only exposed to subdued monochromatic light ( $640 \pm 20$  nm). For dating, we used the coarse grain fraction 63 - 200  $\mu\text{m}$  of quartz and the fine grain fraction 4-11  $\mu\text{m}$  of quartz and of polymineral material. In order to obtain coarse grain quartz extracts, samples were sieved and the fraction 63 – 200  $\mu\text{m}$  was treated with HCl and H<sub>2</sub>O<sub>2</sub> to dissolve carbonate and organic matter. After a subsequent ultrasonic treatment, heavy minerals (density  $> 2.75$  g/cm<sup>3</sup>) and feldspars (density  $< 2.62$  g/cm<sup>3</sup>) were separated in a lithium heteropolytungstate solution (LST). Afterwards, the quartz fraction was etched in 40% HF for at least 45 minutes. The gained material was mounted on aluminium cups (diameter 12 mm) using silicone oil. Polymineral fine grain extracts 4 – 11  $\mu\text{m}$  were obtained by treatment in Atterberg settling tubes after destruction of carbonate and organic carbon with HCl and H<sub>2</sub>O<sub>2</sub> as well as an ultrasonic treatment. The material was subsequently pipetted on aluminium discs (diameter 9.6 mm). Quartz fine grain extracts were produced by etching the fine material with pre-treated 34% hexafluorosilicic acid for some days prior to pipetting.

Optically stimulated luminescence (OSL) using the single aliquot regenerative dose protocol (SAR, see Murray and Wintle 2000) was measured from coarse- and fine grain quartz extracts. Polymineral fine grain extracts were measured with infrared stimulated luminescence (IRSL) applying the multiple aliquot additive dose protocol (MAAD) of Lang et al. (1996).

Measurements of equivalence doses ( $D_e$ 's) were executed at two Risø-Readers TL/OSL-DA-15 (Bøtter-Jensen 1999) with corresponding filter combinations for OSL and IRSL (cf. Lang et al. 1996, Fuchs 2001).  $\beta$ -irradiations were executed using the internal <sup>90</sup>Sr/<sup>90</sup>Y-sources of the Risø-Readers as well as an external <sup>90</sup>Sr/<sup>90</sup>Y-source. For  $\alpha$ -irradiations, necessary to determine the  $a$ -value (sensitivity of the material to  $\alpha$ - compared to its sensitivity to  $\beta$ - irradiation) of fine grain samples, an external <sup>241</sup>Am- $\alpha$ -source was used. Fading tests were done comparing aliquots stored for one month after irradiation with those stored for three months (cf. Lang et al. 1996). Analysis of OSL and IRSL results was executed using the software Analyst 3.07b.

Dose rates ( $\dot{D}$  's) were determined from dry, ground material using the conversion factors of Adamiec and Aitken (1998). Thick source  $\alpha$ -counting was applied to determine U and Th contents (University of Bayreuth), and potassium concentrations were measured either with gas chromatography - combustion - isotope ratio mass spectrometry (ICPMS, Bayreuth

### 3. Material and methods

---

Center for Ecology and Environmental Research, BayCEER) or an atomic adsorption spectrometer (AAS, University of Marburg). Cosmic dose rates were evaluated after Prescott and Hutton (1994). Interstitial water contents were measured gravimetrically. However, due to drying of the outcrops we used the grain size distribution of a sample and the resulting middle pore volume as described in Fuchs (2001) in order to get the presumed palaeo-water content used for age calculations.

Due to in parts insufficient bleaching of the material, we applied the approach of Juyal et al. (2006) (modified by Fuchs et al. (2007), resulting in a simplified age model after Galbraith et al. (1999)) for the determination of coarse grain OSL-De's. Furthermore, younger material dropping through pedogenic cracks or root channels caused outliers towards the lower end of the De-distribution. Hence, we removed those by subtracting the lower 5%-quantil of the sorted De-distribution prior to statistical calculations. In contrast, due to the fact that thousands of grains on each disc give a luminescence signal, for fine grain measurements no correction for insufficient bleaching could be applied.

A more detailed description of luminescence dating is given in chapter 4.2.

### 3. Material and methods

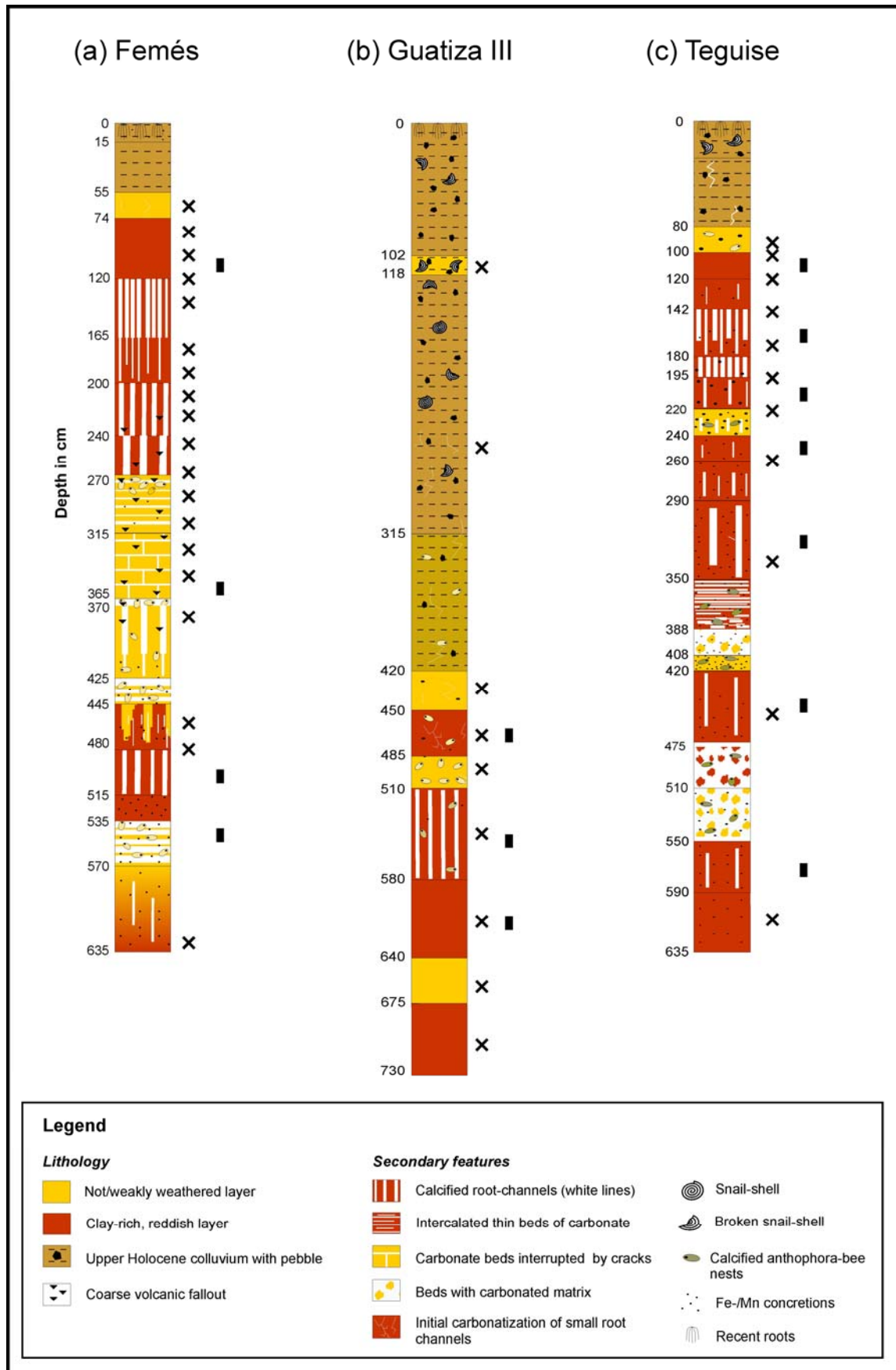


FIGURE 3.1. INVESTIGATED PROFILES ON LANZAROTE WITH LUMINESCENCE (CROSSES) AND MICROMORPHOLOGICAL SAMPLES (RECTANGLES)

### 3. Material and methods

---

#### 3.2.5. Rock magnetism

Dry sediment was filled into plastic boxes, and compressed and fixed with cotton wool prior to closing the lid to prevent movement of sediment particles during measurement. The sediment mass served as normalizer. Because original in situ sediment density and exact filling volume of the boxes are unknown, we assumed an average density of  $1.7 \text{ g}\cdot\text{cm}^{-3}$  in order to calculate volume susceptibilities ( $\kappa$ ).

Initial low field susceptibility was measured in an AC-field of 300 A/m at 920 Hz using the KLY-3-Spinner-Kappa-Bridge (AGICO, Brno, Czech Republic). Frequency dependence of susceptibility ( $\kappa_{fd}$ ) was determined using a MAGNON Susceptibility Bridge (MAGNON, Dassel, Germany) at AC-fields of 80 A/m at 1 and 8 kHz respectively ( $\kappa_{fd} = (\kappa_{@1\text{kHz}} - \kappa_{@8\text{kHz}})/\kappa_{@1\text{kHz}} \cdot 100$  in %). For calculating the S-parameter (S-parameter =  $(IRM_{@(-350)}/IRM_{@(2000)} + 1)/2$ ) we exposed the samples firstly to a field of 2000 mT, and secondly to an antiparallel field of 350 mT using a Magnon PM II pulse magnetizer (MAGNON, Dassel, Germany). Acquired remanence was measured subsequently after each acquisition step with a JR6-spinner magnetometer (AGICO, Brno, Czech Republic).

Rock magnetic measurements were executed by Dr. Ulrich Hambach at the Laboratory for environmental and palaeomagnetism of the University of Bayreuth.

#### 3.2.6. Micromorphology

Sampled oriented blocks were air-dried and impregnated with Oldopal P80-21. Subsequent cutting and polishing to slices of 4.8 x 2.8 cm were done after Beckmann (1997). During preparation, samples were not heated to  $>40^\circ\text{C}$ . Micromorphological description followed the terminology of Stoops (2003).

Micromorphological analyses were done by Dr. Peter Kühn at the University of Tübingen.

#### 3.2.7. Soil analytics

Carbonate contents were determined taking the difference between total organic and total carbon. Total carbon (TC) and total organic carbon (TOC) were analysed using an EuroVector EA3000 Elemental analyser at GFZ Potsdam. For TC, ca. 10 mg sample material was wrapped into tin capsules and combusted under  $\text{O}_2$ -supply at  $> 1000^\circ\text{C}$ . After combustion,  $\text{CO}_2$  was separated by GC column and measured by thermal conductivity. For TOC determination, ca. 3 mg of sample material were weighed into Ag-capsules, dropped with 20% HCl, heated for 3 h at  $75^\circ\text{C}$ , finally wrapped up into Ag-capsules and measured. The calibration was performed using a certified elemental standard (Urea) and proofed with a

### 3. Material and methods

---

soil reference sample (Boden2). The reproducibility for replicate analyses is 0.2 %. Inorganic carbon was calculated subtracting organic from total carbon, resulting in the content of inorganic carbon. Finally, carbonate contents were obtained by multiplying inorganic carbon contents with a stoichiometric factor of 8.33.

For determination of pH values, 20 g of the samples were mixed with a 0.1 n KCl solution and measured with a pH meter (inoLab, WAW). We determined electric conductivity ( $EC_5$ ) by soaking 10 g of sediment in 50 ml of deionized water, filtering and subsequently determining the conductivity with a conductivity electrode (Tetra Con 325). In order to measure Na-saturation, 10 g of sediment were soaked in a  $BaCl_2$ -triethanolamin solution at pH 8.1 and subsequently filtered. Afterwards, Ca, Na, Mg and K of this filtrate were measured using an Atomic Adsorption Spectrometer (AAS, Analytic Jena vario 6). These measurements were carried out at the Laboratory of Physical Geography at the Technical University of Dresden.

Analyses for amorphous clay minerals (allophane) followed the method of Schlichting et al. (1995). To identify the amount of oxalate soluble Al and Si, 1 g air dried material and 50 ml oxalate solution were shook for one hour in darkness and filtrated. The extraction of dithionite soluble Al and Si was performed using 2 g air dried sample material and 50 ml dithionite-citrate solutions. Measurements were carried out after treatment with  $HClO_4$  using a flame atomic adsorption spectrometer (Perkin-Elmmer) at the University of Gießen.

### 4. Results

#### 4.1. Stratigraphy

The lithology of the investigated profiles is described in figure 3.1. The ages of the layers are derived from luminescence datings presented in chapter 4.2.

The profiles are generally divided into two parts: The upper part consists of colluvial sediments of different thickness influenced by anthropogenic activity that contain coarser material including pebbles and boulders. This is followed by a lower part not influenced by anthropogenic activity, showing no coarse material apart from sporadically distributed pebbly volcanic fallout. This lower part is characterised by a change of slightly weathered loess-like layers with those derived from palaeosols. Barely weathered loess-like layers are characterised by yellowish colour and a silty granulometry. Furthermore, they often exhibit secondary carbonatic features like e.g. nodules, calcified root channels and a carbonated matrix, in some layers resulting in the formation of calcrete. In contrast, palaeosol-derived layers have a reddish colour, are clay rich and thus show vertic features with deep vertical cracks. The matrix itself contains no carbonate, whereas root channels and vertical cracks may be calcified.

Most layers were diagenetically overprinted when iron and manganese rich water infiltrated subsequently, producing coatings and concretions of different size. In several layers, calcified nests of anthophora-bees are found in different quantities.

##### 4.1.1. Profile of Femés

The sequence exposed in Femés has a thickness of 635 cm. The upper 55 cm comprise an anthropogenic colluvium underlain by a few weathered, decalcified loess-like layer of Early/Middle Holocene age until 74 cm. The layers between 74 and 270 cm consist of several palaeosol-derived sediments characterised by root pipes carbonated to different extents. These layers were deposited from MIS 4 to upper MIS 2. However, luminescence dating shows that a hiatus not recognizable in the field occurs in these layers (see chapter 4.2.), causing the absence of the lower part of MIS 2 and possibly the uppermost part of MIS 3. Underlying layers until 445 cm comprise the whole MIS 5 apart from MIS 5 e. These layers are generally few weathered, and exhibit a carbonated matrix that is incrustated in some parts and thus forms a calcrete. In some layers carbonated nests of anthophora-bees are found. Between about 220 and 400 cm partly weathered lapilli are sporadically found. From 445 to 535 cm palaeosol-derived sediments dominate, partly showing strongly calcified root channels. These sediments were deposited from upper MIS 6 to MIS 5e. Up to 570 cm

sediments are underlain by a loess-like layer which is strongly calcified, and partly has the appearance of a calcrete where some calcified nests of anthophora bees are found. This layer was deposited during the middle of MIS 6. The lowest outcropping part of this section to 630 cm is characterised by palaeosol-derived sediments sporadically showing calcified root-channels. It was probably deposited during lower MIS 6.

Excluding the upper 55 cm of anthropogenic colluvial material, this sequence shows an average sedimentation rate of 3.2 cm/ka.

##### **4.1.2. Profile of Guatiza III**

The profile of Guatiza III has a thickness of 730 cm. The uppermost 420 cm containing pebbles and ovicaprid bones are colluvial sediments related to anthropogenic activity. As in Femés, these are underlain by a slightly weathered, generally decalcified loess-like layer (420 - 450 cm) dating from the Early/Middle Holocene. However, some pores are secondarily recalcified. The layer between 450 and 485 cm consists of palaeosol-derived sediments with singular secondarily calcified root channels and carbonatized anthophora bee-nests formed during upper MIS 2. From 485 to 510 cm, a carbonatized loess-like layer containing numerous calcified anthophora bee nests is found, deposited during upper MIS 3. According to luminescence dating (see chapter 4.2.), then follows a hiatus not evident in the field. The following part of the section consists of palaeosol sediments and a decalcified loess-like layer between 640 and 675 cm. These layers were deposited during lower and middle MIS3. The palaeosol sediments between 510 and 580 cm show strongly calcified root channels and isolated calcified anthophora bee nests.

Disregarding the upper 420 cm influenced by human activity, the profile of Guatiza III shows an average sedimentation rate of 5.8 cm/ka. However, due to incomplete damming and the low catchment area/vega bottom connectivity (see chapter 4.4.) this rate is rather discontinuous.

##### **4.1.3. Profile of Teguisse**

The profile studied in Teguisse has a thickness of 635 cm. The upper 80 cm consist of an anthropogenically triggered colluvium with pebbles. From 80 to 100 cm, a decalcified loess-like layer containing calcified anthophora bee nests and iron manganese concretions with a length of up to 2 cm is developed. This layer represents the Early/Middle Holocene interval. The layers between 100 to 220 cm are palaeosol sediments and contain different densities of secondarily calcified root channels. These sediments are dated from MIS 5b to lower MIS 2,

where the period between 75 and 50 ka shows a very low time-resolution. No hiatus between these layers and the overlying loess-like layer is recognizable in this profile, although luminescence dating seems to indicate its presence, and it is seen in another profile close to the damming in the south (see chapter 4.2.). A following decalcified loess-like layer (220 to 240 cm) contains singularly calcified anthophora bee nests as well as numerous iron manganese concretions and was deposited during MIS 5d/5e. Underlying palaeosol-derived sediments showing different quantities of secondarily calcified root channels have developed to a depth of 388 cm, where between 388 and 350 cm calcified anthophora bee nests and beds of carbonate are found. These sediments were deposited from mid-MIS 6 to MIS 5e. Between 388 and 408 cm, a calcrete layer developed from slightly weathered loess and is followed by a decalcified loess-like layer containing calcified anthophora bee nests from 408 to 420 cm. Both layers were deposited during mid-MIS 6. From 420 to 475 cm, a soil-derived layer showing secondarily carbonatized root channels has developed. From 475 to 550 cm calcrete horizons containing singular calcified anthophora bee nests and iron manganese concretions (length of up to 0.5 cm) are found. The lowest part of the section consists of two palaeosol-derived sediment layers, the upper containing singular secondarily calcified root channels. Beyond MIS 6, age assignments to sediments were not possible.

Excluding the upper 80 cm consisting of anthropogenically influenced colluvial material, the sequence of Teguse exhibits an average sedimentation rate of ca. 2.1 cm/ka.

**4.2. Dating Saharan dust deposits on Lanzarote (Canary Islands) by luminescence dating techniques and their implication for palaeoclimate reconstruction of NW Africa**

Suchodoletz, H. von\*, Fuchs, M. and L. Zöller

*Published in Geochemistry, Geophysics, and Geosystems 9 (2008), doi:10.1029/2007GC001658*

Department of Geomorphology, University of Bayreuth, Bayreuth/Germany

\*corresponding author

tel: +49-921552266

fax: +49-921552314

E-mail adress: Hans.vonSuchodoletz@uni-bayreuth.de

**Abstract:** Lava flow dammed valleys (Vegas) on Lanzarote (Canary Islands) represent unique sediment traps, filled with autochthonous volcanic material and allochthonous Saharan dust. These sediments and the intercalated palaeosoil sediments document past environmental change of the last glacial-interglacial cycles, both on Lanzarote and in NW Africa. A reliable chronology must be established to use these sediment archives for palaeoclimate reconstructions. Owing to the lack of organic material and the limiting time range of the  $^{14}\text{C}$ -dating method, luminescence dating is the most promising method for these sediments. However, the fluvio-aeolian character of these sediments is a major problem for luminescence dating, because these sediments are prone to insufficient resetting of the parent luminescence signal (bleaching) prior to sedimentation. To check for the best age estimates, we compare the bleaching behaviour of (1) different grain sizes (coarse- versus fine-grain quartz OSL) and (2) different minerals (fine-grain feldspar IRSL versus fine-grain quartz OSL). The results show that owing to its bleaching characteristics, quartz is the preferable mineral for luminescence dating. On the basis of the fine- and coarse-grain quartz OSL age estimates, a chronostratigraphy up to 100 ka could be established. Beyond this age limit for OSL quartz, the chronostratigraphy could be extended up to 180 ka by correlating the vega sediments with dated marine sediment archives.

**Keywords:** luminescence dating, Saharan dust, Canary Islands, insufficient bleaching, land/sea correlation, human occupation.

**4.2.1. Introduction**

Lava flow dammed valleys (Vegas) on Lanzarote (Canary Islands) represent sediment traps, filled with autochthonous volcanic material and allochthonous Saharan dust. These sediments are regarded as unique terrestrial archives for the Quaternary palaeoclimate reconstruction of northwest Africa (Suchodoletz et al. 2009a).

There have been many attempts to reconstruct the palaeoclimate for this region. Marine records that may extend back to the Tertiary (e.g., Dupont 1993, Brunner and Maniscalco 1998, Moreno et al. 2001) have the advantage that they provide continuous records with generally well-preserved proxies. In contrast, terrestrial archives are commonly discontinuous and represent only short periods, which makes their palaeoclimate interpretation difficult (e.g., Gasse et al. 1987, Cheddadi et al. 1998, Lancaster et al. 2002). However, despite the limitation of interpretation and hiatuses, terrestrial archives are essential for investigating palaeoclimate on land, especially the regional patterns and the land-sea interaction. On the Eastern Canary Islands, various terrestrial archives have been used to reconstruct palaeoclimate, for example, dune sequences and their intercalated palaeosols (e.g., Rognon et al. 1989, Criado et al. 2004, Ortiz et al. 2006), calcretes (e.g., Alonso-Zarza and Silva 2002), cave sediments (e.g., Coello et al. 1999) and marine terraces (e.g., Meco et al. 2002). However, these archives show hiatuses and represent limited periods of the Quaternary. Our studies from Lanzarote, where thick Saharan dust had accumulated in volcanic valleys, reveal a generally continuous record, reaching from the Holocene to the Middle Pleistocene (Zöller et al. (2003) and present study), which makes these sediments an outstanding terrestrial archive for a palaeoenvironmental reconstruction of Lanzarote and NW Africa.

For palaeoclimatic interpretation of these archives a sound chronostratigraphy is of crucial importance. Previous studies on the Eastern Canary Islands used the  $^{14}\text{C}$ -dating method (e.g., Petit-Maire et al. 1986) as well as U-Th ages (e.g., Hillaire-Marcel et al. 1995), but the results of both methods suffer from the fact that the ages were determined on land snail shells which may represent open systems. Therefore these dates must be regarded as provisional (Edwards and Meco 2000). The second shortfall of both methods is that they do not directly date the sedimentation process, a drawback that does not apply to luminescence dating. Sporadic studies from the Eastern Canary Islands using luminescence dating were presented by Pomel et al. (1985) and Bouab and Lamothe (1997). Since our initial dating results using infrared stimulated luminescence (IRSL) were promising (Zöller et al. 2003), and in most parts of the investigated profiles there are neither organic matter nor land snail shells, we continued to build up our chronostratigraphy using luminescence dating. Luminescence dating is based on the fact that quartz and feldspar grains accumulate energy in their crystal lattice after burial, that increases in response to ionizing radiation to which the grains are exposed. This signal is discharged when the grains are exposed to sunlight. Measurement of this signal results in the equivalent dose ( $D_e$ ). To determine the time that elapsed since the last bleaching, the  $D_e$  is divided by the ionizing radiation (dose rate  $\dot{D}$ ) of the dated sediment (Singhvi and Krbetschek 1996, Aitken 1998, Wintle 1998).

The advantage of luminescence dating is that it directly dates the last exposure to sunlight, but good optical bleaching prior to burial is of major importance. Pure aeolian sediments such as loess show very good bleaching prior to sedimentation, and have been dated successfully for many years (e.g., Berger et al. 1992, Rousseau et al. 1998, Zöller et al. 2004). It is only recently that the development of coarse-grain dating techniques using optically stimulated luminescence (OSL) facilitated the dating of

poorly bleached materials, for example, fluvial, colluvial or playa sediments (e.g., Olley et al. 1998, Fuchs and Wagner 2003, Bubenzer and Hilgers 2003). Being aware of the largely colluvial character of our sequences (Suchodoletz et al. 2009a), we have compared three different luminescence dating techniques (IRSL of fine-grained feldspars and OSL of fine and coarse-grained quartz) with different bleaching properties to build up a reliable chronostratigraphy for our archives. This methodological comparison should help to evaluate the reliability of the “problematic” IRSL dates in the older parts of the profiles, where they are the only numerical dating method available.

#### **4.2.2. Study area**

Lanzarote (28°50'N-29°13'N, 13°25'W-13°52'W) belongs to the Canary Islands/Spain and is situated ~130 km west of the southern Moroccan coast (figure 4.2.1.). It is a volcanic island, composed of basic to ultrabasic volcanic rocks. Volcanism started around 15.5 Ma ago and has persisted to recent historical times (e.g., Carracedo et al. 1998).

Owing to its limited altitude (maximum 670 m amsl), Lanzarote does not receive precipitation from rising trade winds. It receives 100 mm (at lower elevation) to 250 mm (at higher elevation) precipitation from boreal winter cyclones. Mean annual temperature is 19.9°C (Jahn 1988). Lanzarote is characterized by a very sparse, shrubby and disperse vegetation dominated by xerophytic and halophytic species manifesting a semi desert character.

The island is situated at the northern fringe of the Saharan dust plume over the North Atlantic Ocean. Dust is brought to the island during two different synoptic situations: During the first situation, dust is entrained by so called “Calima” winds: low-level continental African Trade winds (Harmattan) deflected toward the west by Atlantic cyclones especially during boreal winter (Criado and Dorta 2003). The second situation occurs exclusively during boreal summer, when dust is advected by the northern branch of the high-altitude Saharan Air Layer. Subsequently, the material sinks into the lower atmosphere north of the Canary Islands and is finally transported toward the islands via the Northeast Trade wind (Koopmann 1981, Bozzano et al. 2002). Dust can be deposited here during both dry and wet conditions (Criado and Dorta 2003, Menéndez et al. 2007).

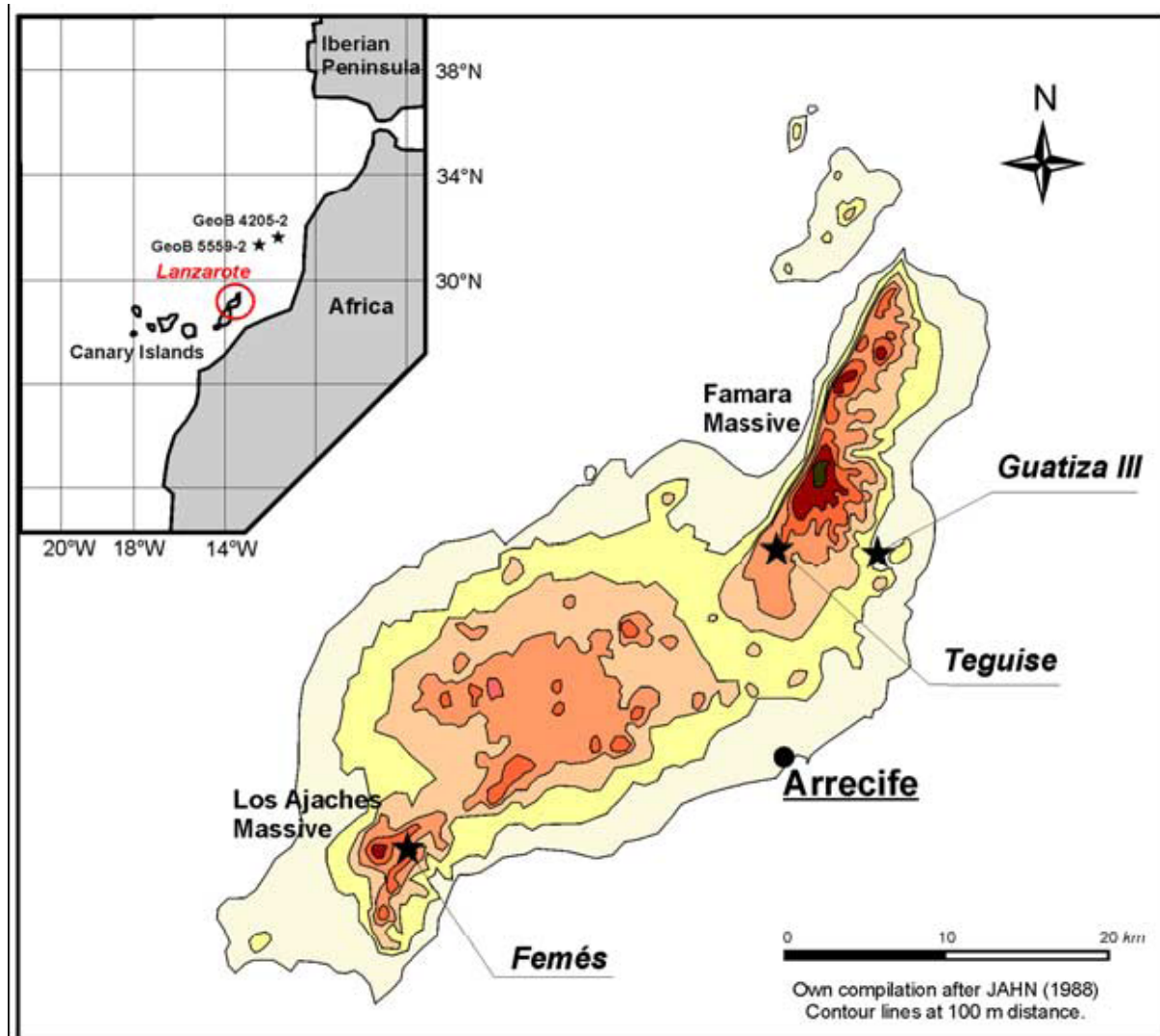


FIGURE 4.2.1. LOCATION MAP OF THE ISLAND OF LANZAROTE WITH THE STUDIED VEGAS OF FEMÉS, TEGUISE AND GUATIZA III. IN ADDITION, MARINE SEDIMENT CORES FROM NEARBY LOCATIONS ARE INDICATED IN THE INSET.

#### 4.2.3. Studied sites

On Lanzarote, palaeo-valleys of Miocene to Pliocene age were dammed during the Early and Middle Pleistocene by lava flows and pyroclastic material. Locally these valleys are called vegas. In our studies we used the outcrops situated in loam pits excavated during the past decades in the vegas of Femés, Guatiza and Teguisse (Valle de San José) (figure 4.2.1.). All studied profiles were chosen in a distal position from geomorphologically active slopes. Hence we chose profile Guatiza III instead of Guatiza I and II (Zöller et al. 2003) for further investigations. Two vegas (Guatiza and Teguisse) are situated on the fringes of the Famara Massif in the north of the island at a distance of ~6 km from each other. Damming of these valleys was never total, so hiatuses can be expected. The valley of Femés is located in the Los Ajaches Massif in the south of Lanzarote about 30 km from the northern sites, and damming was complete until today (Zöller et al. 2006).

The stratigraphies can be seen in figure 4.2.2. The sediments are composed of interbedded in situ and reworked colluvial material originating from allochthonous Saharan dust and autochthonous volcanic

#### 4. Results: 4.2. Dating Saharan dust deposits on Lanzarote (Canary Islands) by luminescence...

products. Parts of these sediments were subject to pedogenesis and are consequently characterized by reddish color and a vertisol texture, whereas other layers are only slightly weathered and show a yellowish color and a silty granulometry. Some beds were overprinted by carbonatic waters and thus contain carbonate nodules, calcified root channels, or are fully developed as calcrete horizons. Many layers were overprinted by water containing Fe and Mn. Consequently, Fe and Mn stains and concretions occur, the largest in the vega of Teguisse. In some horizons, calcified nests of anthophora bees are common. Whereas no coarse colluvial material is found in the lower parts of the sequences, the upper parts consist of anthropogenic colluvium containing pebbles and partly ovicaprid bones. In Femés, coarse volcanic fallout is observed between ~220 and 400 cm. The stratigraphy of this profile is slightly revised compared to that published by Zöller et al. (2003). Consequently, in the case of differing depths both are indicated in tables 4.2.4. and 4.2.5. The properties of the sequences are listed in table 4.2.1.

These sedimentary units record the landscape and palaeoclimatic history from the Lower Pleistocene to the Holocene. The geomorphic system and its sedimentation processes are described in detail by Suchodoletz et al. (2009a).

|   | Femés                                | Guatiza             | Teguisse            |
|---|--------------------------------------|---------------------|---------------------|
| latitude N  | 28°55'32''                           | 29°04'08''          | 29°04'52''          |
| longitude W   | 13°45'19''                           | 13°29'22''          | 13°30'55''          |
| altitude (m a.s.l.)                                     | 300                                  | 100                 | 300                 |
| catchment area (km <sup>2</sup> )                       | 5.07                                 | 10.1                | 3.8                 |
| valley bottom (% of catchment area)                     | 18                                   | 16.1                | 35                  |
| relative elevation difference in the catchment area (m) | 100 (SE slopes) –<br>200 (NW slopes) | > 550               | 100                 |
| time of volcanic damming                                | 1.4 Ma <sup>1</sup>                  | 170 ka <sup>2</sup> | 1.2 Ma <sup>3</sup> |
| volcanic damming complete?                              | yes                                  | no                  | no                  |
| thickness of anthropogenic colluvial deposits (cm)      | 55                                   | 420                 | 80                  |

TABLE 4.2.1. PROPERTIES OF STUDIED SITES ON LANZAROTE

<sup>1</sup> Zöller et al. (2006)

<sup>2</sup> consistent thermoluminescence and ESR data (Suchodoletz et al., in preparation)

<sup>3</sup> Instituto Tecnológico y Geominero de España (2005)

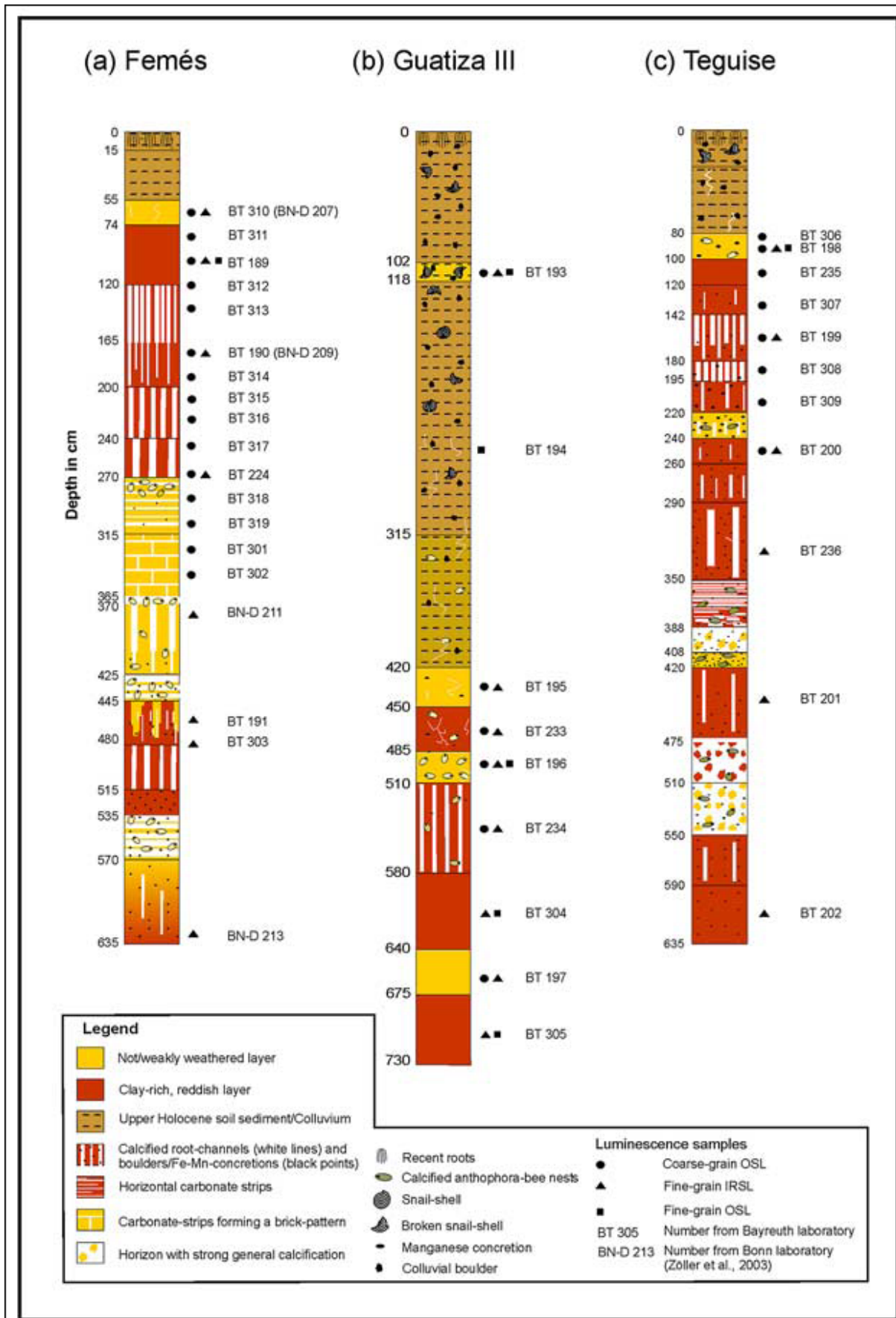


FIGURE 4.2.2. THE PROFILES OF (a) FEMÉS, (b) GUATIZA III AND (c) TEGUISE. GIVEN IS THE SEDIMENTARY CHARACTER OF THE PROFILES AND INDICATED ARE THE SAMPLE LOCATIONS FOR LUMINESCENCE DATING WITH THEIR LAB NUMBERS.

#### **4.2.4. Methods**

For luminescence dating sampling took place during the night, after removing the outer 30 cm of the profile to avoid any contamination with light exposed material. Sampling and sample preparation at the Bayreuth luminescence laboratory (University of Bayreuth/Germany) was done under subdued red light (wavelength  $640 \pm 20$  nm).

##### *4.2.4.1. Sample preparation*

###### *Coarse grain quartz samples*

After sieving, the fraction 63-200  $\mu\text{m}$  was treated with HCl and  $\text{H}_2\text{O}_2$  to destroy carbonate and organic matter, and was held in an ultrasonic bath for 30 min to destroy aggregates. Heavy minerals (density  $> 2.75 \text{ g/cm}^3$ ) and feldspars (density  $< 2.62 \text{ g/cm}^3$ ) were separated in a lithium heteropolytungstate solution (LST). The quartz material was subsequently etched in 40% HF for 45 min in order to remove any remaining feldspar as well as the alpha irradiated outer layer of the quartz grains. The resultant material was fixed on aluminum cups (diameter 12 mm) using silicone oil. The number of grains per cup was between 200 and 600, representing small aliquots according to Fuchs and Wagner (2003).

###### *Fine grain quartz samples*

To remove carbonates and organic carbon, the fraction  $<63 \mu\text{m}$  was treated with HCl and  $\text{H}_2\text{O}_2$ . Subsequent addition of 0.05 M sodium pyrophosphate and treatment in an ultrasonic bath for 30 min dispersed clays and destroyed grain aggregates. Extraction of the 4–11  $\mu\text{m}$  fraction was done in Atterberg-settling tubes up to 50 times. The separated polymineral fraction 4–11  $\mu\text{m}$  was etched for 4–5 days in pretreated 34% hexafluorosilicic acid to remove any remaining feldspars (for methodology, see Fuchs et al. (2005)). After a short IRSL test on two aliquots that included radiation (50 Gy) and IRSL measurement to identify any possible remaining feldspar contamination, the material was pipetted on to 9.6-mm aluminum discs.

###### *Fine grain polymineral samples*

The polymineral fine silt fraction was extracted as described above for fine-grain quartz samples and was directly pipetted on to aluminum discs (diameter 9.6 mm). Each disc had about 1.6 mg of silt.

##### *4.2.4.2. Measurements*

For measurements we used two Risø-Readers TL/OSL-DA-15 combined with a Thorn-EMI 9235QA photomultiplier (Bøtter-Jensen et al. 1999). Sources used for radiation are listed in table 4.2.2. The software Analyst 3.07b was used for analysis of the data.

#### 4. Results: 4.2. Dating Saharan dust deposits on Lanzarote (Canary Islands) by luminescence...

| type of irradiation | type of source  | coarse grain | fine grain |
|---------------------|---|--------------|------------|
| $\beta$             | $^{90}\text{Sr}/^{90}\text{Y}$ (internal Risø-reader 1) | 8.81         | -          |
|                     | $^{90}\text{Sr}/^{90}\text{Y}$ (internal Risø-reader 2) | 2.57         | 2.52       |
|                     | $^{90}\text{Sr}/^{90}\text{Y}$ (external)               | -            | 7.85       |
| $\alpha$            | Littlemore $^{241}\text{Am}$ (external)                 | -            | 1.26       |

TABLE 4.2.2. KIND AND STRENGTH OF USED IRRADIATION-SOURCES

Strengths are given in Gy/min and referred to 21 August 2006, except for the external  $^{90}\text{Sr}/^{90}\text{Y}$ -source which is referred to 15 June 2006.

##### *Fine and coarse grain quartz OSL*

Measurement parameters of fine- and coarse grain quartz samples are listed in table 4.2.3. Equivalent doses (De) were determined using the single aliquot regenerative dose protocol (SAR) (see Murray and Wintle 2000). A saturating exponential growth curve was constructed, using six regeneration cycles after one measurement of the natural OSL: four measurements of regenerated doses, one repeated measurement of the first regenerated dose to determine the recycling ratio and one 0-dose regeneration cycle. The De was determined by subtracting the background from the used OSL integral. A check for possible feldspar contamination was done by stimulating the artificially irradiated samples with infrared and detecting in the blue range (390-450 nm). Depending on the availability of the prepared mineral fraction, we tried to measure a minimum of 30 aliquots from the coarse grained fraction, and 6–7 aliquots from the fine grained samples. In individual cases, the number of measured aliquots was below 30 for coarse-grained samples. To determine a-values of the fine-grain samples, a-irradiation was used.

##### *Polymineral IRSL*

Measurement parameters for polymineral IRSL samples are listed in table 4.2.3.

For De determination, the multiple aliquot additive dose protocol (MAAD) following Lang et al. (1996) was routinely used. After measurement of three natural and three artificially irradiated discs (test dose of 50 Gy) to obtain a rough approximation of the equivalent dose, six dose groups with five discs each were irradiated and stored for 1 month at room temperature. Subsequently, they were measured together with nine natural discs to construct the additive growth curve. The a-value of some representative samples was determined using an a-growth curve with three dose groups of three aliquots each.

Owing to limited laboratory capacity, we did not conduct tests for anomalous fading after Auclair et al. (2003), but used instead a simpler protocol following Lang et al. (1996). We irradiated five discs with the highest irradiation dose, stored them for 3 months at room temperature before measurement and compared them to the measurements done after 1 month of storage.

#### 4. Results: 4.2. Dating Saharan dust deposits on Lanzarote (Canary Islands) by luminescence...

|                       | OSL                                       | IRSL   |
|-----------------------|---|--|
| Stimulation-LEDs      | 470 ± 20 nm                               | 845 ± 20 nm  |
| Detection-filter      | U-340 Hoya<br>(transmission 290 - 380 nm) | BG 39, GG 400, 2xBG 3<br>(transmission 390-450 nm)             |
| Preheat (rate 10°/s)  | 240°C for 10 s                            | 220°C for 120 s (age < 10 ka)<br>220°C for 300 s (age > 10 ka) |
| Cut-heat (rate 5°C/s) | 160°C                                     |  |
| Test dose             | Reader 1: 2.2 Gy<br>Reader 2: 0.64 Gy     |  |
| Measurement           | 20 s at 125°C                             | 60 s at room temperature                                       |
| Used integral         | 0.0 - 0.4 s                               | 0 - 15 s   |
| Background interval   | 16 - 20 s                                 | 55 - 60 s  |

TABLE 4.2.3. USED MEASUREMENT-PARAMETERS FOR OSL AND IRSL

##### 4.2.4.3. Dose rate determination

The dose rate ( $\dot{D}$ ) is the energy that accumulates in a mineral and thus creates the luminescence signal. The dose rate is composed of the natural radioactivity ( $\alpha$ -,  $\beta$ -,  $\gamma$ -radiation) and the cosmic radiation affecting the sample. Since the outer rims of coarse grains are etched away using HF,  $\alpha$ -radiation influences only the fine-grain material. Thus, for fine grains, the  $a$ -value giving the effectivity of  $\alpha$ - compared to  $\beta$ -radiation must be determined.

We determined natural radioactivity by measuring the concentration of the radioactive elements U, Th and K using dry, ground material. U and Th contents were calculated using thick source  $\alpha$ -counting (42 mm) at the University of Bayreuth. Potassium concentrations were measured at the Bayreuth Center for Ecology and Environmental Research (BayCEER), Bayreuth/Germany using inductively coupled plasma source mass spectrometry (ICPMS), and at the University of Marburg/Germany using an atomic adsorption spectrometer (AAS). Dose rates were calculated using the conversion factors given by Adamiec and Aitken (1998). Cosmic dose rates were evaluated according to Prescott and Hutton (1994). All dose rates are listed in table 4.2.4.

##### 4.2.4.4. Water content

For every sample the water content was measured gravimetrically. Since the outcrops have been open for many years and the sediments have been desiccated, measured values are obviously underestimations compared to the palaeovalues as already stated by Zöllner et al. (2003). Thus, using the grain size distribution of a sample and the resulting middle pore volume, we estimated potential minimal and maximal water contents of a sample as described by Fuchs (2001). For age calculation, an average value was taken. The error is assumed to be generally 0.1. Measured and corrected water contents are given in table 4.2.4.

#### 4. Results: 4.2. Dating Saharan dust deposits on Lanzarote (Canary Islands) by luminescence...

| Sample depth (cm) | Sample             | $\alpha$ -count rate (cpm) | U-content (ppm) | Th-content (ppm) | K-content (%)<br><sup>1</sup> from ICPMS<br><sup>2</sup> from AAS | $\beta$ -dose rate* | $\gamma$ -dose rate* | cosm. dose rate | Measured water content | Corrected water content |
|-------------------|--------------------|----------------------------|-----------------|------------------|---|---------------------|----------------------|-----------------|------------------------|-------------------------|
| <b>Femés</b>      |                    |                            |                 |                  |   |                     |                      |                 |                        |                         |
| 60                | BT 310, (BN-D 207) | 0.58*                      | -               | -                | -   | 2.58 ± 0.13         | 1.12 ± 0.06          | 0.21 ± 0.011    | 1.1*                   | 1.19                    |
| 80                | BT 311             | 0.48 ± 0.012               | 2.34 ± 0.058    | 8.00 ± 0.20      | 2.45 ± 0.07 <sup>2</sup>  | -                   | -                    | 0.21 ± 0.010    | 1.13                   | 1.24                    |
| 100               | BT 189             | 0.46 ± 0.009               | 2.25 ± 0.044    | 7.70 ± 0.15      | 3.19 ± 0.10 <sup>1</sup>  | -                   | -                    | 0.20 ± 0.010    | 1.13                   | 1.24                    |
| 120               | BT 312             | 0.36 ± 0.008               | 1.75 ± 0.039    | 6.01 ± 0.13      | 3.32 ± 0.10 <sup>2</sup>  | -                   | -                    | 0.20 ± 0.010    | 1.13                   | 1.24                    |
| 140               | BT 313             | 0.43 ± 0.006               | 2.09 ± 0.029    | 7.16 ± 0.10      | 2.12 ± 0.06 <sup>2</sup>  | -                   | -                    | 0.20 ± 0.010    | 1.14                   | 1.22                    |
| 170               | BT 190, (BN-D 209) | 0.47*                      | -               | -                | -   | 3.25 ± 0.05         | 1.08 ± 0.05          | 0.19 ± 0.010    | 1.19*                  | 1.25                    |
| 190               | BT 314             | 0.40 ± 0.008               | 1.96 ± 0.040    | 6.71 ± 0.14      | 1.91 ± 0.06 <sup>2</sup>  | -                   | -                    | 0.19 ± 0.010    | 1.17                   | 1.26                    |
| 210               | BT 315             | 0.44 ± 0.001               | 2.12 ± 0.004    | 7.25 ± 0.02      | 2.61 ± 0.08 <sup>2</sup>  | -                   | -                    | 0.19 ± 0.009    | 1.20                   | 1.27                    |
| 225               | BT 316             | 0.39 ± 0.010               | 1.87 ± 0.047    | 6.39 ± 0.16      | 2.66 ± 0.08 <sup>2</sup>  | -                   | -                    | 0.19 ± 0.009    | 1.20                   | 1.28                    |
| 245               | BT 317             | 0.41 ± 0.010               | 2.01 ± 0.047    | 6.87 ± 0.16      | 2.99 ± 0.09 <sup>2</sup>  | -                   | -                    | 0.18 ± 0.009    | 1.19                   | 1.30                    |
| 270               | BT 224             | 0.44 ± 0.008               | 2.13 ± 0.039    | 7.28 ± 0.13      | 2.89 ± 0.09 <sup>1</sup>  | -                   | -                    | 0.18 ± 0.009    | 1.18                   | 1.24                    |
| 290               | BT 318             | 0.30 ± 0.008               | 1.46 ± 0.039    | 5.01 ± 0.13      | 1.78 ± 0.05 <sup>2</sup>  | -                   | -                    | 0.18 ± 0.009    | 1.11                   | 1.24                    |
| 310               | BT 319             | 0.30 ± 0.006               | 1.46 ± 0.027    | 5.01 ± 0.09      | 2.07 ± 0.06 <sup>2</sup>  | -                   | -                    | 0.18 ± 0.009    | 1.11                   | 1.23                    |
| 330               | BT 301             | 0.44 ± 0.009               | 2.12 ± 0.044    | 7.27 ± 0.15      | 2.24 ± 0.07 <sup>2</sup>  | -                   | -                    | 0.17 ± 0.009    | 1.14                   | 1.25                    |
| 350               | BT 302             | 0.43 ± 0.010               | 2.09 ± 0.048    | 7.16 ± 0.17      | 1.70 ± 0.05 <sup>2</sup>  | -                   | -                    | 0.17 ± 0.009    | 1.18                   | 1.28                    |
| 380 (400*)        | BN-D 211           | 0.45*                      | -               | -                | -   | 3.27 ± 0.05         | 1.09 ± 0.06          | 0.17 ± 0.008    | 1.15*                  | 1.27                    |
| 460               | BT 191             | 0.47 ± 0.010               | 2.28 ± 0.050    | 7.16 ± 0.17      | 3.39 ± 0.10 <sup>1</sup>  | -                   | -                    | 0.16 ± 0.008    | 1.12                   | 1.26                    |
| 480               | BT 303             | 0.44 ± 0.007               | 2.11 ± 0.034    | 7.23 ± 0.12      | 2.83 ± 0.08 <sup>1</sup>  | -                   | -                    | 0.15 ± 0.008    | 1.17                   | 1.28                    |
| 630 (670*)        | BN-D 213           | 0.45*                      | -               | -                | -   | 3.12 ± 0.16         | 0.99 ± 0.05          | 0.14 ± 0.007    | 1.30*                  | 1.3                     |
| <b>Teguise</b>    |                    |                            |                 |                  |   |                     |                      |                 |                        |                         |
| 80                | BT 306             | 0.52 ± 0.018               | 2.5 ± 0.087     | 8.57 ± 0.30      | 2.53 ± 0.08 <sup>2</sup>  | -                   | -                    | 0.21 ± 0.010    | 1.05                   | 1.16                    |
| 90                | BT 198             | 0.65 ± 0.013               | 3.12 ± 0.061    | 10.70 ± 0.21     | 2.49 ± 0.07 <sup>1</sup>  | -                   | -                    | 0.21 ± 0.010    | 1.04                   | 1.16                    |
| 110               | BT 235             | 0.52 ± 0.010               | 2.51 ± 0.048    | 8.60 ± 0.17      | 2.86 ± 0.09 <sup>2</sup>  | -                   | -                    | 0.20 ± 0.010    | 1.09                   | 1.27                    |
| 135               | BT 307             | 0.44 ± 0.016               | 2.11 ± 0.078    | 7.22 ± 0.27      | 3.19 ± 0.10 <sup>2</sup>  | -                   | -                    | 0.20 ± 0.010    | 1.19                   | 1.28                    |
| 160               | BT 199             | 0.46 ± 0.007               | 2.21 ± 0.033    | 7.57 ± 0.11      | 3.69 ± 0.11 <sup>1</sup>  | -                   | -                    | 0.20 ± 0.010    | 1.13                   | 1.31                    |
| 185               | BT 308             | 0.32 ± 0.006               | 1.56 ± 0.030    | 5.35 ± 0.10      | 2.24 ± 0.07 <sup>2</sup>  | -                   | -                    | 0.19 ± 0.010    | 1.14                   | 1.26                    |
| 210               | BT 309             | 0.39 ± 0.008               | 1.86 ± 0.039    | 6.38 ± 0.13      | 2.32 ± 0.07 <sup>2</sup>  | -                   | -                    | 0.19 ± 0.009    | 1.17                   | 1.24                    |

#### 4. Results: 4.2. Dating Saharan dust deposits on Lanzarote (Canary Islands) by luminescence...

|                    |             |                 |                 |             |                          |                |                |                 |      |      |
|--------------------|-------------|-----------------|-----------------|-------------|--------------------------|----------------|----------------|-----------------|------|------|
| 250                | BT 200      | 0.56 ±<br>0.010 | 2.69 ±<br>0.048 | 9.21 ± 0.17 | 2.90 ± 0.09 <sup>1</sup> | -              | -              | 0.18 ±<br>0.009 | 1.1  | 1.26 |
| 330                | BT 236      | 0.40 ±<br>0.007 | 1.92 ±<br>0.034 | 6.57 ± 0.12 | 4.08 ± 0.12 <sup>1</sup> | -              | -              | 0.17 ±<br>0.009 | 1.14 | 1.26 |
| 450                | BT 201      | 0.42 ±<br>0.009 | 2.05 ±<br>0.044 | 7.03 ± 0.15 | 3.73 ± 0.11 <sup>1</sup> | -              | -              | 0.16 ±<br>0.008 | 1.18 | 1.26 |
| 610                | BT 202      | 0.43 ±<br>0.007 | 2.10 ±<br>0.034 | 7.19 ± 0.12 | 2.93 ± 0.09 <sup>1</sup> | -              | -              | 0.14 ±<br>0.007 | 1.09 | 1.27 |
| <i>Guatiza III</i> |             |                 |                 |             |                          |                |                |                 |      |      |
| 110                | BT 193      | 0.39 ±<br>0.008 | 1.88 ±<br>0.039 | 6.44 ± 0.13 | 2.89 ± 0.09 <sup>1</sup> | -              | -              | 0.2 ±<br>0.010  | 1.09 | 1.24 |
| 250                | BT 194      | 0.40 ±<br>0.009 | 1.96 ±<br>0.044 | 6.71 ± 0.15 | 2.53 ± 0.08 <sup>1</sup> | -              | -              | 0.18 ±<br>0.009 | 1.10 | 1.26 |
| 435                | BT 195      | 0.51 ±<br>0.009 | 2.49 ±<br>0.044 | 8.53 ± 0.15 | 3.96 ± 0.12 <sup>1</sup> | -              | -              | 0.16 ±<br>0.008 | 1.07 | 1.21 |
| 470                | BT 233      | 0.43 ±<br>0.006 | 2.06 ±<br>0.029 | 7.05 ± 0.10 | 2.51 ± 0.08 <sup>1</sup> | -              | -              | 0.15 ±<br>0.008 | 1.11 | 1.25 |
| 495                | BT 196      | 0.48 ±<br>0.009 | 2.35 ±<br>0.044 | 8.03 ± 0.15 | 2.73 ± 0.08 <sup>1</sup> | -              | -              | 0.15 ±<br>0.008 | 1.08 | 1.25 |
| 550                | BT 234      | 0.44 ±<br>0.006 | 2.11 ±<br>0.029 | 7.22 ± 0.10 | 3.22 ± 0.10 <sup>1</sup> | -              | -              | 0.15 ±<br>0.008 | 1.14 | 1.26 |
| 610                | BT 304      | 0.39 ±<br>0.011 | 1.90 ±<br>0.053 | 6.51 ± 0.18 | 4.02 ± 0.12 <sup>2</sup> | -              | -              | 0.14 ±<br>0.007 | 1.13 | 1.28 |
| 660                | BT 197      | 0.53 ±<br>0.009 | 2.58 ±<br>0.044 | 8.84 ± 0.15 | 2.99 ± 0.09 <sup>1</sup> | -              | -              | 0.14 ±<br>0.007 | 1.09 | 1.22 |
| 700                | BT 305      | 0.50 ±<br>0.013 | 2.43 ±<br>0.063 | 8.32 ± 0.22 | 3.86 ± 0.12 <sup>2</sup> | -              | -              | 0.13 ±<br>0.007 | 1.11 | 1.23 |
| <i>Guatiza I</i>   |             |                 |                 |             |                          |                |                |                 |      |      |
| 210                | BN-D<br>219 | 0.46*           | -               | -           | -                        | 2.58 ±<br>0.04 | 0.85 ±<br>0.04 | 0.18 ±<br>0.009 | 1.20 | -    |
| <i>Tahiche</i>     |             |                 |                 |             |                          |                |                |                 |      |      |
| recent             | BT 204      | 0.42 ±<br>0.009 | 2.04 ±<br>0.043 | 6.98 ± 0.15 | 2.00 ± 0.06 <sup>1</sup> | -              | -              | 0.21 ±<br>0.011 | 1.10 | -    |

TABLE 4.2.4. LUMINESCENCE DATING: ANALYTICAL RESULTS

Dose rates ( $\dot{D}$ ) are given in Gy/ka. U- and Th-contents were calculated from the  $\alpha$ -count rate. Measured water contents present the ratio moist/dry weight, the correction was done using the clay contents of the samples. The error of water contents is assumed to be 0.1.

\* data taken from Zöller et al. (2003)

##### 4.2.4.5. Age calculation

Suchodoletz et al. (2009a) demonstrate that most of the sediments filling the vegas are reworked and deposited by colluvial and fluvial processes. These processes are problematic for luminescence dating because they are occurring rather rapidly, and often the finer material is transported in the form of aggregates. Hence bleaching of these sediments during colluvial transport was presumably not always complete, thus resulting in overestimated De values as detected in other studies (e.g., Porat et al. 2001, Fuchs and Wagner 2003).

For fine grains, insufficient bleaching is not easily detectable since every disc contains thousands of grains giving a luminescence signal so that De differences between the discs are averaged. Instead, for coarse grains single aliquot and single grain methods offer the possibility to detect and correct

insufficient bleaching by looking at their De scatter and the type of De distribution (Gaussian, left-skewed, right-skewed) (e.g., Olley et al. 1998, Lepper et al. 2000, Bailey and Arnold 2006, Fuchs and Wagner 2003). Since most of our De distributions are positively skewed which may indicate insufficient bleaching, we had to find a way to obtain the De corresponding to the last reworking of the sediments. Different techniques were developed on the basis of the assumption that the last bleaching event is equivalent to the left maximum of a right skewed De distribution. However, some of these techniques are not applicable to our De distributions for different reasons: the approach of Olley et al. (1998) taking the lowest 5% of the De distribution is not applicable owing to a relatively broad rising limb of the De distribution resulting in greatly underestimated De. Accordingly, this method is generally judged to be useful only in case of young, poorly bleached fluvial samples (Bailey and Arnold 2006). The leading edge method developed by Lepper et al. (2000) was inapplicable since the quantity of measured aliquots was not sufficient to get a good Gaussian fit through the rising limb of our distributions (cf. Fuchs et al. 2007). The method of Fuchs and Lang (2001), using an empirically derived threshold to identify the well bleached proportion of an insufficiently bleached sample is also not applicable in our case. This is due to the fact that for many samples the threshold was already exceeded using the first two De from the sorted low to high De value data set. Thus we decided to use the approach of Juyal et al. (2006), modified by Fuchs et al. (2007). Basically, this is a simplified minimum age model of Galbraith et al. (1999).

$$De = De_{\min} + 2 * \sigma_{\max} + 4\%$$

where  $De_{\min}$  is the minimal equivalent dose after subtraction of the lower 5% quantil (see below),  $\sigma_{\max}$  is the maximal error occurring in the data from the lower end to the first maximum of the De histogram and 4% are added as general instrumentation error of the used Risø reader.

A common problem is the mixing of younger material dropped through pedogenic cracks or root channels as described by Bateman et al. (2003). We have observed this process in the vega of Guatiza. This phenomenon would cause an underestimation of the De and is visible as individual outliers not linked to the form of the De distribution toward lower values in many histograms (figure 4.2.3.). To neutralize this frequently occurring effect, we decided to subtract the lower 5% quantil of the sorted De distribution from all samples prior to statistical calculations. Depending on the number of measured aliquots, one to two De had to be rejected.

For fine grains, insufficient bleaching is hardly detectable. Thus the arithmetic mean of obtained De from the measurements was taken for age calculation. IRSL ages by Zöller et al. (2003) were recalculated using corrected water contents (see above) and new cosmic dose rates.

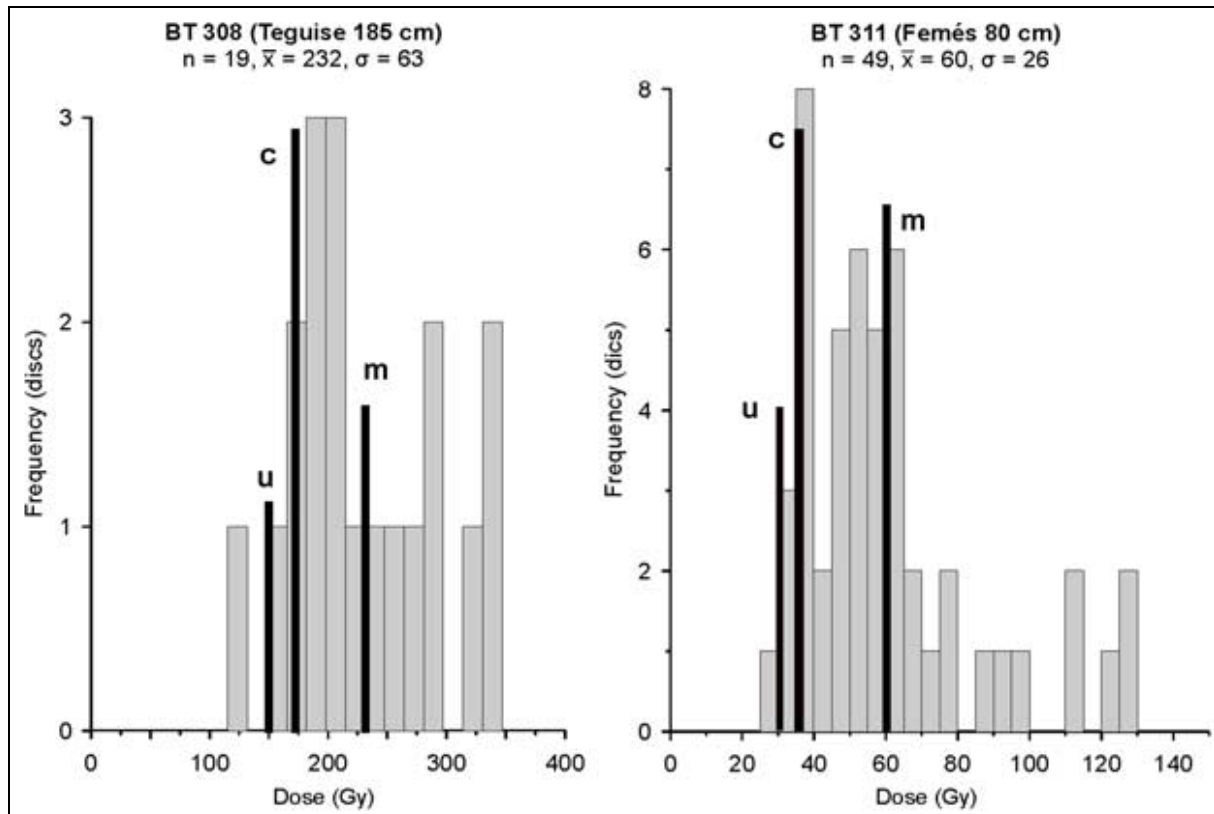


FIGURE 4.2.3. SELECTED *De*-HISTOGRAMS OF RATHER POORLY BLEACHED COARSE-GRAIN OSL-SAMPLES FROM TEGUIŠE AND FEMÉS.

Note the younger outlier in sample BT 308. In black are indicated calculated *De*'s after Juyal *et al.* (2006) and arithmetic means: *u*, uncorrected values; *c*, corrected values after removal of the upper 5% quantil; *m*, arithmetic mean.

#### 4.2.5. Results

##### 4.2.5.1. Dose rates

Results of dose rate ( $\dot{D}$ ) determinations are given in table 4.2.4. with their  $1\sigma$ -errors.

Uranium contents calculated from thicksources  $\alpha$ -counting range from 1.46 to 3.1 ppm and thorium values from 5.0 to 10.7 ppm. Potassium contents determined either by AAS or ICPMS range from 1.7 to 4.1%. Rather low dose rate values generally occur in calcareous horizons (e.g., BT 318, BT 319, BT 308). The occurrence of radioactive disequilibria in calcareous horizons cannot be excluded. However, the U-content of calcite presents only a very small proportion compared to the total U-content, so that disequilibria in the U-decay chain are not expected to have a significant influence on the total dose rate. Furthermore, Schäfer and Zöller (1996) demonstrated from a Middle Palaeolithic site in Thuringia/Germany showing significant disequilibria detected by low level  $\gamma$ -spectrometry, that using dose rates from U and Th based on  $\alpha$ -counting is a good approach if radioactive disequilibrium has regenerated more or less permanently since deposition. Carbonate precipitation posterior to deposition may dilute concentrations of radioelements and thus lower the dose rate. However, carbonate-free layers deposited over carbonate-rich beds indicate that secondary calcification was more or less

contemporaneous to sedimentation. The consequences of this effect should not have played a major role although a slight underestimation of dose rates due to this effect cannot be excluded.

#### *4.2.5.2. Equivalent doses*

Equivalent doses of quartz OSL and feldspar IRSL measurements are listed in table 4.2.5. with their  $1\sigma$ -errors. Due to their own characteristics and accuracies, the applied luminescence methods (coarse and fine grain OSL, fine grain IRSL) are discussed separately.

#### *Quartz coarse grain OSL measurements*

The potential for total bleaching of the investigated sediments was tested by exposure of the prepared coarse-grain quartz extracts to 10 hours of natural daylight (Bayreuth/Germany,  $\sim 50^\circ\text{N}$ , November 2005) with a subsequent OSL measurement. This test was carried out for samples BT 190, BT 195 and BT 196 which showed no OSL signal after daylight exposure. Furthermore, a dose recovery test was carried out using the same samples as for the bleaching test. After the bleaching of the samples they were given  $\beta$ -radiations of 4.28 Gy (sample BT 195), 17.13 Gy (sample BT 196) and 38.55 Gy (sample BT 190). Subsequently, the OSL measurements for  $D_e$  determination were performed with preheat temperatures of  $220^\circ$ ,  $240^\circ$ ,  $260^\circ$  and  $280^\circ\text{C}$ , with four aliquots for each temperature. In figure 4.2.4. the results of these measurements can be seen, with a  $D_e$  plateau between  $220^\circ$  and  $280^\circ\text{C}$  within error bars. Thus, in spite of a slight overestimation of given doses, for all further  $D_e$  measurements a preheat temperature of  $240^\circ\text{C}$  was applied.

All quartz samples show typical exponential saturating growth. From the growth curves it can be seen that saturation, on average, is reached around 350 Gy but can also be somewhat higher for several samples. Thus highest  $D_e$  estimations above 300 Gy have to be treated with caution.

Measured aliquots were excluded from further analysis when test dose error, palaeodose error, or recycling ratio error were  $>10\%$ . The same applies to aliquots giving a signal less than three times the standard deviation of the background. This was true for about 7% of the measured aliquots.

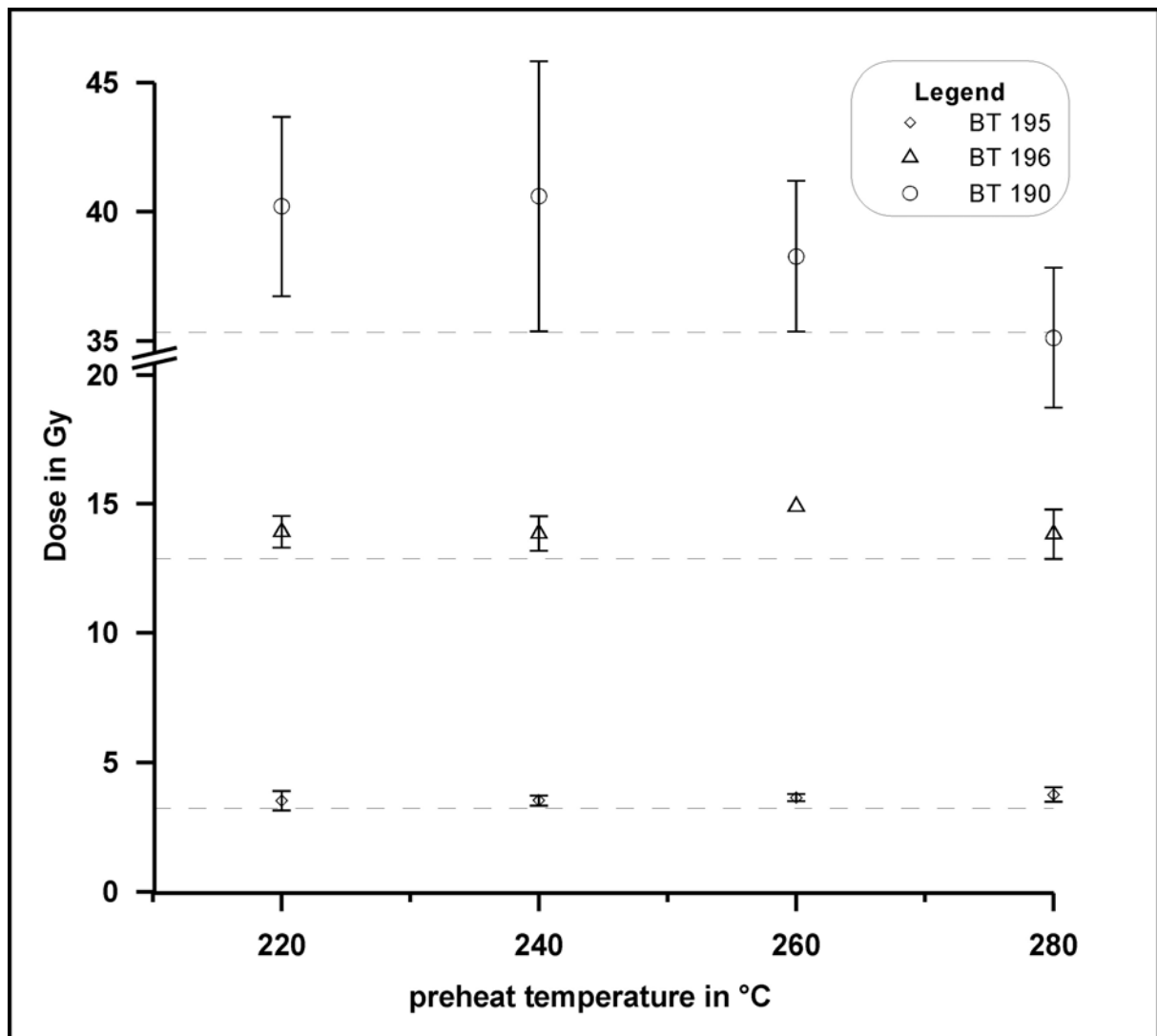


FIGURE 4.2.4. RESULTS OF THE DOSE RECOVERY TEST OF COARSE GRAIN SAMPLES MEASURED WITH OSL, SHOWN WITH ERROR BARS ( $2\sigma$ ). Every data point is the average of 4 single measurements. Dashed lines below a graph indicate the given palaeodose. Mean ratios given/measured dose were: 220°C, 1.08; 440°C, 1.09; 260°C, 1.1; 280°C, 1.07.

#### Quartz fine grain OSL measurements

Fine-grain OSL  $D_e$  range from 5.6 to 211 Gy. The frequency distribution of the measured aliquots per sample yielded a standard deviation between 2 to 12%. About 3% of the measured aliquots had to be removed owing to the exclusion criteria defined above. All growth curves show an exponential behaviour, with saturation attained around 350 Gy (highest calculated  $D_e$  = 211 Gy). Typical measurements of  $a$ -values range between 0.03 and 0.05. Consequently, a mean value of 0.04 was used for calculations.

#### IRSL fine grain measurements

As can be seen from the IRSL growth curves, saturation of the investigated feldspars is attained around 1800-2000 Gy. Hence all investigated samples (highest  $D_e$  ~700 Gy) are within the datable dose range. IRSL growth curves from Lower to Middle Holocene samples show an almost linear

#### 4. Results: 4.2. Dating Saharan dust deposits on Lanzarote (Canary Islands) by luminescence...

behaviour, whereas the older ones are clearly saturating exponential. Fitting error of the growth curves was between 0.3 and 3.5%, giving lower values for higher doses. As already stated by Pomel et al. (1985), measured a-values are very low with values between 0.029 and 0.063, being in general higher in Teguisse (average 0.06) than in Femés (average 0.04) and Guatiza (average 0.05). Owing to long a-irradiation times only some representative a-values were determined, whereas for the missing values the mean for every profile was taken. Almost half of the samples show significant anomalous fading up to 40%.

| Sample depth (cm) | Code              | IRSL-De     | a-value IRSL  | IRSL age     | Anomalous Fading | Fine-grain quartz OSL-De | a-value fine grain quartz OSL | Fine-grain quartz OSL age | Coarse-grain quartz OSL-De | Coarse-grain quartz OSL age |
|-------------------|-------------------|-------------|---------------|--------------|------------------|--------------------------|-------------------------------|---------------------------|----------------------------|-----------------------------|
| <b>Femés</b>      |                   |             |               |              |                  |                          |                               |                           |                            |                             |
| 60                | BT 310 (BN-D 207) | 18.3 ± 4.7* | 0.04 ± 0.001* | 4.9 ± 1.3    | yes*             | -                        | -                             | -                         | 20.5 ± 1.5                 | 6.4 ± 0.7                   |
| 80                | BT 311            | -           | -             | -            | -                | -                        | -                             | -                         | 38.0 ± 3.4                 | 12.4 ± 1.6                  |
| 100               | BT 189            | 65.5 ± 0.8  | 0.04 ± 0.002  | 16.7 ± 1.5   | yes              | 65.3 ± 4.9               | 0.03 ± 0.01                   | 16.8 ± 1.9                | 47.9 ± 3.7                 | 13.6 ± 1.6                  |
| 120               | BT 312            | -           | -             | -            | -                | -                        | -                             | -                         | 122 ± 11.9                 | 35.4 ± 4.7                  |
| 140               | BT 313            | -           | -             | -            | -                | -                        | -                             | -                         | 150 ± 10.8                 | 56.0 ± 6.5                  |
| 170               | BT 190 (BN-D 209) | 166 ± 12*   | 0.04 ± 0.002* | 41.0 ± 3.8   | no*              | -                        | -                             | -                         | 165 ± 31.4                 | 45.9 ± 9.7                  |
| 190               | BT 314            | -           | -             | -            | -                | -                        | -                             | -                         | 194 ± 22.6                 | 55.9 ± 8.2                  |
| 210               | BT 315            | -           | -             | -            | -                | -                        | -                             | -                         | 164 ± 22.8                 | 47.7 ± 7.8                  |
| 225               | BT 316            | -           | -             | -            | -                | -                        | -                             | -                         | 204 ± 25.1                 | 54.8 ± 7.2                  |
| 245               | BT 317            | -           | -             | -            | -                | -                        | -                             | -                         | 193 ± 17.4                 | 57.6 ± 7.2                  |
| 270               | BT 224            | 328 ± 2     | 0.04 ± 0.002  | 91.2 ± 8.1   | no               | -                        | -                             | -                         | 208 ± 16.6                 | 64.8 ± 7.8                  |
| 290               | BT 318            | -           | -             | -            | -                | -                        | -                             | -                         | 213 ± 49.2                 | 101.0 ± 24.9                |
| 310               | BT 319            | -           | -             | -            | -                | -                        | -                             | -                         | 219 ± 65.7                 | 93.3 ± 29.2                 |
| 330               | BT 301            | -           | -             | -            | -                | -                        | -                             | -                         | 237 ± 21.0                 | 88.3 ± 11.1                 |
| 350               | BT 302            | -           | -             | -            | -                | -                        | -                             | -                         | 275 ± 46.8                 | 125.0 ± 23.8                |
| 380 (400*)        | BN-D 211          | 419 ± 46*   | 0.04 ± 0.002* | 106 ± 15     | no*              | -                        | -                             | -                         | -                          | -                           |
| 460               | BT 191            | 568 ± 3     | 0.04 ± 0.002  | 144 ± 13     | no               | -                        | -                             | -                         | -                          | -                           |
| 480               | BT 303            | 529 ± 3     | 0.04 ± 0.002  | 156.3 ± 13.8 | no               | -                        | -                             | -                         | -                          | -                           |
| 630 (670*)        | BN-D 213          | 709 ± 79*   | 0.03 ± 0.009* | 207 ± 27     | no*              | -                        | -                             | -                         | -                          | -                           |
| <b>Teguisse</b>   |                   |             |               |              |                  |                          |                               |                           |                            |                             |
| 80                | BT 306            | -           | -             | -            | -                | -                        | -                             | -                         | 18.1 ± 0.5                 | 5.4 ± 0.6                   |
| 90                | BT 198            | 36.2 ± 0.4  | 0.06 ± 0.001  | 8.3 ± 0.8    | no               | 35.3 ± 1.5               | 0.05 ± 0.013                  | 8.5 ± 0.9                 | 25.7 ± 0.9                 | 7.2 ± 0.8                   |
| 110               | BT 235            | -           | -             | -            | -                | -                        | -                             | -                         | 72.1 ± 4.3                 | 22.0 ± 2.3                  |
| 135               | BT 307            | -           | -             | -            | -                | -                        | -                             | -                         | 103 ± 6.1                  | 30.7 ± 3.2                  |
| 160               | BT 199            | 287 ± 3     | 0.06 ± 0.0004 | 68 ± 6.2     | yes              | -                        | -                             | -                         | 163 ± 11.5                 | 44.4 ± 4.9                  |
| 185               | BT 308            | -           | -             | -            | -                | -                        | -                             | -                         | 172 ± 15.9                 | 69.4 ± 6.0                  |
| 210               | BT 309            | -           | -             | -            | -                | -                        | -                             | -                         | 327 ± 47.8                 | 121.6 ± 10.8                |
| 250               | BT 200            | 485 ± 1.4   | 0.06 ± 0.0003 | 121.3 ± 11   | yes              | -                        | -                             | -                         | 386 ± 67                   | 114.3 ± 22.3                |

#### 4. Results: 4.2. Dating Saharan dust deposits on Lanzarote (Canary Islands) by luminescence...

|                       |        |             |                      |              |     |           |                     |            |             |             |
|-----------------------|--------|-------------|----------------------|--------------|-----|-----------|---------------------|------------|-------------|-------------|
| 330                   | BT 236 | 583 ± 2     | <i>0.06 ± 0.0005</i> | 129.3 ± 11.5 | no  | -         | -                   | -          | -           | -           |
| 450                   | BT 201 | 592 ± 2     | <i>0.06 ± 0.0005</i> | 138.0 ± 12.3 | yes | -         | -                   | -          | -           | -           |
| 610                   | BT 202 | 688 ± 3     | <i>0.06 ± 0.0005</i> | 189.1 ± 16.7 | no  | -         | -                   | -          | -           | -           |
| <b>Guatiza III</b>    |        |             |                      |              |     |           |                     |            |             |             |
| 110                   | BT 193 | 8.7 ± 0.2   | 0.05 ± 0.001         | 2.4 ± 0.2    | no  | 8.2 ± 0.8 | <i>0.04 ± 0.007</i> | 2.3 ± 0.3  | 1.77 ± 0.2  | 0.54 ± 0.07 |
| 250                   | BT 194 | -           | -                    | -            | -   | 5.6 ± 0.2 | <i>0.04 ± 0.007</i> | 1.8 ± 0.2  | -           | -           |
| 435                   | BT 195 | 16.5 ± 0.5  | 0.06 ± 0.003         | 3.4 ± 0.3    | no  | -         | -                   | -          | 11.6 ± 0.5  | 2.7 ± 0.3   |
| 470                   | BT 233 | 42.0 ± 0.4  | 0.04 ± 0.0004        | 13.0 ± 1.1   | no  | 43.9 ± 2  | 0.04 ± 0.005        | 13.6 ± 1.3 | 36.7 ± 2.9  | 12.9 ± 1.5  |
| 495                   | BT 196 | 113 ± 2     | 0.03 ± 0.001         | 32.4 ± 2.9   | no  | 109 ± 2   | 0.04 ± 0.002        | 30.1 ± 2.7 | 99.4 ± 14.1 | 31.9 ± 5.4  |
| 550                   | BT 234 | 99.7 ± 0.8  | <i>0.05 ± 0.001</i>  | 26.1 ± 2.3   | yes | -         | -                   | -          | 168 ± 9.1   | 49.7 ± 5.2  |
| 610                   | BT 304 | 138 ± 0.7   | <i>0.05 ± 0.001</i>  | 32.3 ± 2.9   | no  | 174 ± 9.5 | 0.04 ± 0.004        | 41.0 ± 4.3 | -           | -           |
| 660                   | BT 197 | 153 ± 2.5   | 0.05 ± 0.001         | 37.7 ± 3.4   | yes | -         | -                   | -          | 115 ± 19.9  | 33.0 ± 6.5  |
| 700                   | BT 305 | 258 ± 2.4   | <i>0.05 ± 0.001</i>  | 55.9 ± 5.0   | no  | 211 ± 25  | 0.04 ± 0.007        | 46.2 ± 6.6 | -           | -           |
| <b>Guatiza I</b>      |        |             |                      |              |     |           |                     |            |             |             |
| 210                   | BT     | 15.7 ± 1.3* | 0.08 ± 0.025*        | 4.3 ± 0.5    | yes | -         | -                   | -          | 3.5 ± 0.2   | 1.2 ± 0.1   |
| <b>Tahiche recent</b> |        |             |                      |              |     |           |                     |            |             |             |
|                       | BT 204 | 7.3 ± 0.3   | 0.05 ± 0.001         | 2.2 ± 0.2    | no  | 6.3 ± 0.6 | <i>0.04 ± 0.007</i> | 2.1 ± 0.3  | 3.5 ± 1     | 1.2 ± 0.4   |

TABLE 4.2.5. LUMINESCENCE DATING: EQUIVALENT DOSES AND AGES

*De's are given in Gy. Coarse grain OSL-De's were calculated after Juyal et al. (2006). All ages are given in ka. Measured a-values are given in standard, assumed a-values in italic letters.*

\* data taken from Zöllner et al. (2003)

#### 4.2.6. Discussion

##### 4.2.6.1. Reliability of different luminescence methods

###### Coarse grain OSL ages

Most of our coarse-grain single aliquot histograms are right skewed (mean skewness 1.24), indicating insufficient bleaching during colluvial transport. Several outliers toward lower doses were also observed (figure 4.2.3.).

Owing to the strong scatter of the equivalent doses, age errors are between 9 and 31%. The occurrence of colluvial reworking during most periods was also proven by micromorphological studies (Sauer and Zöllner 2006). This occurs in all vegas, however the histogram asymmetry is generally lower in Teguisse compared to Femés and Guatiza III. This is explained by the lower catchment area-valley bottom ratio, which means a lower proportion of (insufficiently bleached) colluvial material originating from the slopes relative to in situ aeolian dust is found in the vega bottom sediments (Suchodoletz et al. 2009a). Correspondingly, lowest errors were observed in the vega of Teguisse. Using the approach of Juyal et

al. (2006), most  $D_e$  values are now situated at the upper rising left limb of our distribution (figure 4.2.3.). Here we believe that the equivalent doses corresponding to the last bleaching event should be located. The general omission of the lower 5% of measured aliquots from all samples strongly improved our  $D_e$  calculation in samples exhibiting outliers toward the lower end of the distribution, and thus  $D_e$ 's of most of these samples fall at the upper rising limb of our histograms as well. In cases without outliers, owing to the broad rising limb, the resulting shift toward higher  $D_e$ 's is very small. Thus this method appears to be a justified approach for  $D_e$  determination.

For two samples, however, this approach seems to fail: Sample BT 200 shows an exceptional  $D_e$  histogram with a left skewed distribution (figure 4.2.5.a). Since the  $D_e$  of this sample is close to saturation level it is very likely that the aliquots normally forming the right (older) tail of the distribution were already in saturation and thus are not present in the histogram. Additionally, the number of aliquots is strongly limited so that a rising limb is not well developed. The arithmetic mean  $D_e$  of this sample gives a value at the rising limb close to the first maximum of the distribution (figure 4.2.5a). However, owing to the non-Gaussian form of the distribution this arithmetic mean can only be a rough estimation. Caused by the limited amount of aliquots, the calculated  $D_e$  of sample BT 197 may be underestimated and should be regarded as a minimum age (figure 4.2.5.b).

Luminescence tests investigating insufficient bleaching (due to iron stains around the grains) during aeolian transport were carried out with recent Saharan dust from the Canary Islands (Suchodoletz et al., submitted). They show that for coarse grains inherited doses with respect to dose rates from Lanzarote are in the range of only 0.1-0.2 ka and are thus negligible. A sample from colluvial material overlying a historic lava flow dating from 1736 AD (sample BT 204) yields an apparent coarse-grain OSL age of about 1.2 ka, thus indicating an overestimation  $<1$  ka. These tests show that coarse-grain OSL basically offers the required conditions for dating Lower Holocene or older fluvio-aeolian sediments. The problem of a slight overestimation of given doses during the preheat tests (see figure 4.2.4.) must be seen against the background of generally relatively large errors of coarse-grain OSL ages: owing to the uncertainty caused by insufficient bleaching, dating errors are rather large, so that the overestimation effect is smaller than calculated errors. This shows, however, that our luminescence ages are points of reference rather than precise dates.

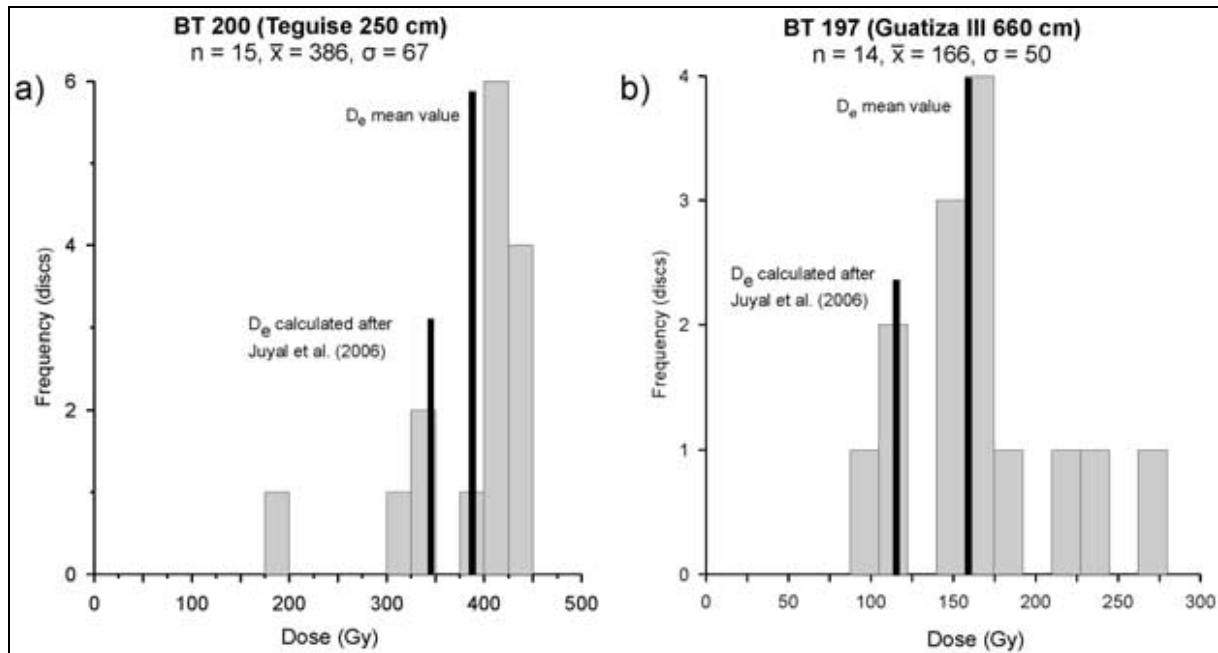


FIGURE 4.2.5. DE-HISTOGRAMS OF SAMPLES (a) BT 200 AND (b) BT 197 WITH DIFFERENT DE.

#### *Fine grain quartz OSL ages*

Comparison of coarse and fine-grain quartz OSL ages reveals that the latter do not show significant age overestimations as could be expected owing to insufficient bleaching. Young Holocene samples show, however, a regular overestimation of about 1 to 3 ka. (samples BT 189, BT 198, BT 310). Overestimation of the same magnitude is found for recent sample BT 204. Thus bleaching of fine grains is not as complete as for coarse-grain OSL. This could be due to their colluvial transport as aggregates. Since quartz OSL does not exhibit anomalous fading (Aitken 1998), fine-grain quartz OSL yielded reasonable ages in a suitable time interval. Additionally, it provides consistent ages for parts of the sedimentary sequence where owing to the lack of fine sand or the occurrence of anomalous fading, neither coarse-grain OSL nor reliable IRSL ages are available. This was the case for samples BT 304 and BT 305.

#### *Fine grain IRSL ages*

Depending on the dose rate, the OSL of quartz from Lanzarote saturates between 100 and 130 ka. Thus, owing to their higher saturation level, only IRSL feldspar ages are available in the lower parts of the profiles. Anomalous fading that was detected during the fading tests for almost half of the samples (see table 4.2.5) is a problem. This could be due to the properties of local volcanic plagioclases as described by Wintle (1973), although no correlation between the fading rate and volcanic input could be found.

Even if anomalous fading was not detected during the test, the so called midterm fading cannot be excluded (Xie and Aitken 1991). For instance, the age of sample BT 304 is underestimated compared to the fine-grain OSL age, even though the former exhibits no anomalous fading during the test. In this

case midterm fading can possibly be the cause. Another possible cause for age uncertainty is insufficient bleaching: since colluvial transport of fine grains takes mostly place as aggregates, they are more vulnerable to insufficient bleaching than coarse grains as shown for fine-grain OSL ages above. A third possibility could be the somewhat slower bleaching of feldspar IRSL compared to quartz OSL (Godfrey-Smith et al. 1988). Furthermore, an effect described by Trautmann et al. (2000) could cause unreliable ages: above ~800 Gy the IRSL-signal of potassium feldspars may be expected not to grow in a single exponential manner during artificial irradiation. Above this threshold, radiofluorescence of K-feldspars already slows down more than expected, indicating the failure of further conduction band-electron trap transition. A further growth of the IRSL signal beyond an absorbed dose of ~800 Gy may thus not directly be connected to electron filling of traps carrying the correct age information. Thus extrapolations using these dose points are problematic. It should be noted, however, that so far Trautmann et al. (2000) stated this effect for K-feldspars only.

In order to check the reliability of IRSL ages suspected of potentially showing much larger age overestimations in comparison to coarse-grain OSL ages, we conducted double measurements of fine grain IRSL and coarse-grain OSL in the younger parts of the profiles. These show that, within error limits, 8 out of 16 double measurements yield IRSL ages in agreement with coarse-grain OSL. Two IRSL ages (samples BT 199 and BT 224) are overestimated by 20-25 ka compared to coarse grain OSL ages. In case of sample BT 199, this strong overestimation occurs despite strong anomalous fading. Although samples BT 189 and BT 200 show signals close to real palaeodoses today, we assume that they originally had an inherited signal during burial since they show substantial anomalous fading that reduced the original signal. In case of sample BT 189 exhibiting similar IRSL  $D_e$  and fine-grain OSL  $D_e$ , an original higher IRSL  $D_e$  compared to the OSL  $D_e$  was possibly caused by the slower bleaching of feldspar compared to quartz (Godfrey-Smith et al. 1988). In total, insufficient bleaching obviously affects almost 30% of the IRSL test samples. Therefore IRSL ages from the lower parts of the profiles that are not corroborated by coarse-grain OSL ages should be considered with caution.

Looking at young Holocene samples, fine grain IRSL ages are regularly overestimated by 0.5 to 3 ka (samples BT 193, BT 195, BT 198) compared to coarse-grain OSL ages. Overestimation of the same magnitude is found for a recent sample (BT 204) taken above a lava flow dating from 1736 AD, as well as for recently investigated present-day dust exhibiting a residual IRSL-dose equivalent to <0.93 ka. For fine-grain OSL ages, overestimation is in the same range as for IRSL ages. This indicates that at least a part of the overestimation is due to a residual dose that existed prior to the arrival of Saharan dust at Lanzarote, possibly caused by aggregation during transport (Suchodoletz et al., submitted). This effect is negligible for older samples, but Middle Holocene IRSL ages like some of those published by Zöllner et al. (2003) should be regarded with care: remeasurement of IRSL sample BN-D 219 from profile Guatiza I giving an IRSL age of  $4.3 \pm 0.5$  ka yielded an age of  $1.2 \pm 0.1$  ka using coarse-grain quartz OSL.

*4.2.6.2. Establishing a chronostratigraphy*

Considering the uncertainties of the applied luminescence methods and the lack of independent dating methods, coarse-grain OSL dating yields the most reliable dates since it offers the only possibility to recognize insufficient bleaching. Thus we regard these ages as the age base of our chronostratigraphical model.

Owing to the uncertainty even when using that method, we have to look for a possibility to correlate proxies yielded from the vegas with those from other studies. The composition of aeolian components of the vega fillings should be similar to that from nearby marine cores. However, owing to the intermixed in situ and colluvial material of the vegas, this can only be recognized at ka timescales (Suchodoletz et al. 2009a).

Kaolinite, a mineral originating from the Southern Sahara/Sahel belt (Caquineau et al. 1998) was found in variable quantities in our archives using semiquantitative XRD measurements. Since aeolian quartz and kaolinite contents exhibit, except for the upper profile in Teguisse, an almost identical pattern (Suchodoletz et al. 2009b), a formation or destruction of kaolinite can mostly be excluded here. A marine study from the Northern Canary Basin about 300 km north of Lanzarote investigated the wind system off NW Africa and interpreted the aluminum content in core GeoB 5559-2 as a tracer of kaolinite that was brought to the study area by southerly winds (Moreno et al. 2001). Likewise, another nearby marine study (Bozzano et al. 2002) interpreted iron contents in core GeoB 4205-2 as derived from the Southern Sahara/Sahel belt (for core locations, see figure 4.2.1.). Both proxies show good agreement with each other (figure 4.2.6.). The marine stratigraphies use the stable oxygen isotopes of fine-fraction carbonate (GeoB 5559-2) and of the planktonic foraminifera *Globigerinoides ruber* (GeoB 4205-2) for correlation with the established marine oxygen isotope stratigraphy of Martinson et al. (1987). Owing to assumed similar wind systems over Lanzarote and the North Canary Basin, our kaolinite contents should exhibit the same pattern as the marine proxies. We therefore correlated marine aluminum and iron concentrations with kaolinite contents of our vega sediments, using the chronology established by the coarse grain OSL ages. From this correlation, a similarity is identifiable between the marine proxies and kaolinite contents from the upper parts of our profiles Femés and Guatiza III, whereas this pattern is biased in Teguisse (figure 4.2.6.). In the latter vega, we found large concretions and ubiquitous coatings of ferromanganese character. These indicate that the biased signal could be due to stronger pedogenic mixing and kaolinite destruction generated by higher humidity and a more intensive iron and manganese dynamics here compared to the other vegas (Hurst and Kunkle 1985).

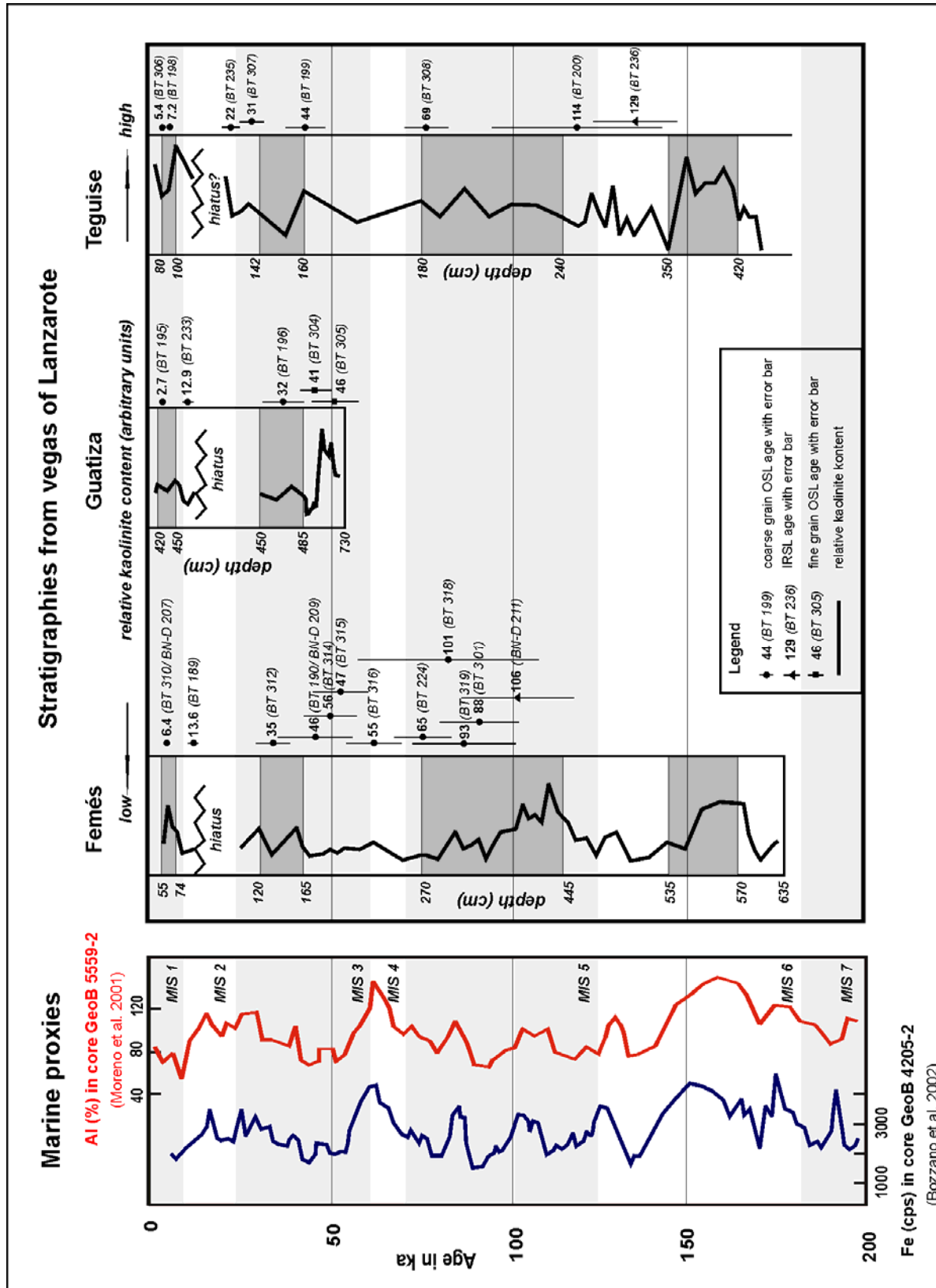


FIGURE 4.2.6. VEGA STRATIGRAPHIES WITH RELATIVE KAOLINITE CONTENTS ADJUSTED TO NUMERICAL CHRONOSTRATIGRAPHY AND TO MARINE AL AND FE CONTENTS.

Luminescence dates giving correct sedimentation ages are shown with their error bars (in kiloannums), whereas the minimum age of sample BT 197 is not presented. Shaded areas in the profiles indicate generally unweathered/less weathered layers visible in the field and used for correlation between the vegas. Horizon depths in centimeters (not in scale) are indicated on the left side of the profiles.

However, this drawback could be overcome by a cross correlation of sedimentary stratigraphies and luminescence ages from the different vegas, supported by the correlation with the marine proxies. The resulting coherent chronological pattern results in fundamental conclusions concerning the different luminescence methods (see figure 4.2.7.). (1) If the result from sample BT 197 is regarded as a minimum age, almost 80% ( $n = 29$ ) of the coarse-grain quartz OSL ages appear to be conclusive within their error bars. (2) Taking into account the effects of strong anomalous fading but disregarding the overestimation of a few ka in very young samples, only about 50% ( $n = 14$ ) of the fine-grain IRSL samples yield correct ages within their error bars. (3) Disregarding the overestimation of a few ka in very young samples, >80% ( $n = 6$ ) of the fine-grain quartz OSL ages are consistent within their error bars.

The high rate of concordant coarse and fine grain quartz OSL ages, coherent during the cross correlation demonstrates that the obvious correlation pattern of local kaolinite with marine proxies can be confirmed. Unfortunately, reliable luminescence dating of the older parts of the profiles is not possible owing to anomalous fading and insufficient bleaching of the IRSL signal.

Thus, beyond the range of quartz OSL dating (between about 100 to 130 ka), having no reliable luminescence dates we tried to continue the correlation between local kaolinite in Femés and the marine proxies in order to build up a tentative chronostratigraphy. However, this correlation must be regarded as tentative. Following this correlation, IRSL ages from Femés older than 100 ka (samples BT 191, BT 303, BN-D 213) would overestimate burial ages by around 20 to 30 ka (figure 4.2.7.), which in case of sample BN-D 213 would be close to its  $1\sigma$  confidence interval. In turn, in Teguisse the two lowermost IRSL ages (samples BT 201 and 202) would by far underestimate burial ages of sediments, when extrapolating the cross correlation with the stratigraphy of Femés and with marine proxies. This underestimation in Teguisse is also visible in figure 4.2.7., where the IRSL ages indicate a strongly enhanced sedimentation rate prior to 130 ka not seen in Femés and not probable in the extremely material limited vega system of Teguisse (lowest vega bottom/catchment area ratio). Thus the agreement of the ages of the lowest samples in Femés (BN-D 213) and Teguisse (BT 202) within error bars seems not to be an argument for similar ages of the concerned layers, and sample BT 202 must be regarded as strongly underestimated in spite of the lack of anomalous fading. This underestimated age could thus either be due to midterm fading (Xie and Aitken 1991) or to the effect described by Trautmann et al. (2000) as mentioned above. In contrast, the underestimation of sample BT 201 is explainable by strong anomalous fading.

Our chronostratigraphy shows that in all vegas, above a ubiquitously found unweathered layer, certainly anthropogenically triggered colluvia often including ovicaprid bones occur, varying in thickness between 0.55 m in Femés and 4.2 m in Guatiza III (see Zöller et al. 2003, Suchodoletz et al. 2009a) (figure 4.2.2.). The beginning of these colluvia is dated between ~2.5 and 5 ka and probably marks the beginning of human activity on the island. Thus human activity probably started later than 5–10 ka as proposed by Zöller et al. (2003), but also somewhat earlier than the first century AC as assumed by Criado and Atoche-Peña (2004).

#### 4. Results: 4.2. Dating Saharan dust deposits on Lanzarote (Canary Islands) by luminescence...

During Upper MIS 3 and Lower MIS 2, a hiatus seems to be present in all vegas. Whereas it can clearly be detected in Femés and Guatiza between about 15 and 30 ka, owing to the lower time resolution it is difficult to detect in Teguisse where it may exist between about 8.5 (sample BT 198) and 22 ka (sample BT 235). In Teguisse, this hiatus would be located at the same stratigraphic position as a clearly visible one observed in another outcrop of the same vega, near the incomplete damming in the south. The hiatuses in the vegas of Teguisse and Guatiza are explainable by erosion caused by the incomplete damming of the sediment traps. Rognon and Coudé-Gaussen (1987) describe a “geomorphological crisis” in Fuerteventura and NW Morocco from 14 to 11 ka BP (equivalent to about 12.8–17.4 cal ka BP using the program calpal-online). This crisis was characterized by strong erosion due to heavy precipitation. The temporal coincidence with the hiatuses observed in the incompletely dammed vegas Guatiza and Teguisse makes this crisis a probable cause. In Femés, however, the hiatus is hard to explain owing to the low position of the profile in the vega bottom and the completely closed sediment trap.

It emerges that the bottom of profile Guatiza III has the youngest age, starting only at the beginning of MIS 3. When taking the tentative chronostratigraphy of the lower parts of profiles Femés and Teguisse based on correlations, the maximum age of the exposed sequence in the vega of Femés would be around 175–180 ka, thus reaching back to the beginning of Marine Isotope Stage (MIS) 6. Owing to the low sedimentation rate caused by a low catchment area-vega bottom ratio (Suchodoletz et al. 2009a), the profile of Teguisse appears to reach back farthest into the past. Extrapolating the average sedimentation rate of the upper dated part to the bottom, a maximal sedimentation age of about 300–350 ka could be expected for this profile.

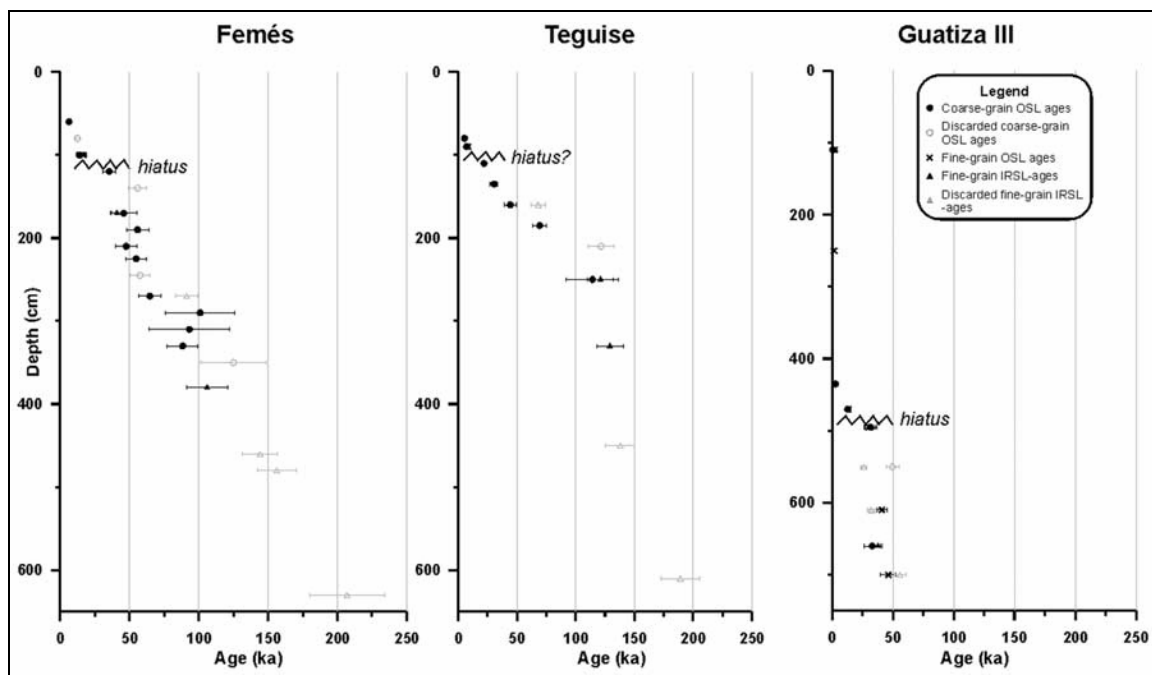


FIGURE 4.2.7. OVERVIEW OF MEASURED LUMINESCENCE AGES WITH HIATAE. Reliable and unreliable ages are discriminated.

#### **4.2.7. Conclusions**

Luminescence dating faces some problems in the vegas of Lanzarote. This is due to the fluvioaeolian geomorphic dynamics with its inherent insufficient bleaching of the sediments as well as to strong anomalous fading of the IRSL signals probably caused by volcanic plagioclases. However, these problems could be overcome by using a combination of OSL datings as well as stratigraphic cross correlations between different profiles supported by correlations with nearby marine proxies, giving credibility to the chronology of the profiles.

Consequently, a sound chronostratigraphy based on luminescence datings could be established until around 130 ka, whereas for the period between 130 and 180 ka a tentative chronostratigraphy is based on correlations and thus needs to be further confirmed (figure 4.2.6.). Altogether, this age model can serve as a timescale for palaeoclimatic interpretations derived from the vegas.

#### **4.2.8. Acknowledgements**

The work of the first author was funded for 2 years by a postgraduate grant from the Free State of Bavaria, Germany, channeled through the University of Bayreuth. Financial support for further work was granted by Deutsche Forschungsgemeinschaft (project Zo 51/29-1).

We thank Marie Ruppel (Dresden/Germany) for help during sampling and Manfred Fischer (University of Bayreuth/Germany) for help during sample preparation, as well as Gunter Ilgen (Bayreuth Center for Ecology and Environmental Research, Bayreuth/Germany) and Walter Jungmann (University of Marburg/Germany) for potassium analyses. Beate Mocek and Max Wilke (University of Potsdam/Germany) are thanked for their help during XRD-measurements. We give special thanks to the participants of the international Workshop ‘Lower Latitudes Loess—Dust Transport Past and Present’ held at Lanzarote during March 2006, for numerous helpful critics and discussions. Sushma Prasad (GFZ Potsdam, Germany) is thanked for language corrections.

**4.3. Luminescence bleaching characteristics of Saharan dust – A case study from Lanzarote, Canary Islands (Spain)**

Suchodoletz, H. von<sup>1\*</sup>, Fuchs, M.<sup>1</sup>, Zöller, L.<sup>1</sup> & I. Menéndez<sup>2</sup>

*Submitted to Quaternary Geochronology*

<sup>1</sup> Chair of Geomorphology, University of Bayreuth, Bayreuth/Germany

<sup>2</sup> Departamento de Física, Universidad de Las Palmas de Gran Canaria/Spain

\*corresponding author

tel: +49-921552266

fax: +49-921552314

E-mail adress: Hans.vonSuchodoletz@uni-bayreuth.de

**Abstract:** “Warm loess” deposits composed of Saharan dust constitute important palaeoclimate archives in the circum-Saharan area. For dating of these deposits, luminescence dating is one of the most important methods. However, insufficient sediment bleaching can alter the results of luminescence dating, yielding overestimated ages. In order to check Saharan dust for insufficient bleaching after its aeolian transport, different luminescence methods were applied to recently deposited aeolian material collected from the Canary Islands/Spain. The results show that Saharan dust contains a very small inherited dose which could bias the dating results of very young Holocene samples.

Furthermore, we investigate the bleaching behaviour of recently reworked colluvial sediments from Lanzarote. The luminescence measurements demonstrate that due to pedogenetic overprinting bleaching during colluvial transport takes much more time than for samples from Central Europe.

*Keywords:* luminescence dating, insufficient bleaching, Saharan dust, Canary Islands, colluvial transport

**4.3.1. Introduction**

Saharan dust deposits are well known from the circum-Saharan region, representing valuable palaeoenvironmental and palaeoclimatic archives (Yaalon and Bruins 1977, Coudé-Gaussen 1991, Dearing et al. 2001, Wright 2001, Zöller et al. 2003, Menéndez et al. 2009). In order to use proxies derived from these archives for reconstructing former palaeoenvironmental and climate conditions, the establishment of a reliable chronostratigraphy is of crucial importance. For dating sediments, luminescence dating techniques are the most important methods due to their ability to directly determine the age of the last process of sediment reworking. In order to obtain a correct luminescence age, the resetting of the inherited luminescence signal by sediment exposure to daylight during the last

reworking process must be complete. If incomplete resetting occurs, a remnant signal remains, causing an age overestimation (e.g. Porat et al. 2001, Fuchs and Wagner 2003, Jain et al. 2004).

Wind-borne sediments are generally well-bleached since they are normally transported as single grains and thus sufficiently exposed to daylight (Hilgers et al. 2001). However, next to the well known phenomena of insufficient bleaching of waterlain sediments (Wallinga 2002, Fuchs et al. 2005) this may also concern aeolian sediments (e.g. Singhvi et al. 1986, Frechen et al. 1999). Consequently, in order to gain a reliable luminescence age, the detection of insufficient bleaching is of crucial importance and appropriate analytical procedures should be applied to correct for this effect (Fuchs and Lang 2001, Lepper and McKeever 2002, Fuchs and Wagner 2003, Olley et al. 2004, Juyal et al. 2006, Fuchs et al. 2007).

In this study, the bleaching behaviour of actual Saharan dust collected on the Canary Islands is investigated. Former studies on Saharan dust report iron and manganese stains on individual grains as well as wind-transported clay aggregates (Koopmann et al. 1981, Coudé-Gausson et al. 1987, Balsam and Otto-Bliesner 1995, Evans et al. 2004). Both features may inhibit a sufficient bleaching of the aeolian sediments, thus leading to an age overestimation (e.g. Singhvi et al. 1986, Frechen et al. 1999, Lian and Huntley 1999).

Next to the bleaching behaviour of purely aeolian Saharan dust, the resetting of the luminescence signal from reworked aeolian sediments is investigated. The Saharan dust was originally trapped in valleys dammed by lavaflows and afterwards fluvially transported over short distances (Suchodoletz et al. 2009a). Such colluvial sediments derived from Saharan dust are important palaeoclimate archives for the NW African region (e.g. Zöller et al. 2003, Criado and Atoche-Peña 2004, Menéndez et al. 2009).

In order to examine the bleaching behaviour of aeolian and colluvial sediments from the Canary Islands, the grain size specific bleaching behaviour of middle/coarse versus fine grains (Fuchs et al. 2005) from both types of samples is investigated .

#### **4.3.2. Regional setting**

The Canary Islands are a volcanic archipelago consisting of seven main islands, situated between 100 and 400 km off the southern Moroccan coast in the subtropical Northeast Atlantic (figure 4.3.1.).

The northeasternmost island Lanzarote (28°50′-29°13′N, 13°25′-13°52′W) has a NE-SW extension of ca. 57 km and a maximal width of about 20 km. Its topography is moderately mountainous with a maximal altitude of ca. 670 m a.s.l.

The island of Gran Canaria (27°44′-28°10′N, 15°22′-15°50′W) in the center of the archipelago has a nearly circular shape of ca. 45 km in diameter. Its topography is rather steep since the highest summit reaches up to an altitude of 1949 m a.s.l.

A special geomorphic feature of the islands are valleys dammed by volcanic material, locally called vegas. These valleys contain thick colluvial sediments of Saharan origin and represent archives for

#### 4. Results: 4.3. Luminescence characteristics of Saharan dust – A case study...

reconstructing the palaeoenvironment and palaeoclimate of the source area (Suchodoletz et al. 2009a, Suchodoletz et al. 2009b).

Saharan dust-bearing winds are associated with the position of the Canary Islands at the northern fringe of the Saharan dust plume over the North Atlantic (figure 4.3.1.). Two different atmospheric situations are mainly responsible for Saharan dust reaching the islands:

1. The first situation frequently occurs during boreal winter when dust is advected by so called “Calima” winds. Calima winds are low-level continental African Trade winds (Harmattan) deflected towards the west by Atlantic cyclones situated close to the Canary Islands (cf. Criado and Dorta 2003). This wind transports considerable amounts of dust originating from northern as well as from southern Saharan sources at low altitude (0-1500 m) towards the Canary Islands, whereas the upper atmosphere is free of dust.
2. During the second situation mainly occurring during boreal summer, dust from southern Sahara - Sahel areas (especially the Bodélé depression) is brought to the Canary Islands. Dust transport to latitudes north of the Canary Islands is enabled by the northern branch of the Saharan Air Layer blowing in an altitude of about 1500 to 5500 m. From there, the dust sinks into the lower atmosphere and is finally transported towards the islands by the Northeast Trade wind (e.g. Koopmann 1981, Bozzano et al. 2002)

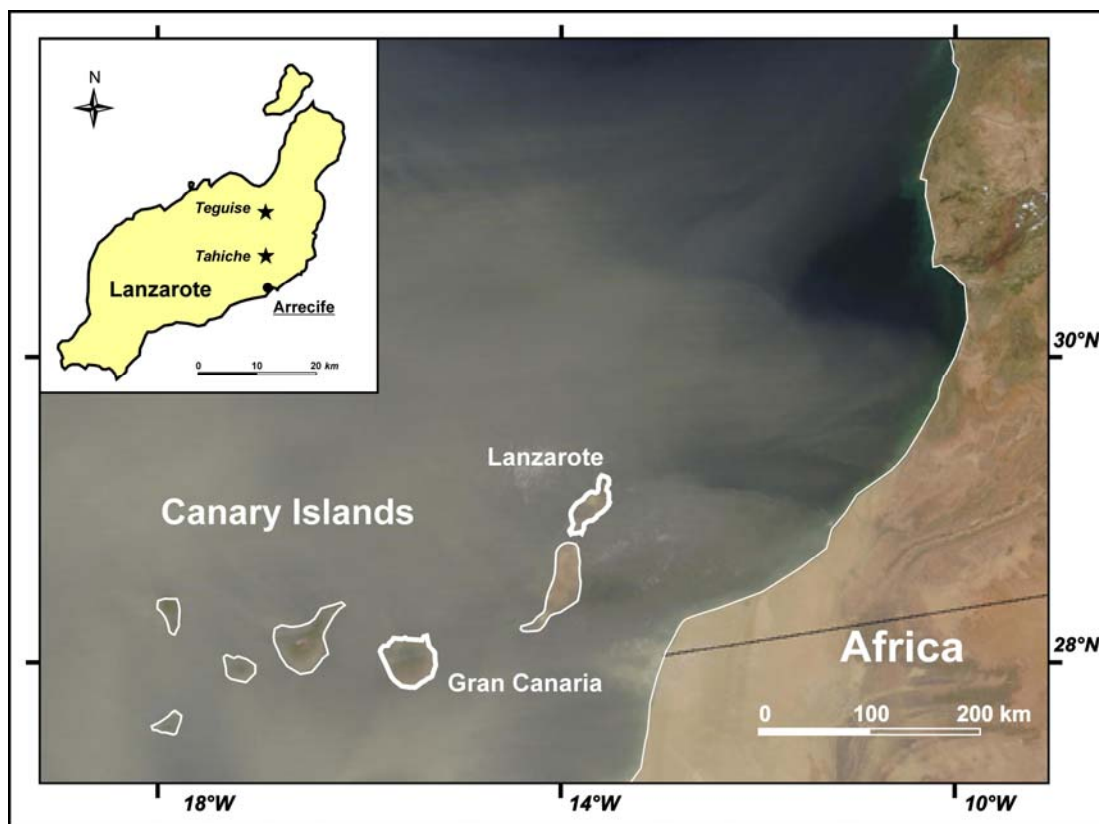


FIGURE 4.3.1. THE CANARY ISLANDS AFFECTED BY A SAHARAN DUST STORM, 22TH OF APRIL 2002. LANZAROTE AND GRAN CANARIA ARE HIGHLIGHTED. THE INSET INDICATES SAMPLING SITES ON LANZAROTE  
Image taken from: <http://earthobservatory.nasa.gov>

### **4.3.3. Material**

From the islands of Lanzarote and Gran Canaria dust samples from three different dust events were collected in 2006. Sample SD1 was collected during a Calima event from the southeast coast of Lanzarote at an altitude of ca. 15 m a.s.l. in the period from 8<sup>th</sup> to 9<sup>th</sup> of February (6-days backward-trajectories in figure 4.3.2.a.) For sampling, a 1 m<sup>2</sup> planar sediment trap at 1 m height above ground surface was used.

Dust samples SD2 and SD3 were collected in the northeastern part of Gran Canaria at an altitude of 300 m a.s.l. during the periods from 19<sup>th</sup> to 31<sup>st</sup> of July and 3<sup>rd</sup> to 13<sup>th</sup> of September. During these periods, the northern branch of the Saharan Air layer was active, incorporating dust into the NE trade wind which finally transported the material to the Canary Islands (6-days backward-trajectories in figures 4.3.2.b and 4.3.2.c). Here, the sampling technique was applied as described in Menéndez et al. (2007).

Additionally, two samples were taken from recently reworked colluvial sediments on Lanzarote: The first sample (CS1) was collected in a loam pit close to the village of Tahiche in the center of the island (29°01'31''N, 13°33'01''W) (figure 4.3.1.). The sediments represent a colluvium which was transported less than 1 km and finally accumulated on top of a lavaflow from 1736 AD (Rothe 1996) (see figure 4.3.3.a). This sample was already described in Suchodoletz et al. (2008, sample BT 204).

The second sample (CS2) was taken in a loam pit close to the village of Teguisse in the north of Lanzarote (29°04'52''N, 13°30'55''W) (figure 4.3.1.). This sediment was fluviially transported over a distance of ca. 10 m and derives from a formerly aeolian deposit with an age of > 200 ka (Suchodoletz et al. 2008) (see figure 4.3.3.b).

#### 4. Results: 4.3. Luminescence characteristics of Saharan dust – A case study...

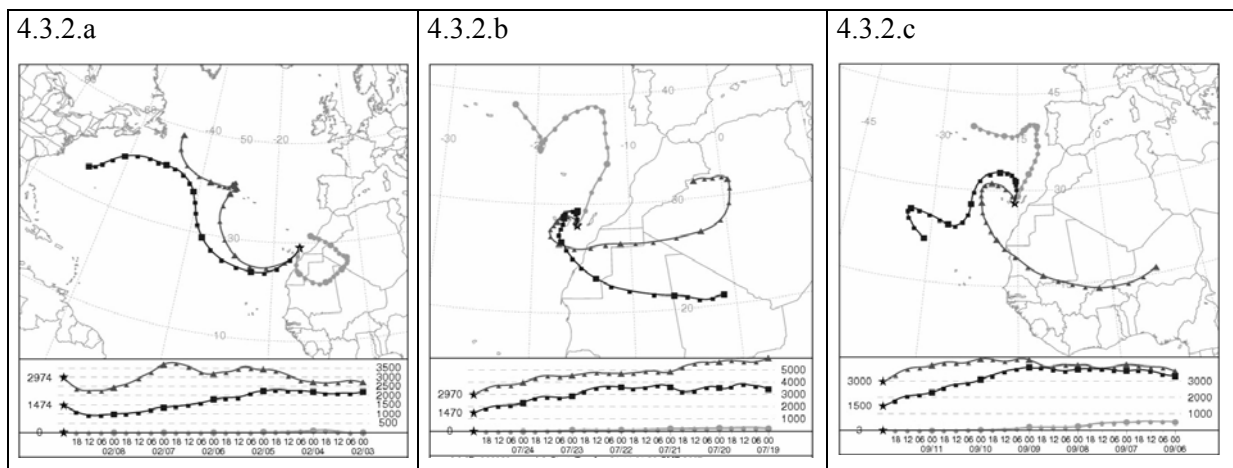


FIGURE 4.3.2. SIX DAYS BACKWARD-TRAJECTORIES OF THE SAMPLED DUST PERIODS DURING 2006

Backward trajectories show the way that an imaginary air molecule probably must have passed in order to arrive at a certain point at a certain time. The first date is the starting-, and the second date the arriving date (on the Canary Islands) of the air molecule.

Figure 4.3.2.a = 04. - 09.02. (dust sample SD1), Figure 4.3.2.b = 20. - 25.07. (dust sample SD2), Figure 4.3.2.c = 07. - 12.09. (dust sample SD3)

Circles indicate the air mass arriving at ground level, rectangles arriving at an altitude of 1500 m, and triangles arriving at 3000 m.

These backward-trajectories were obtained using the HYSPLIT-model from the NOAA-READY website: <http://www.arl.noaa.gov/ready/hysplit4.html>

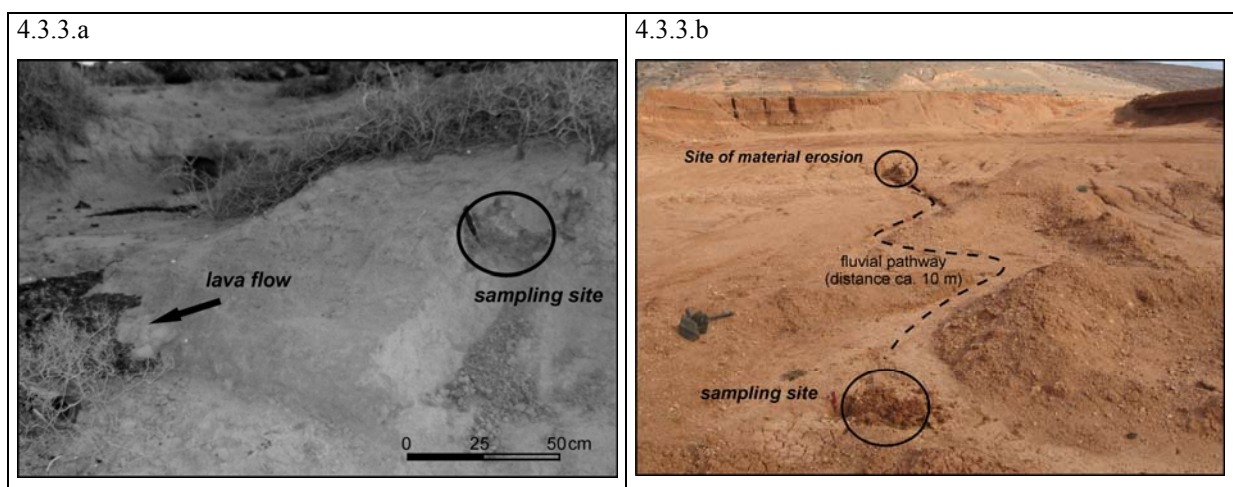


FIGURE 4.3.3. RECENT SEDIMENT SAMPLES

Figure 4.3.3.a: sample CS1 from Tahiche taken above the lava flow from 1736 AD., Figure 4.3.3.b: sample CS2 taken from the loam pit of Teguisse after a fluvial transport of about 10 m. The sediment at the erosion site is estimated > 200 ka old.

#### 4.3.4. Methods

##### 4.3.4.1. Microscopy

In order to investigate dust samples for the occurrence of aggregates and iron stains, the samples were analysed and photographed using a microscope ZEISS "Axiophot" with the digital camera "Axiocam".

*4.3.4.2. Luminescence measurements*

All samples were processed under subdued red light ( $640 \pm 20$  nm) in the Bayreuth luminescence laboratory.

Dust samples were first treated with HCl and H<sub>2</sub>O<sub>2</sub> in order to remove any carbonates and organic matter. Afterwards, the samples were held in an ultrasonic bath for 10 min to destroy possible mineral aggregates. Due to the limited amount of material, a middle/coarse grain fraction (39 - 250  $\mu$ m) was separated by sieving, but neither density separation nor HF-etching were carried out. Thus, this middle/coarse grain fraction represents a polymineralic extract, consisting dominantly of silt quartz and feldspar grains (cf. Coudé-Gaussen et al. 1987, Menéndez et al. 2007). Additionally to this middle/coarse grain fraction, polymineral fine grain silt (4-11  $\mu$ m) was separated using settling tubes.

For colluvial sample CS1, coarse (63-200  $\mu$ m) and fine grain (4-11  $\mu$ m) quartz as well as the polymineral fine grain fraction (4-11  $\mu$ m) could be extracted (Suchodoletz et al. 2008), whereas for sample CS2 we only obtained the last fraction. After sieving, the different grain size fractions were treated with HCl and H<sub>2</sub>O<sub>2</sub> to remove carbonate and organic matter. In order to extract quartz coarse grains, density separation with lithium-heteropolytungstate (LST) and HF etching (40 min) were applied. To gain quartz extracts from the polymineral fine grain fraction, the material was etched with pre-treated 34% hexafluorosilicic acid for 4-5 days to remove any feldspars (Fuchs et al. 2005).

For luminescence measurements, quartz coarse grain and polymineral middle/coarse grain extracts were mounted on aluminum cups (diameter 12 mm) using silicone oil. Fine grains were pipetted on aluminium discs (diameter 9.6 mm).

Optically stimulated luminescence of fine and coarse grained quartz (quartz-OSL) as well as of polymineral middle/coarse grains was measured on a Risø-Reader TL/OSL-DA-15 (Bøtter-Jensen et al. 1999). This reader is equipped with blue LEDs ( $470 \pm 30$  nm) for stimulation and a Thorn-EMI 9235QA photomultiplier combined with a 7.5 mm U-340 Hoya filter (transmission 290 - 380 nm) for detection.  $\beta$ -irradiation was executed using the internal <sup>90</sup>Sr/<sup>90</sup>Y-source of the Risø-Reader (coarse grains: ca. 2.57 Gy/min; fine grains: ca. 2.52 Gy/min). For equivalent dose (De) determination, a Single Aliquot Regenerative dose protocol (SAR, Murray and Wintle 2000) was applied. A saturating exponential growth curve was constructed, using six regeneration cycles after measurement of the natural luminescence signal: Four measurements of regenerated doses, one repeated measurement of the first regenerated dose to determine the recycling ratio and one 0-dose regeneration cycle. OSL decay curves were recorded for 20 s at a temperature of 125°C. Prior to measurement, samples were preheated to 240°C for 10 s (heating rate 10°C/s) for natural and regenerated doses, and with a cut-heat of 160°C (heating rate 5°C/s) for the test dose of 0.64 Gy (cf. Suchodoletz et al. 2008). The De was determined using the integral OSL in the stimulation interval 0.0 – 0.4 s after subtracting the background interval 16 – 20 s. For colluvial quartz samples, a check for possible feldspar contamination was performed by stimulating the artificially irradiated samples with infrared and detecting in the blue range (390-450 nm).

Infrared stimulated luminescence (IRSL) of polymineral fine grains from both colluvial and dust samples was measured with the described TL/OSL-DA-15 reader, in this case equipped with a filter-combination transmitting 390-450 nm (BG 39, GG 400, 2xBG 3). De's were determined applying the Multiple Aliquot Additive Dose protocol (MAAD) after Lang et al. (1996). Due to the limited amount of material, neither test dose measurements nor fading tests could be performed. According to the amount of material, three (SD1), six (SD2) and five (SD3) dose groups, each including two to four discs were irradiated and stored for one week at a temperature of 70°C. Subsequently, these discs were measured together with three (SD1), ten (SD2) and eight (SD3) natural discs to construct the additive growth curve. Prior to measurements, samples were preheated to 220°C for 120 s with a heating rate of 10°C/s. IRSL-decay curves were recorded for 60 s at room temperature. For De calculation, the integral of the first 15 s was taken after subtracting the background (the interval from 55 to 60 s).

All luminescence measurements were analysed using the software Analyst 3.07b.

Apart from colluvial sediment sample CS1 from Tahiche (cf. Suchodoletz et al. 2008), no dose rates were determined. Instead, for all calculations of apparent ages we used a minimal dose rate of 2 Gy/ka and a maximal dose rate of 3.5 Gy/ka. These values were averaged from several samples from Lanzarote analysed by Suchodoletz et al. (2008).

#### **4.3.5. Results**

##### *4.3.5.1. Microscopy*

Dust samples SD2 and SD3 were investigated under a microscope prior to sample treatment. Both samples clearly exhibit aggregates as well as iron-manganese coatings and stains as described by other authors (Koopmann et al. 1981, Coudé-Gaussen et al. 1987, Mason et al. 2003, Evans et al. 2004) (figure 4.3.4.).

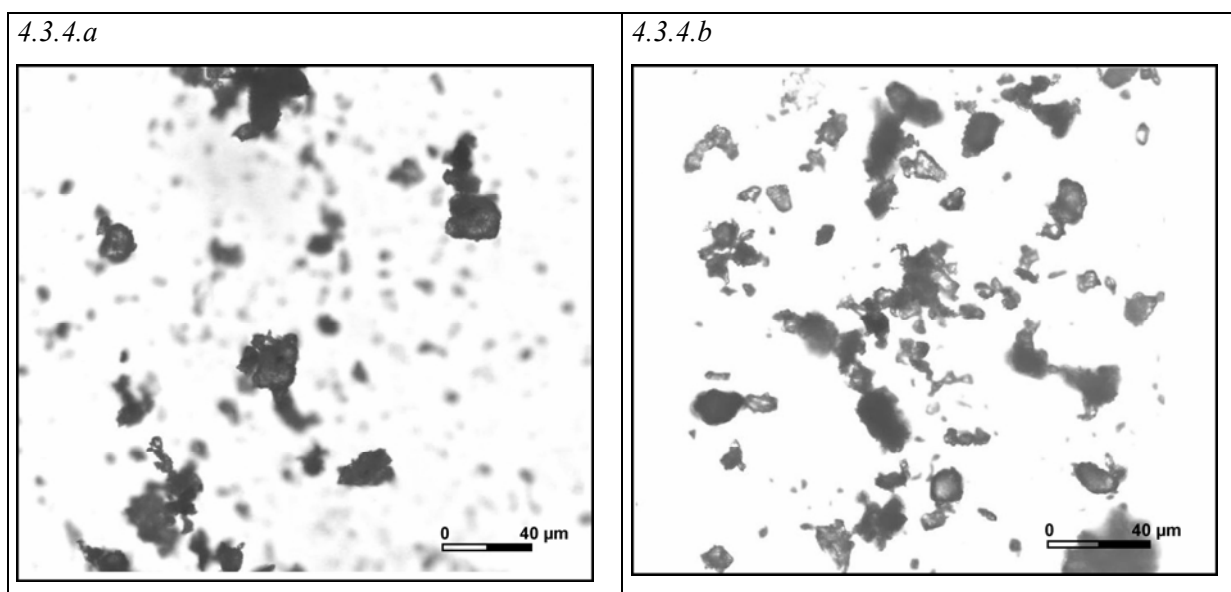


*FIGURE 4.3.4. MICROSCOPE IMAGES OF SAMPLES SD2 (FIGURE 4.3.4.a) AND SD3 (FIGURE 4.3.4.b) Aggregates are clearly recognizable.*

*4.3.5.2. Luminescence measurements*

*Dust samples*

All SAR measurements of polymineral middle/coarse grains show a linear growth behaviour in the measured dose range (figure 4.3.5.). For De-determination, eight aliquots were measured from sample SD2. The histogram shows a peak at ca. 0.5 Gy, scattering between 0.2 and 0.9 Gy ( $\sigma = 0.14$ ; figure 4.3.6.). From sample SD3, eleven aliquots were measured. The histogram shows a peak at ca. 0.1 Gy, but due to the positively skewed distribution the mean De is slightly higher with 0.27 Gy. The De-scatter of sample SD3 is between 0.1 and 0.7 Gy ( $\sigma = 0.19$ ; figure 4.3.6.). Due to the limited amount of measured aliquots, an exact determination of middle/coarse grain palaeodoses following statistical approaches (e.g. Fuchs and Lang 2001, Lepper and McKeever 2002, Olley et al. 2004, Juyal et al. 2006) could not be achieved. Instead, middle/coarse grain De's were defined using the highest peak of the De-distribution in the histogram. Thus, the equivalent dose is 0.5 Gy for sample SD2 and 0.1 Gy for sample SD3, respectively (see table 4.3.1.).

| Sample                   | Sample location | Collection period<br>2006 | De (Gy)<br>CG-Q (in brackets<br>number of discs) | De (Gy)<br>MCG-P<br>(in brackets<br>number of discs) | De (Gy)<br>FG-Q | De (Gy)<br>FG-P |
|--------------------------|-----------------|---------------------------|--|--|-----------------|-----------------|
| <i>Dust samples 2006</i> |                 |                           |  |  |                 |                 |
| SD1                      | L               | 08.-09.02                 | -  | -  | -               | 0.97± 0.2       |
| SD2                      | G               | 19.-31.07                 | -  | ca. 0.5 (8)  | -               | 1.86 ± 0.8      |
| SD3                      | G               | 03.-13.09.                | -  | ca. 0.1 (11)   | -               | 1.44 ± 0.4      |
| <i>Colluvial samples</i> |                 |                           |  |  |                 |                 |
| CS1 (BT 204*)            | L               | -                         | 3.5 ± 1 (4)*                                     | -  | 6.3 ± 0.6*      | 7.3 ± 0.3*      |
| CS2                      | L               | -                         | -  | -  | -               | 319 ± 7         |

TABLE 4.3.1. EQUIVALENT DOSES (DE) FOR DUST AND COLLUVIAL SAMPLES FROM THE ISLANDS OF LANZAROTE (L) AND GRAN CANARIA (GC).

CG-Q: coarse grain quartz; MCG-P: middle/coarse grain polymineral; FG-Q: fine grain quartz; FG-P: fine grain polymineral.

\* Data taken from Suchodoletz et al. (2008)

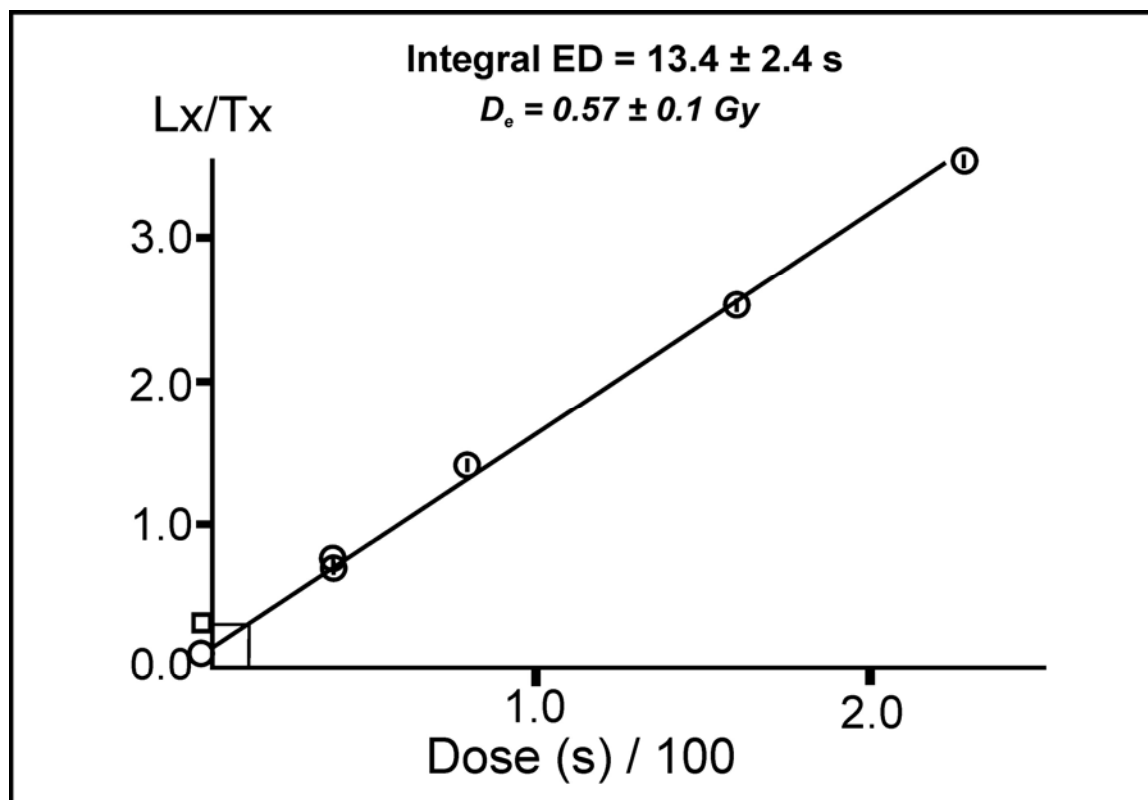


FIGURE 4.3.5. POLYMINERAL MIDDLE/COARSE GRAIN OSL GROWTH CURVE OF SAMPLE SD3

The x-axis shows given irradiation doses in s/100, the y-axis the luminescence signal normalised to the test dose signal ( $Lx/Tx$ ). The equivalent dose is obtained by relating the natural luminescence signal (rectangle at the y-axis) with the growth-curve constructed from regenerative doses (circles).

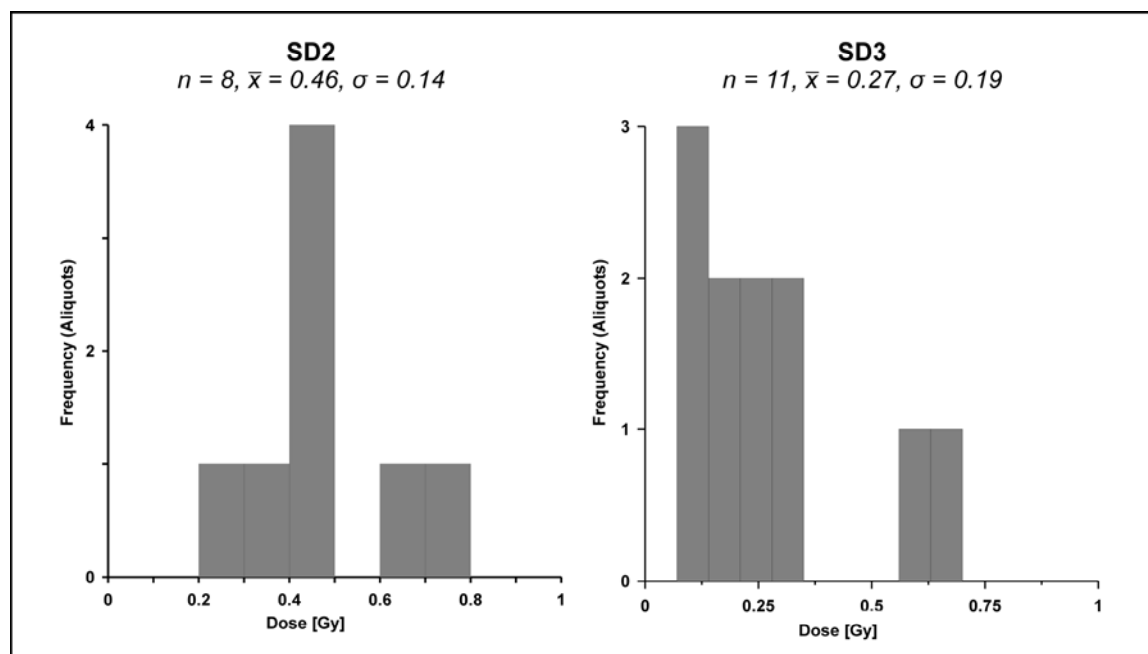


FIGURE 4.3.6. EQUIVALENT DOSE HISTOGRAMS OF POLYMINERAL MIDDLE/COARSE GRAIN DUST SAMPLES SD2 AND SD3

Polymineral fine grain IRSL-measurements also show a linear growth behaviour in the measured dose range, with a high luminescence scatter within each dose group (figure 4.3.7.). Due to expected low  $D_e$ 's, aliquots were not normalised prior to measurement.  $D_e$ 's of measured samples were 1.0 Gy

#### 4. Results: 4.3. Luminescence characteristics of Saharan dust – A case study...

(SD1), 1.9 Gy (SD2) and 1.4 Gy (SD3), respectively. Relatively large errors between 21% (SD1) to 43% (SD2) are caused by the large scatter between measured aliquots and the fact that measured signals were only slightly above the background (see table 4.3.1.).

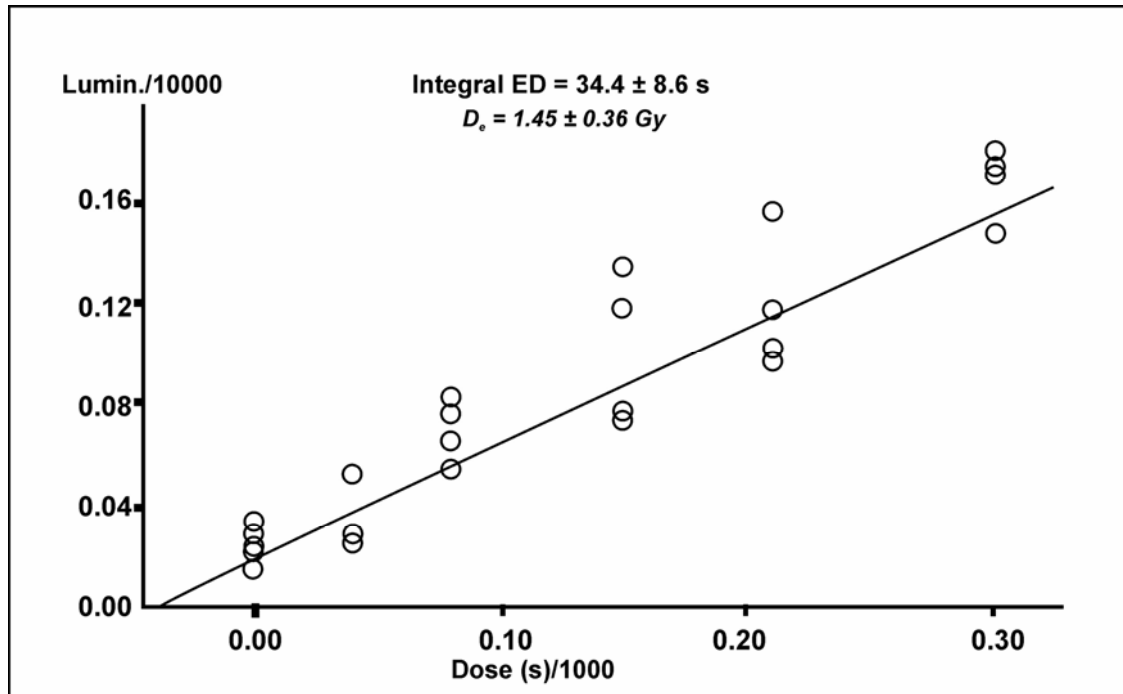


FIGURE 4.3.7. FINE GRAIN IRSL GROWTH-CURVE OF SAMPLE SD3.

#### Colluvial samples

De's from colluvial samples yielded systematically higher values compared to those of Saharan dust samples as will be shown in this chapter.

From sample CS1 from Tahiche (sample BT 204, Suchodoletz et al. 2008) only four coarse grain quartz De's could be measured, showing an approximate De of  $3.5 \pm 1$  Gy. Fine grain quartz measurements were based on seven aliquots, yielding an OSL-De of  $6.3 \pm 0.6$  Gy. Polymineal fine grain IRSL measurements resulted in a De of  $7.3 \pm 0.3$  Gy (see table 4.3.1.).

Sample CS2 from Teguse yields a fine grain IRSL-De of  $319 \pm 7$  Gy. No coarse and fine quartz material was gained, thus no OSL measurements could be executed.

#### 4.3.6. Discussion

Equivalent doses from Saharan dust samples from the Canary Islands clearly show that insufficient bleaching of the luminescence signal is a minor problem for dating Pleistocene samples. This holds true for both types of sediments:

- Dust originating from the entire Sahara transported by low level Calima winds (sample SD1).
- Dust mainly originating from sources in the south Sahara/Sahel transported by a combination of the high level Saharan Air Layer and NE trade winds (samples SD2 and SD3).

Comparing different grain sizes from Saharan dust samples, results from middle/coarse grains show almost negligible  $D_e$ 's which are lower than  $D_e$ 's from fine grains. Since  $D_e$ -values of middle/coarse grains were only slightly above 0, the lack of an exact determination of middle/coarse grain palaeodoses following statistical approaches as discussed above is irrelevant for this study. Since polymineral instead of pure quartz material was measured, obtained low  $D_e$ 's should be even lower for pure quartz extracts, since the polymineral signal is composed of that from quartz and that from feldspar.

Low  $D_e$ -values gained from middle/coarse polymineral dust material are probably due to the aeolian transport of coarser material as single grains rather than as aggregates. Taking average dose rates of 2 to 3.5 Gy/ka determined from Mid Pleistocene to Holocene samples from Lanzarote (Suchodoletz et al. 2008), inherited coarse grain quartz  $D_e$ 's would correspond to an age overestimation of ca. 0.03 to 0.25 ka.

In contrast to coarser grains, fine grain material from the Sahara is often transported as aggregates (e.g. Evans et al. 2004). Since  $\alpha$ -values and thus the contribution of the  $\alpha$ -dose to the dose rate are very low for Saharan dust material dated on Lanzarote (Suchodoletz et al. 2008), aggregates may be the main reason why IRSL fine grain  $D_e$ 's are slightly higher than middle/coarse grain  $D_e$ 's, corresponding to maximal ages between 0.5 and 0.93 ka. Furthermore, fine grain material from southern sources brought by the Saharan Air Layer (samples SD2 and SD3;  $D_e$ 's 1.9 and 1.4 Gy) seems to exhibit slightly higher fine grain-IRSL- $D_e$ 's compared to dust derived from Calima winds also including material from northern sources (sample SD1,  $D_e$  1.0 Gy). This could be due to environmental differences between northern and southern sources, with southern sources representing mostly dry lake beds and eroded red soils. This kind of material is known to be potentially stronger affected by Fe stains and aggregation (Bozzano et al. 2002, Evans et al. 2004). However, due to the limited number of datings and their large  $D_e$ -errors this effect can only be assumed here and should be further investigated.

Results from recently transported colluvial deposits on Lanzarote show that bleaching during redeposition was not complete, and even after a transport distance of some 100 m in Tahiche the luminescence signal of sample CS1 still shows a dominant luminescence signal. Applying minimal and maximal dose rates of 2 or 3.5 Gy/ka and subtracting a theoretical maximal apparent sediment age of 0.25 ka, sample CS1 shows an age of 0.75 – 1.5 ka for quartz coarse grains and 1.75 – 3.25 ka for quartz and feldspar fine grains. Since this sample overlies a lavaflow from the middle of the 18<sup>th</sup> century, this sample must be significantly overestimated. Similarly, sample CS2 from Teguisse shows very limited bleaching after a colluvial transport of ca. 10 m, yielding a fine grain IRSL- $D_e$  of ca. 320 Gy. Corresponding to minimal and maximal dose rates reported from Lanzarote (Suchodoletz et al. 2008) this results in an apparent age of 160 – 90 ka. Since only a part of this  $D_e$ -overestimation is inherited from the original Saharan dust as shown above, additional signal inheritance has to originate from local factors: As shown by Suchodoletz et al. (2009a), colluvial fine grain material is frequently

#### **4. Results: 4.3. Luminescence characteristics of Saharan dust – A case study...**

---

transported as aggregates. Additionally, in situ iron staining of the grains occurs in the sediments on Lanzarote due to pedogenesis (figure 4.3.8.) (Zarei 1989). Consequently, older soil material is only slowly bleached when eroded and transported, showing an unbleachable luminescence residual even after longer colluvial transport. Results from sample CS2 clearly demonstrate that, unlike in central Europe, a colluvial transport of < 100 m is not sufficient for a complete bleaching of the luminescence signal (see Lang 1996), probably caused by coatings and soil aggregates formed during pedogenesis on Lanzarote.

Thus, Upper Holocene ages from the Eastern Canary Islands derived from colluvially redeposited aeolian deposits are systematically overestimated by some 100 to 1000 years. This holds especially true for fine grain samples. Dating older (Pleistocene) sediments, this systematic overestimation becomes negligible because this difference will be included in the overall error. However, sufficient bleaching should be checked individually for each sample from partly redeposited aeolian deposits, using single aliquot or single grain techniques for quartz coarse grains (e.g. Fuchs and Lang 2001, Juyal et al. 2006, Jacobs et al. 2006).

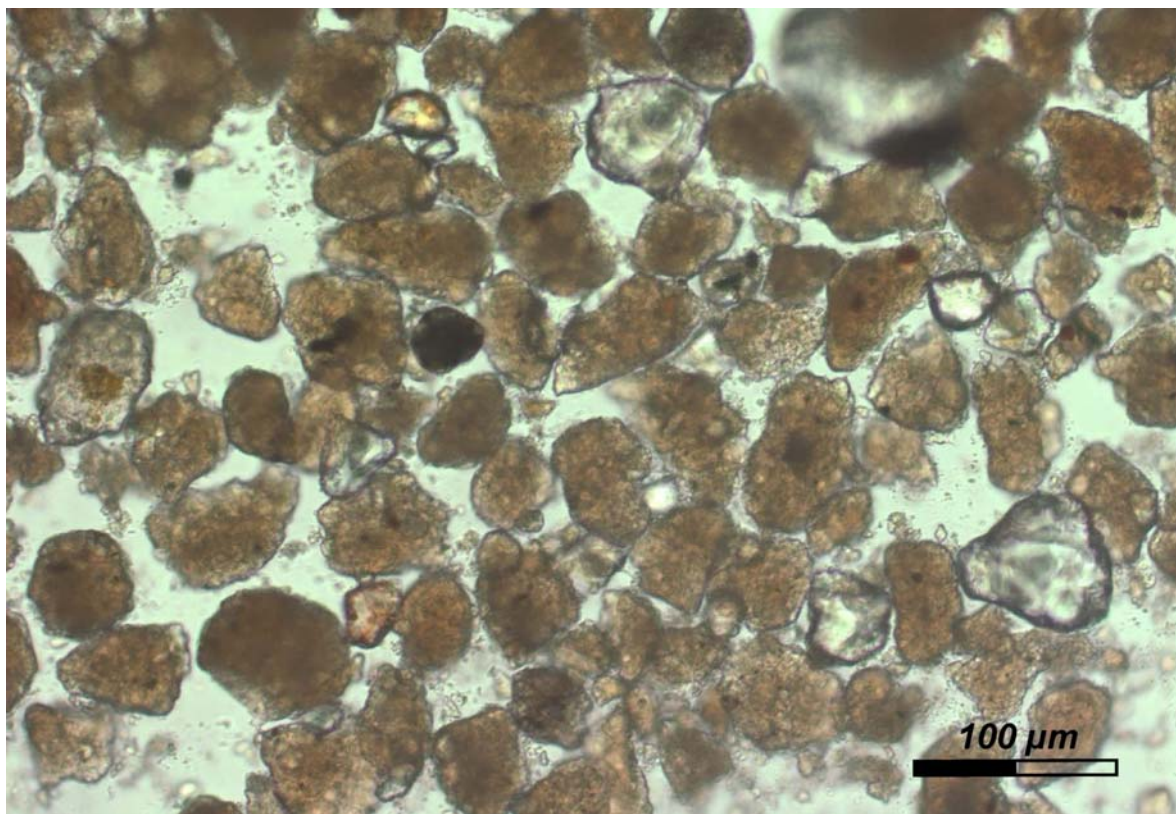


*FIGURE 4.3.8. SECONDARY CONCRETIONS IN THE FRACTION < 63μm IN A SOIL SEDIMENT LAYER FROM LANZAROTE, FORMED BY AMORPHOUS PLASMA CONSISTING OF IRON OXIDES/HYDROXIDES AND CLAY (CF. ZAREI ET AL. 1989).*

#### **4.3.7. Conclusions**

Investigations of the bleaching behaviour of Saharan dust show that the material transported from NW-Africa to the Canary Islands is well suited for luminescence dating. This is confirmed by only very small inherited luminescence signals in middle/coarse grains after an aeolian transport of at least

some days. However, somewhat larger inherited doses in fine grained material could be problematic if very young Holocene aeolian samples ( $< 2$  ka) are dated. Consequently, in order to avoid age uncertainties  $> 10\%$  caused by inherited doses, coarse instead of fine grain luminescence techniques should generally be used for Upper Holocene samples derived from Saharan dust.

Results of recently reworked colluvial samples from Lanzarote demonstrate that this kind of material holds an additional inherited palaeodose due to the local environmental dynamics of the geomorphological and pedological system, confirming the results of Suchodoletz et al. (2008). This signal is only slowly bleached during colluvial transport and still detectable even after a transport of some 100 m. Thus, colluvial samples from the island used for luminescence dating should have been transported for at least some 100 m. These results also show that the use of fine grain techniques for Holocene colluvial samples is even more critical than for exclusively aeolian samples.

#### ***4.3.8. Acknowledgements***

The work of the first author was funded for two years by a post-graduate grant of the Free State of Bavaria, Germany, supplied by the University of Bayreuth. Further financial support was given by Deutsche Forschungsgemeinschaft (project Zo 51/29-1).

We thank Barbara Wallraff for collecting sample SD1 on Lanzarote and Manfred Fischer for sample preparation at the Bayreuth luminescence laboratory. We are also indebted to Achim Brauer and Jens Mingram (GFZ Potsdam, Germany) for facilitating microscope investigations.

**4.4. Geomorphological investigations of sediment traps on Lanzarote (Canary Islands) as a key for the interpretation of a palaeoclimate archive off NW Africa**

H. von Suchodoletz<sup>1</sup>, D. Faust<sup>2</sup> & L. Zöller<sup>1</sup>

*This article is published in Quaternary International 196, 44-56.*

<sup>1</sup>Chair of Geomorphology, University of Bayreuth, D-95440 Bayreuth, Germany

<sup>2</sup>Institute of Geography, Technical University of Dresden, D-01062 Dresden, Germany

\*corresponding author

tel: +49-921552266

fax: +49-921552314

E-mail address: Hans.vonSuchodoletz@uni-bayreuth.de

**Abstract**

On Lanzarote (Canary Islands) Late Quaternary Saharan dust and volcanic material were trapped in Miocene to Pliocene valleys dammed by volcanic lava flows. These trapped sediments are potentially interesting as they can be natural archives useful to reconstruct the terrestrial palaeoclimate history of the NW African margin. Nevertheless, slope wash processes altered the primarily aeolian deposits, making climatic interpretation not straightforward. Geomorphological mapping, GIS calculations and sedimentological investigations were used to unravel these processes influencing the temporal resolution of the palaeoclimatic archive, demonstrating that they average the palaeoclimatic signal by some ka. Thus, despite the colluvial geomorphic environment the valley fillings can be used for palaeoclimatic interpretation of events with a length of at least some ka. The youngest sediments, deposited since at least 2.5 ka, are anthropogenically triggered and thus cannot be used for palaeoclimatic interpretation. The results show that the input of Saharan dust at Lanzarote increased during the last 1.0 Ma and especially during the Early/Middle Holocene.

**4.4.1. Introduction**

Loess–palaeosol sequences are an important type of terrestrial palaeoclimate archive. Such sequences have been used in both hemispheres to derive terrestrial climate variations during past few million years including changing wind dynamics and moisture regimes (e.g. Issar and Bruins 1983, Dodonov and Baiguzina 1995, Antoine et al. 2001, Berger et al. 2001, Markovic et al. 2006, Schellenberger and Veit 2006, Mason et al. 2007). Accordingly, loess–palaeosol sequences derived from Saharan dust were investigated in the Mediterranean area and are regarded as valuable palaeoclimate archives (e.g. Yaalon and Bruins 1977, Coudé-Gaussen 1991, Dearing et al. 2001).

#### **4. Results: 4.4. Geomorphological investigations of sediment traps....**

---

Lanzarote (Canary Islands) is situated on the northern fringe of the Saharan dust plume over the Atlantic Ocean and annually receives aeolian material derived from the Sahara (e.g. Jahn 1995). This study investigates valleys dammed by volcanic activity representing sediment traps, where continuous sedimentation of Saharan dust and volcanic material occurred over a longer time span during the Quaternary (Zöller et al. 2003). The layered deposits filling the valleys show continuity and therefore could be used as palaeoenvironmental archives (figure 4.4.1). However, steep and strongly eroded slopes of the valleys indicate that colluvial input contributed to the infilling of the valleys (figure 4.4.2). When sediments were only partly directly deposited by aeolian input and another part was later reworked by colluvial processes, the understanding of the link between erosional and depositional area and the type of material transport (high frequency/low magnitude or low frequency/high magnitude) becomes important for palaeoenvironmental interpretation. These issues are important since a weak link and low frequency/high-magnitude processes can cause a time lag between environmental signal and time of deposition or destroy older sediments (e.g. Lang 2003, Fuchs et al. 2004, Rommens et al. 2006). Hence, the interpretability of a colluvial sedimentary archive depends on the way of transport, making its investigation a crucial prerequisite for a subsequent palaeoenvironmental interpretation of the archive.

Consequently, in order to know whether the sediments trapped on Lanzarote bear useful palaeoenvironmental information about the regional climate of the NW African region and to what extent they can be stratigraphically and palaeoclimatologically interpreted, our investigation of the sedimentation path focussed on the link between erosional and depositional areas as well as the frequency–magnitude relation of colluvial transport. For this, we use geomorphological mapping and GIS calculations supported by luminescence dating and sedimentological analyses. The investigations allow the development of different sedimentation scenarios, which can serve as a base for further palaeoclimatic interpretation of these deposits. Furthermore, quantitative estimations from a selected sediment trap allow evaluating the dynamics of Saharan dust input during the Quaternary as well as the influence of anthropogenic activity on the local semiarid ecosystem.

#### 4. Results: 4.4. Geomorphological investigations of sediment traps....

---



FIGURE 4.4.1. HORIZONTALLY STRATIFIED LAYERS IN THE BOTTOM OF THE VEGA OF TEGUISE. Darker layers indicate layers derived from palaeosol material, lighter layers consist of slightly weathered loess-like sediments.

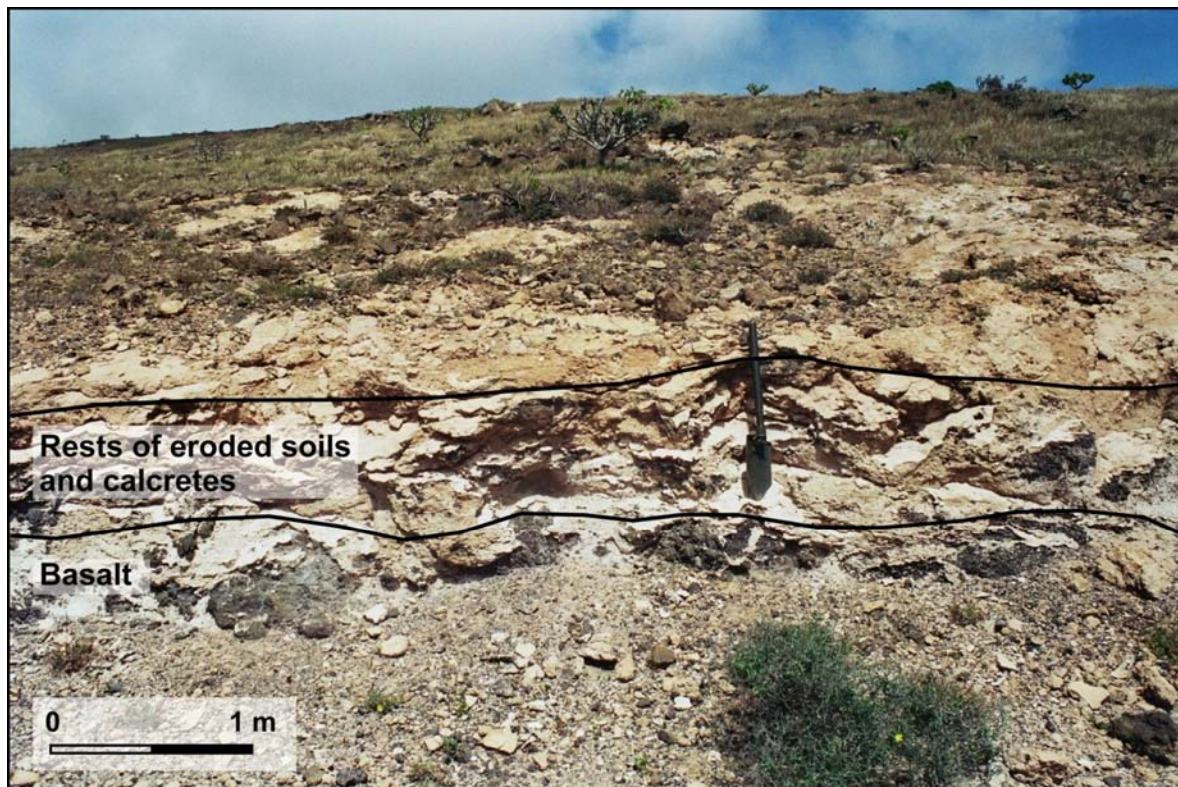


FIGURE 4.4.2. ERODED SLOPE WITH CALCRETE IN THE VEGA OF FEMÉS

### 4.4.2. Geographical setting

Lanzarote is the northeasternmost island of the volcanic Canary islands 130 km off the coast of Southern Morocco at 28–29°N and 13–18°W (figure 4.4.3). Volcanism on Lanzarote started during the Miocene about 15.5 Ma ago and lasted until the Late Holocene (last volcanic eruptions 1730–36 and 1824) (e.g. Carracedo et al. 1998). Both the northern and the southern part of the island are dominated by volcanic massifs with Miocene to Pliocene age. The volcanism is basic and pyroclastics were formed (cf. Rothe 1996). Given this basic volcanism of the island, Mizota and Matsuhisa (1995) and Jahn (1988) demonstrate that all quartz found on the island has an allochthonous origin. The relief of the island is strongly eroded so that the maximum altitude of Lanzarote is only 670m (Jahn 1988). Slopes are generally smoothed and concave. Several phases of soil forming processes led to the formation of polygenetic calcretes, which are exposed on the slopes of the volcanoes due to erosion processes. The two volcanic complexes are separated by the central part of the island showing a smoother topography, and are dissected by numerous U-shaped valleys and smaller gullies. Some of the larger valleys were dammed by volcanic material (lava flows, pyroclastica) during the Early and Middle Pleistocene so that they served as sediment traps for Saharan dust and local volcanic material. Locally, these dammed valleys are called vegas.

The climate of the Canary Islands is maritime-semiarid. Due to the limited altitude of Lanzarote compared to the western Canary Islands, the island gets no orographic precipitation from rising trade winds. Thus, it gains only very sparse precipitation (100–250 mm) from boreal winter cyclones decreasing from higher to lower altitudes. Mean annual temperature at sea level is 19.9°C, with a minimum of 17.0°C in January and a maximum of 23.0°C in August (Jahn 1988). The vegetation has a very sparse, shrubby and dispersed character and is dominated by xerophytic and halophytic species. This kind of vegetation cover is mainly caused by anthropogenic activity (Jahn 1988, Kunkel 1993).

Lanzarote is situated at the northern fringe of the Saharan dust plume over the North Atlantic. Today, Saharan dust is brought to Lanzarote during two different synoptic situations. During winter, dust is advected at low altitude (0–1500 m) to the archipelago by Calima-winds, continental African Trade winds (Harmattan) which are deflected towards the west by Atlantic cyclones situated close to the Canary Islands (cf. Criado and Dorta, 2003). During summer, dust is transported to the north of the Canary Islands by the northern branch of the Saharan Air Layer blowing at an altitude of about 1500–5500 m. There, the material sinks into the lower atmosphere due to changes in the geopotential fields and is finally transported towards the island by the Northeast Trade wind (cf. Koopmann 1981, Bozzano et al. 2002).

#### 4. Results: 4.4. Geomorphological investigations of sediment traps....

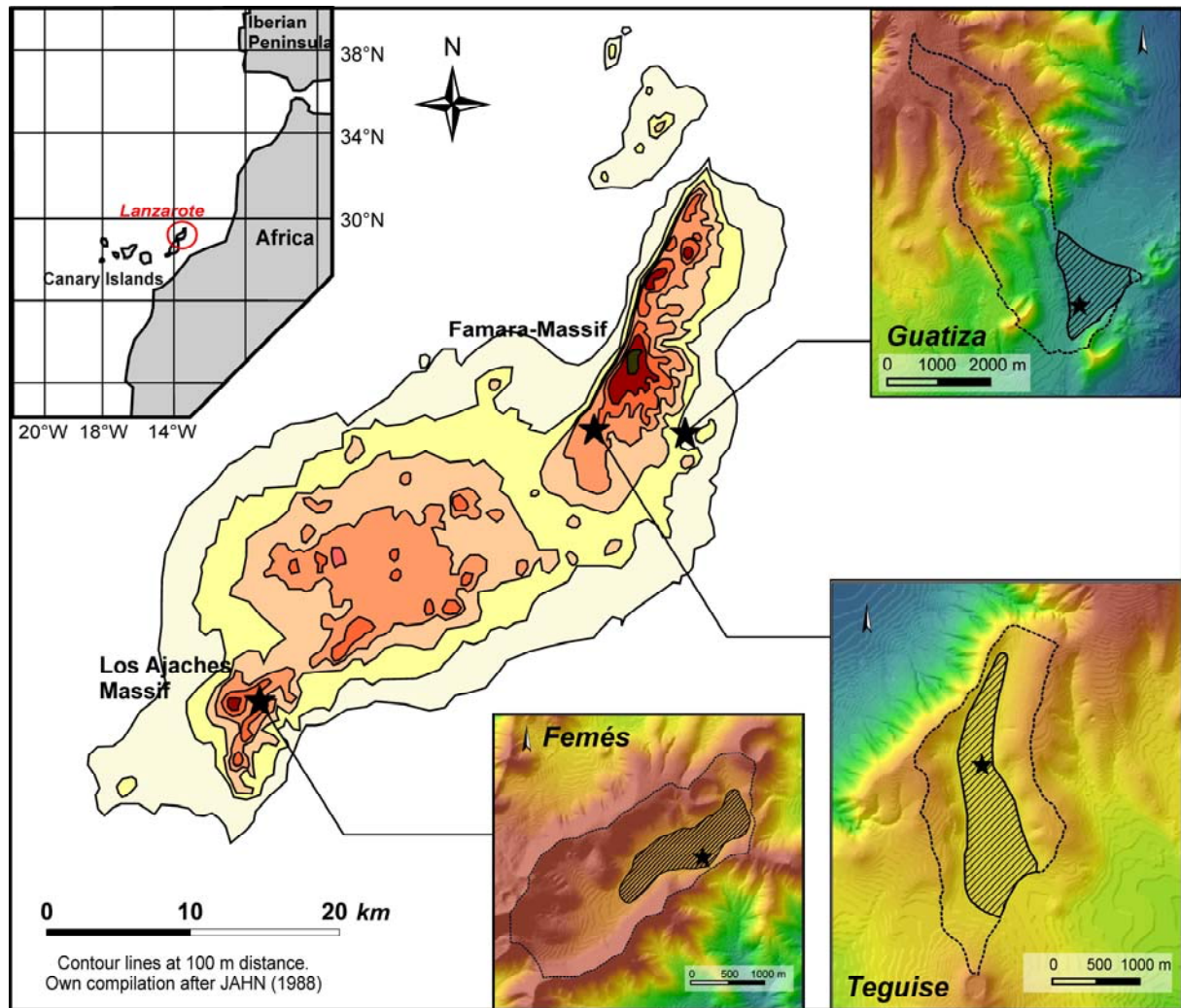


FIGURE 4.4.3. GEOGRAPHIC POSITION OF THE CANARY ISLANDS (INSET) AND INVESTIGATED SEDIMENT TRAPS ON LANZAROTE (STARS).

On the right and lower margins elevation models of the sediment traps with locations of the investigated profiles (stars). Hatched areas indicate the valley bottom and dashed lines the catchment areas.

#### 4.4.3. Methods

*Geomorphological mapping of the vega catchments and calculations with the GIS-program Arc Map 9.0 (ESRI)* were used to determine the ratios between catchment area surfaces and those of the recent valley floors. The digital database of elevation contour lines was provided by GRAFCAN, Cartografía de Canarias S.A. The vector data were triangulated for the calculation of a digital elevation model, where the height information is referenced per pixel. Due to the temporarily incomplete damming of the vegas of Teguisse and Guatiza, the continuously completely closed Femés sediment trap was chosen in order to establish a semi-quantitative sediment mass balance by calculating volumes of sediment deposited in the vega bottom and temporarily stored in the catchment area (table 4.4.1). Due to the lack of geophysical investigations, the depths of the different valley segments prior to damming were estimated using slope extrapolations from various vega transects as shown in figures 4.4.4 and 4.4.5.

#### 4. Results: 4.4. Geomorphological investigations of sediment traps....

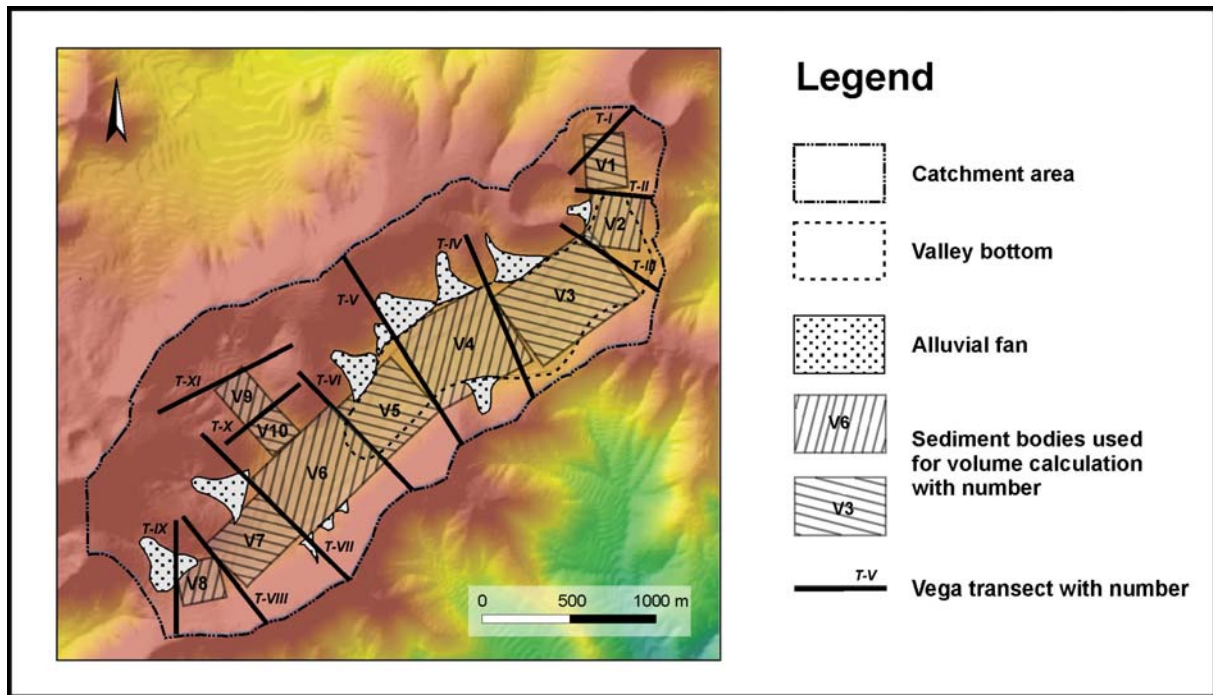


FIGURE 4.4.4. VEGA TRANSECTS, SURFACE OF SEDIMENT BODIES AND ALLUVIAL FANS USED FOR THE CALCULATION OF STORED SEDIMENT IN FEMÉS

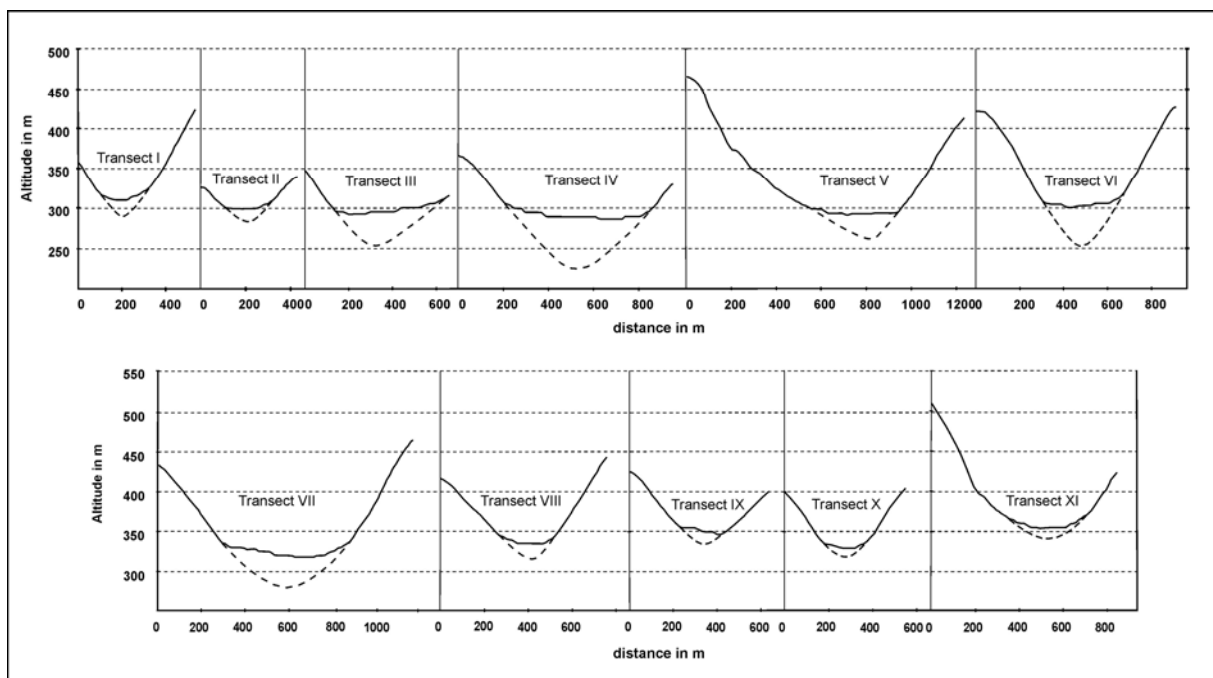


FIGURE 4.4.5. VEGA TRANSECTS IN FEMÉS (LEFT SIDE: N/W-SLOPE, RIGHT SIDE: S/E-SLOPE)  
Dashed lines show extrapolated slopes.

Close to the damming in the northeast, a value of about 50 m is proposed which is confirmed by the estimation of Zöllner et al. (2006). Using the estimated depth of a vega transect produced a triangle-shaped cut through the sediment body. Considering a probable U-shaped valley, the triangle was

#### 4. Results: 4.4. Geomorphological investigations of sediment traps....

horizontally cut at 75% of the depth so that the cut became trapezoid shaped, similar to most of the Miocene/Pliocene valleys found on Lanzarote today (figure 4.4.6).

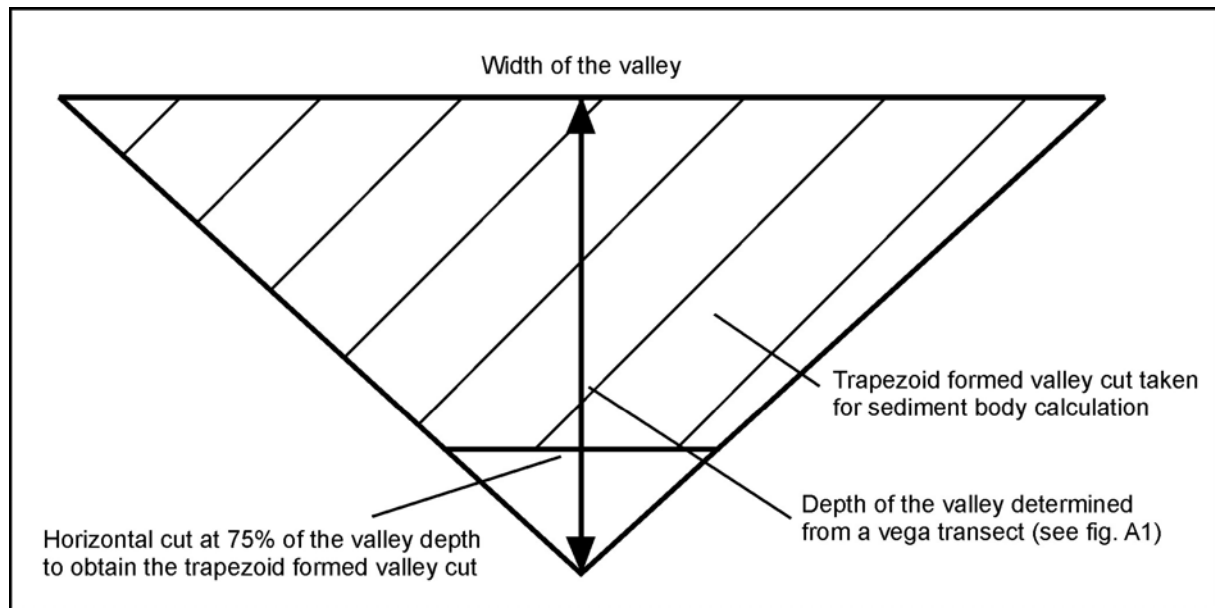


FIGURE 4.4.6. MODEL OF A HORIZONTAL CUT THROUGH A SEDIMENT BODY ALONG A VEGA TRANSECT.

Taking into account different valley widths, the vega was subdivided into 10 different sediment bodies (figure 4.4.4, table 4.4.1). To determine their lateral surfaces, the trapezoid cuts from adjacent vega transects were used, e.g. for sediment body V1 the cuts of the northward transect T-I and the southward transect T-II (figure 4.4.4) were taken. Sediment bodies V2–V5 were added to calculate the volume of the sediment deposited in the lower vega bottom, which is equivalent to the erosion base. The remaining sediment bodies served for calculations of the sediment trapped in small valleys and the upper vega, comprising the material that did not reach the erosion base in the lower vega bottom.

In order to estimate the volume stored in the alluvial fans, an average sediment thickness of 5 m, the average value observed during geomorphological mapping, was multiplied with the total area of the fans (figure 4.4.4). The partial overlapping of the fan areas with the sediment bodies is not relevant as a problem since the calculations are semi-quantitative. Geomorphological mapping showed that all slopes are covered by thick calcretes and in the lower segments partly by soils. Thus, an average sediment thickness of 0.8 m was estimated for the remaining slopes. Consequently, the material deposited in the vega bottom was calculated by the formula

$$V_{\text{vega}} = V_2 + V_3 + V_4 + V_5$$

The material in the remaining catchment areas ( $V_{\text{catchment}}$ ) was calculated by the formula

$$V_{\text{catchment}} = V_1 + V_6 + V_7 + V_8 + V_9 + V_{10} + V_{\text{af}} + V_s$$

where  $V_{1-10}$  represent sediment bodies in the valley,  $V_{\text{af}}$  the sediment stored in alluvial fans and  $V_s$  the sediment deposited on the slopes.

#### 4. Results: 4.4. Geomorphological investigations of sediment traps....

| Vega bottom ( $V_{\text{vega}}$ ) |                   | Remaining catchment area ( $V_{\text{catchment}}$ ) |                   |
|-----------------------------------|-------------------|---|-------------------|
| $V_2$                             | 1 185 890         | $V_1$   | 696 120           |
| $V_3$                             | 7 843 660         | $V_6$   | 6 151 370         |
| $V_4$                             | 6 819 200         | $V_7$   | 2 218 780         |
| $V_5$                             | 3 637 560         | $V_8$   | 502 740           |
|                                   |                   | $V_9$   | 258 390           |
|                                   |                   | $V_{10}$  | 511 960           |
|                                   |                   | alluvial fans ( $V_{\text{af}}$ )                   | 1 602 180         |
|                                   |                   | Slopes ( $V_s$ )                                    | 2 509 120         |
| <b>Sum</b>                        | <b>19 486 310</b> |   | <b>14 450 660</b> |
| <b>% of total volume</b>          | <b>57.4</b>       |   | <b>42.6</b>       |

TABLE 4.4.1. SEDIMENT VOLUMES STORED IN DIFFERENT STORAGEES (IN  $M^3$ ) IN FEMÉS.

**Micromorphological images** were interpreted after Stoops (2003) by Peter Kühn (University of Tübingen). Preparation of thin sections was executed after the method of Beckmann (1997).

**Electric conductivities** of sediment layers were measured by mixing 10 g of sediment with 50 ml of deionized water, and filtrating and measuring the filtrate with the conductivity electrode of a pH meter (inoLab, WAW).

**Wet sieving** yielded the grain size fractions of fine (63–125  $\mu\text{m}$ ) and coarse sand (250–2000  $\mu\text{m}$ ). Prior to sieving, an aliquot of 8–10 g (equidistant 5 cm) was treated with HCl and  $\text{H}_2\text{O}_2$  to remove carbonate and organic matter. After sieving, dried fractions were weighed and related to the total mass of the sample.

**X-ray diffraction (XRD) analyses** were used to determine quartz contents. Aliquots of 5 g (equidistance 10 cm) were ground in an agate mortar. Subsequently, carbonate was dissolved using 10% acetic acid at room temperature. Afterwards, the material was washed, dried, ground again and 2% Md-IV sulfide were added as a standard (Krischner 1990). Measurements were executed at a Siemens D 5005 diffractometer at the University of Potsdam (2s/point, 4–42°2 $\theta$ , Cu-tube FLCu-4KE), results were interpreted using the program MacDiff 4.2.5. on a Macintosh computer (Petschick 2000). For analysis, the highest peaks of Md-IV-sulphide (molybdenite) and quartz were used: for Md-IV-sulfide the peak at 14.39°2 $\theta$  and for quartz the peak at 26.67°2 $\theta$ . Absolute quartz contents were obtained applying a calibration curve consisting of 11 well defined quartz contents in an artificial mineral composite (feldspars, muscovite, olivine), spiked with 5% Md-IVsulphide.

**Age determinations** used luminescence dating, as discussed elsewhere (Suchodoletz et al. 2008).

#### 4.4.4. Studied sites

## **4. Results: 4.4. Geomorphological investigations of sediment traps....**

---

Three dammed palaeovalleys (vegas) were investigated on Lanzarote (figure 4.4.3). The flat valley slopes underwent a long-term alteration with several soil forming periods as could be seen in polygenetic calcretes (figure 4.4.2). The valley bottoms are filled with quartz-rich sediments, thus indicating that they mainly consist of Saharan dust and to a minor degree of volcanic material including bombs, lapilli and ashes (Jahn 1988, Zöller et al. 2004).

### ***4.4.4.1. Vega of Femés***

The vega of Femés is a SW to NE oriented palaeovalley with a length of about 3 km in the Los Ajaches Massif in the south of Lanzarote (figure 4.4.3). According to datings of volcanites originating from the same volcanic group as those that form the damming of the vega (Coello et al. 1992, Instituto Tecnológico y Geominero de España 2005), this damming occurred about 1.0 Ma ago and lasted until recent time. The valley bottom is situated about 300 m a.s.l. The catchment area extends about 5.07 km<sup>2</sup> whereof 18.4% are covered by the recent valley floor, giving a ratio of 5.4:1 (figure 4.4.3). The northwestern slopes are on average two times higher than the southeastern ones and reach up to 200 m relative height above the valley bottom.

The topography is characterized by steep slopes, a nearby erosion base and relatively simple catchment topography. Although most of the valley bottom is filled up with horizontally deposited sediments, alluvial fans are common along the margin. The contact between valley bottom and slopes is abrupt. However, lower footslopes even in case of steep slope angles are covered by well preserved soils, which thin out upslope within a few metres.

### ***4.4.4.2. Vega of Teguisse***

The Teguisse sediment trap (vega de San José) is a 3 km long north–south directed palaeovalley at the southern margin of the Famara Massif in the north of Lanzarote (figure 4.4.3). Volcanic damming in the south occurred about 1.2 Ma ago (Instituto Tecnológico y Geominero de España 2005) and was not complete, as was detected during geomorphological mapping. The valley bottom is situated at about 300 m a.s.l. Surrounding slopes reach about 100 m above the bottom. They are obviously gentler and the topography is simpler compared with the geomorphic situation in Femés. The contact between valley bottom and slopes is gentle. However, the slope toes are covered with clayey reddish soil sediments, which thin out upslope within a few meters. The catchment area extends over 3.8 km<sup>2</sup>, whereof 35% are covered by the recent valley floor yielding a ratio of 2.9:1 (figure 4.4.3). Due to incomplete damming, temporarily discharge of sediments happened and the sedimentary sequences show a conspicuous hiatus, close to the damming in the south of the vega.

### ***4.4.4.3. Vega of Guatiza***

The vega of Guatiza in northern Lanzarote is a flat area situated at the southeastern foot of the Famara Massif close to the mouth of a canyon draining the highest parts of the volcanic complex reaching

#### **4. Results: 4.4. Geomorphological investigations of sediment traps....**

---

about 670 m a.s.l. (ig. 4.4.3). The valley bottom is at about 100 m a.s.l. To the east, the vega was dammed by a chain of younger volcanoes whose ages are described as Holocene (Instituto Tecnológico y Geominero de España 2005). However, thermoluminescence (TL) dating of heated palaeosols point to a damming 170 ka ago (Suchodoletz et al., in preparation). Since damming was not complete to the north, the calculation of the ratio catchment-vega bottom is an approximation. A rough estimation yields a catchment area of about 10 km<sup>2</sup> whereof the valley bottom covers approximately 16%, resulting in a ratio of 6.2:1 (figure 4.4.3). Since this ratio is even higher than that in Femés, the sedimentation rate would be the highest of the three studied vegas. However, due to incomplete damming hiatuses could be expected which would lower the sedimentation rate.

#### **4.4.5. Results and discussion**

##### **4.4.5.1. Sedimentation system of the vegas**

###### *4.4.5.1.1. Connection between areas of erosion and deposition*

Geomorphological mapping of the whole catchment areas, supported in Femés by the sediment–mass balance of the vega system, demonstrates that depending on their geomorphology the coupling between erosional and depositional area is different in the three valleys.

In Femés, intermediate storage within the sedimentation pathway is limited to slopes covered by calcretes, foot slope positions, slope flattenings, tributary valley bottoms, the upper parts of the alluvial fans and most of the upper part of the main vega itself. Thus, from a total volume of about 34 million m<sup>3</sup> of sediment deposited in the vega system since damming 1.0 Ma ago a volume of 19.5 million m<sup>3</sup> was deposited in the vega bottom, whereas 14.5 million m<sup>3</sup> were deposited in storage positions of the catchment areas (see table 4.4.1). This means that only 42.6% of the material deposited in the catchment area is temporarily stored, whereas about 57.4% has definitely accumulated at the vega bottom. Since only 18.4% of the total material could have been deposited in the area of the vega bottom itself as in situ aeolian fallout, there must have been a significant contribution of colluvial material from the slopes in order to get the recent proportion of 57.4% of total sediment stored in the valley bottom. This yields a sediment delivery ratio from the remaining catchment area (without the valley bottom itself) into the valley bottom of around 48%, indicating that almost half of the sediment originally deposited on the slopes was reworked and is found in the vega bottom today, here forming 68.6% of the total vega bottom sediments. This demonstrates a high slope–vega connectivity.

In Tegui, sediment storage on the slopes is negligible apart from calcretes inherited from older soil forming processes. Thus, the sediment path leads more directly into the valley bottom than in Femés. As a consequence of the close slope–bottom connection, it is estimated that about 75% of the mobilized sediment from the catchment was deposited in the valley bottom.

Guatiza has a relatively large and branched catchment area with comparatively large flat areas. On the other hand, it shows a steep topography (450 m difference in altitude). It is assumed that slightly less

#### **4. Results: 4.4. Geomorphological investigations of sediment traps....**

---

than 50% of all mobilized sediments reach the vega bottom so that the coupling between erosional and depositional area is the least in this vega.

These results demonstrate that due to very steep vega morphologies a system of sediment cascades as observed in larger catchment areas generally plays a minor role in valley bottom sediment supply (e.g. Faust and Herkommer (1995) calculated a delivery ratio of only 8% in a catchment of Lower Andalusia). Due to the generally high slope–vega bottom connectivity the amount of sediment never exceeded the potential sediment transport capacity, so that calculations of the dependencies between geomorphologic features of the vegas and sedimentation in the vega bottoms are possible. Hence, the sedimentation rate in the vega bottom sediments directly increases with increasing catchment area when compared to the size of the vega bottom. This means that time resolution in the vegas is directly linked to the ratio catchment area/vega bottom surface. As an example, the much smaller ratio catchment area–vega bottom in Teguisse compared to Femés means that the sedimentation rate in the vega bottom should be much smaller in Teguisse. Hence, a sediment package in the same depth with a comparable thickness is much older and should have a lower time resolution in Teguisse when compared to Femés.

##### *4.4.5.1.2. Types of vega sediments and colluvial transport*

The material filling the valleys consists of two different components:

- Saharan dust either brought by Calima winds or by the Saharan Air Layer (SAL)
- Volcanic material originating from local sources in form of ashes, lapilli and bombs

This material was originally deposited on the slopes and in the valley bottom. However, the valley bottom additionally received colluvial sediments (soils, volcanic material and Saharan dust) reworked from the slopes, in the case of Femés almost 70% of total deposited sediment as shown in the calculations above. The importance of colluvial input during the studied periods is documented by several thin sections taken from different horizontally stratified sedimentary layers in the Vegas, since all show comparable colluvial characteristics (figure 4.4.7).

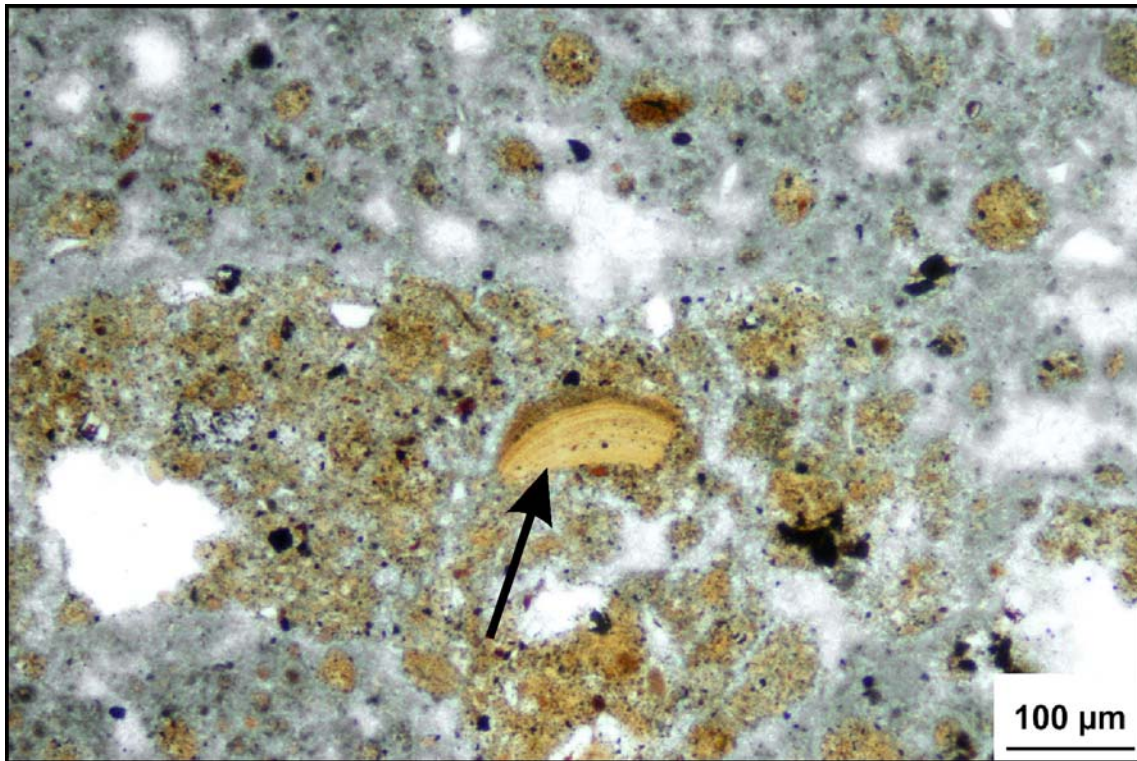


FIGURE 4.4.7. THIN SECTION OF A CARBONATIC HORIZON FROM FEMÉS SHOWING A LARGE PED FRAGMENT (ARROW) WITHIN THE FINE SILTY MATRIX.  
*Analysis by Peter Kühn.*

After deposition in the vega bottoms, sediments underwent postsedimentary overprinting (swelling and shrinking, secondary carbonate and iron–manganese precipitation, formation of soil aggregates, bioturbation). Hence, neither quantification of colluvial material in an individual layer nor discrimination between in situ and colluvial sediment layers is possible in the vega bottom sediments today.

Looking at horizontally stratified layers across the valley bottoms reveals that a general sorting from proximal to distal positions—relative to the surrounding slopes—took place during the erosional process. Thus the layer material is generally coarse near the slope but rapidly becomes finer (clayey-silty) towards the vega centre, independent of the magnitude of the erosional event. Thus, discrimination between material deposited in situ as aeolian and reworked material derived from colluvial input processes of different intensity is not possible in a more distal position from the slopes. This is demonstrated by the example from Femés shown in figure 4.4.8, where the depth plot of the fine sand content (63–125  $\mu\text{m}$ ) is similar to that of the total quartz content. Since quartz has an exclusively aeolian origin, variations of fine sand must be mainly controlled by Saharan dust whereas the erosional dynamics is not reflected here. Occasionally, this dust signal is overprinted by volcanic fallout, as can be seen between 220 and 400 cm (with strongest influence between 280 and 315 cm) where lapilli and volcanic ash caused two peaks in the fine sand depth plot (63–125  $\mu\text{m}$ ) which are paralleled by peaks in the coarse sand fraction (250–2000  $\mu\text{m}$ ) (figure 4.4.8). This demonstrates that grain sizes in the distal vega bottom sediments only display the variability of arid and humid periods

#### 4. Results: 4.4. Geomorphological investigations of sediment traps....

(variations of clay and silt) and the dynamics of aeolian dust input (fine sand), whereas the erosional dynamics is not impacting here.

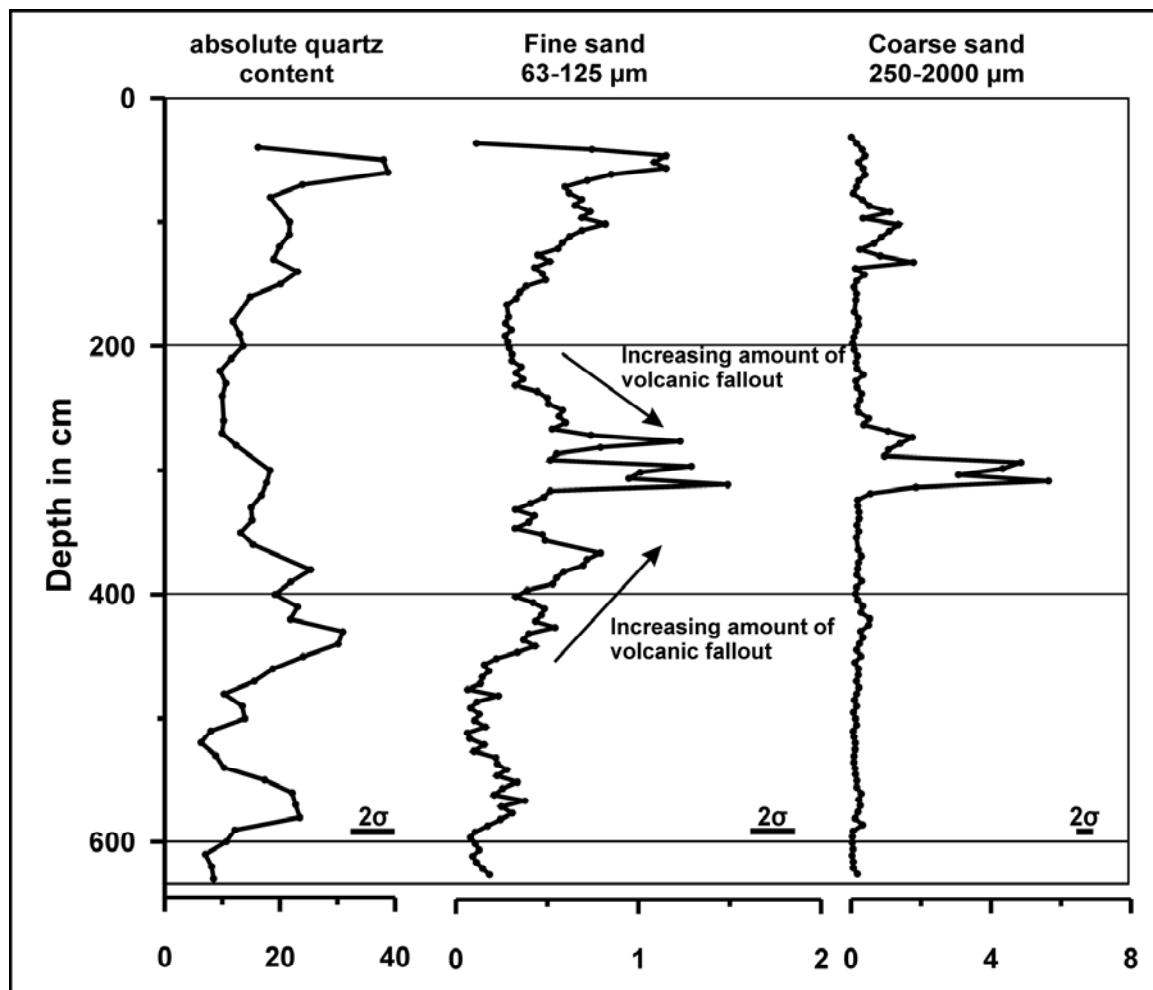


FIGURE 4.4.8. QUARTZ CONTENTS AND GRAIN SIZE FRACTIONS FROM A PROFILE IN THE CENTRE OF THE VEGA OF FEMÉS (IN %).

Error bars ( $2\sigma$ ) are given in the lower right parts of the graphs. Increasing influence of coarse volcanic fallout on the fine sand fraction is indicated with arrows.

When looking at the vega bottom sediments proximal to the slopes in order to reveal the erosional dynamics, it is conspicuous that in silty layers probably deposited during drier periods coarse volcanic material with a diameter of up to 10 cm is found. This material was probably eroded from the slopes since it thins towards the vega bottom as described above. In contrast, in clayey horizons probably originating from more humid periods the content of coarse, pebbly material is systematically negligible. This could indicate that erosional processes during drier periods were more intensive than those during more humid ones. However, this differentiation could at least partly be caused by the upward transport of pebbles to the palaeosurface in clayey, swellable material similar to processes occurring in Bt horizons of desert pavements. Once the sedimentation of clayey material stopped, the stones were stuck in the silty, not-swellable material where this process could not be active, thus generating the observed distribution of stone-rich layers (e.g. Springer 1958, Dan et al. 1982). Desert

#### **4. Results: 4.4. Geomorphological investigations of sediment traps....**

---

pavements, possessing a largely stone-free Bt-horizon underneath of the surface stone layer, cover large parts of Lanzarote today and thus prove the existence of such processes under local conditions.

##### *4.4.5.1.3. Case studies for sediment accumulation*

In order to better understand the sedimentation process of in situ aeolian and colluvial material into the vega bottom, different scenarios were constructed. The vega of Femés, due to its complete damming from the beginning, offers the best model conditions. It seems that comparable erosion and sedimentation processes took place in all other dammed vegas of Lanzarote. The scenarios assume that dust and ash fallout happened all over the catchment area at similar ratios. Subsequently, soils and/or fresh material were eroded and transported into the vega bottom. All scenarios are based on the ratio total catchment area/valley bottom of 5.4:1. That means, taking into account the ratio of 48% of eroded sediment reaching the valley bottom, that 32% of the sediment in the vega bottom was deposited here as in situ fallout. The remaining 68% of the material were eroded from the catchment area, yielding a ratio in situ/reworked sediment of 1:2.2. In situ and colluvial sediments cannot be distinguished in singular thin layers due to postsedimentary processes. Based on luminescence dates (Suchodoletz et al. 2008), the average sedimentation rate in the valley bottom of Femés between about 180 and 2.5 ka is ca. 3.2 cm/ka. Supposing a period of 10 ka, the whole sediment package would thus have a thickness of 32 cm of which 10 cm are in situ material and 22 cm are transported and deposited above. For this 10 ka- period, three different cases are proposed.

**Scenario I.** During a period of dry climate, material deriving from Saharan dust and to a minor degree from volcanic ash is deposited in the vega bottom and on the slopes. During this time no soil forming processes takes place. As a consequence of erosion, the vega bottom will be covered with unweathered in situ material (Av) and unweathered transported material (As) in a ratio of 1:2.2. The profile would exclusively contain sediments indicating arid conditions (figure 4.4.9a).

In this scenario, the frequency of erosion is supposed to be very high, as slopes in such an arid environment (recent precipitation in the vega catchment areas ca. 150–250 mm) are unstable over the whole period as shown in figure 4.4.10. This results in closely interbedded strata of in situ and colluvial unweathered material.

**Scenario II.** During a wetter climatic period, aeolian material is deposited in the vega bottom as well as on slopes. Soil formation happens symsedimentarily in the vega bottom and on slopes. After erosion, the sediment package in the vega bottom consists of in situ soil material (Bv) below redeposited soil sediment deriving from the slopes (Bs) in the ratio of 1:2.2. Both kinds of sediment indicate a wetter climate, but due to peloturbation they cannot be distinguished (figure 4.4.9b).

In contrast to scenario I, slopes would be vegetated and consequently more stable so that the frequency of erosion events should be reduced. Nevertheless, elevated precipitation compared to today also falls in a range of low geomorphic stability (figure 4.4.10). Furthermore, palaeoenvironmental research indicates that stable conditions in the northwest African area over a time span of more than 10 ka

#### 4. Results: 4.4. Geomorphological investigations of sediment traps....

---

would not be expected. Thus, a strong influence of climatic cycles like Heinrich-events and D-O cycles occurring with a high frequency of some ka on this region is reported from several studies (Cacho et al. 1999, Moreno et al. 2002a, Moreno and Canals 2004), which play an important role in this geomorphic environment instable even during generally wetter periods. Furthermore, high electric conductivity of the sediments (e.g. in Femés up to 571 and in Teguise to 2400  $\mu\text{S}/\text{cm}$ ) caused by the adjacency of the vegas to the sea permitted a dispersion of clayey material during the slightest runoff and thus soil sediments are easily mobilized. Consequently, although the frequency of erosion should be lower than in scenario I, steady state conditions over a time span of 10 ka are not assumed.

**Scenario III.** This case assumes that climate changes from dry to wet or vice versa occurred during a 10 ka lasting period. These cases are regarded in scenarios III-I and III-II.

(I) Assuming that climate will change from dry to wetter conditions, soils will be formed synchronously in the vega bottom and on the slopes during the wetter period. When erosion occurs, interbedded strata in the vega bottom form, consisting of unweathered in situ and colluvial material ( $A_v$  and  $A_s$ ) below in situ soil ( $B_v$ ) covered by eroded soil sediment ( $B_s$ ). As mentioned above, the in situ soil will mix with the overlying soil sediment. As a result, unweathered material ( $A_{v,s}$ ) will be covered by soil material ( $B_{v,s}$ ) in a ratio depending on the duration of each period (figure 4.4.9c).

(II) When climate changes from wetter to drier conditions, first soils will develop symsedimentarily in the deposited sediments in the vega bottom as well as on the slopes, whereas the latter is regularly eroded into the vega bottom. After climate changed, aeolian sediment will be deposited everywhere and not be overprinted by pedogenesis, and slope material will immediately be transported into the valley bottom. As a result, the vega bottom will have a layer consisting of in situ and colluvial soil ( $B_{v,s}$ ) mixed by peloturbation below interbedded unweathered in situ and colluvial material ( $A_{v,s}$ ). As in scenario III-I, the ratio between soil ( $B_{v,s}$ ) and unweathered material ( $A_{v,s}$ ) depends on the duration of each period (figure 4.4.9d).

#### 4. Results: 4.4. Geomorphological investigations of sediment traps....

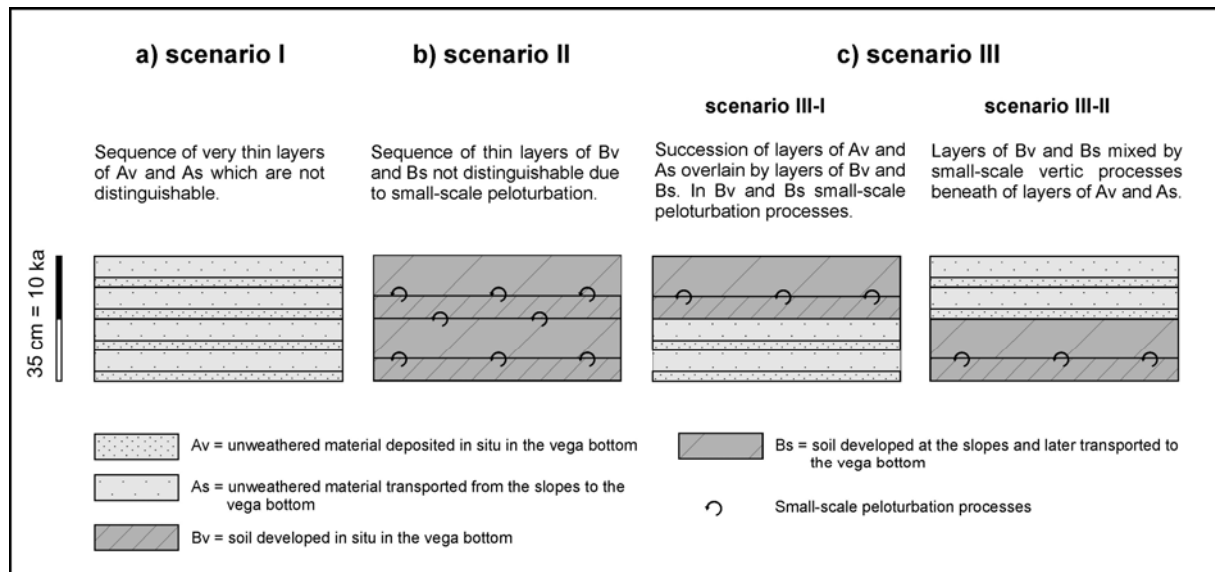


FIGURE 4.4.9. SEDIMENTATION SCENARIOS ASSUMING A TIME SPAN OF 10 KA AND A CONSTANT SEDIMENTATION RATE OF 3.5 CM/KA.

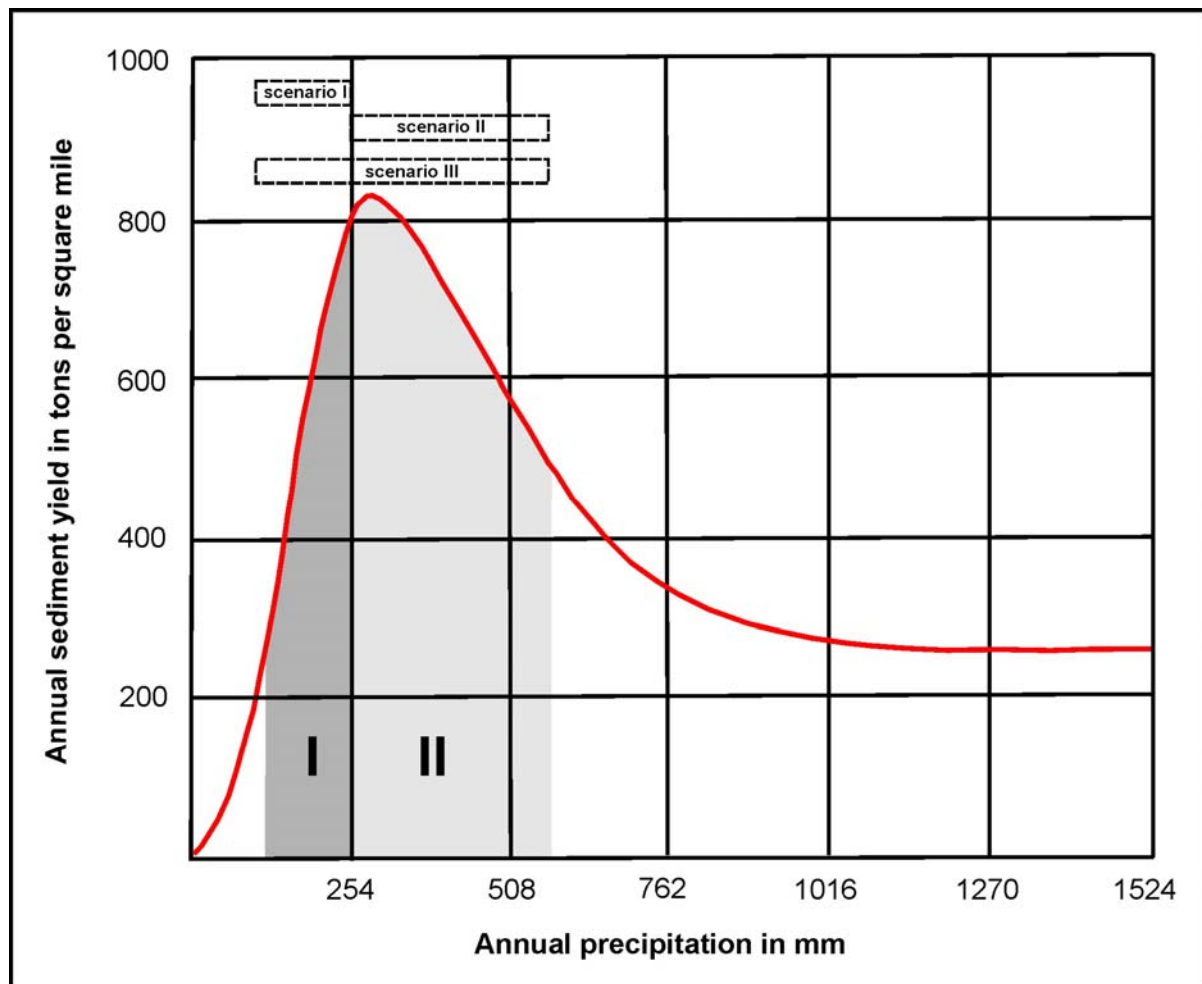


FIGURE 4.4.10. SEDIMENT YIELD CORRELATED WITH ANNUAL AVERAGE PRECIPITATION AND SEDIMENTATION SCENARIOS (DASHED RECTANGLES).

I = recent average precipitation in the vega catchment areas, II = assumed precipitation range during moister palaeoclimatic periods, III = assumed precipitation range during a change from moist to dry or vice versa  
After Langbein and Schumm (1958), modified.

### 4.4.5.2. *Palaeoenvironmental interpretation*

Knowledge about sedimentation processes and sediment budget of the vegas is useful when addressing different items of palaeoenvironmental research on Lanzarote.

#### 4.4.5.2.1. *Limitations of the resolution of palaeoclimatic events in vega sediments*

Understanding the interaction between in situ and colluvial sedimentation is crucial for correct palaeoclimatic interpretation, and even more important when considering the time resolution of palaeoclimatic events. The chronology of the vega sediments was established using optical and infrared stimulated luminescence, where partial insufficient bleaching during colluvial transport caused inaccurate zero setting of the luminescence signal. In consequence, dating errors are up to 10%, so that an age of 100 ka yields an error of about 10 ka (Suchodoletz et al. 2008). Although these luminescence ages are supported by correlations between similar proxies from the vegas and nearby marine cores as well as a stratigraphic correlation between different profiles (Suchodoletz et al. 2008), a climatic interpretation of sediments could only have a coarse temporal resolution. For younger sediments, due to smaller numerical dating errors of luminescence ages, climatic interpretability becomes naturally better. However, this improvement of time resolution for younger sediments has an intrinsic limit caused by the colluvial sedimentation process including time lags between sedimentation and colluvial transport as shown above. Therefore, resolution in scenario III including climatic shifts shorter than 10 ka (e.g. D-O cycles, Heinrich-events) is almost impossible. Consequently, due to regular colluvial input climatic proxies are expected to average the palaeoclimatic information of a level of some ka. Thus, only palaeoclimatic events that encompass at least this time span offer good possibilities for identification and interpretation.

Youngest sediments overlying an Early/Middle Holocene dust layer which were deposited since at least 2.5 ka are characterized by an extreme rate of material delivery into the valley bottom of Femés. In the central basin of the vega these sediments have a thickness of up to 75 cm as shown in figure 4.4.11, and reach up to 420 cm in the vega of Guatiza. Geoarchaeological studies (e.g. Atoche-Peña et al. 1995) report an intensified Roman colonization with strong pasturing of the slopes from ca. 2 ka BP. The intensive pasturing triggered accelerated erosion including a mobilization of material from sediment storages (filled during longer periods of the past) due to the high vulnerability of the instable semiarid ecosystem to anthropogenic activity. Since the anthropogenic sediment transport mechanism is completely different from that of the period before, this recently deposited material is not useful for palaeoclimatic interpretations based on the actualistic principle.

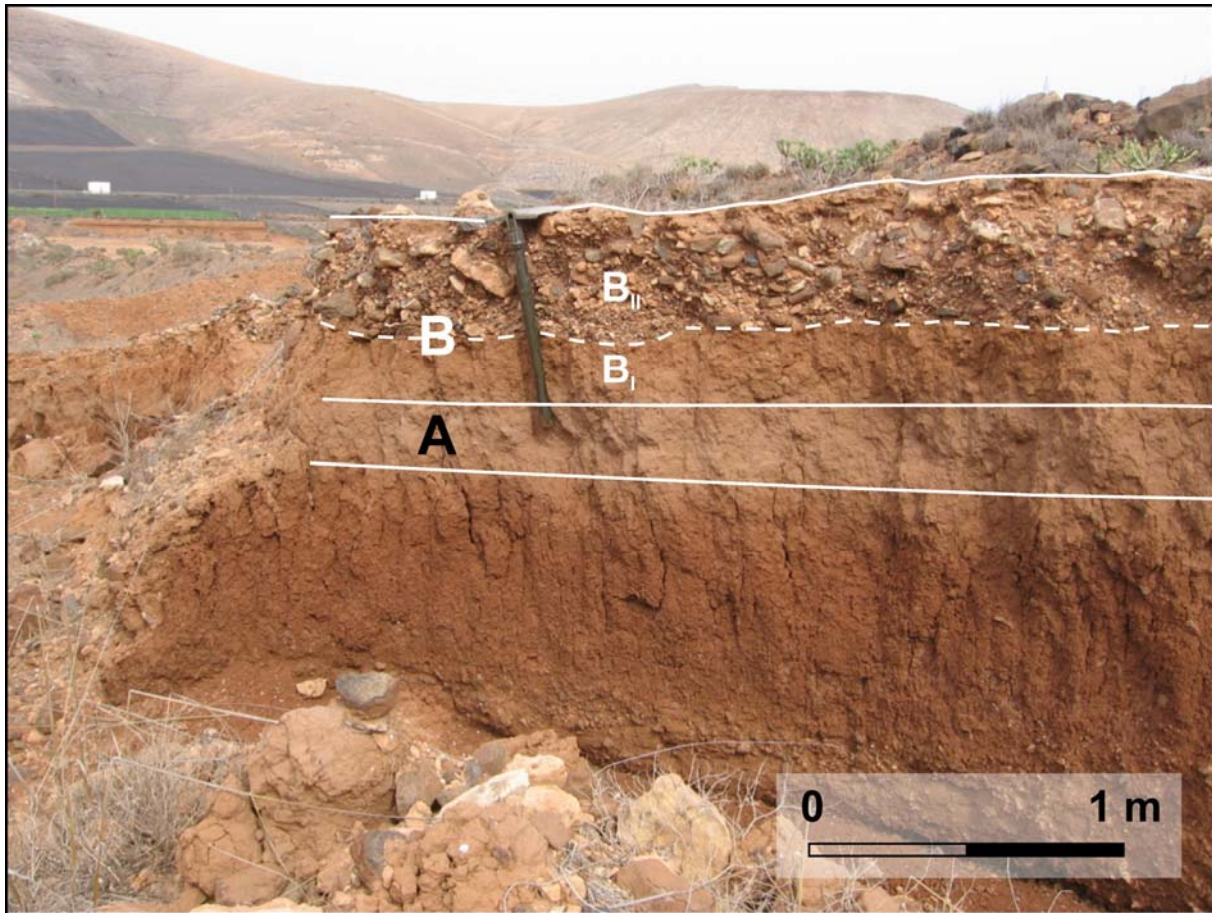


FIGURE 4.4.11. MIDDLE HOLOCENE LAYER DEPOSITED 8 TO 2.5 (OR 5) KA (A) BENEATH A YOUNG HOLOCENE COLLUVIUM CONSISTING OF TWO LAYERS (B<sub>I</sub> AND B<sub>II</sub>).

##### 4.4.5.2.2. Dynamics of Saharan dust input during the Quaternary

The export of Saharan dust to the North Atlantic has been a study issue for a long time. Thus, it is established that dust export from North Africa has existed since the Lower Cretaceous (Goudie and Middleton 2001). During the Neogene, dust export increased in parallel with the desiccation of the African continent, showing prominent steps at 6–5, 2.5 and between 1.6 and 1.2 Ma (Pflaumann et al. 1998, Goudie and Middleton 2001). However, a quantitative estimation for the development of dust input to the region of the Canary Islands during the Quaternary does still not exist. This problem is addressed using the sediment mass-balance of the vega of Femés.

The recent period is obviously one of the driest during the last 180 ka at Lanzarote (unpublished results). Furthermore, the landscape shows a high degree of anthropogenic destabilization. Nevertheless, vega bottoms still have a vegetation cover, and a geoarchaeologic study reports much moister conditions with a denser vegetation prior to Spanish influence starting from the 15th century (Santana-Santana 2003). Thus, remobilization of dust from the vega bottoms did probably not play an important role during most of the Quaternary, so that calculated dust deposition rates should correspond to real values. Assuming a continuous input for the whole period of 1.0 Ma, a total volume of 34 000 m<sup>3</sup> was in average deposited during 1 ka (cf. Chapter 4.4.5.1.1.). Converted to thickness (total catchment area 5.07 km<sup>2</sup>) this yields an approximate material deposition of 0.67 cm/ka over the

#### **4. Results: 4.4. Geomorphological investigations of sediment traps....**

---

whole catchment area. If this value was exceeded, the valley would have been filled up by now which is not the case. The deposited material is composed of Saharan dust and volcanic material. Thus, the average yearly deposition rate of 0.67 cm/ka for the whole catchment is the theoretically maximal value of dust deposition during the last 1.0 Ma. Comparing the average material deposition of 0.67 cm/ka in the vega catchment area during the whole period of the 1.0 Ma to a value of 1.0 cm/ka for the last 180 ka (derived from the sedimentation rate of 3.2 cm/ka in the valley bottom as described in Chapter 4.4.5.1.3), the former is much lower than the value for the last 180 ka, indicating an increase of dust sedimentation during the Early or Middle Pleistocene.

A persistent layer deposited during the Early/Middle Holocene shown in figure 4.4.11 has a thickness of about 20 cm in Femés and was deposited within at most 6 ka in the studied vegas (from about 8.5 to latest 2.5 ka, Suchodoletz et al. 2008). This yields an average in situ accumulation rate in the whole vega catchment area of 1.1 cm/ka. This accumulation rate in the vega bottom is much higher than the average accumulation rate of 0.67 cm/ka calculated for the last 1.0 Ma, and slightly higher than the average rate of ca. 1.0 cm/ka during the last 180 ka. New dating has shifted the eruption period of the Corona-volcano system (the last volcanic event prior to the 18th century) from formerly ca. 4–6 to 21 ka (Carracedo et al. 2003). Thus, there was no strong contribution of volcanic material during the Early and Middle Holocene, meaning that the value of 1.1 cm/ka must be close to the real sedimentation rate of Saharan dust during the Early/Middle Holocene. Furthermore, luminescence dates from Femés do not exclude the possibility that the sedimentation of this layer ended already ca. 5 ka, thereby limiting the period of its formation to ca. 3.5 ka and thus yielding a maximum possible accumulation rate of 1.8 cm/ka. Hence, Saharan dust sedimentation during the Early/Middle Holocene was probably somewhat elevated compared to the average of the period from 180 ka to the Holocene. This is in contrast to a study which reports a strongly reduced export of Saharan dust during the Early/Middle Holocene from 12 to 5.5 ka due to moist conditions in the Sahel area (de Menocal et al. 2000). Thus, a high dust input on the Canary Islands could also be forced by other factors than aridity, including a change of the origin of dust or human activity connected to destabilization in the dust mobilization area.

These results were compared with studies on recent Saharan dust accumulation on the Canary Islands: One study points to an actual dust accumulation rate between 1.3 and 6.6 cm/ka depending on the altitude, an average value between 4 and 2 cm/ka seems representative for the altitude of the catchment area of Femés (Menéndez et al. 2007). A pedologic study points to an accumulation rate of about 1.5 cm/ka during the last 260 a (Herrmann et al. 1996). On the other hand, model estimates indicate a recent dust fall of only 0.46 cm/ka for the geographic position of the Canary Islands (Prospero 1996), which seems to be an underestimate. Altogether, most results confirm that dust input on the Canary Islands intensified at the latest during the Early and Middle Holocene and obviously maintained this elevated level until the recent. Hence, the Holocene is a climate period with an exceptional high dust mobilization and a comparatively high morphodynamic activity compared to

#### **4. Results: 4.4. Geomorphological investigations of sediment traps....**

---

former periods. Summing up, the calculations show that the dust input to the Canary Islands increased during the last 1.0 Ma, whereas the highest values were reached at the latest during the Early/Middle Holocene lasting (and probably accelerating) until today.

##### **4.4.6. Conclusion**

Geomorphologic calculations supported by sedimentologic analyses and luminescence dating established a quantitative sediment-mass budget of volcanic sediment traps on Lanzarote. These investigations demonstrate that despite the colluvial transport system of the sediment traps on Lanzarote they can serve as palaeoclimate archives, although time resolution is limited to some ka. The youngest sediments deposited since at least 2.5 ka are climatically not interpretable, as they were mobilized by human activity rather than by climatic processes. These results will serve as a base for following palaeoclimatic analyses of the trapped sediments. Furthermore, the quantitative sediment budget together with luminescence dating allows an estimation of Saharan dust input to the Canary Islands, demonstrating that this strongly intensified during a large part of the Quaternary, cumulating since the Early/Middle Holocene.

##### **Acknowledgements**

The work of the first author was funded for two years by a post-graduate grant of the Free State of Bavaria, Germany, supplied by the University of Bayreuth. Further financial support was given by Deutsche Forschungsgemeinschaft (project Zo 51/29-1). We are especially indebted to Constantino Criado (Universidad of La Laguna de Tenerife) for supplying the GIS database. Daniela Sauer (University of Hohenheim) and Peter Kühn (University of Tübingen) did the investigation of thin sections. Melanie Kappes (University of Bayreuth) and Jens Schumann (GFZ Potsdam) helped us building the GIS-models of the vegas, Max Wilke and Beate Mocek (University of Potsdam) during XRD analyses. E. Mateo and A. Miguélez-López (Cabildo de Lanzarote) are thanked for their uncomplicated support and cooperation. H. Oberhänsli (GFZ Potsdam) is thanked for a critical review of the manuscript.

**4.5. Loess-like and palaeosol sediments from Lanzarote (Canary Islands/Spain) – indicators of palaeoenvironmental change during the Late Quaternary**

Suchodoletz, H. von<sup>1\*</sup>, Kühn, P.<sup>2</sup>, Hambach, U.<sup>1</sup>, Dietze, M.<sup>3</sup>, Zöller, L.<sup>1</sup> & D. Faust<sup>3</sup>

*This article is in press in Palaeogeography, Palaeoclimatology, Palaeoecology  
(doi:10.1016/j.palaeo.2009.03.019).*

<sup>1</sup>Chair of Geomorphology, University of Bayreuth, Germany

<sup>2</sup>Institute of Geography, Chair of Physical Geography, Eberhard Karls University of Tübingen, Germany

<sup>3</sup>Institute of Geography, Technical University of Dresden, Germany

\*corresponding author

Hans.vonSuchodoletz@uni-bayreuth.de

tel: +49-921552266

fax: +49-921552314

**Abstract:**

On Lanzarote (Canary Islands) Quaternary Saharan dust and weathered local volcanic material were trapped in Miocene to Pliocene valleys dammed by younger volcanic edifices. These sediments show sequences of alternating reddish/clayey and loess-like yellowish/silty material. In order to investigate if reddish/clayey layers contain material derived from local pedogenesis and if so, which pedogenetic processes were active, we performed sedimentological, micromorphological and environmental magnetic analyses. The analyses demonstrate that these layers contain material derived from local soils. These soils were characterised by clay formation, rubefication and the formation of superparamagnetic particles during periods of enhanced soil moisture. Thus, they can serve as natural archives in order to reconstruct the terrestrial palaeoclimatic history of Lanzarote. The distribution of soil material in the profiles shows that cold periods of the Late Quaternary were characterised by more humid conditions than today. Using palaeontological remains and a comparison with recent soils on Tenerife, we can roughly estimate maximal palaeoprecipitation values during more humid periods.

**Keywords:** Canary Islands, Saharan dust, pedogenesis, geomorphology, palaeosols, micromorphology, environmental magnetism, X-ray diffraction, soil moisture

**4.5.1. Introduction**

#### **4. Results: 4.5. Loess-like and palaeosol sediments – indicators of palaeoenvironmental change...**

Loess-palaeosol sequences are important terrestrial palaeoclimate archives for the past few million years as documented by numerous multiproxy-studies from both hemispheres (e.g. Bronger 1976, Maher and Thompson 1992, Dodonov and Baiguzina 1995, Antoine et al. 2001, Schellenberger and Veit 2006). In these sediments, palaeosol horizons are formed by various pedogenetic processes such as clay formation, rubefication or humus accumulation and indicate enhanced soil moisture compared to periods when unweathered loess was deposited. Enhanced soil moisture indicates a more positive landscape water budget and is therefore connected to more humid climate conditions (e.g. Bush et al. 2004, Carter-Stiglitz et al. 2006). Pedogenetic processes and thus the intensity of pedogenesis in such sequences can be traced back using variations of several proxies, e.g. clay content, clay mineral assemblages, carbonate contents, isotopic composition of organic matter and soil carbonates, micromorphological features or environmental magnetic parameters (e.g. Bronger and Heinkele 1989, Heinkele 1990, Junfeng et al. 1999, Hatté et al. 2001, Maher et al. 2002, Markovic et al. 2008).

Enviromagnetism, the magnetism of sediments and soils, describes the occurrence, abundance and properties of iron-bearing minerals in the environment. Magnetic grains, exclusively iron oxides/hydroxides and sulphides, occur virtually ubiquitously in Quaternary sediments, soils, dust and organisms, albeit often in minor or trace concentrations. After sedimentation and/or reworking, they undergo diagenesis and pedogenesis when, for example, more humid conditions predominate. This can result in their transformation, depletion, neo-formation or enhancement. Ferrimagnetic minerals in particular react several orders of magnitude more strongly in ambient laboratory magnetic fields than other iron-bearing minerals. These minerals control the magnetic properties of sediments or soils even when present in very small amounts. Since climate changes and human activity produce changes in sedimentary and soil-forming environments, magnetic properties from a wide range of marine and continental sedimentary archives reflect alternating warm/humid and cold/dry climates during the Quaternary (e.g. Walden et al. 1999, Hambach et al. 2008).

The properties of a magnetic assemblage depend not merely on the composition of the minerals, but largely on the grain size distribution of the particles. For a given mineral, initial magnetic susceptibility ( $\kappa$ ) varies over orders of magnitude depending only on grain size.  $\kappa$  is largest for very fine superparamagnetic (SP) particles (roughly  $< 30$  nm), is reduced for single domain (SD) grains and increases again for multi domain grains (roughly  $> 140$  nm, valid for magnetite), although not reaching the values of superparamagnetic particles (e.g. Evans & Heller 2003). Nowadays, essentially three models of the origin of ultrafine superparamagnetic minerals are discussed. (i) Firstly, large magnetic mineral grains may be decomposed or even “split” into smaller grains by weathering processes, producing large amounts of superparamagnetic particles when a relatively high concentration of magnetic minerals is present (Maher 1998, van Velzen & Dekkers 1999). (ii) Secondly, bacteria produce extracellular superparamagnetic Fe-minerals in different sedimentary or soil environments, a process obviously omnipresent in soils (Maher 1998). Fassbinder et al. (1990) first demonstrated the occurrence of so-called magnetotactic bacteria in soils. These bacteria produce

#### **4. Results: 4.5. Loess-like and palaeosol sediments – indicators of palaeoenvironmental change...**

intracellular low susceptible, but highly magnetic particles in the single domain state as means of spatial orientation, thereby causing magnetic enhancement as observed in non-volcanic soils. (iii) Thirdly, recent works of Torrent et al. (2006) and Liu et al. (2008) demonstrate the importance of the ferrihydrite → hydromaghemite → hematite transformation. This transformation may constitute a major pathway accounting for the magnetic enhancement in many soils. The production of superparamagnetic hydromaghemite particles concurrently increases both the initial and frequency dependent magnetic susceptibility.

The Saharan desert is the largest source of dust in the world, contributing about 50% of all mobilised mineral aeolols (Aléon et al. 2002). This dust accumulates in the circum-Saharan area and is called “warm” or “desert” loess, in contrast to lithologically similar deposits in boreal and temperate zones derived from material mobilised by periglacial processes (e.g. Yaalon and Bruins 1977, Coudé-Gausson 1991, Wright 2001, Dearing et al. 2001).

About 30-50% of the dust originating from the Saharan desert is transported to the Atlantic Ocean (Goudie and Middleton 2001, Prospero and Lamb 2003). The Canary Islands are located at the northern fringe of this Atlantic Saharan dust plume, and aerosol deposition is well documented since the Middle Pleistocene (Moreno et al. 2001, Bozzano et al. 2002). On Lanzarote, Saharan dust and volcanic material are trapped in valleys which have developed in Miocene to Pliocene volcanic massifs and were at least partly dammed by younger volcanic material during the Early to Middle Pleistocene (Instituto Tecnológico y Geominero de España 2005, Coello et al. 1992). The trapped sediments show alternating distinct beds of reddish/clayey and loess-like yellowish/silty material. Previous soil studies in Lanzarote mainly focussed on slope sediments (Jahn 1988, Zarei 1989, Schüle et al. 1989), whereas the sequences developed in valley positions and exposed in profiles up to 7 m thickness (Zöller et al. 2003) have not yet been the focus of pedostratigraphical investigations. Recent geomorphological investigations revealed that a part of these valley sediments were directly deposited as aeolian fallout, whereas the larger part was colluvially reworked from the slopes. Both types of sediment alternate frequently (high frequency/low magnitude) and are partly mixed by vertic peloturbation processes, thus appearing as homogenous layers today (Suchodoletz et al. 2009a). The fact that erosion occurred with high frequency and low magnitude is demonstrated by a recent (and as demonstrated in this paper, past-) precipitation regime causing high landscape instability (cf. Langbein and Schumm 1958). It is further demonstrated by the largely continuous sedimentation rate found in the valley base. This is revealed by luminescence datings, yielding sediment ages ranging from Holocene to Mid-Pleistocene (> 180 ka)(Zöller et al. 2003, Suchodoletz et al. 2008).

We propose that the alternation of loess-like yellowish/silty and reddish/clayey layers reflects differing periods of weathering on the island, regardless of the geomorphic position of the material (slope, valley) during weathering. Therefore, these sequences should reflect climatic changes, where properties such as reddish color and high clay content developed during more humid periods (Zöller et al. 2003, Suchodoletz et al. 2009a).

#### 4. Results: 4.5. Loess-like and palaeosol sediments – indicators of palaeoenvironmental change...

In this paper, we apply various sedimentological and pedological methods such as investigations of clay content, environmental magnetic parameters (measurement of initial and frequency dependent magnetic susceptibility as well as remanence properties), clay mineral composition and micromorphological features, in order to understand pedogenetic properties and processes. Based on this understanding, we are able to attempt a reconstruction of palaeoenvironmental conditions.

##### 4.5.2. Geographic setting

Lanzarote is the northeasternmost of the volcanic Canary islands, and is situated 130 km off the coast of NW Africa between 28°50' to 29°13'N and 13°25' to 13°52'W (figure 4.5.1). Volcanism started during the Miocene about 15.5 Ma ago and lasted until recent (1730-36 last volcanic eruptions) (e.g. Carracedo et al. 1998). Both the northern and the southern part of the island are dominated by Miocene to Pliocene volcanic massifs. Volcanism is basic, forming basalts and pyroclastics (cf. Rothe 1996). Consequently, Jahn (1988) and Mizota and Matsuhisia (1995) demonstrate that all quartz found on the island must have an allochthonous origin.

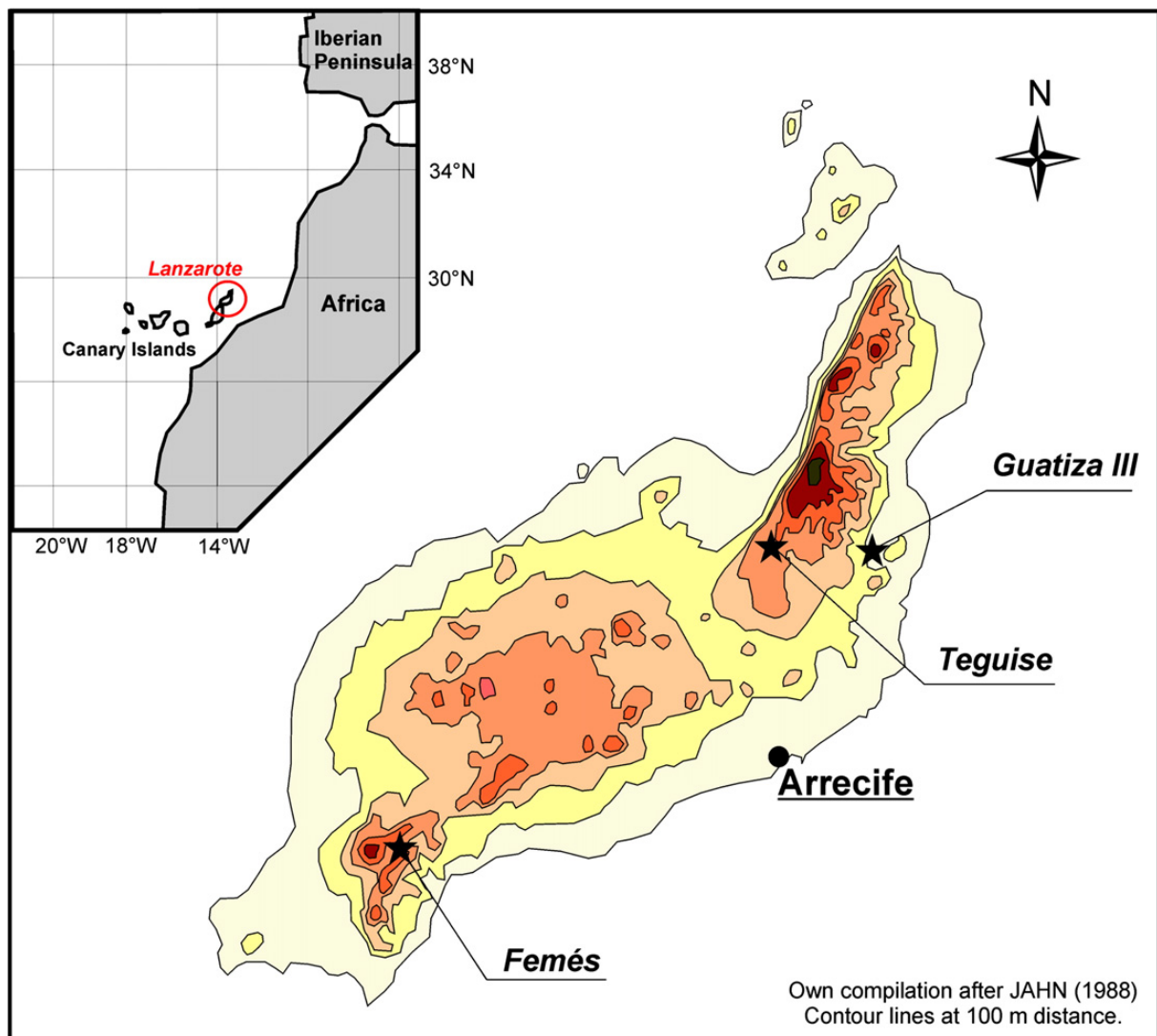


FIGURE 4.5.1. LOCATION OF LANZAROTE AND STUDIED SITES

#### **4. Results: 4.5. Loess-like and palaeosol sediments – indicators of palaeoenvironmental change...**

Due to strong erosion, the relief of Lanzarote is generally smooth with concave slopes. The maximal altitude of the island is only 670 m. Several phases of soil forming processes resulted in the formation of polygenetic calcretes exposed along the slopes through erosion. The volcanic complexes in the north and the south of the island are separated by a central part exhibiting a smoother topography, and they are further dissected by numerous U-shaped valleys and smaller gullies. Some of the larger valleys were dammed by volcanic material (lava flows, pyroclastica) during the Early and Middle Pleistocene and thus served as sediment traps for Saharan dust and local volcanic material. On Lanzarote, these dammed valleys are called vegas.

The climate of Lanzarote is maritime-semiarid. Due to the limited elevation of the island, Lanzarote gets no precipitation from orographically raising trade wind air. Thus, it receives only very sparse precipitation from boreal winter cyclones, ranging from 100 to 250 mm/a and decreasing from higher to lower altitudes. Mean annual temperature at sea level is  $19.9 \pm 3^\circ\text{C}$  (Jahn 1988). The vegetation is very sparse, shrubby and disperse, dominated by xerophytic and halophytic species. The vegetation cover is mainly controlled by anthropogenic activity (Jahn 1988, Kunkel 1993).

Saharan dust is brought to the island mainly during two different synoptic situations: During winter, Calima events advect dust at low latitude (0-1500 m) to the archipelago. Calima-winds are continental African Trade winds (Harmattan) deflected towards the west by Atlantic cyclones situated close to the Canary Islands (cf. Criado and Dorta 2003). During summer, dust is transported to latitudes north of the Canary Islands by the northern branch of the Saharan Air Layer which is active within an altitude of about 1500 to 5500 m a.s.l. There, the material advects into the lowermost troposphere and is finally transported towards the island by the Northeast Trade wind (cf. Koopmann 1981, Bozzano et al. 2002). Finally, dust sedimentation is either by dry or wet deposition (Criado and Dorta 2003, Menéndez et al. 2007).

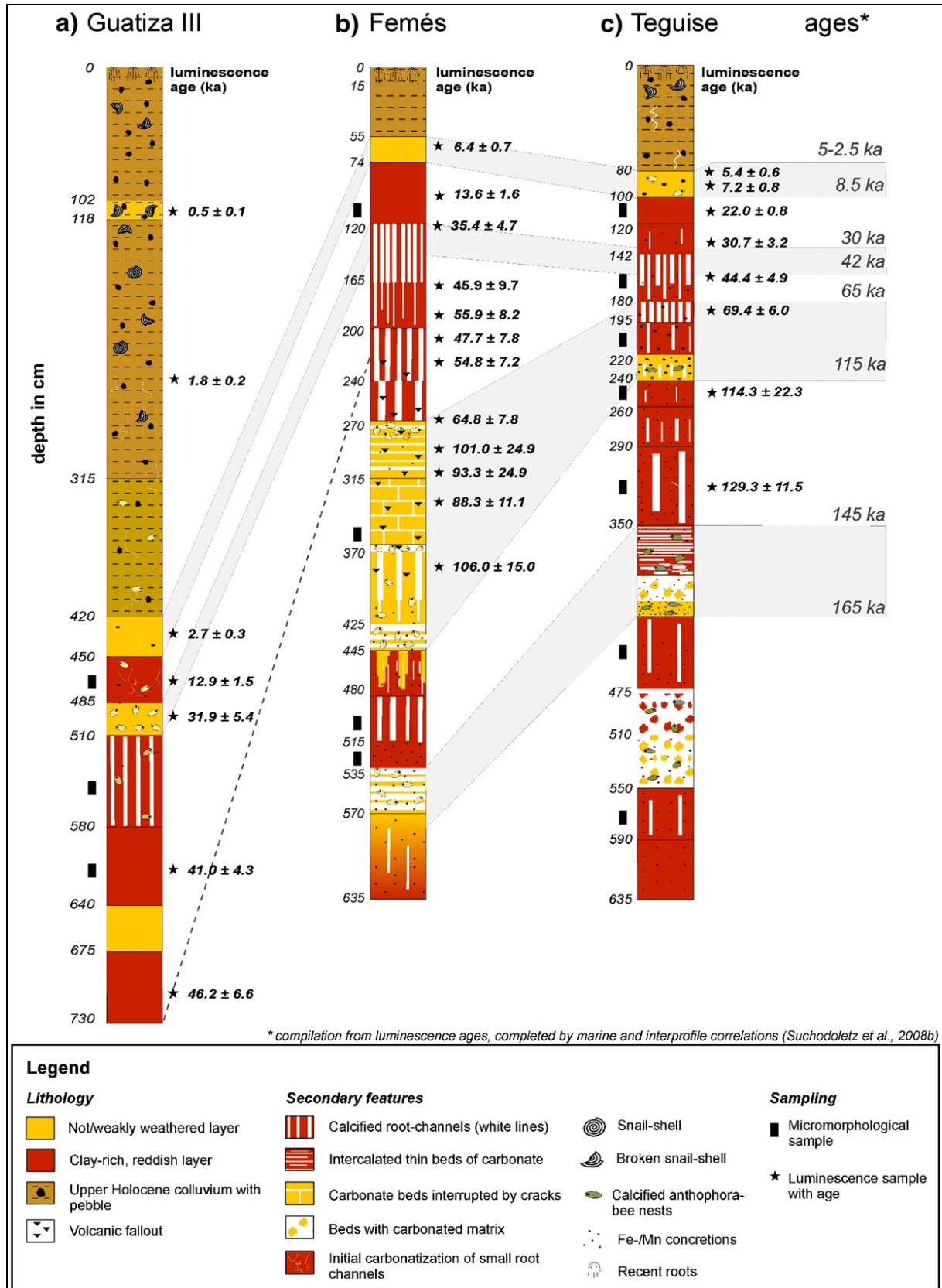
##### **4.5.3. Studied sites**

Three vegas in the north and the south of Lanzarote were investigated (figure 4.5.1, table 4.5.1). The valley slopes underwent long-term alteration through several soil forming periods, as evidenced by polygenetic calcretes, and thus have a flat shape. The profiles investigated are taken from sites remote from geomorphic active slopes. The sediments consist of a mixture of in situ and reworked fluvioaeolian material, derived from both allochthonous Saharan dust and from autochthonous volcanic material. High quartz contents in the sediments (Jahn 1988, Zöller et al. 2004) indicate that Saharan dust is the main contributor. The sequences are characterised by a change of reddish/clayey and loess-like, yellowish/silty layers. Several layers exhibit carbonate nodules as well as calcified root channels and vertical cracks, in some cases hardened to calcrete horizons. Loess-like layers in particular show ferromanganese concretions up to 2 cm in diameter or calcified nests of ground-nesting anthophora bees (figure 4.5.2). The upper parts of the sequences are characterised by

#### 4. Results: 4.5. Loess-like and palaeosol sediments – indicators of palaeoenvironmental change...

anthropogenically influenced colluvial deposits of varying thickness, some containing ovicaprid bones (Zöller et al. 2003, Suchodoletz et al. 2009a).

Details of the studied sites are listed in table 4.5.1.



#### 4. Results: 4.5. Loess-like and palaeosol sediments – indicators of palaeoenvironmental change...

FIGURE 4.5.2. INVESTIGATED PROFILES WITH LUMINESCENCE AGES

|   | Guatiza             | Femés               | Teguisse            |
|---|---------------------|---------------------|---------------------|
| latitude N  | 29°04'08''          | 28°55'32''          | 29°04'52''          |
| longitude W   | 13°29'22''          | 13°45'19''          | 13°30'55''          |
| altitude (m a.s.l.)                                     | 100                 | 300                 | 300                 |
| catchment area (km <sup>2</sup> )                       | 10.1                | 5.07                | 3.8                 |
| valley bottom (% of catchment area)                     | 16.1                | 18                  | 35                  |
| relative elevation difference in the catchment area (m) | > 550               | 100-200             | 100                 |
| time of volcanic damming                                | 170 ka <sup>1</sup> | 1.0 Ma <sup>2</sup> | 1.2 Ma <sup>3</sup> |
| volcanic damming complete?                              | no                  | yes                 | no                  |
| thickness of anthropogenic colluvial deposits (cm)      | 420                 | 55                  | 80                  |

TABLE 4.5.1. PROPERTIES OF STUDIED SITES ON LANZAROTE.

<sup>1</sup> consistent thermoluminescence and ESR data, Suchodoletz *et al.* (in preparation)

<sup>2</sup> Instituto Tecnológico y Geominero de España (2005), Coello *et al.* (1992)

<sup>3</sup> Instituto Tecnológico y Geominero de España (2005)

#### 4.5.4. Methods

**Grain size analyses** were performed in two different ways:

- For relative analyses, sediment samples were collected in an equidistant interval of 5 cm. 10 g of sediment were treated with 10 and 30% HCl at 65°C to remove carbonate and dolomite. Subsequently, organic carbon was destroyed using 32% H<sub>2</sub>O<sub>2</sub>. Sand was removed by wet sieving, and the fraction < 63 µm was treated for some hours in an ultrasonic bath to desintegrate abundant aggregates containing clay and ferromanganese oxides and -hydroxides which would strongly bias the grain size results (figure 4.5.3). After adding 0.1 M sodium pyrophosphate and subsequent shaking for 24 h in order to disperse clay particles, the samples were measured using a Malvern 2600C Analyser at GFZ Potsdam/Germany. For interpretation, the mean of three successive measurements recording 32 grain size classes was taken. Following Konert and Vandenberghe (1997), we used a conspicuous inflection point of the grain size distributions separating the first dominant peak from the following, thus obtaining a limit clay/silt of 6.18 µm. In order to get the weathering signal, the ratio of clay and the fraction < 42 µm was taken to remove the signal of coarse silt. Coarse silt and fine sand show very similar depth functions, and due to their smaller specific surface they are believed not to contribute to weathering on the island as strongly as fine/middle silt (cf. Helgeson *et al.* 1984).

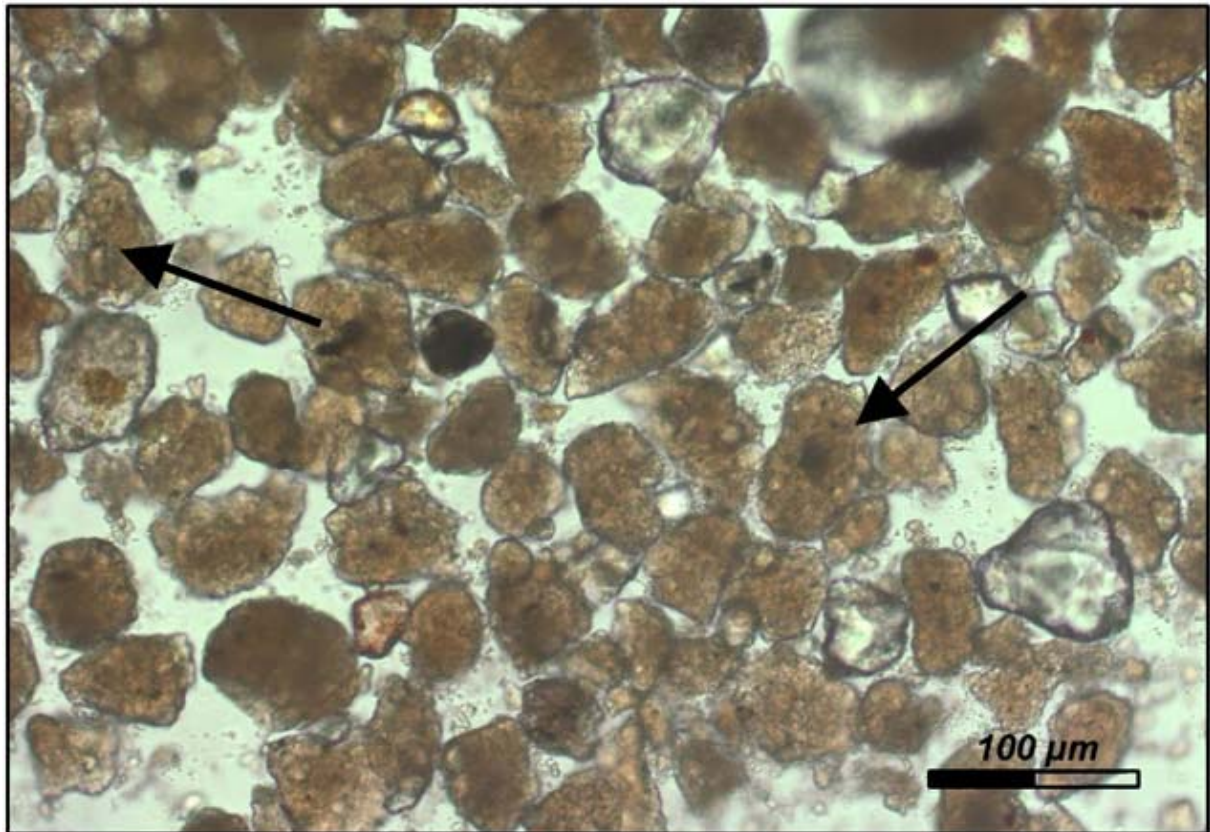


*FIGURE 4.5.3. DARK-BROWN AGGREGATES INCLOSING SMALLER GRAINS IN THE SIEVED AND HCL-TREATED FRACTION < 63 μm FROM A REDDISH CLAY HORIZON IN FEMÉS (230 CM). Two examples are marked with arrows.*

- Absolute clay contents from selected layers in Femés were determined using pipette analyses (cf. Konert and Vandenberghe 1997). A suspension of 20 g pretreated and sieved sample material < 63 μm and of 1 l deionized water was filled into a Koehn-cylinder and shaken. Aliquots of clay, fine, middle and coarse silt were taken from the suspension at time intervals determined by Stoke's law. Obtained aliquots were dried and weighed and related to the original sample weight.

**Environmental magnetic analyses** were carried out on bulk samples taken in a distance of 5 cm. The dried sediment was packed into plastic boxes, and subsequently compressed and fixed with cotton wool in order to prevent movement of sediment particles during measurement before closing the lid. The sediment mass served as a normalizer. Because the original in situ sediment density and the exact volume of the boxes were unknown, we assumed an average density of  $1.7 \cdot 10^3 \text{ kg}\cdot\text{m}^{-3}$  in order to calculate volume susceptibility ( $\kappa$ ).

The initial low field susceptibility was measured in an AC-field of 300 A/m at 920 Hz using the KLY-3-Spinner-Kappa-Bridge (AGICO, Brno, Czech Republic). The frequency dependence of susceptibility ( $\kappa_{fd}$ ) was determined with a MAGNON Susceptibility Bridge (MAGNON, Dassel, Germany) at AC-fields of 80 A/m at 1 and 8 kHz respectively ( $\kappa_{fd} = (\kappa_{@1\text{kHz}} \cdot \kappa_{@8\text{kHz}}) / \kappa_{@1\text{kHz}} \cdot 100$  in %). In order to investigate the remanence properties we exposed the samples to pulse-fields of 2 T and 0.35 T (antiparallel), respectively, using a Magnon PM II pulse magnetizer (MAGNON, Dassel,

#### **4. Results: 4.5. Loess-like and palaeosol sediments – indicators of palaeoenvironmental change...**

Germany). Acquired remanence (isothermal remanent magnetization, IRM@2T) was subsequently measured with a JR6-spinner magnetometer (AGICO, Brno, Czech Republic).

Analyses with *X-ray diffraction (XRD)* were performed using bulk and clay samples:

- For X-ray analyses of bulk material, aliquots of 5 g were taken from samples collected in an equidistance of 10 cm and ground in an agate mortar. In order to improve the peak intensity of investigated minerals, carbonate was dissolved at room temperature using acetic acid (10%). The air dried material was then ground again. In order to get semi quantitative mineral contents, 2% Md-IV sulfide was added as a standard (Krischner 1990). Measurements were performed with a Siemens D 5005 diffractometer at the University of Potsdam with 2s/point from 4 to 42°2 $\theta$ , using the Cu-tube FLCu-4KE. Interpretation was executed using MacDiff 4.2.5. software on a Macintosh computer (Petschick 2000). For analysis, we used the highest peaks of the investigated minerals: For Md-IV-sulfide the molybdenite peak at 14.39°2 $\theta$ , for quartz the peak at 26.67°2 $\theta$ , for kaolinite the peak at 12.34°2 $\theta$  and for illite the peak at 8.84°2 $\theta$ . The relative amounts of kaolinite and illite were obtained from the ratio mineral/standard of the peak areas. In order to obtain the absolute quartz content, a calibration-curve was constructed using 11 different contents of quartz in an artificial composite of feldspars, muscovite and olivine, spiked with 5% Md-IV-sulfide. The linear regression-curve yields the equation  $y = 0,138*x + 3.07$  ( $R^2 = 0.99$ ). The intersect >0 reflects that a main-peak of muscovite is close to the investigated quartz-peak. Given that the amount of the various minerals in the standard is constant, this effect was non-significant and the regression quartz/sulphide ( $y = 0.138*x$ ) was used for further calculations.
- In order to analyse the clay fraction of selected samples from Femés (50, 170, 205, 485, 525 and 580 cm), aliquots of 7 g were dispersed and the fraction < 2  $\mu$ m was separated. The suspension was poured on a glass slide allowing the clay minerals to orientate. Measurements were executed at a Seifert XRD C 3000 TT diffractometer (CuK $\alpha$ , 40 kV, 30 mA, 2,5-30,01°2 $\theta$ ; step scan 15,0 s; step size 0,03°) at Dresden University of Technology. Samples were measured three times after each of the following preparation steps: air drying, solvation with ethylene glycol (48 hours) and heat treatment (2 h at 550°C). Interpretation was completed using the programme Siemens Diffracplus BASIC 4.0#1.

In order to obtain *carbonate contents* from samples equidistantly sampled every 10 cm, we determined total carbon (TC) and total organic carbon (TOC) contents using an Euro Vector EA3000 Elemental Analyser at GFZ Potsdam/Germany. For TC around 10 mg sample material was wrapped into tin capsules and combusted under oxygen supply at > 1000 °C. After combustion, CO<sub>2</sub> was separated in a gas chromatographic column and detected by thermal conductivity. For TOC analysis, around 3 mg of sample material were weighed into Ag-capsules, dropped with 20% HCl, heated for 3 h at 75°C, finally wrapped in the Ag-capsules and measured with the EA3000. Calibration was

#### **4. Results: 4.5. Loess-like and palaeosol sediments – indicators of palaeoenvironmental change...**

performed with the elemental standard “Urea” and verified with a soil reference sample (Boden2). The reproducibility for replicate analyses is 0.2 %. Inorganic carbon was calculated by subtraction of organic from total carbon. Finally, carbonate contents were determined by multiplying inorganic carbon contents with a stoichiometric factor of 8.33.

***Pedologic analyses*** at Dresden University of Technology included measurements of pH values, electric conductivity and Na-saturation. We analysed from all three profiles one sample per distinct lithological bed (figure 4.5.2). In order to determine pH values, 20 g of the samples were mixed with a 0.1 n KCl solution and measured with a pH meter (inoLab, WAW). We determined electric conductivity (EC<sub>s</sub>) by soaking 10 g of sediment in 50 ml of deionized water, filtering the suspension and subsequently determining the conductivity with a conductivity electrode (Tetra Con 325). For measurements of Na-saturation, 10 g of sediment were soaked in a BaCl<sub>2</sub>-triethanolamin solution at pH 8.1 and subsequently filtered. Afterwards, Ca, Na, Mg and K of this filtrate were measured using an Atomic Adsorption Spectrometer (AAS, Analytic Jena vario 6).

Three representative samples (65, 205 and 525 cm) from Femés were investigated for amorphous clay minerals (allophane) following the method of Schlichting et al. (1995): In order to identify the amount of oxalate soluble Al and Si, 1 g air dried material and 50 ml oxalate solution were shaken in darkness for one hour, and subsequently filtrated. The extraction of dithionite soluble Al and Si was performed using 2 g air dried sample material and 50 ml of a dithionite-citrate solution. Measurements were carried out after treatment with HClO<sub>4</sub> using a flame atomic adsorption spectrometer (Perkin-Elmer) at the University of Gießen/Germany.

For ***micromorphological investigations***, undisturbed orientated samples were collected at depths shown in figure 4.5.2. Following air-drying, the blocks were impregnated with Oldopal P80-21. Once hardened, the blocks were cut and polished to 4.8 cm x 2.8 cm slices following the procedure outlined by Beckmann (1997). During preparation, samples were not heated > 40°C. Micromorphological description at the University of Tübingen/Germany follows the terminology of Stoops (2003).

The ***chronostratigraphy*** was established using luminescence datings (see figure 4.5.2), supported by both a correlation between kaolinite contents measured in the valley sediments and nearby marine proxies (kaolinite and iron contents), and by an interprofile stratigraphic correlation between the vegas. Since reliable luminescence datings only cover the period from the Holocene to about 130 ka, the stratigraphy of the lower parts of Femés and Teguisse is based solely on the correlation with marine proxies and the interprofile stratigraphic correlation and thus implies some uncertainty. The chronology is discussed in Suchodoletz et al. (2008).

#### 4. Results: 4.5. Loess-like and palaeosol sediments – indicators of palaeoenvironmental change...

##### 4.5.5. Results

**Grain size:** Although the depth dependent distribution of the ratio clay/< 42 µm indicates that ultrasonic treatment prior to laser analysis caused widespread scattering of individual datapoints, a clear temporal signal is recognizable in the underlying trend of the graphs (figure 4.5.4, figure 4.5.5 column e). Due to enormous problems in determining the absolute clay content by laser analysis (cf. Mc Cave and Syvitsky 1991, Konert and Vandenberghe 1997), only relative estimates are possible. The depth dependent distribution of absolute clay contents from Femés as determined by pipette analyses parallels that of relative clay values obtained using the laser method (figure 4.5.4), yielding values between 23 and 80%. This demonstrates that despite the lack of absolute clay values the relative results of laser analysis are reliable. This is not disproved by the low correlation coefficient between both curves of only 0.32, since this value is somewhat biased by the large scattering of individual laser data points.

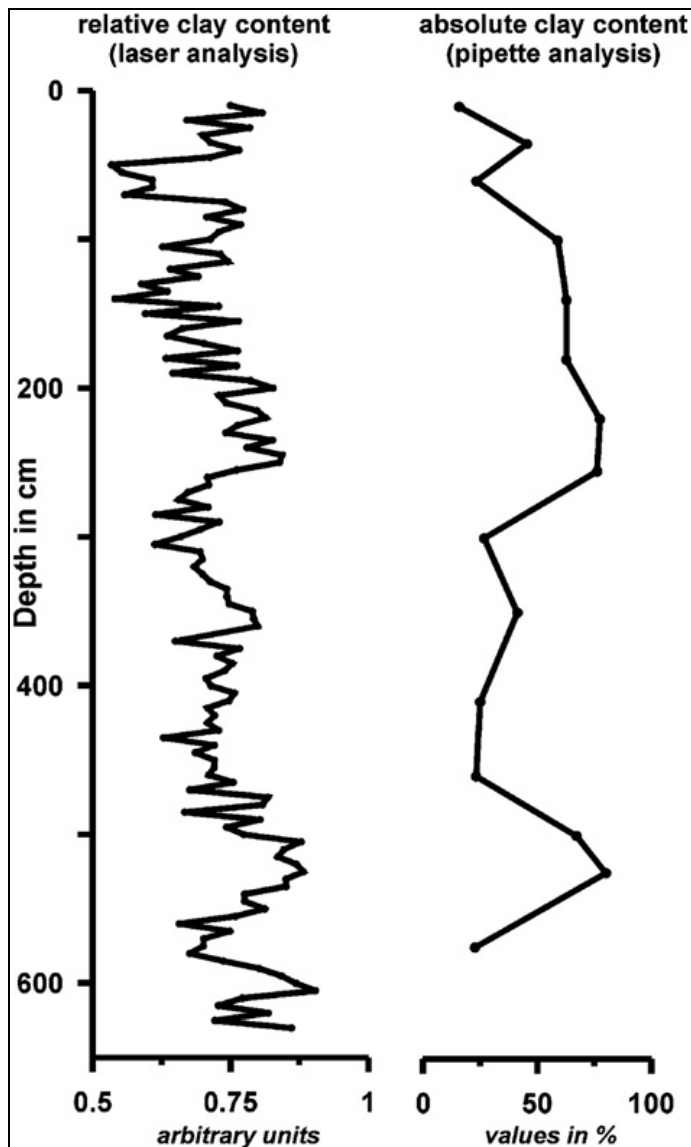


FIGURE 4.5.4. COMPARISON OF RELATIVE CLAY CONTENTS DERIVED BY LASER ANALYSIS WITH ABSOLUTE CLAY CONTENTS DERIVED BY PIPETTE ANALYSIS FROM THE PROFILE OF FÉMES.

#### **4. Results: 4.5. Loess-like and palaeosol sediments – indicators of palaeoenvironmental change...**

*XRD-analyses of bulk samples* yield mostly parallel depth dependent distributions of kaolinite and quartz, except for the upper part of Teguisse (figure 4.5.5 columns g, h). Both show strong variations within one profile, where higher values are generally found in yellowish/silty layers. Absolute quartz contents fluctuate between 6 and 39% in Femés, 4 and 31% in Guatiza III and 7 and 65% in Teguisse (figure 4.5.5 column h). Due to the lack of a calibration curve, relative instead of absolute kaolinite values must be given. The location of the illite-peaks in the XRD-diffractograms is very close to those of mica which has a similar structure. Thus, illite is not distinguishable from mica. Since mica is exclusively derived from Saharan dust (Coudé-Gaussen et al. 1987, Mizota and Matsuhisa 1995), the proportion of mica/illite is influenced by both pedogenetically formed illite and a change in the composition of the aeolian material. The latter influence is seen in the partial similarity of the depth dependent distributions of illite/mica, quartz and kaolinite in Guatiza III and in the central part of the Femés profile (figure 4.5.5 column f).

#### 4. Results: 4.5. Loess-like and palaeosol sediments – indicators of palaeoenvironmental change...

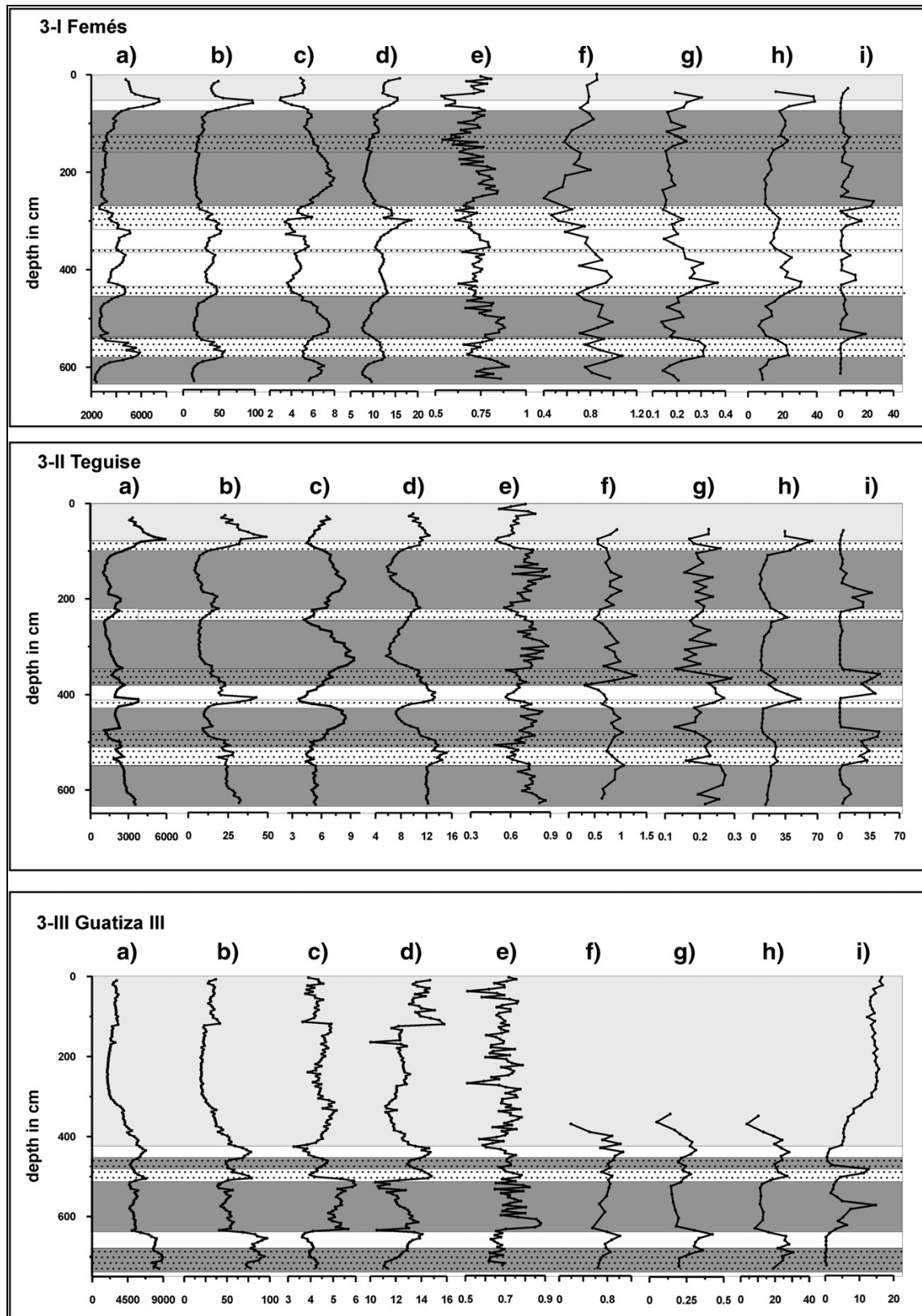


FIGURE 4.5.5. PROXIES FROM THE VEGÁS OF LANZAROTE:

a) initial magnetic susceptibility ( $\kappa$ ,  $10^{-6}$  SI-units), b) isothermal remanent magnetisation (IRM,  $A \cdot m^l$ ), c) frequency dependent susceptibility ( $\kappa_{fd}$ , %), d) IRM/ $\kappa$  ( $kA \cdot m^{-l}$ ), e) relative clay content (arbitrary units), f) relative bulk illite content (arbitrary units), g) relative bulk kaolinite content (arbitrary units), h) absolute bulk quartz content (%), i) carbonate in matrix (%).

Shaded layers indicate soil sediment layers and upper hatched layers anthropogenic colluvial deposits

#### 4. Results: 4.5. Loess-like and palaeosol sediments – indicators of palaeoenvironmental change...

*XRD- analyses of clay samples* from Femés (figure 4.5.6) show a clear peak at 10.0 Å (8.85°2θ), indicating the presence of illite/mica. As mentioned above, a further distinction of illite and mica is not possible. A second prominent peak occurs around 7.16 Å (12.35°2θ), recording the presence of kaolinite. Further secondary peaks of the mentioned clay minerals can be seen. Quartz (3.34 Å) also appears to be ubiquitous. Only some samples (170, 485 and 525 cm) show a faint signal around 15 Å (5.9°2θ) in the air dried record moving towards 16.5 Å (5.4°2θ) after ethylene glycol treatment. This may indicate swellable phyllosilicates, presumably mixed layer minerals.

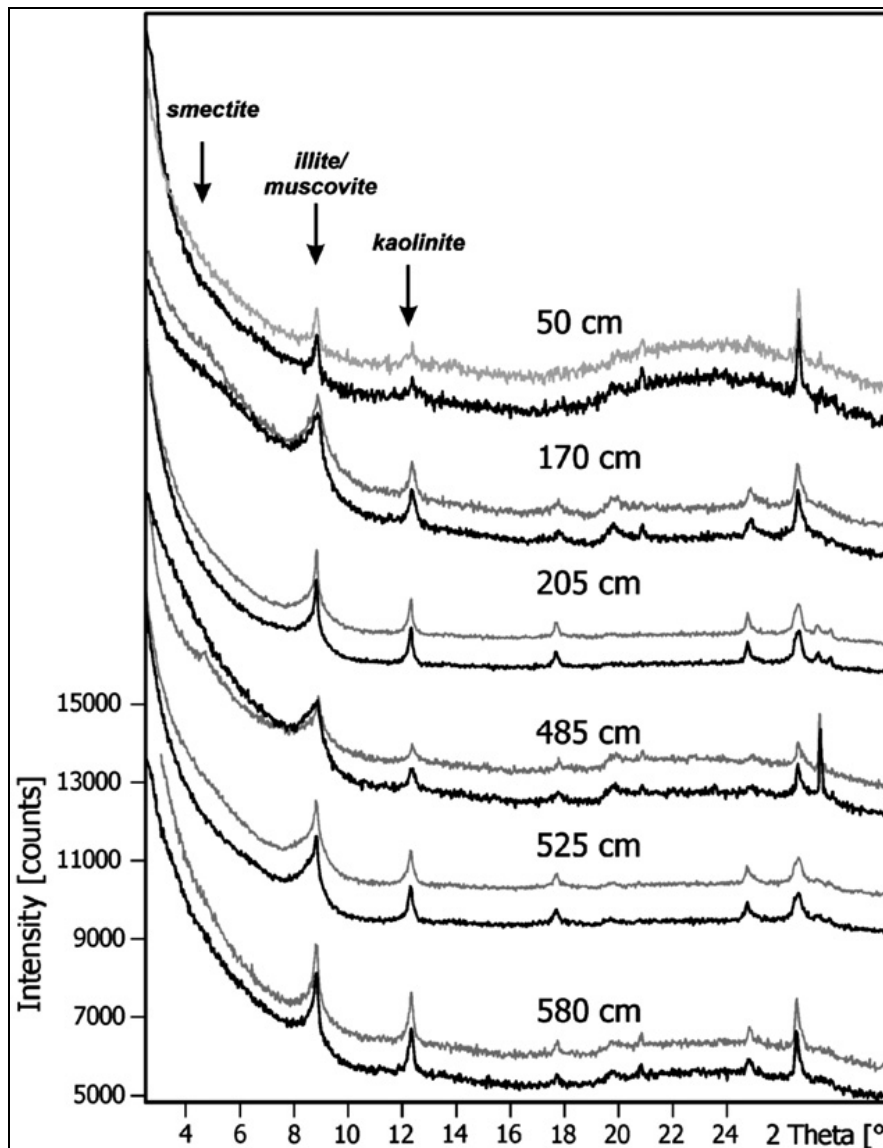


FIGURE 4.5.6. X-RAY DIFFRACTOGRAMS FROM THE INVESTIGATED CLAY SAMPLES  $< 2 \mu\text{m}$  FROM FEMÉS. The peaks of kaolinite and illite/muscovite are clearly recognizable, whereas that of smectite is absent or very faint.

Black lines indicate graphs of untreated pulver aliquots, grey lines show measurements after a treatment of the material with glycole.

#### **4. Results: 4.5. Loess-like and palaeosol sediments – indicators of palaeoenvironmental change...**

*Environmental magnetic analyses* provide both concentration dependent parameters such as initial magnetic susceptibility ( $\kappa$ ) and isothermal remanent magnetisation (IRM), and grain size and mineral specific parameters such as frequency dependent susceptibility ( $\kappa_{fd}$ ) and interparametric ratios, e.g. IRM/ $\kappa$ .  $\kappa$  roughly reflects the bulk amount of magnetic minerals (remanence and non-remanence carrying minerals) in the sediment, whereas IRM reflects only the amount of remanence carriers.  $\kappa_{fd}$  and IRM/ $\kappa$  do not depend on concentration changes at all but provide important information on the composition and grain size distribution of magnetic mineral assemblages.

The measurements yielded high  $\kappa$ - and IRM-values in loess-like yellowish/silty layers, whereas lower values are found in reddish/clayey strata. Absolute values of  $\kappa$  (IRM) vary between 1000 - 5900  $10^{-6}$  SI-units (4-49 A/m) in Teguse, between 2300 - 7400  $10^{-6}$  SI-units (12-97 A/m) in Femés and between 1900 - 8900  $10^{-6}$  SI-units (19-97 A/m) in Guatiza III, respectively (figure 4.5. columns a, b). These extreme values of  $\kappa$  and IRM - at least one order of magnitude higher than those typical for loess or loessic soils in mid-latitude settings - indicate that the signal is strongly dominated by ferrimagnetic minerals of detrital origin (e.g. Maher 1998, Spassov et al. 2003).

Frequency dependent susceptibility ( $\kappa_{fd}$ ), indicating so called superparamagnetic particles, shows a generally anticorrelated pattern to initial magnetic susceptibility and IRM, with highest values in reddish/clayey layers and lowest in yellowish/silty beds. Absolute values vary between 3.7 – 9.4 % in Teguse, between 3 – 8% in Femés and between 3.3 - 6 % in Guatiza III (figure 5, column c). Although the courses of IRM and  $\kappa$  look almost identical, their ratio (IRM/ $\kappa$ ) reveals clear differences. This is expressed by variations on the same wave length as  $\kappa_{fd}$ , but showing an opposite trend. Values range from 5-15  $\text{kA/m}^{-1}$  in Teguse, from 7-18  $\text{kA/m}^{-1}$  in Femés and from 10-16  $\text{kA/m}^{-1}$  in Guatiza III (figure 5, column d). Low IRM/ $\kappa$  values in the reddish/clayey layers point to the dominance of non-remanence carrying minerals in the magnetic assemblage.

In figure 4.5.7a, the correlation between  $\kappa$  and IRM is shown. Both parameters are strongly concentration dependent and show a strong linear correlation with distinct grouping of the individual sites. The linear fit shows an intersection  $\neq 0$  with the susceptibility axis. The cross-plot of the frequency dependent susceptibility ( $\kappa_{fd}$ ) to the IRM/ $\kappa$  ratio is displayed in figure 4.5.7b. These parameters are generally mineral and/or grain size dependent and anticorrelated, with distinct grouping of individual sites.

Overall, the depth-dependent variability of initial magnetic susceptibility ( $\kappa$ ) and IRM with depth is much greater than that of  $\kappa_{fd}$ .  $\kappa$  and IRM show abrupt changes and a wide range of values which are at least partially independent of lithology and/or pedostratigraphy. IRM/ $\kappa$  and  $\kappa_{fd}$ , however, exhibit a more or less regular relationship to depth.

Detailed results of our environmental magnetic investigations will be discussed in a forthcoming paper (Hambach et al., in prep.).

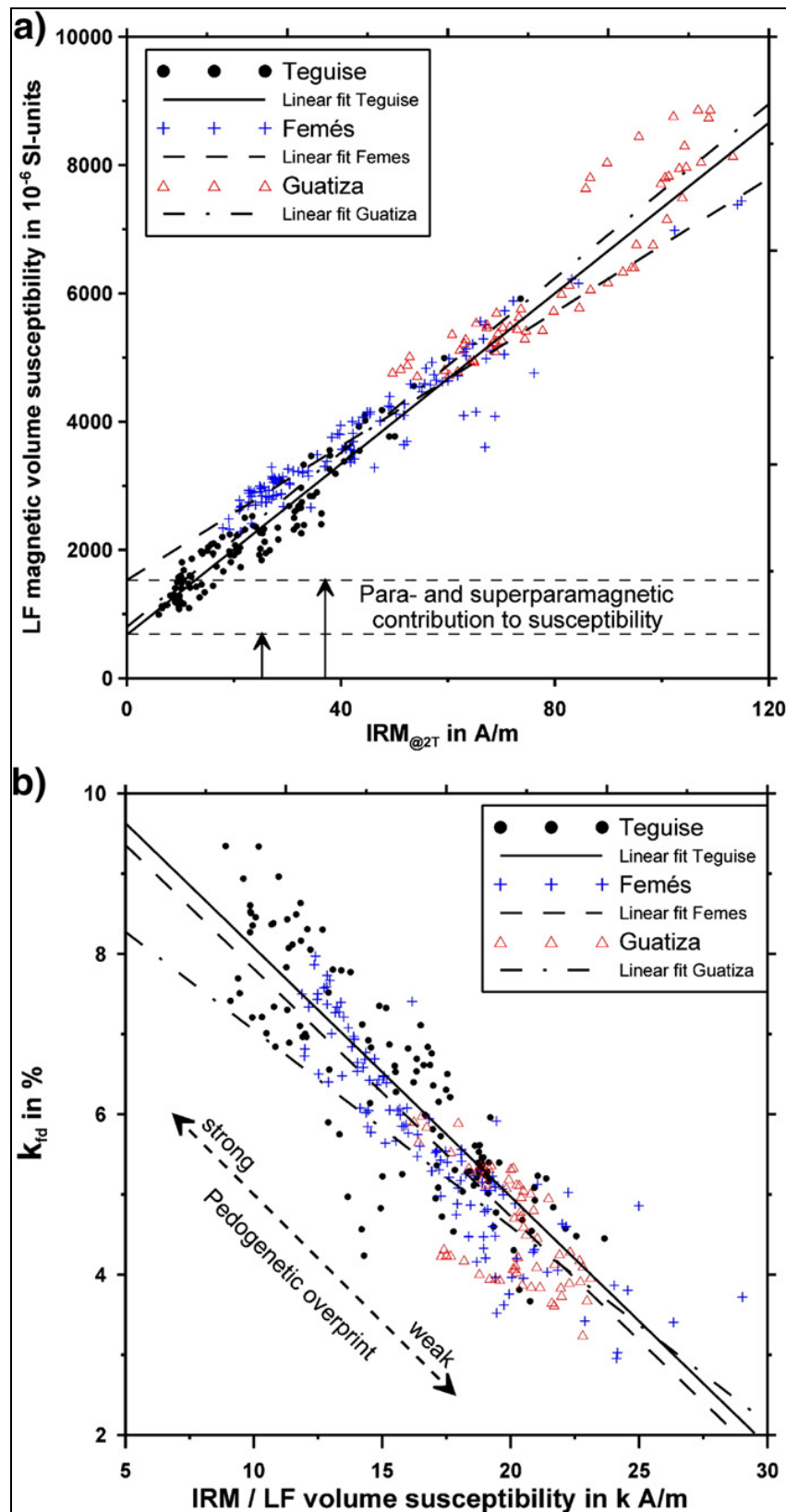


FIGURE 4.5.7. CROSS-PLOTS OF ENVIRONMENTAL MAGNETIC PARAMETERS FROM DIFFERENT SITES  
 a: Cross-plot of IRM acquired at fields of 2 Tesla to low field magnetic volume susceptibility ( $\kappa$ ). Both parameters are strongly concentration dependent. The strong linear correlation proves the dependency of the magnetic susceptibility signal on remanence carrying –probably ferrimagnetic– minerals. The intersections of the linear fits with the susceptibility axis clearly indicate the para- and superparamagnetic contributions to the magnetic susceptibility signal. Note the distinct grouping of the individual sites. For Guatiza only the data from the non-anthropogenic interval are plotted.

#### **4. Results: 4.5. Loess-like and palaeosol sediments – indicators of palaeoenvironmental change...**

*b: Cross-plot of the frequency dependent susceptibility ( $\kappa_{FD}$ ) to the IRM/ $\kappa$  ratio. Both parameters are generally mineral and/or grain size dependent, but absolutely independent from variations in concentration. The obvious anticorrelation indicates the overall control of the parameters by a non-remanence carrying but highly susceptible mineral fraction. This fraction is most probably formed by superparamagnetic particles derived from weathering of the primarily detrital ferrimagnetic minerals. Note the distinct grouping of the individual sites. The obvious stronger pedogenetic overprint in Teguisse compared to the other profiles is also visible in the field and can be explained by enhanced humidity due to the close proximity of this profile to the sea. For Guatiza only the data from the non-anthropogenic interval are plotted.*

**Carbonate contents** of the sediment matrix vary between 0 % and 47%, highest values showing the Teguisse section. Generally, loess-like layers contain primary carbonate, whereas the matrix of the majority of reddish-clayey layers is non-calcareous (figure 4.5.5 column i). In the latter, secondary carbonate is found as infillings of cracks and channels.

**pH-values** in all profiles vary between 7.6 and 8.2, indicating alkaline conditions. An exception is one horizon in Femés (74-120 cm) showing a pH value of 6.6 (table 4.5.2).

**Na-saturation** varies between 5.8 and 34.2 %. Generally, values in Femés show no correlation with indicators of the alternation of loess-like and reddish/clayey material but exhibit a general increase towards the bottom of the profile. In Teguisse, absolute values are generally higher, showing highest values in reddish/clayey layers (table 4.5.2).

**Electric conductivity** ( $EC_5$ ) values are between 70 and 2400  $\mu\text{S}/\text{cm}$  with highest values found in the profile of Teguisse. This could be explained by the close proximity of this profile to the sea (table 4.5.2).

Exemplary **analyses for amorphous clay minerals** yield a proportion of oxalate-soluble silicon ( $\text{Si}_0$ ) below 0.1 - 0.2%, indicating that amorphous clay minerals are not significant (table 4.5.3) (Dahlgren 1994).

**4. Results: 4.5. Loess-like and palaeosol sediments – indicators of palaeoenvironmental change...**

| horizon        | pH value | Na-saturation (%) | conductivity EC <sub>5</sub> | clay, pipette-analysis (mass-%, error 5%) | slickensides in the field | micromorphological features |              |                   |             | Antophora bees     | derived soil moisture |
|----------------|----------|-------------------|------------------------------|---|---------------------------|-----------------------------|--------------|-------------------|-------------|--------------------|-----------------------|
|                |          |                   |                              |   |                           | vertic prop.                | redox. Feat. | second. calcific. | clay illuv. |                    |                       |
| <b>Femés</b>   |          |                   |                              |   |                           |                             |              |                   |             |                    |                       |
| 55 – 74        | 7.7      | 17.4              | 459                          | 23  | -                         |                             |              |                   |             |                    | -                     |
| 74 – 120       | 6.6      | 17.2              | 245                          | 59  | +                         | ++                          |              |                   |             |                    | +                     |
| 120 – 165      | 7.7      | 13.9              | 219                          | 63  | +                         |                             |              |                   |             | ++ (100 m upslope) | O                     |
| 165 – 200      | 7.6      | 17.3              | 227                          | 63  | ++                        |                             |              |                   |             |                    | ++                    |
| 200 – 240      | 7.6      | 14.2              | 236                          | 78  | + / ++                    |                             |              |                   |             |                    | ++                    |
| 240 – 270      | 7.7      | 15.0              | 250                          | 76  | +                         |                             |              |                   |             |                    | +                     |
| 270 – 315      | 7.8      | 12.6              | 288                          | 27  | -                         |                             |              |                   |             | ++                 | O                     |
| 315 – 365      | 7.7      | 18.8              | 289                          | 41  | +                         | -                           | ++           |                   |             |                    | + / O                 |
| 365 – 370      |          |                   |                              |   | -                         |                             |              |                   |             | +                  | O                     |
| 370 – 425      | 7.7      | 25.6              | 267                          | 25  | -                         |                             |              |                   |             |                    | -                     |
| 425 – 445      |          |                   |                              |   | -                         |                             |              |                   |             | +                  | O                     |
| 445 – 480      | 7.6      | 32.5              | 110.7                        | 23  | - / +                     |                             |              |                   |             |                    | O / +                 |
| 480 – 515      | 7.7      | 24.3              | 328                          | 67  | +                         | ++                          |              |                   |             |                    | +                     |
| 515 – 535      | 7.6      | 9.9               | 333                          | 80  | + / ++                    | ++                          |              |                   |             |                    | ++                    |
| 535 – 570      | 7.8      | 34.2              | 270                          |   | -                         | ++                          |              |                   |             | +                  | O                     |
| 570 – 635      | 7.9      | 24.8              | 391                          | 23  | +                         |                             |              |                   |             |                    | +                     |
| <b>Guatiza</b> |          |                   |                              |   |                           |                             |              |                   |             |                    |                       |
| 420-450        | 7.8      |                   | 260                          |   |                           |                             |              |                   |             |                    |                       |
| 450-485        | 7.7      |                   | 206                          |   |                           | -                           | ++           |                   |             | +                  | O / +                 |
| 485-510        | 7.9      |                   | 176.1                        |   |                           |                             |              |                   |             | ++                 | O                     |
| 510-580        | 7.8      |                   | 233                          |   |                           | -                           | ++           |                   |             |                    | ?                     |
| 580-640        | 7.8      |                   | 325                          |   |                           |                             |              |                   |             |                    | ?                     |
| 640-675        | 7.8      |                   | 133                          |   |                           |                             |              |                   |             |                    | ?                     |
| 675-730        | 7.8      |                   | 70                           |   |                           | -                           | ++           |                   |             | +                  | ?                     |
| <b>Tegui</b>   |          |                   |                              |   |                           |                             |              |                   |             |                    |                       |
| 80-100         | 8.0      | 5.8               | 394                          |   | -                         |                             |              |                   |             | +                  | - / O                 |
| 100-120        | 7.8      | 14.6              | 1365                         |   | +                         |                             |              |                   |             |                    | - / O                 |
| 120-142        | 8.0      | 14.1              | 1178                         |   | +                         |                             |              |                   |             |                    | +                     |
| 142-180        | 8.0      | 15.2              | 1494                         |   | +++                       | ++                          |              |                   |             |                    | ++                    |
| 180-195        | 8.0      | 12.9              | 1423                         |   | ++                        |                             |              |                   |             |                    | ++                    |
| 195-220        | 8.0      | 12.2              | 1361                         |   | ++                        | ++                          |              |                   |             |                    | ++                    |

TABLE 4.5.2. RESULTS OF PEDOLOGIC ANALYSES AND ABSOLUTE CLAY CONTENTS.

Furthermore, the detection of slickensides in the field as well as of anthophora bee nests are indicated and micromorphological features are interpreted (+ slight occurrence, ++ medium occurrence, +++ strong occurrence, - no occurrence)

From these data, soil moisture relative to the lower precipitation limit of anthophora bees (200-300 mm/a) is derived for every layer (- < 200-300 mm/a; O 200-300 mm/a; + / ++ somewhat/much more than 200-300 mm/a)

#### 4. Results: 4.5. Loess-like and palaeosol sediments – indicators of palaeoenvironmental change...

| depth (cm) | Al <sub>o</sub><br>(mg/kg) | Si <sub>o</sub><br>(mg/kg) | Al <sub>d</sub><br>(mg/kg) | Si <sub>d</sub><br>(mg/kg) |
|------------|----------------------------|----------------------------|----------------------------|----------------------------|
| 65         | 1343                       | 231                        | 1168                       | 101                        |
| 205        | 1463                       | < 180                      | 1134                       | < 90                       |
| 525        | 1394                       | < 180                      | 972                        | < 90                       |

TABLE 4.5.3. ALLOPHANE ANALYSES FROM FEMÉS.

Al<sub>o</sub> = oxalate soluble Al, Si<sub>o</sub> = oxalate soluble Si, Al<sub>d</sub> = dithionite soluble Al, Si<sub>d</sub> = dithionite soluble Si.

**Micromorphological analyses** show well developed pedality, pyroclasts and vitric shards with a different degree of weathering in all thin sections. Grainy peds have a regular size of 20 – 50µm, mostly compacted to bigger subangular to angular peds (grainy intrapedal microstructure) comparable to the agglomerates of allophane mentioned by Zarei (1989). The depth function of main micromorphological features can be taken from table 4.5.4, whereas specific features are described and explained below:

- *Vega de Femés*

- o 108 - 113 cm: Few thin (around 10 µm) limpid yellow brown clay coatings indicate clay illuviation, rather more than expected for semi arid climate conditions (Bronger 1976). At least two redoximorphic phases occurred: (i) granostriated b-fabric around typical and concentric Fe-Mn nodules (mostly > 100 µm) indicates physical stress (figure 4.5.8a), attributed to transport or swelling/shrinking processes. These nodules were formed allochthonously and/or were subject to vertic processes. (ii) Ferruginous hypocoatings and aggregate nodules without granostriated b-fabric (figure 4.5.8a) are younger, since no signs of physical stress are visible. Therefore, we assume that the vertic process is relic.
- o 358- 363 cm: Fragments of yellow brown clay coatings occurring within non-calcareous peds (figure 4.5.8b) suggest a formation of clay coatings followed by their destruction. The thickness of these fragments of up to 50 µm in diameter indicates elevated clay illuviation (see chapter 6.2.). Peds and pyroclasts surrounded by non calcareous fine material are embedded in a calcareous micritic groundmass (crystallitic b-fabric) as remnants of a formerly decalcified horizon.
- o 498-503 cm: A stipple speckled b-fabric was found only in this section from Femés, indicating neoformation of clay minerals (Stephan 2000). Secondary calcification phenomena such as micritic hypocoatings are weakly developed and can generally not be related to distinct palaeoenvironmental changes within the relevant period of time.
- o 535 – 545 cm: Undisturbed yellow brown clay coatings lie next to pressure aggregate surfaces and predate their formation, indicating swelling and shrinking phenomena (figure 4.5.8c). Fragments of clay coatings within peds denote clay illuviation followed by formation of peds by vertic processes (figure 4.5.8d). A subangular blocky to crumb microstructure indicates a distinct overprint by bioturbation.

#### **4. Results: 4.5. Loess-like and palaeosol sediments – indicators of palaeoenvironmental change...**

- *Vega de Guatiza*

- o 450-485 cm: Numerous pyroclasts and vitric shards with voids occur. Most pyroclasts have a small rim of precipitated iron hydroxide as a sign of in situ weathering. Many pyroclasts have inclusions of olivine with no signs of weathering. Limpid yellow brown clay coatings with a thickness of ~10 µm demonstrate weak clay illuviation. Micritic nodules in channels are a result of secondary calcification.
- o 510-580 cm: Limpid yellow brown clay coatings represent a first phase of clay translocation. These were often covered by a subsequent secondary calcification corresponding to micritic coatings. Dusty brown clay coatings covering limpid yellow brown clay coatings in compound coatings characterise the second phase of clay illuviation. Locally, complete dense micritic infillings occur with fragments of limpid yellow brown clay coatings.
- o 675-730 cm: Silt coatings partly cover dusty yellow brown clay coatings, indicating rapid transport of suspended material. Strongly altered remnants of vitric shards and/or pumice were also apparent somewhat darker than the groundmass (400-500 µm diameter).

- *Vega de Teguisse*

- o 100-120 cm: The occurrence of glauconite shows an influence of marine sediments. Numerous typical manganese-ferruginous nodules with external ferruginous hypocoatings are a result of an in situ redoximorphic phase. Abundant pyroclasts with included unweathered minerals occur only in this thin section. Secondary calcification processes formed micritic hypocoatings predominantly occurring at the lower sides of channels and micritic nodules (up to 500 µm in diameter).
- o 142-180 cm: Few limpid yellow brown clay coatings result from weak clay illuviation processes. Abundant tissue and root residues and carbonate pseudomorphs of root cells in channels reveal a distinct influence of rooting. Micritic nodules occur frequently in areas with coarse monic c/f-related distribution that may also be connected to bioturbation. On the other hand, nodules with a higher content of coarse material than the surrounding groundmass (c/f<sub>5µm</sub> ratio: 1/9) can be regarded as allochthonous.
- o 195-220 cm: Two phases of clay illuviation: (i) fragments of 100 µm thick, limpid yellow brown clay coatings represent the older phase, (ii) reddish brown dusty clay coatings the younger phase. Numerous tissue residues, sometimes reddish under plane polarised light, are remnants of rooting and, therefore, bioturbation. Manganese aggregate nodules and ferruginous hypocoatings on groundmass are a result of in situ redoximorphic processes.
- o 240-260 cm: Numerous pyroclasts (200-300 µm) with external ferruginous hypocoatings as well as manganese-ferruginous aggregate nodules can be explained by redoximorphic influence and in-situ weathering. Most of the occurring ferruginous typical nodules (up to 1.5 mm in diameter) are altered/ weathered pyroclasts, therefore, the non-calcareous groundmass seems not to

#### **4. Results: 4.5. Loess-like and palaeosol sediments – indicators of palaeoenvironmental change...**

be a weathering product of pyroclasts. Micritic nodules in channels as well as complete dense infillings and micritic hypocoatings on the channel-surrounding groundmass indicate secondary calcification (figure 4.5.8e).

- o *290-350 cm*: Channels with dense rims and perpendicular fissures developed similarly to those in 550-590 cm. Microstructure is similar to that in 420-475 cm and 550-590 cm. Nevertheless, the porosity is much higher within the peds than in other thin sections. Strongly altered vitric shards can be found within the groundmass (figure 4.5.8f)
- o *420-475 cm*: Channels with dense rims and perpendicular fissures are more distinctly developed than in 550-590 cm. Limpid yellow brown clay coatings (10-20 µm thick) occur within peds. Disorthic typical manganese ferruginous nodules show allochthonous influence, since the size of the included minerals is bigger compared to the minerals in the groundmass (cf. 142-180 cm).
- o *550-590 cm*: The influence of marine sediments can be demonstrated by the occurrence of numerous glauconites in the groundmass (figure 4.5.8g). Fissures perpendicular to the walls of channels occur frequently. Channel walls are more compacted than the surrounding groundmass. Limpid yellow brown clay coatings (10-20 µm in thickness) occur within granules. Those intrapedal granules are packed to subangular peds defining a subangular blocky microstructure. During the development of subangular blocky peds, some of the limpid yellow brown clay coatings were fragmented and incorporated into these subangular peds. Locally occurring pressure faces demonstrate weakly developed vertic properties. Vitric shards and pumice are partly strongly weathered, but their shapes are still visible.



4. Results: 4.5. Loess-like and palaeosol sediments – indicators of palaeoenvironmental change...

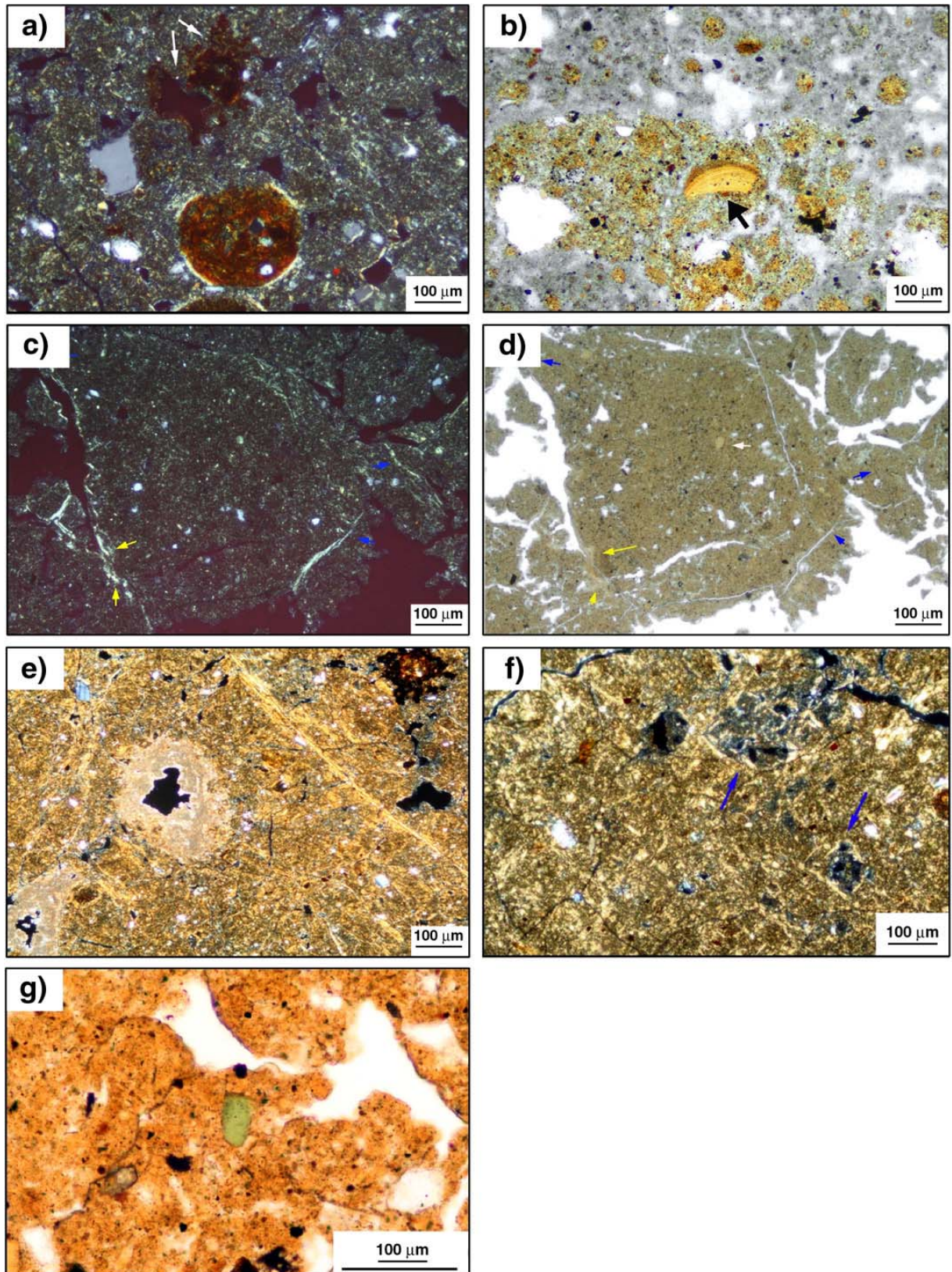


FIGURE 4.5.8. MICROMORPHOLOGICAL FEATURES  
a: Ferruginous hypocointing on groundmass (white arrows) and typical ferruginous nodules. Note the granostriated b-fabric resulting from physical stress. – Femés, 108 – 113 cm, crossed polariser.  
b: Fragment of clay coating (black arrow) within non calcareous ped. Grey areas indicate secondary calcification by micritic carbonate. – Femés, 358 – 363 cm, one polariser.

## **4. Results: 4.5. Loess-like and palaeosol sediments – indicators of palaeoenvironmental change...**

*c: Small yellow brown clay coatings (yellow arrows). Porostriated b-fabric and pressure faces (blue arrows) indicating physical stress. – Femés, 535-545 cm, crossed polariser.*

*d: Small yellow brown clay coatings (yellow arrows) and pressure faces (blue arrows). Pressure faces are not distinguishable from groundmass using one polariser. Fragment of clay coating within ped (white arrow). – Femés, 535-545 cm, same as 7-c, but with one polariser.*

*e: Micritic hypocoatings around channels and pressure faces (yellowish striae). Note the ferruginous nodule without granostratification in the upper right corner. – Teguisse, 240-260 cm, crossed polariser.*

*f: Weathered volcanic glass (blue arrows) with granostratified b-fabric. Clay domains within the glass indicate weathering to clay. – Teguisse, 240-260 cm, crossed polariser.*

*g: Numerous grains of glauconite (e.g. in the centre) indicate the influence of marine sediments. – Teguisse, 550-590 cm.*

### **4.5.6. Discussion**

#### **4.5.6.1. Are reddish/clayey layers linked to pedogenesis?**

We intend to use sediment properties for palaeoenvironmental interpretation. For this it is crucial to know if these properties are neoformed by pedogenesis or inherited from Saharan dust which could have changed provenance and thus properties during the Quaternary.

Recently collected Saharan dust close to the Canary Islands shows clay contents < 15 % (Criado and Dorta 2003, Holz et al. 2004, Menendez et al. 2007). A slightly weathered Early/Middle Holocene loess-like layer in the Femés section (55-74 cm) contains 23 % clay (figure 4.5.2, cf. table 4.5.2). Accordingly, in marine sediments ca. 300 km north of Lanzarote, Moreno et al. (2001) observed maximal clay contents of < 25 % in sediments derived from Saharan dust during the last 250 ka. This indicates that the geogenic clay content inherited from Saharan dust is between 15 and 25 %, so that clay contents up to 80% found in the valley sediments must be neoformed on Lanzarote (table 4.5.2).

The extent of pedogenetic processes can be estimated from environmental magnetic properties. Frequency dependent magnetic susceptibility ( $\kappa_{fd}$ ) as well as IRM/ $\kappa$  ratio reflect the proportion of very small superparamagnetic particles newly formed during pedogenesis or, alternatively, produced by weathering controlled maghemitization of local volcanic or aeolian/detrital magnetite derived from Africa (Maher 1998, Liu et al. 2008). In figure 4.5.5 (columns a - e) we observe that frequency dependent magnetic susceptibility ( $\kappa_{fd}$ ) and clay content show similar distribution patterns, while initial magnetic susceptibility ( $\kappa$ ), IRM and IRM/ $\kappa$  are generally anticorrelated. Whereas  $\kappa$ , IRM and IRM/ $\kappa$  are increased in the pedogenically unaltered intervals of the sections and significantly decreased in the soil sediment layers,  $\kappa_{fd}$  exhibits an opposite trend, showing higher values in the soil sediment layers, indicating an increased contribution of SP particles here. Interestingly, the relationship of IRM/ $\kappa$  to depth is almost perfectly anti-correlated to  $\kappa_{fd}$ . This can be explained by the greater decrease in remanence in the soil sediment layers as compared to the weaker decay of  $\kappa$ . This observation also points to the relatively increased contribution of SP particles.

Values of  $\kappa$  and IRM, found to be very high in loess-like layers probably indicating local volcanic input or a primary ferrimagnetic contribution from Saharan dust, are strongly reduced in reddish/clayey strata, indicating a lower concentration of ferrimagnetic material here. Although this general pattern can be somewhat biased by a change of volcanic input, as seen in the lower part of

#### **4. Results: 4.5. Loess-like and palaeosol sediments – indicators of palaeoenvironmental change...**

Teguisse, the general negative correlation with clay contents and  $\kappa_{fd}$  excludes the change of volcanic input to be a main cause for these fluctuations (figure 4.5.5 columns a, b, c, e). We propose that reduced values of  $\kappa$  and IRM in reddish/clayey layers reflect the transformation of ferrimagnetic magnetite/maghemite to less susceptible para- and/or antiferromagnetic phases during rubefication. These environmental magnetic results show that increasing clay contents are paralleled by rubefication processes that are also indicated by the reddish colour of the soil sediment layers (see below). This clearly demonstrates that reddish/clayey layers were neoformed on the island and are not inherited from Saharan dust.

As shown by Suchodoletz et al. (2009a), valley base sediments derive from Saharan dust and volcanic material, either deposited as aeolian fallout or as colluvially reworked material derived from the slopes. Taking the vega of Femés, we find a catchment area/valley base ratio of 5.4 : 1 (see table 4.5.1), meaning that only 18% of all sediments deposited in the total catchment area were directly deposited as aeolian fallout in the valley base. However, 57% of the total sediment found in the vega system is now stored in the valley base. Thus, most of these sediments were originally deposited and stored somewhere in the catchment area and subsequently colluvially transported into the valley base, yielding a ratio between material deposited as aeolian fallout in the valley base and that deposited as reworked material from the slopes of 1 : 2.2 or 30 : 70 % (Suchodoletz et al. 2009a). Consequently, most (70%) of the reddish/clayey material found in the vega base must be regarded as soil sediment whose properties are mainly derived from pedogenetic processes active along the slopes. We have to identify ways to discriminate between these properties and those which subsequently formed in the valley base after deposition.

##### **4.5.6.2. Soil forming processes**

*Decalcification* is one of the first processes active during pedogenesis. Today, Saharan dust arriving at the Canary Islands contains a carbonate content of about 18 – 40 % (Criado and Dorta 2003, Menéndez et al. 2007). All studies on recent dust collected north and south of the Sahara detected a certain carbonate content, although material from southern sources contains less carbonate than northern dust (Herrmann et al. 1996, Goudie and Middleton 2001, Guieu et al. 2002). These findings show that even in case of a change of provenance during the Quaternary Saharan dust deposited on Lanzarote must always have contained a certain proportion of carbonate. The majority of mainly dust-borne soil-sediment layers shows a completely decalcified sediment-matrix (figure 4.5.5, column i). This demonstrates that those sediments which are now alkaline (caused by the presence of carbonate and high salt-content indicated by high electric conductivities)(table 4.5.2) may have been at least slightly acidic along the slopes and in the valley base during pedogenesis as in one horizon from Femés (74-120 cm) showing a pH value below 7. A loess-like layer deposited between 8.5 and 5 – 2.5 ka in all valleys shows only negligible amounts of carbonate today (figures 4.5.2, 4.5.5 column i). Since this layer hardly shows other weathering features such as increased clay content and frequency

#### **4. Results: 4.5. Loess-like and palaeosol sediments – indicators of palaeoenvironmental change...**

dependent susceptibility, we suggest that similar loess-like layers of Pleistocene age were also decalcified shortly after their deposition on the island. Increased carbonate content in their matrices must hence be caused by secondary recalcification after burial at a later stage of soil formation, when carbonate-rich groundwater was reaching the topmost sediments of the valley bases. This secondary recalcification is also supported by micromorphological analyses (figure 4.5.8e).

So-called *superparamagnetic grains* are found in the magnetic assemblage of soil sediments as indicated by strongly enhanced frequency dependent susceptibility ( $\kappa_{fd}$ ) values. In the cross-plot of figure 4.5.7a, the correlation between  $\kappa$  and IRM is shown. Both parameters are strongly concentration dependent. The almost perfect linear correlation proves the dependency of the magnetic susceptibility signal on remanence-carrying – probably ferrimagnetic – minerals. The intersections of the linear fits with the susceptibility axis clearly indicate a para- and superparamagnetic contribution to the magnetic susceptibility. The cross-plot of frequency-dependent susceptibility ( $\kappa_{fd}$ ) to IRM/ $\kappa$  is displayed in figure 4.5.7b. Both parameters are generally mineral and/or grain size dependent, but absolutely independent from variations in concentration. The obvious negative correlation indicates the overall control of the parameters by a non-remanence carrying but highly susceptible mineral fraction. This fraction is most probably composed of superparamagnetic particles derived from weathering of the primarily detrital ferrimagnetic minerals. The distinct grouping of the individual sites gives evidence for the locally variant intensity of pedogenetic processes, in which the more intensive pedogenesis in the profile of Teguisse is explained by its closer position to the sea and thus the greater influence from sea spray.

The loess-like sediments found in the sediment traps on Lanzarote are mainly composed of Saharan dust with a minor contribution of local volcanic fallout, both either directly deposited as aeolian fallout or as hill-wash material (Suchodoletz et al 2009a). These sediments underwent intense pedogenesis during humid periods which also affected the magnetic minerals. The unaltered magnetic mineralogy of the loess-like sediments stems from Saharan dust, occasionally from volcanic fallout and regularly from the additive of local volcanic material derived from the erosion of the volcanic rocks of the island. This magnetic mineralogy is probably characterised by magnetite/maghemite in a grain size distribution lying within the superparamagnetic/single domain (SP/SD) range with significant proportions in both parts (Hambach et al., in preparation). During more humid periods, when pedogenesis prevails, low temperature oxidation of primarily detrital magnetite to maghemite and/or the neo-formation of superparamagnetic particles formed by dehydration of pedogenic ferrihydrite shift the grain size distribution slightly to the SP range (Liu et al. 2008). The presence of SD bacterial magnetite, which suffered the same fate, cannot be excluded. The resulting magnetic grain assemblage shows significant lower remanence, slightly lower initial susceptibility, but increased  $\kappa_{fd}$  (cf. figure 4.5.5 a, b, c). Thus, we are facing the relative increase of the SP-grain-size-fraction at the expenses of the SD-fraction. This observation can be solely explained by processes affecting a quite homogenous primary magnetic mineralogy in a setting of varying pedogenetic intensity with time.

#### **4. Results: 4.5. Loess-like and palaeosol sediments – indicators of palaeoenvironmental change...**

As mentioned above, pedogenesis is characterised by a strong *neof ormation of clay minerals*, increasing the content of clay up to 80%. The volcanic environment of Lanzarote facilitates a steady supply of dissolved cations in ground and slope water. Cations are not directly leached due to the semi-arid climate (Zarei 1989). These are ideal conditions for a formation of smectite, as reported from soils in a similar environment in Central Mexico (Solleiro-Rebolledo et al. 2003) and from soils on Lanzarote (Jahn 1988, Zarei 1989). For testing the presence of smectite in the sediments found in the valley floor, we performed XRD analyses of the clay fraction from the Femés section. A colluvium sample (50 cm) was composed of material derived from a loess-like layer originating from the Early/Middle Holocene (cf. figures 4.5.2; 4.5.5 column e), showing a clay content of 23 % (table 4.5.2). This sample is mainly composed of kaolinite and illite and shows no smectite, confirming the minor smectite content of Saharan dust (Criado and Dorta 2003, Holz et al. 2004, Menéndez et al. 2007). Five samples were collected from layers showing medium to high clay contents between 23 and 77% (170, 205, 485, 525 and 580 cm; cf. figure 4.5.5 column e). But, unlike the results of Zöller et al. (2004) who found a significant proportion of smectite in the profile of Femés, only small amounts were detected here (figure 4.5.6). The absence of large quantities of smectite is confirmed by parallel XRD analyses of the clay fraction of four samples (50, 170, 485, 580 cm) performed at the USGS in Boulder/USA. Obviously, the formation of smectite is not the main cause for high clay content in the valley base sediments.

Other clay minerals such as illite, kaolinite and chlorite are abundant, but also frequently found in Saharan dust (Coudé-Gaussen 1987, Caquineau et al. 1998, Menéndez et al. 2007). Accordingly, they are regularly observed in slightly weathered loess-like layers of the valley base sediments (for kaolinite and illite see figure 4.5.5 columns f, g). However, Zarei (1989) hypothesizes that all these clay minerals could also have formed during weathering.

Nevertheless, strong in situ formation of illite is unlikely because there is no general relationship between illite/mica and the indicators of pedogenesis such as frequency dependent susceptibility or clay content (figure 4.5.5 columns c, e, f). Only in Teguisse we can see some similar trends indicating some neof ormation during pedogenesis. The occurrence pattern of kaolinite is largely parallel to that of quartz (figure 4.5.5 columns f, g). Quartz has a completely aeolian origin since it does not form from the weathering of basaltic rock (Jahn 1995, Mizota and Matsuhisa 1995). The close similarity of quartz and kaolinite suggests that it is unlikely that the latter was formed in the soils of Lanzarote. This is supported by Bronger and Sedov (2003) who found no neof ormation of kaolinite in terrae rossa (Rhodoxeralfs) developing from the Middle Pleistocene until today at the SW coast of Morocco, in climatic conditions similar to those on Lanzarote. Clay minerals such as chlorite can hardly be distinguished from montmorillonite and vermiculite, because they appear rather diffuse in the diffractograms. Since Zarei (1989) reported only a rare occurrence of chlorite on Lanzarote, it is obviously not largely formed here.

#### **4. Results: 4.5. Loess-like and palaeosol sediments – indicators of palaeoenvironmental change...**

Clay minerals such as allophane and halloysite described in former studies (Zarei 1989) could not be detected in XRD-diffractograms due to the fact that they are X-ray amorphous. Zarei (1989) describes these minerals from a horizon with an age of around 21 ka (formerly called series IV<sub>A</sub>, Carracedo et al. 2003), and attributed them to weathering of volcanic glass in soils. Direct weathering of pyroclasts to clay could be observed by micromorphology in our profiles (cf. chapter 4.5.4, figure 4.5.8f). Weathering features on the surfaces of volcanic material even in slightly weathered loess-like horizons show that this process starts already very early during pedogenesis. Weathering of volcanic material can also be tracked by a lowering of initial magnetic susceptibility  $\kappa$  in soil sediments as described above and seen in figure 4.5.5 (column a). Zarei (1989) describes the formation of subangular to round dark-brown microaggregates with an average size of 10 – 50  $\mu\text{m}$  in soil horizons showing high amounts of allophane, oxides and hydroxides on Lanzarote. We also found large amounts of similar aggregates in clay rich soil sediment layers characterised by shrinking and swelling (figure 4.5.3). In conclusion, these observations suggest that XRD-amorphous clay should have formed in the valley base soils of Lanzarote. However, analyses of three samples (two showing high clay contents) from Femés did not indicate its presence (table 4.5.3).

*Clay Illuviation* is traceable by clay coatings found in thin sections and occurred during periods of pedogenesis along the slopes as well as in the valley bases (tables 4.5.2, 4.5.4). However, those coatings formed on the slopes were destroyed during colluvial transport and are only preserved as fragments in the valley base sediments (figure 4.5.8b). Dispersion and transportation of clay from the palaeosurface downwards were easily facilitated by high sodium saturation caused by sea spray, destabilizing the soil structure (table 4.5.2, Jahn 1988). Furthermore, soluble salts as found in large quantities (high electric conductivities, cf. table 4.5.2) were probably washed away since they would have inhibited the dispersion of clay. Thus, this process can not directly be compared to clay illuviation processes found e.g. in Central Europe, where they indicate special environmental conditions (e.g. Kühn et al. 2006).

The majority of soil-sediment layers exhibit *a strong vertic texture*. Periods of shrinking and swelling are reported by slickensides and vertical cracks at different scales, observed in outcrops and in thin sections (figure 4.5.8 a, c, figure 4.5.9, table 4.5.2). Most commonly, smectite produces vertic features in soils (Duchaufour 1982, Nordt et al. 2004), but allophane may also cause shrinking and swelling (Wan et al. 2002). Intense vertic properties demonstrate that either smectite or amorphous clay minerals must be present in larger amounts, being responsible for high clay contents in soil-derived horizons. Yet, it is not clear why analyses show converse results (see above). Consequently, the solution to this problem requires further investigation.



*FIGURE 4.5.9. STRONG SHRINKING CRACKS DEVELOPED ON THE SURFACE OF RECENTLY FORMED COLLUVIAL DEPOSITS IN GUATIZA.*

The smooth courses of frequency dependent susceptibility ( $\kappa_{fd}$ ) and  $IRM/\kappa$  reflect in situ pedogenetic processes. They clearly demonstrate that they were not affected by the vertic processes reaching depths as large as 100 cm described in other studies (e.g. Kovda et al. 2001). The smooth pattern, however, is in contrast to the pattern of initial magnetic susceptibility ( $\kappa$ ) controlled by the primary mixture of Saharan dust and local volcanic material, characterised by abrupt changes in its depth dependent function.

Strong **rubefication** as indicated by Munsell-colors in the range of 2.5 YR and 5 YR in the soil sediments (cf. Schwertmann et al. 1982, Michalet et al. 1993) is contemporaneous to the formation of superparamagnetic particles and clay minerals (see above). Michalet et al. (1993) demonstrate that in Moroccan soils the formation of clay-microaggregates such as those found in the soil sediments of the vegas (see above) generally favours the rubefication process. Rubefication causes the dark-red colour of the soil sediments, in contrast to the yellowish colour of slightly weathered loess-like layers. This process is typical for seasonally humid tropic and subtropic soils and occurs in a slightly acidic/neutral milieu, thus confirming an early decalcification of the sediments shortly after their deposition (Zech and Hintermaier-Erhard 2002).

Iron-manganese nodules of different size and hypocoatings on ped surfaces (figure 4.5.8a) indicate strong **redoximorphic dynamics** in the valley base sediments. Polygenetic neoformation of

#### **4. Results: 4.5. Loess-like and palaeosol sediments – indicators of palaeoenvironmental change...**

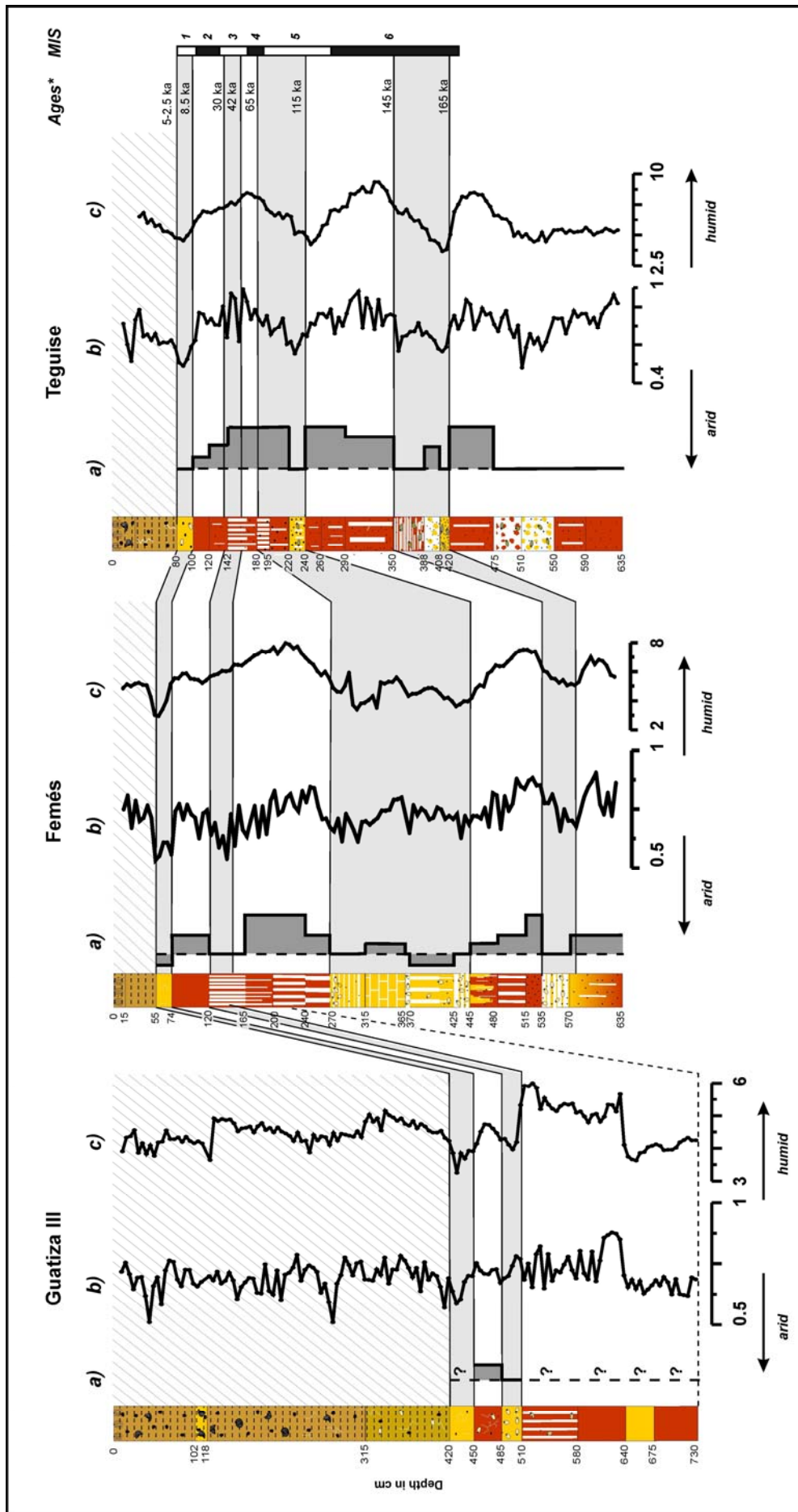
ferromanganese features (figure 4.5.8a) within one layer and their disappearing upslope suggest that these dynamics take mainly place in valley base environments, probably beginning during sedimentation and lasting until today.

##### **4.5.6.3. Palaeoenvironmental conditions as inferred from pedogenetic proxies**

Luminescence datings show that soil sediment layers generally have similar sedimentation rates as slightly weathered loess-like horizons (Suchodoletz et al. 2008). Therefore, differences in the intensity of pedogenetic properties are mainly caused by a change of climate conditions rather than by variation in the time span available for pedogenesis (Busacca and Cremaschi 1998, Sedov et al. 2003, Faust and Haubold 2007). Since the climate of Lanzarote is semiarid, the main factor limiting pedogenesis is humidity. Hence, soil properties can yield information about palaeoedaphic moisture conditions.

We have demonstrated that pedogenetic processes may take place along slopes and to some degree in the valley bases. Consequently, only some of the pedogenetic features observed in the valley base sediments can be used as indicators for primary pedogenesis and may therefore be useful palaeoenvironmental proxies. From genetic relationships and analysis we would classify some characteristics as primary pedogenetic features, more or less contemporaneous to the first material deposition in the vega catchments. Some of these can be traced by proxies: (i) vertic processes (as evidenced by outcrop and micromorphological investigations; table 4.5.2, figure 4.5.10 column a) (ii) clay mineral formation (clay contents; figure 4.5.10, column b) (iii) formation of superparamagnetic minerals linked with rubefication (traceable with frequency dependent susceptibility; figure 4.5.10 column c), and (v) clay illuviation. The vertic processes information was combined with the rate of occurrence of calcified anthophora-bee nests as direct indicators of soil moisture, leading to a combined soil moisture proxy (figure 4.5.10 column a). Due to the lack of continuous micromorphological samples, clay illuviation can not be traced. Furthermore, due to its fostering by high Na-saturation it is not useful as a palaeoenvironmental proxy here. As shown above (chapter 4.5.6.2.), vertic processes occurred a very short time after deposition into the vega base, and the other processes predominantly took place on the slopes prior to erosion. These processes have to be separated from processes restricted to later stages of pedogenesis of incertain duration, overprinting primary pedogenetic features of soils and soil sediments in the valley bases. Such subsequent processes are the mobilisation of Fe and Mn and carbonate dissolution or precipitation.

4. Results: 4.5. Loess-like and palaeosol sediments – indicators of palaeoenvironmental change...



#### **4. Results: 4.5. Loess-like and palaeosol sediments – indicators of palaeoenvironmental change...**

*FIGURE 4.5.10. COMPILATION OF PROFILES, AGES AND PALAEOENVIRONMENTAL PROXIES.*

*a) vertic properties derived from field and micromorphological analysis, merged with the occurrence of ground-nesting anthophora-bees (arbitrary scale), b) relative clay content (arbitrary scale), c) frequency dependent magnetic susceptibility (%).*

*Shaded sections indicate more arid periods, hatched areas anthropogenically triggered colluvia. Due to the lack of palaeoenvironmental significance of these layers, vertic properties were not investigated in these colluvia.*

*Ages and Marine Isotope Stages (MIS) are indicated on the right side.*

With a few singular exceptions (e.g. in Teguisé 388-408 cm), soil moisture (derived from vertic properties and the occurrence of anthophora bee nests), clay contents and frequency dependent susceptibility show parallel depth dependent functions, increasing in soil-sediment layers and decreasing in less weathered loess-like material. Altogether, these proxies display a coherent isochronous pattern of pedogenetic intensity exclusively controlled by climate (enhanced soil moisture). The chronological evidence, when considered alongside the correlating patterns across vegas, indicate general robust support of a soil moisture pattern based on pedogenesis. These results show that parts of MIS 2, 3, 4 and 6 exhibited higher soil moisture levels than today, whereas most parts of MIS 1 and 5 were obviously as dry or even drier when compared to recent conditions. In general, cold periods were obviously characterised by moisture, and warm periods by drier conditions (figure 4.5.10).

Furthermore, the occurrence of fossilised nests of anthophora-bees can provide some hints about precipitation intensity (table 4.5.3). The nests occur almost exclusively in weakly developed soil sediments showing clay contents between 26 and 63% in Femés (table 4.5.2), and were formed during slightly moister periods compared to today (figures 4.5.2, 4.5.10). According to Edwards and Meco (2000) and Genise and Edwards (2003) these bees thrive during periods of increased precipitation in semiarid areas with 200 to 500 mm annual precipitation, slightly above the actual rainfall rates of 100 to 200 mm\*a<sup>-1</sup> (Jahn 1988). The bees probably inhabited these environments when precipitation reached 200 to 300 mm\*a<sup>-1</sup>. It is likely that they had left the nests already before reaching their upper ecological humidity limit of 500 mm\*a<sup>-1</sup>, presumably caused by something similar to the seasonal lagoons reported prior to the 15<sup>th</sup> century here (Santana-Santana 2003), with stagnant water collecting in the valleys and increasing humidity covering the valley centres. Since anthophora bee nests are not found in strongly developed soil-sediments, it is evident that strong soil formation with rubefication and clay formation must have happened under climatic conditions of more than 300 mm annual precipitation.

While ground-nesting bees indicate that the moisture regime during periods of slight pedogenesis on Lanzarote were a little more intensive than today, we can estimate the humidity range during periods of strong pedogenesis through recent soil forming processes described in a catena in Tenerife covering the last 10 ka (Fernandez-Caldas et al. 1981): Today, brunification, rubefaction and the formation of amorphous allophane and smectite occur in a comparable geological situation attributed to climatic conditions with precipitation up to 560 mm (Kämmer 1974). However, soil moisture is influenced by

#### **4. Results: 4.5. Loess-like and palaeosol sediments – indicators of palaeoenvironmental change...**

various factors such as cloudiness, air temperature and precipitation, and these soils from Tenerife are found in a region that has on the one hand strong cloud cover and on the other hand a mean annual temperature below that of Lanzarote. Thus, this value is not directly comparable to past conditions on Lanzarote. Nevertheless, it can give about a reasonable estimate of the water budget on Lanzarote during more humid periods of the Quaternary.

Altogether, the water budget was obviously more positive during most parts of the investigated time period, namely during glacial stages.

#### **4.5.7. Conclusions**

Using grain size analyses, environmental magnetic investigations, micromorphology and pedological analyses, we could support the hypothesis that reddish/clayey layers in valley base sediments on Lanzarote are derived from local palaeosols. These palaeosols were formed by various pedogenetic processes such as clay formation and rubefication during periods of enhanced soil moisture in the valley bases and especially along the slopes. Subsequently, the material derived from the slopes was transported to the valley bases by colluvial processes during low amplitude and high frequency sedimentation events, so that the layers consist of soil sediments rather than in situ soils. Using clay contents, environmental magnetic parameters, palaeontological remains and the occurrence of vertic properties, a chronology of periods with enhanced soil moisture could be established for the Late Quaternary. This chronology demonstrates that cold periods like parts of MIS 2, 3 and 4 and 6 were characterised by a higher soil moisture than currently, whereas most parts of warm MIS 1 and 5 were obviously as dry or even drier than today. Since various factors influence soil moisture, it is not possible to derive palaeoprecipitation values from these valley base sediment samples directly. However, using palaeontological findings and a comparison with recent soils on Tenerife, rough estimations are possible. These show that maximal soil moisture corresponds to that found in regions of Tenerife with a recent precipitation of up to 560 mm\*a<sup>-1</sup>; however, a direct comparison with this value is not possible due to the variance in climatic conditions between both islands as well as between glacials and the recent period. Since most parts of the profiles consist of soil sediments rather than loess-like material, the water budget of Lanzarote was obviously more positive during most parts of the investigated time period. Hence, the recent dry climate of Lanzarote is rather an exception than the rule.

#### **Acknowledgements:**

The work of the first author was funded for two years by a post-graduate grant of the Free State of Bavaria, Germany, supplied by the University of Bayreuth. Further financial support was given by Deutsche Forschungsgemeinschaft (project Zo 51/29-1).

We are indebted to Dan Muhs (USGS Boulder, CO/USA) for comparative XRD analyses of clay minerals. Furthermore, we thank Beate Mocek and Max Wilke (University of Potsdam/Germany) for

#### **4. Results: 4.5. Loess-like and palaeosol sediments – indicators of palaeoenvironmental change...**

help during XRD analyses of bulk samples, Birgit Plessen (GFZ Potsdam/Germany) for her support during carbonate analyses and Georg Schettler (GFZ Potsdam/Germany) for facilitating grain size analyses. Peter Felix-Henningsen (University of Gießen/Germany) we thank for allophane analyses. For help during grain sizes analyses we are grateful to Gert Herold, David Sonnabend and Sebastian Breitenbach (all GFZ Potsdam/Germany). We thank Hedi Oberhänsli (GFZ Potsdam/Germany) for a critical revision of structure and language of the manuscript. The Student's Parish of the Catholic University Eichstätt/Germany is thanked for offering conference facilities. We thank John Dearing (University of Liverpool) and an anonymous reviewer for their helpful critiques, and Fiona Mulvey (Technical University of Dresden/Germany) for a strong improvement of the English manuscript.

### **5. Synthesis: Palaeoclimatic scenarios for more humid periods on Lanzarote**

In chapter 4 we could demonstrate that vega sediments of Lanzarote older than 5/2.5 ka are archives registering changes of palaeohumidity from MIS 6 to the Holocene with a time resolution of some ka, resolving palaeoclimatic events at a scale of marine isotope stages (MIS) and substages. As demonstrated in figure 5.1., these changes can be traced by frequency dependent susceptibility and clay contents, showing that glacials and stadials are generally characterised by enhanced soil humidity which culminates between 145 - 125 ka and 75 - 45 ka. By contrast, interglacials and interstadials exhibit equal or even drier conditions than at recent. A comparison between the depth dependent functions of clay content and frequency dependent susceptibility from different vegas shows that these are in general parallel. Minor differences are probably caused by different time resolutions of the vega profiles. Apart from a probable hiatus between 15 and 25 ka, the profile of Femés shows an almost complete sequence for the last 180 ka. Along with its intermediate temporal resolution throughout the profile, this sequence seems to be the best choice for palaeoclimatic interpretation and will thus be the key profile for our palaeoclimatic interpretation.

The comparison with previous palaeoclimatic studies from the Eastern Canary Islands based on  $^{14}\text{C}$  dating (Meco and Pomel 1985, Petit-Maire et al. 1986, Rognon and Coudé-Gaussen 1987, Rognon and Coudé-Gaussen 1989, Damnati et al. 1996, Meco et al. 1997, Coello et al. 1999) shown in figure 5.1. indicates that several palaeosols occur in different archives in parallel to most of the period between 25 and 75 ka recorded in our vega sediments as generally moister than at recent. However, no consistent pattern is seen there. This inconsistency could be due to problems of  $^{14}\text{C}$  dating on Lanzarote as reported by Meco et al. (2002) and confirmed by own investigations (see chapter 7), so that wetter spells could be somewhat older than the ages derived from  $^{14}\text{C}$  dating. The results of studies based on U/Th and especially TL dating (Rognon and Coudé-Gaussen 1996, Pomel et al. 1985, Hillaire-Marcel et al. 1995) are regarded as more reliable, and they agree better with our findings in the vega sediments. These studies interpret the period between 50 ka and the Last Glacial Maximum (LGM; ca. 20 ka) as a time of a generally wetter but instable climate, whereas the period prior to 50 ka was characterised by a more humid and stable climate. This shift from wetter to somewhat drier, instable conditions between about 50 – 40 ka is also seen in the vegas of Femés and Guatiza III, when frequency dependent susceptibility and clay contents decrease especially during the period between 40 and 30 ka but still exhibit a generally increased level. Thus, in spite of problems with  $^{14}\text{C}$ -dating and although somewhat masked by

## 5. Synthesis

different time resolution, our findings generally fit with the results of former palaeoclimate studies from the eastern Canary Islands.

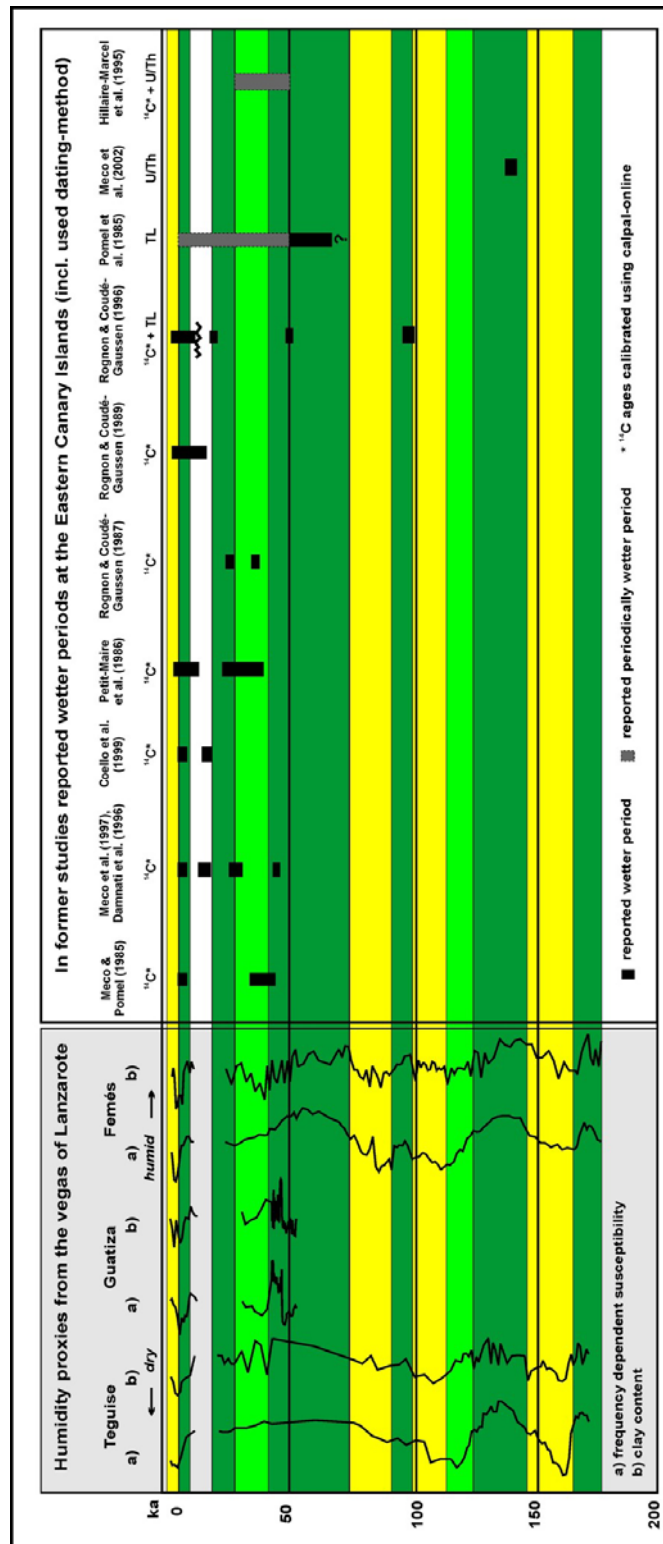


FIGURE 5.1. SOIL HUMIDITY PROXIES FROM THE VEGAS OF LANZAROTE IN COMPARISON WITH PREVIOUS PALAEOCLIMATE STUDIES FROM THE EASTERN CANARY ISLANDS.

Yellow areas indicate fewly weathered layers (= drier periods), light green areas slightly pedogenised layers (= slightly enhanced humidity) and dark green areas layers with strong pedogenesis (= strongly enhanced humidity) in the vega soils from Lanzarote.

TL ages are regarded as the most reliable ones, followed by U/Th ages. Especially older sections from studies based on  $^{14}\text{C}$  ages must be regarded with caution.

## 5. Synthesis

---

Comparing soil humidity proxies from Lanzarote with palaeoclimatic proxies from the NW African and Mediterranean area, three characteristics are evident (figure 5.2.):

- Our vega proxies are inversely correlated with the extension of arboreal vegetation in the Mediterranean area, reconstructed from marine and terrestrial pollen studies off Iberia and NW Africa (Hooghiemstra et al. 1992) and a lake from Greece (Tzedakis et al. 2003).
- Our vega proxies generally match well with organic carbon and pollen contents derived from marine cores off NW-Africa and the Canary Islands indicating stronger trade winds off NW Africa (de Menocal et al. 1993, Freudenthal et al. 2002). Furthermore, they generally agree with lower Sea surface temperatures (SST's) inferred from foraminifera distributions in marine cores retrieved off Cap Blanc/Mauritania (Crowley 1981).
- Periods of enhanced soil humidity on Lanzarote are coeval with most sapropels in the Eastern Mediterranean Sea (S1, S2, S4, S5, S6), whereas sapropel S3 is contemporary with a generally dry period on Lanzarote (Kallel et al. 2000). Although the advance of the African summer monsoon to the north into the Sahara is not well studied over the last 200 ka, the occurrence of sapropels in the Eastern Mediterranean Sea reflecting high Nile river discharge indicates the feeding of the Nile catchment by the African monsoon.

## 5. Synthesis

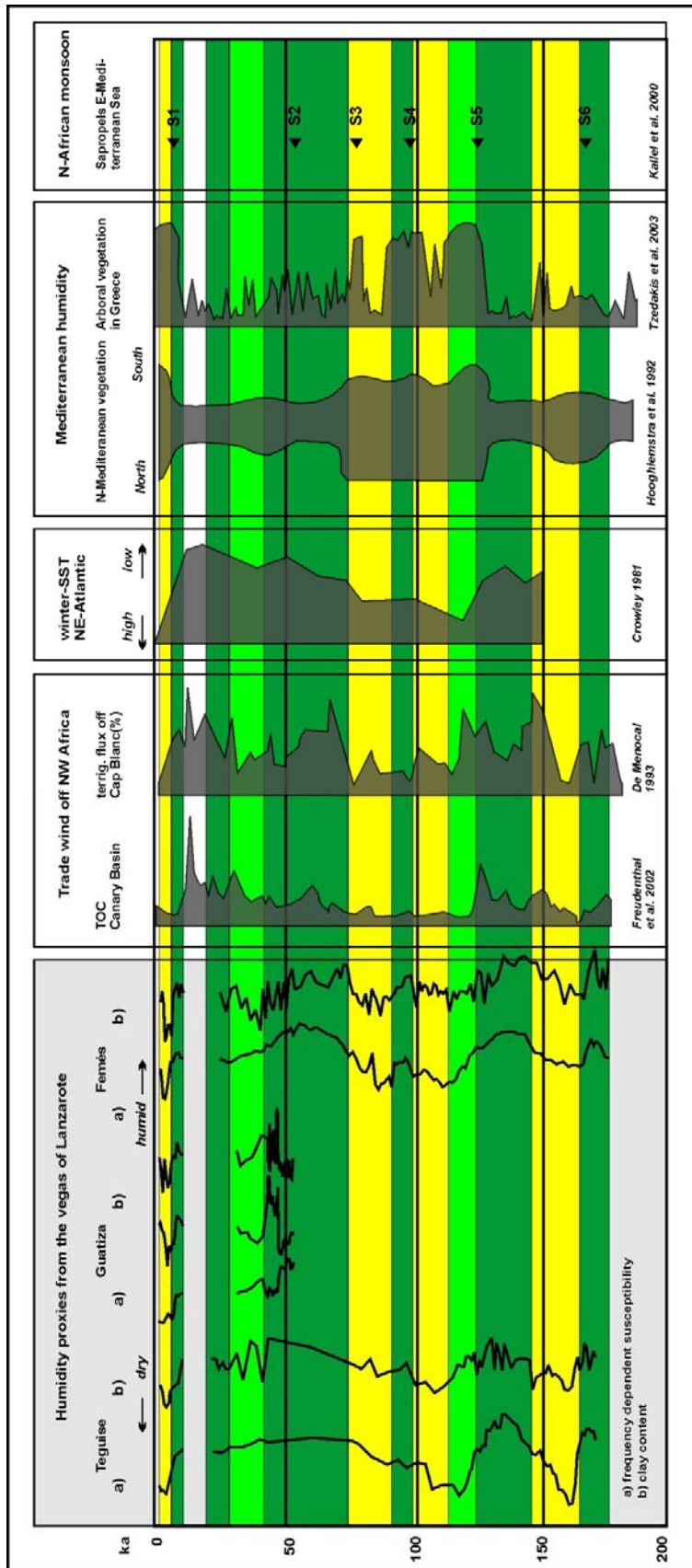


FIGURE 5.2. SOIL HUMIDITY PROXIES FROM LANZAROTE IN COMPARISON WITH PALAEOCLIMATE PROXIES FROM STUDIES OF THE NW AFRICAN AND MEDITERRANEAN AREA.

Yellow areas indicate fewly weathered layers (= drier periods), light green areas slightly pedogenised layers (= slightly enhanced humidity) and dark green areas layers with strong pedogenesis (= strongly enhanced humidity) in the vega soils from Lanzarote.

## 5. Synthesis

---

Based on these comparisons, in the following we will discuss palaeoclimatic scenarios for periods characterised by enhanced soil humidity on Lanzarote during the Late Quaternary. Each scenario is based on a factor that could have caused a more positive hydrologic budget of the vegas and thus should have enhanced soil humidity.

This positive hydrologic budget could be caused by:

1. An increase of precipitation. On Lanzarote, this could either be brought by:
  - a) North Atlantic cyclones
  - b) The African summer monsoon
2. A decrease of temperatures (and thus of evaporation).

*1.a. Could higher precipitation from North Atlantic cyclones be a possible cause for enhanced soil humidity?*

At present, the amount of precipitation on the Canary Islands is negatively correlated with the North Atlantic Oscillation (NAO) (García-Herrera et al. 2001). Like for the Mediterranean region and southern Morocco, precipitation is higher during negative NAO phases (Hurrell 1995, Knippertz et al. 2003). This is caused by Deep Atlantic Low pressure systems breaking the trade wind layer that prevails over the islands during most of the year (García-Herrera et al. 2001). This link shows that recent changes in precipitation on the Canary Islands are generally connected to dynamic atmospheric features generated over of the Mediterranean area.

Previous studies report a southward shift of the westerlies during glacial periods, bringing precipitation to the Mediterranean area as well as to North Africa. Narcisi et al. (1992) and Narcisi (2001) describe high levels from lakes in Italy, probably caused by wetter winters during the Last Glacial Maximum (LGM). Likewise, Maley (2000) reports high lake levels from the central Saharan Hoggar Massif which he ascribed to a shift of Saharan depressions related to a southern position of the Subtropical Jet Stream. Accordingly, Edmunds et al. (2004) compiled groundwater studies from the Northern Sahara, and found a significant recharge period between 45 and 23.5 ka caused by Atlantic westerlies. This southward shift under “glacial-like” boundary conditions in connection with the European glaciation is also reported in modeling studies such as that by Ganopolski et al. (1998) and Kageyama et al. (1999). Hence, these results plead for increased westerly precipitation in the Mediterranean region (and thus on the Canary Islands) during glacial periods.

On the other hand, the limited extension of arboreal Mediterranean vegetation contemporaneous with more humid glacial and stadial periods on Lanzarote (Hooghiemstra et

al. 1992, Tzedakis et al. 2003) is somewhat contradictory. To focus on this problem, we looked at studies dealing with cold Heinrich events. These represent the most extreme periods during the glacials in the Mediterranean area and will serve here as exemplary periods for glacial conditions. From pollen studies we understand that during these events steppic prevailed over arboral vegetation (Turon et al. 2003, Sanchez-Goni et al. 2000, Boessenkool 2001). Whereas some authors assume generally dry conditions during the Heinrich-events (Turon et al. 2003, Sanchez-Goni et al. 2000), others plead for wet and very cold winter conditions with increased runoff and an enhanced anticyclonic-driven summer aridity (e.g. Boessenkool 2001). The latter hypothesis is supported by Ruddiman and McIntyre (1981) who proposed a southward shift of the Arctic Front in the N-Atlantic during these events, pushing the cyclonic trajectories off Iberia towards latitudes of about 40°N.

Transmitting this scenario from Heinrich-events to glacial periods in general, stronger trade winds off NW Africa were generated by a seasonally increased anticyclonic circulation during summer. Consequently, the development of a thermophilous arboral vegetation in the Mediterranean area was hampered by summer aridity caused by this anticyclonal circulation, as well as by generally lower annual temperatures. During winter, this anticyclonic precipitation was probably replaced by North Atlantic cyclones which brought precipitation to the Mediterranean and the Canary Islands, causing more humid edaphic conditions in the vegas of Lanzarote (figure 5.3.).

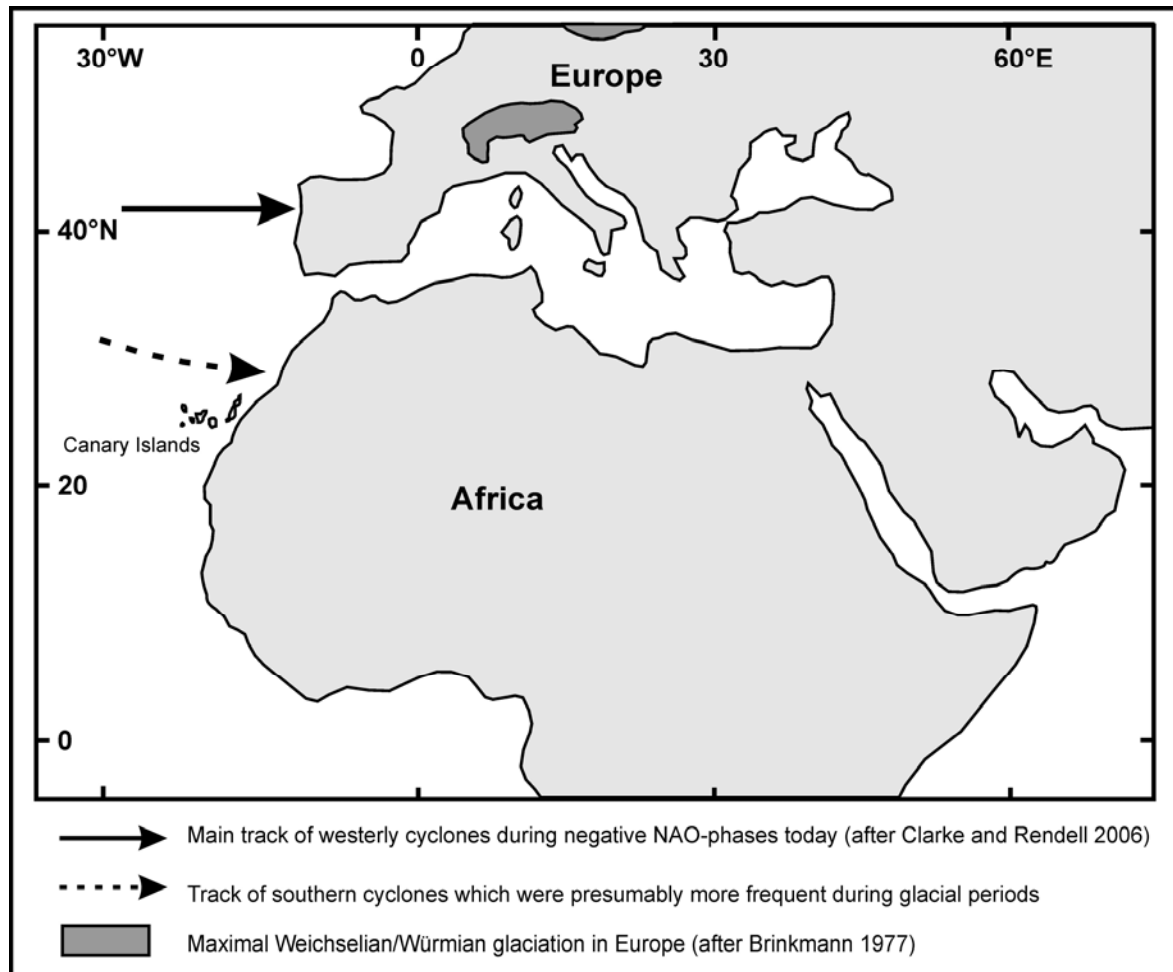


FIGURE 5.3. RECENT MAIN TRACK OF WESTERLY CYCLONES DURING NEGATIVE PHASES OF THE NORTH ATLANTIC OSCILLATION (NAO) COMPARED TO THE TRACK OF SOUTHERN CYCLONES THAT WERE PRESUMABLY MORE FREQUENT DURING GLACIALS.

*1.b. Could precipitation from the African summer monsoon be a cause for enhanced soil humidity on Lanzarote?*

Apart from the exception of sapropel S 3 formed about 80 ka ago, eastern Mediterranean sapropels occur concomitantly with enhanced soil humidity on Lanzarote. An advance of the African summer monsoon to the latitude and longitude of the Canary Islands is assumed by Kuhlmann (2003) for the Early Holocene and MIS 5e (Eemian) as shown in figure 5.4. Advance and retreat of the African summer monsoon were generally progressive from south to north and back again (e.g. Yan and Petit-Maire 1994), meaning that the monsoon arrived later at and retreated earlier from northernmost sites. In the palaeoclimatic compilation of Hoelzmann et al. (2004) it is demonstrated that the climatic optimum in the Sahara/Sahel zone was reached around 9.5 ka ago. Since vega sediments from Lanzarote indicate dryness from about 8.5 ka ago, this means that at the latitude of the Canary Islands as the northernmost outpost of the monsoonal area the influence of the monsoon could not have lasted longer than about 2 ka, and was probably restricted to the interval between 10.5 and 8.5 ka.

## 5. Synthesis

Looking at the time window when palaeosol-derived sediments are occurring it is clear that more humid phases on Lanzarote are much too long to be exclusively explained by such a monsoonal influence. However, our results do not exclude the assumption of Kuhlmann (2003) that the African summer monsoon progressed to the latitude of the Canary Islands during some short periods of the Quaternary, where it contributed to the observed increase in soil humidity (figure 5.4.). A monsoonal influence coeval with sapropel S 5 could possibly explain intermediate humidity during MIS 5e on Lanzarote (between 126 and 115 ka) (figure 5.1.), a period that is expected to be very dry from the general circulation pattern.

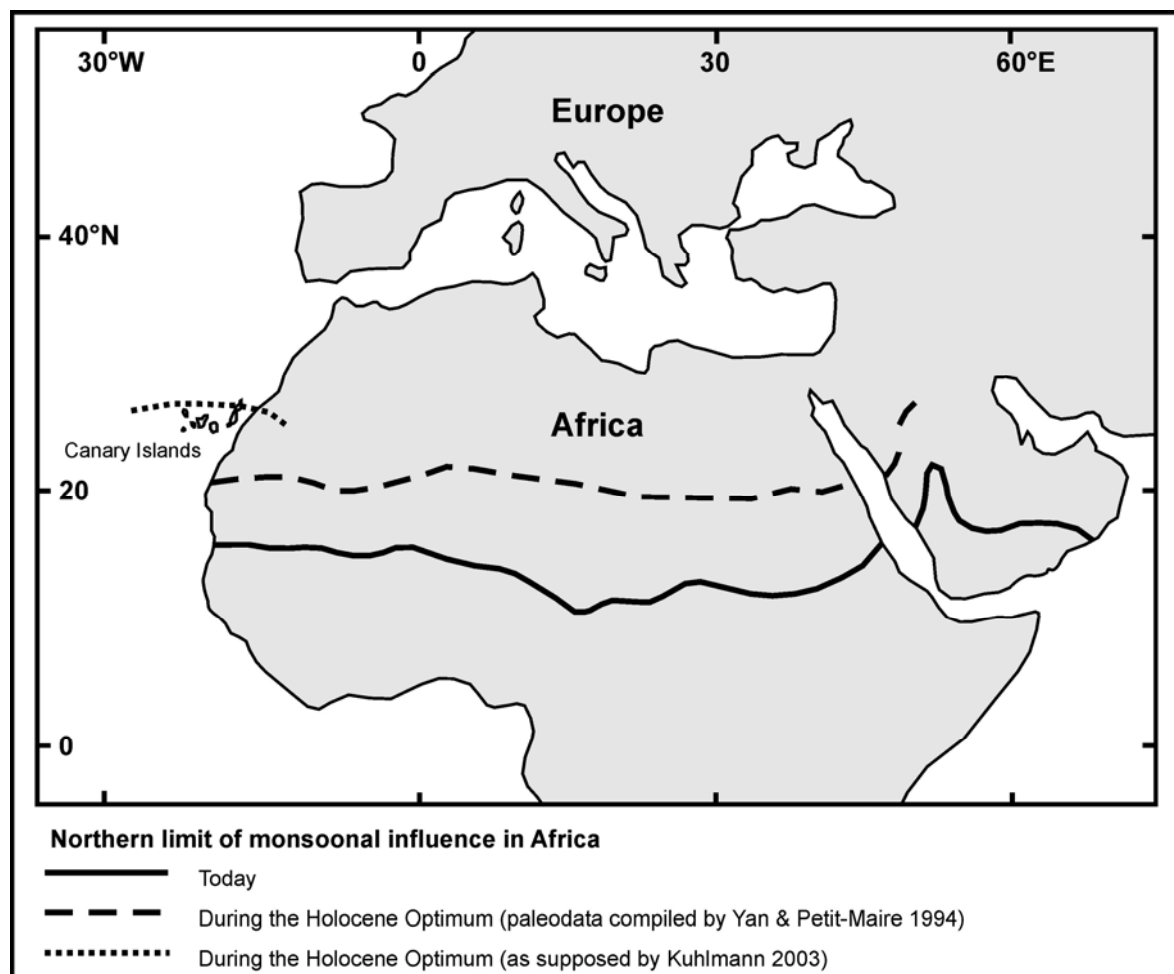


FIGURE 5.4. THE NORTHERN LIMIT OF MONSOONAL INFLUENCE IN AFRICA AT PRESENT AND DURING THE HOLOCENE OPTIMUM, THE LATTER BOTH SHOWN AS COMPILED BY YAN AND PETIT-MAIRE (1994) AND A SUPPOSED BY KUHLMANN (2003).

### 2. Did a decrease of temperature cause a relative increase in soil humidity?

At recent, the Canary current advects relatively cold water from High Northern Latitudes to the Canary Islands. The activity of this current was proven by Crowley (1981) for the Pleistocene who reports a general decrease of glacial sea surface temperatures (SST) by 5-7°C compared to recent conditions in a site off Cap Blanc/Mauritania around 650 km SW of

Lanzarote. Looking more in detail at a core off southern Iberia, 1000 km upstream Lanzarote, Cayre et al. (1999) report a general decrease of glacial SST of about 4°C, whereas the lowering of SST during Heinrich events was found to be about 10°C.

Lower SST directly influence overlying air temperatures, and a lowering of air temperatures would have the following consequences for the vega sediments:

- Evapo-transpiration in soils should be reduced (Hölting 1996).
- Decreased air temperatures should have lowered the altitude of the condensation level. At recent, the minimum altitude of trade wind clouds is in average around 1000 m, and during some days of the year it also affects the highest peaks of the Famara Massif with an altitude of 670 m (Kämmer 1974). Consequently, when lower glacial air temperatures caused a parallel lowering of the altitude of condensation level and trade wind inversion layer (T. Foken, oral communication, Schubert et al. 1995), a moistening effect of trade wind clouds on Lanzarote similar to the situation at the NE slopes of the higher western Canary Islands (e.g. Tenerife, Gran Canaria) as shown in figure 5.5. can not be ruled out. However, a lowered water vapour content of the atmosphere during colder glacials (e.g. Ganopolski et al. 1998, Clark et al. 1999) should have reduced the density of trade wind clouds so that they contained less water vapour. On the other hand, increased trade wind speeds shown for glacial periods (figure 5.1.) should have increased the amount of trade wind cumulus clouds (Albrecht 1981).
- Lowered SST in parallel with a relatively warm land surface during summer would have fostered the formation of coastal fog, similar to the situation described for recent conditions at the SW-Moroccan coast by Kämmer (1974).

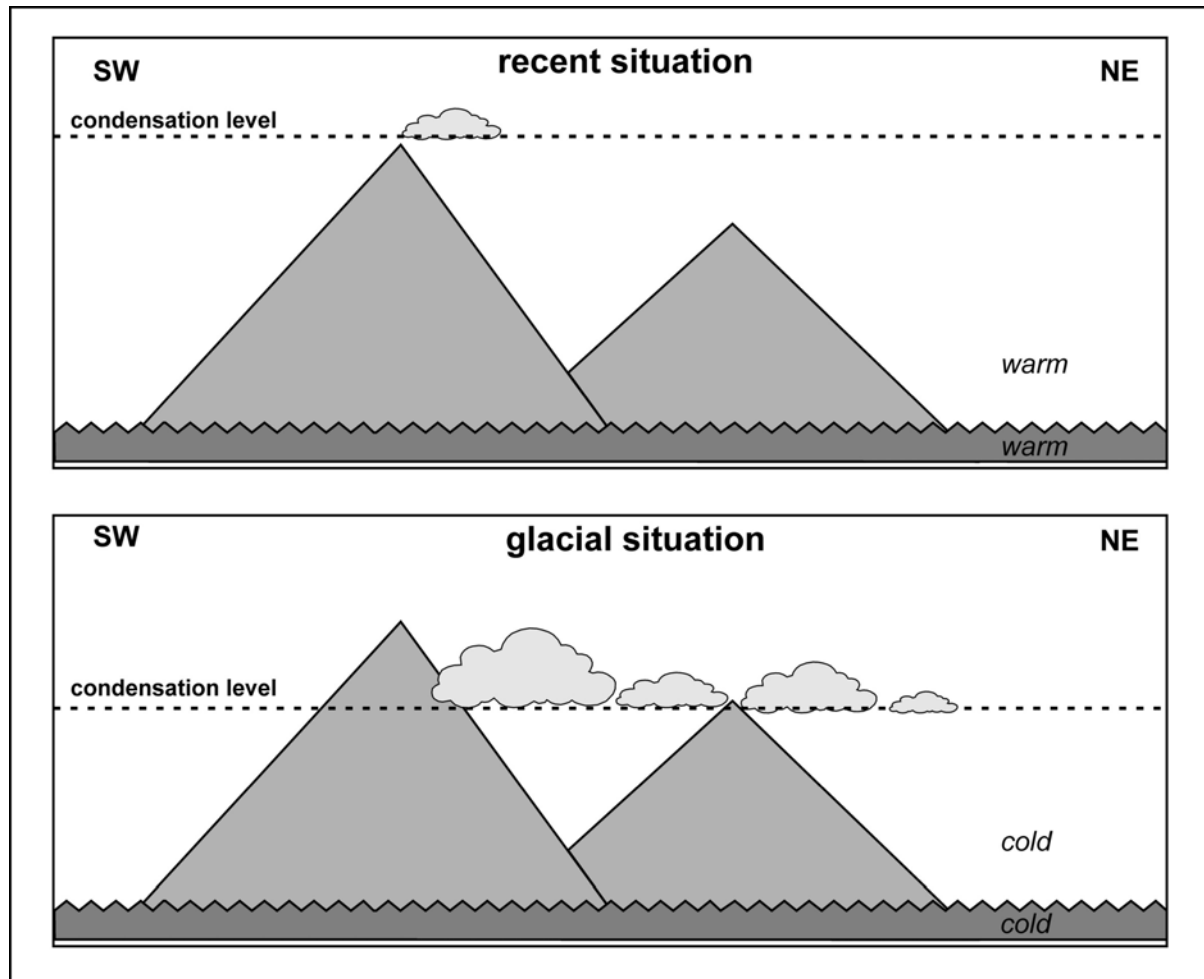


FIGURE 5.5. RECENT SITUATION WITH (RELATIVELY) WARM SST AND AIR TEMPERATURE COMPARED TO THAT DURING GLACIAL PERIODS, WHEN SST AND AIR TEMPERATURE WERE MUCH COLDER.

The discussion above shows that all three hypothesized causes for enhanced soil humidity during glacial periods could be possible. However, a discrimination of the effects of different causes for specific time periods is not possible, as will be shown in the following example from the Lower Holocene. Proxies from the vega sediments indicate quite humid conditions from about 15 to 8.5 ka before continuous aridity started to prevail. The compilation of Verschuren et al. (2004) shows that most climate studies from the westerly-influenced Mediterranean area witness fairly humid conditions between ca. 10 and 4 ka. Thus, the change towards drier conditions about 8.5 ka ago seems not be influenced by precipitation from westerly cyclones.

Kuhlmann (2003) finds a major change in the sedimentation pattern off the Canary Islands ca. 8.5 ka ago. Using wavelet-analyses, he interprets this as the end of monsoonal influence in this region. Hence, humid conditions in the vegas of Lanzarote during the Lower Holocene could be caused by monsoonal precipitation. On the other hand, Boessenkool (2001) reports a steep increase of SST up to recent values in the Canary current about 1000 km upstream from

## 5. Synthesis

---

the Canary Islands at about 8.7 ka. A parallel SST-rise is seen by Zhao et al. (1995) about 900 km downstream off Cap Blanc between 10 and 7.5 ka (two different cores), whereas Kim et al. (2007) do not confirm this rise close to the Canary Islands. Hence, in spite of some uncertainty, decreased temperatures could be another explanation for humid conditions in the vega soils until about 8.5 ka.

Although an unraveling of different causes for enhanced soil humidity on Lanzarote is not yet possible, we can propose that increased precipitation activity from glacial westerly cyclones in combination with lowered glacial temperatures must have been the main triggers for soil humidity on Lanzarote. This was perhaps occasionally amplified by precipitation from the African summer monsoon. Similar to Moreno et al. (2002b), we propose that these results clearly demonstrate that the major part of Late Quaternary climate variability at the latitude of the Canary Islands was controlled by northern High Latitude Processes.

### 6. Conclusion

In this study we could demonstrate, that in spite of their mostly colluvial character sedimentary sequences containing loess-like and palaeosol-derived material developed in dammed valleys on Lanzarote (Canary Islands) are valuable archives for the palaeoclimate of the NW African margin during the Late Quaternary. Based on these archives, it could be demonstrated that soils on Lanzarote generally developed during glacials and stadials and indicate more humid conditions during those periods, whereas interglacials and interstadials were mostly characterised by drier conditions. Causes for generally more humid conditions during glacials and stadials could have been enhanced winterly cyclonic precipitation and/or a lowered temperature and thus evapo-transpiration. During certain periods as the Lower Holocene or MIS 5e, a possible advance of the African summer monsoon could have caused more humid conditions that are observed during these generally warm periods. Unfortunately, an unraveling of these causes is not possible yet so that absolute palaeoprecipitation values can not be proposed. However, it is possible to give a rough estimation of palaeohumidity by a comparison with recent soils found on Tenerife, an island of the western Canary Islands. From this comparison emerges that the properties of palaeosol-derived sediments accumulated in the vega bottoms correspond to those developed in a region of Tenerife receiving a recent annual precipitation up to 560 mm. Although due to different glacial air temperatures these values are not directly comparable to the past, they clearly show that the humidity conditions on Lanzarote were always semi-arid to semi-humid and never reached a humid level.

### 7. Outlook and perspectives

The presented work stimulated several ideas for further palaeoclimatic research topics on Lanzarote. In this chapter we will present some of these ideas which are about to be realized.

*Extending the time range of the investigations:* Our research showed that complete damming and a medium sedimentation rate make the vega of Femés the most appropriate one for palaeoclimatic research on Lanzarote. Up to now, the investigated time span only reaches back to 180 ka, hence comprising MIS 6 to 1. As shown in chapter 4.2., the earlier part of this period is already beyond the limit of quartz OSL dating, whereas potentially possible IRSL dating so far often fails due to anomalous fading. Consequently, sediments older than the investigated period can not be dated using established luminescence methods. However, a new luminescence technique was developed recently: This method uses an infrared emission during the transition of electrons from the conductive band into light sensitive traps in K-feldspars (radioluminescence). A higher saturation level compared to conventional luminescence techniques allows a dating of samples that are much older, yielding ages up to 300 ka in samples from Central Europe (Trautmann et al. 2000, Krbetschek et al 2000). A further advantage of radioluminescence dating is the absence of anomalous fading, whereas a slightly slower bleaching behaviour than for conventional luminescence constitutes a real drawback of this method. Using radioluminescence SAR techniques, a dating of samples from Lanzarote with an assumed Middle Pleistocene age is currently attempted by Dr. M. Krbetschek at the Technical University of Freiberg. If successful, coring in the vega sediments of Femés would offer the possibility to extend the range of palaeoclimatic investigations far into the Middle Pleistocene.

*Reconstruction of palaeovegetation:* Recently, techniques were developed that allow a determination of compound specific isotope ratios ( $\delta^{13}\text{C}$ ) of terrestrial biomarkers using gas chromatography - combustion - isotope ratio mass spectrometry (GC-C-IRMS). These compound specific  $\delta^{13}\text{C}$ -ratios ratios allow a much more reliable reconstruction of the palaeovegetation than that of bulk samples (e.g. Schmitt et al. 2003, Zech 2006, Tipple and Pagani 2007). A set of exemplary samples is currently investigated by Dr. Bruno Glaser, Dr. Michael Zech and Björn Buggle at the pedologic laboratory of the University of Bayreuth. If successful, this would allow obtaining valuable information about the palaeovegetation during more humid phases, and to improve our understanding of the palaeoclimate during the Late Quaternary on Lanzarote.

*Investigating Middle and Upper Quaternary dune-palaeosol sequences:* A sand pit close to the village of Mála at northern Lanzarote exposes carbonatic dune sands intercalated with

## 7. Outlook and perspectives

---

reddish/brownish palaeosols (e.g. Damnati 1996, Williamson et al. 2004, Ortiz et al. 2006). Former investigations (Ortiz et al. 2006) point to a Late Pleistocene/Holocene age of these sediments, and the sediment alternation has been interpreted as a result of small-scale climatic fluctuations during the last millenia. A preliminary red thermoluminescence dating was performed on a heated palaeosol in the upper part of this sequence, pointing to a Middle Pleistocene age of about  $173 \pm 23$  ka. This age diverges significantly from the  $^{14}\text{C}$  age of about 25 ka that we think should be questioned. The age range of TL age is principally supported by Electron spin resonance (ESR) datings of land snail shells by Prof. Dr. U. Radtke (University of Cologne), also yielding late Middle Pleistocene ages (Suchodoletz et al., in preparation). These results demonstrate once more the difficulties with radiocarbon dating in this area as previously already described by Meco et al. (2002). A reliable dating of these palaeosols is a precondition for a correct palaeoclimatic interpretation of the dune-palaeosol sequence in Mala. Furthermore, the same holds for several similar dune-palaeosol sequences distributed over the Eastern Canary Islands since they are linked with Mala via a detailed aminochronostratigraphy (Ortiz et al. 2006). Consequently, further quartz OSL and ESR datings (the latter done by Prof. Dr. U. Radtke, University of Cologne) are in progress, and detailed pedologic investigations are planned by the author and Prof. Dr. D. Faust (Technical University of Dresden).

Results from this geomorphologically different archive could be useful for a better understanding of climate and landscape development on Lanzarote during more humid periods as seen in the investigated vega soil sediments.

### 8. References

- Adamiec, G. & M. Aitken (1998): Dose-rate conversion factors: update. *Aciert TL* 16/2, 37-50.
- Aitken, M.J. (1998): *An Introduction to Optical Dating*. Oxford University Press, New York, 267 pp.
- Albrecht, B.A. (1981): Parametrization of trade-cumulus cloud amounts. *Journal of the Atmospheric Sciences* 38, 97-105.
- Aléon, J., Chaussidon, M., Marty, B., Schütz, L. & R. Jaenicke (2002): Oxygen isotopes in single micrometer-sized quartz grains: Tracing the source of Saharan dust over long-distance atmospheric transport. *Geochimica et Cosmochimica Acta* 66/19, 3351-3365.
- Alonso-Zarza, A.M. & P.G. Silva (2002): Quaternary laminar calcretes with bee nests: Evidences of small-scale climatic fluctuations, Eastern Canary Islands, Spain. *Palaeogeography, Palaeoclimatology, Palaeoecology* 178, 119–135.
- Allen, J.R.M., Brandt, U., Brauer, A., Hubberten, H.-W., Huntley, B., Keller, J., Kraml, M., Mackensen, A., Mingram, J., Negendank, J.F.W., Nowaczyk, N.R., Oberhänsli, H., Watts, W.A., Wulff, S. & B. Zolitschka (1999): Rapid environmental changes in southern Europe during the last glacial period. *Nature* 400, 740-743.
- Antoine, P., Rousseau, D.-D., Zöller, L., Lang, A., Munaut, A.-V., Hatté, C. & M. Fontugne (2001): High-resolution record of the last interglacial–glacial cycle in the Nussloch loess–palaeosol sequences, Upper Rhine Area, Germany. *Quaternary International* 76-77, 211-229.
- Atoche-Peña, P., Paz-Altera, J.A., Ramirez-Rodriguez, A. & E. Ortiz-Palomar (1995): *Evidencias arqueológicas del mundo romano en Lanzarote (Islas Canarias)*. Servicio de publicaciones del excmo. Cabildo Insular de Lanzarote, Arrecife.
- Auclair, M., Lamothe, M. & S. Huot (2003): The measurement of anomalous fading for feldspar IRSL using SAR. *Radiation Measurements* 37, 487–492.
- Bailey, R.M. & R.J. Arnold (2006): Statistical modelling of single grain quartz De distributions and an assessment of procedures for estimating burial dose. *Quaternary Science Reviews* 25, 2475–2502.
- Balsam, W.L. & B.L. Otto-Bliesner (1995): Modern and last glacial maximum aeolian sedimentation patterns in the Atlantic Ocean interpreted from sediment iron oxide content. *Palaeoceanography* 10/3, 493-507.
- Bateman, M.D., Frederick, C.D., Jaiswal, M.K. & A.K. Singhvi (2003): Investigations into the potential effects of pedoturbation on luminescence dating. *Quaternary Science Reviews* 22, 1169–1176.
- Beckmann, T. (1997): *Präparation bodenkundlicher Dünnschliffe für mikromorphologische Untersuchungen*. *Hohenheimer Bodenkundliche Hefte* 40, 89–103.
- Berger, G.W., Pillans, B.J. & A.S. Palmer (1992): Dating loess up to 800 ka by thermoluminescence. *Geology* 20, 403–406.

## 8. References

---

- Berger, G.W., Pillans, B.J. & P.J. Tonkin, P.J. (2001): Luminescence chronology of loess-palaeosol sequences from Canterbury, South Island, New Zealand. *New Zealand Journal of Geology and Geophysics* 44, 501-516.
- Boessenkool, K.P. (2001): Environmental changes in the North Atlantic region during the last deglaciation. PhD-thesis University Utrecht/Netherlands, 128 pp.
- Bøtter-Jensen, L., Duller, G.A.T., Murray, A.S. & D. Banerjee (1999): Blue light emitting diodes for optical stimulation of quartz in retrospective dosimetry and dating. *Radiation Protection Dosimetry* 84, 335–340.
- Bouab, N. & M. Lamothe (1997): Geochronological framework for the Quaternary paleoclimatic record of the Rosa Negra section (Fuerteventura-Canary Islands, Spain). In: *Climates of the Past: Proceedings of the International Union of Geological Sciences*. Edited by J. Meco and N. Petit-Maire, pp. 37–42, Univ. de Las Palmas de Gran Canaria, Las Palmas de Gran Canaria, Spain.
- Bozzano, G., Kuhlmann, H. & B. Alonso (2002): Storminess control over African dust input to the Moroccan Atlantic margin (NW Africa) at the time of maxima boreal summer insolation: a record of the last 220 kyr. *Palaeogeography, Palaeoclimatology, Palaeoecology* 183, 155-168.
- Brinkmann, R. (1977): *Historische Geologie. - Abriss der Geologie*. volume 2, Stuttgart, 400 pp.
- Bronger, A. (1976): Zur quartären Klima- und Landschaftsentwicklung des Karpatenbeckens auf (paläo-) pedologischer und bodengeographischer Grundlage. *Kieler Geographische Schriften* 45, 268 pp.
- Bronger, A. & T. Heinkele (1989): Micromorphology and genesis of palaeosols in the Luochuan loess section, China: Pedostratigraphic and environmental implications. *Geoderma* 45/2, 123-143.
- Bronger, A., Winter, R. & S. Sedov (1998): Weathering and clay mineral formation in two Holocene soils and in buried palaeosols in Tadjikistan: towards a Quaternary palaeoclimatic record in Central Asia. *Catena* 34, 19-34.
- Bronger, A. & S.N. Sedov (2003): Vetusols and paleosols: Natural versus man-induced environmental change in the Atlantic coastal region of Morocco. *Quaternary International* 106/107, 33-60.
- Broström, A., Coe, M., Harrison, S.P., Gallimore, R., Kutzbach, J.E., Foley, J., Prentice, I.C. & P. Behling (1998): Land surface feedbacks and palaeomonsoons in northern Africa. *Geophysical Research Letters* 25/19, 3615-3618.
- Brunner, C.A. & R. Maniscalco (1998): Late Pliocene and Quaternary paleoceanography of the Canary Island Region inferred from planctonic foraminifer assemblages of site 953. *Proceedings of the Ocean Drilling Program, Scientific Results* 157, 73–82.
- Bubbenzer, O. & A. Hilgers (2003): Luminescence-dating of Holocene playa sediments of the Egyptian Plateau Western Desert. *Quaternary Science Reviews* 22, 1077–1084.
- Busacca, A. & M. Cremaschi (1998): The role of time versus climate in the formation of deep soils of the Apennine Fringe of the Po Valley, Italy. *Quaternary International* 51/52, 95-107.

## 8. References

---

- Bush, A.B.G., Little, E.C., Rokosh, D., White, D. & N.W. Rutter (2004): Investigation of the spatio-temporal variability in Eurasian Late Quaternary loess–paleosol sequences using a coupled atmosphere–ocean general circulation model. *Quaternary Science Reviews* 23, 481-498.
- Cacho, I., Grimalt, J.O., Pelejero, C., Canals, M., Sierro, F.J., Flores, J.A. & N. Shackleton (1999): Dansgaard-Oeschger and Heinrich event imprints in Alboran Sea palaeotemperatures. *Paleoceanography* 14/6, 698–705.
- Caquineau, S., Gaudichet, A., Gomes, L., Magonthier, M.-C. & B. Chatenet (1998): Saharan dust: Clay ratio as a relevant tracer to assess the origin of soil-derived aerosols. *Geophysical Research Letters* 25, 983–986.
- Carracedo, J.C., Day, S., Guillou, H., Rodríguez-Badiola, E., Canas, J.A. & F.J. Pérez-Torrado (1998): Hotspot volcanism close to a passive continental margin: the Canary Islands. *Geological Magazine* 135/5, 591-604.
- Carracedo, J.C., Singer, B., Jicha, B., Guillou, H., Rodríguez-Badiola, E., Meco, J., Pérez-Torrado, J., Gimeno, D., Socorro, S. & A. Láinez (2003): La erupción y el tubo volcánico del volcán Corona (Lanzarote, Islas Canarias). *Estudios Geológicos* 59, 277–302.
- Carter-Stiglitz, B., Banerjee, S.K., Gurlan, A. & E. Oches (2006): A multi-proxy study of Argentina loess: Marine oxygen isotope stage 4 and 5 environmental record from pedogenic hematite. *Palaeogeography, Palaeoclimatology, Palaeoecology* 239, 45-62.
- Cayre, O., Lancelot, Y. & E. Vincent (1999): Palaeoceanographic reconstructions from planktonic foraminifera off the Iberian Margin: Temperature, salinity, and Heinrich events. *Paleoceanography* 14/3, 384-396.
- Cheddadi, R., Lamb, H.F., Guiot, J. & S. van der Kaars (1998): Holocene climate change in Morocco: A quantitative reconstruction from pollen data. *Climate Dynamics* 14, 883-890.
- Clark, P.U., Alley, R.B. & D. Pollard (1999): Northern Hemisphere ice-sheet influences on global climate change. *Science* 286, 1104-1111.
- Coello, J., Cantagrel, J.-M., Hernán, F., Fúster, J.-M., Ibarrola, E., Ancochea, E., Casquet, C., Jamond, C., de Téran, J.-R.D. & A. Cendrero (1992): Evolution of the eastern volcanic ridge of the Canary Islands based on new K-Ar data. *Journal of Volcanology and Geothermal Research* 53, 251-274.
- Coello, J.J., Castillo, C. & E.M. González (1999): Stratigraphy, Chronology, and Palaeoenvironmental reconstruction of the quaternary sedimentary infilling of a volcanic tube in Fuerteventura, Canary Islands. *Quaternary Research* 52, 360-368.
- Coudé-Gaussen, G., Rognon, P., Bergametti, G., Gomes, L., Strauss, B., Gros, J.M. & M.N. le Coustumer (1987): Saharan dust of Fuerteventura island (Canaries): Chemical and mineralogical characteristics, air mass trajectories, and probable sources. *Journal of Geophysical Research* 92/D8, 9753-9771.

## 8. References

---

- Coudé-Gaussen, G. (1991): Les poussières sahariennes. Edition John Libbey Eurotext, Paris, 485 pp.
- Criado, C. & P. Dorta (2003): An unusual 'blood rain' over the Canary Islands (Spain). The storm of January 1999. *Journal of Arid Environments* 55, 765-783.
- Criado, C. & P. Atoche-Peña (2004): Influyó la ganadería de los mahos en el deterioro paleoambiental de la isla de Lanzarote? *Revista Tenique* 6, 137-157.
- Criado, C., Guillou, H., Hansen, A., Hansen, C., Lillo, P., Torres, J.M. & A. Naranjo (2004): Geomorphological evolution of parque natural de Las Dunas de Corralejo (Fuerteventura, Canary Islands). In: *Contribuciones recientes sobre geomorfología. (Actas de la VIII Reunión de Geomorfología, Toledo, 22-25 de septiembre de 2004)*, edited by G. Benito and A. Diez-Herrero, pp. 291 - 297, Cons. Super. de Invest. Cient., Madrid.
- Crowley, T.J. (1981): Temperature and circulation changes in the Eastern North Atlantic during the last 150 000 years: Evidence from the planktonic foraminiferal record. *Marine Micropalaeontology* 6, 97-129.
- Dahlgren, R.A. (1994): Quantification of allophane and imogolite. *Quantitative methods in soil mineralogy*, SSSA Miscellaneous Publications, Madison, WI, 430-450.
- Damnati, B. (1996): Mineralogical and sedimentological characterization of Quaternary aeolian formations and palaeosols in Fuerteventura and Lanzarote (Canary Islands, Spain). In: J. Meco & N. Petit-Maire (Eds.): *Climates of the past, Proceedings of the CLIP meeting held in June 2-7, 1995 - Lanzarote und Fuerteventura (Canary Islands, Spain)*, IUGS-UNESCO, Las Palmas de Gran Canaria, 71-77.
- Damnati, B., Petit-Maire, N., Fontugne, M., Meco & J. D. Williamson (1996): Quaternary palaeoclimates in the eastern Canary Islands. *Quaternary International* 31, 37-46.
- Dan, J., Yaalon, D.H., Moshe, R. & S. Nissim (1982): Evolution of reg soils in southern Israel and Sinai. *Geoderma* 28, 172-202.
- Dearing, J.A., Livingstone, I.P., Bateman, M.D. & K. White (2001): Palaeoclimate records from OIS 8.0-5.4 recorded in loess-palaeosol sequences on the Matmata Plateau, southern Tunisia, based on mineral magnetism and new luminescence dating. *Quaternary International* 76/77, 43-56.
- Ding Z.L., Rutter, N.W., Sun, J.M., Yang S.L. & T.S. Liu (2000): Re-arrangement of atmospheric circulation at about 2.6 Ma over northern China: evidence from grain size records of loess-palaeosol and red clay sequences. *Quaternary Science Reviews* 19/6, 547-558.
- Ding, Z.L. & S.L. Yang (2000): C3/C4 vegetation evolution over the last 7.0 Myr in the Chinese Loess Plateau: evidence from pedogenic carbonate  $\delta^{13}\text{C}$ . *Palaeogeography, Palaeoclimatology, Palaeoecology* 160/3, 291-299.
- Dodonov, A.E. & L.L. Baiguzina (1995): Loess stratigraphy of Central Asia: Palaeoclimatic and palaeoenvironmental aspects. *Quaternary Science Reviews* 14, 707-720.

## 8. References

---

- Duchaufour, P. (1982): *Pedology. Pedogenesis and classification*. George Allen & Unwin, London, Boston, Sydney.
- Dupont, L. M. (1993): Vegetation zones in NW Africa during the Brunhes chron reconstructed from marine palynological data, *Quaternary Science Reviews* 12, 189–202.
- Edmunds, W.M., Dodo, A., Djoret, D., Gasse, F., Gaye, C.B., Goni, I.B., Travi, Y., Zouari, K. & G.-M. Zuppi (2004): Groundwater as an archive of climatic and environmental change: Europe to Africa. In: Battarbee, R.W., Gasse, F. & C.E. Stickley (eds.): *Past climate variability through Europe and Africa*. Springer, Dordrecht, 279-306.
- Edwards, N. & J. Meco (2000): Morphology and paleoenvironment of brood cells of Quaternary ground-nesting solitary bees (Hymenoptera. Apidae) from Fuerteventura, Canary Islands, Spain. *Proceedings of the Geological Association* 111, 173–183.
- Evans, M. E. & F. Heller (2003): *Environmental Magnetism – Principles and Applications of Enviromagnetics*. Academic Press, 299 pp.
- Evans, R.D., Jefferson, I.F., Kumar, R., O’Hara-Dhand, K. & I.J. Smalley (2004): The nature and early history of airborne dust from North Africa; in particular the Lake Chad basin. *Journal of African Earth Sciences* 39, 81-87.
- Fassbinder, J.W.E., Stanjek, H. & H. Vali (1990): Occurrence of magnetic bacteria in soil. *Nature* 343, 161-163.
- Faust, D. & M. Herkommer (1995): Rill erosion in Lower Andalusia. A statistical evaluation of rills. *Zeitschrift für Geomorphologie N.F. Suppl.* 99, 17–28.
- Faust, D., Zielhofer, C., Baena-Escudero, R. & F.D. del Olmo (2004): High-resolution fluvial record of late Holocene geomorphic change in northern Tunisia: climatic or human impact? *Quaternary Science Reviews* 23, 1757-1775.
- Faust, D. & F. Haubold (2007): Was können Böden uns verraten ? *Local Land and Soil News* 20/21, 13-15.
- Fernandez-Caldas, E., Quantin, P. & M.L. Tejedor-Salguero (1981): Séquences climatiques des sol dérivés de roches volcaniques aux Iles Canaries. *Geoderma* 26, 47-62.
- Frechen M., Horvat, E. & G. Gabris (1997): Geochronology of Middle and Upper Pleistocene Loess Sections in Hungary. *Quaternary Research* 48/3, 291-312.
- Frechen, M., Zander, A., Cilek, V. & V. Ložek (1999): Loess chronology of the Last Interglacial/Glacial cycle in Bohemia and Moravia, Czech Republic. *Quaternary Science Reviews* 18, 1467-1493.
- Freudenthal, T., Meggers, H., Henderiks, J., Kuhlmann, H., Moreno, A. & G. Wefer (2002): Upwelling intensity and filament activity off Morocco during the last 250.000 years. *Deep-Sea Research II*/49, 3655-3674.
- Fuchs, M. (2001): *Die OSL-Datierung von Archäosedimenten zur Rekonstruktion anthropogen bedingter Sedimentumlagerung*. PhD thesis, University of Heidelberg, 179 pp.

## 8. References

---

- Fuchs, M. & A. Lang (2001): OSL dating of coarse-grain fluvial quartz using single-aliquot protocols on sediments from NE Peloponnes, Greece. *Quaternary Science Reviews* 20, 783–787.
- Fuchs, M. & G. A. Wagner (2003): Recognition of insufficient bleaching by small aliquots of quartz for reconstructing soil erosion in Greece. *Quaternary Science Reviews* 22, 1161–1167.
- Fuchs, M., Lang, A. & G.A. Wagner (2004): The history of Holocene soil erosion in the Phlious Basin, NE Peloponnes, Greece, based on optical dating. *The Holocene* 14/3, 334–345.
- Fuchs, M., Straub, J & L. Zöller (2005): Residual Luminescence signals of recent river flood sediments: A Comparison between quartz and feldspar of fine- and coarse-grain sediments. *Ancient TL* 23, 25-30.
- Fuchs, M., Woda, C. & A. Bürkert (2007): Chronostratigraphy of a sediment record from the Hajar mountain range in north Oman: Implications for optical dating of insufficiently bleached sediments. *Quaternary Geochronology* 2, 202-207.
- Galbraith, R.F., Roberts, R.G., Laslett, G.M., Yoshida, H. & J.M. Olley (1999): Optical dating of single and multiple grains of quartz from Jinmium Rock Shelter, northern Australia: Part I, experimental design and statistical models. *Archaeometry* 1/2, 339-364.
- Ganopolski, A., Rahmstorf, S., Petoukhov, V. & M. Claussen (1998): Simulation of modern and glacial climates with a coupled global model of intermediate complexity. *Nature* 391, 351-356.
- Garcia-Herrera, R., Gallego-Puyol, D. & E. Hernandez-Martin (2001): Influence of the North Atlantic Oscillation on the Canary Islands precipitation. *Journal of Climate* 14, 3889-3903.
- Gasse, F., Fontes, J.C., Plaziat, J.C., Carbonel, P., Kaczmarek, I., de Deckker, P., Soulié-Marsche, I., Callot, Y. & P.A. Dupeuble (1987): Biological remains, geochemistry and stable isotopes for the reconstruction of environmental and hydrological changes in the Holocene lakes from North Sahara. *Palaeogeography, Palaeoclimatology, Palaeoecology* 60, 1-46.
- Geldmacher, J., Hoernle, K., van den Bogaard, P., Zankl, G. & D. Garbe-Schönberg (2001): Earlier history of the >70 Ma old Canary hotspot based on the temporal and geochemical evolution of the Selvagen Archipelago and neighboring seamounts in the eastern North Atlantic. *Journal of Volcanology and Geothermal Research* 111, 55-87.
- Genise, J.F. & N. Edwards (2003): Ichnotaxonomy, origin, and paleoenvironment of Quaternary insect cells from Fuerteventura, Canary Islands, Spain. *Journal of the Kansas Entomological Society* 76/2, 320-327.
- Godfrey-Smith, D. I., Huntley, D.J. & W.H. Chen (1988): Optical dating studies of quartz and feldspar extracts. *Quaternary Science Reviews* 7, 373–380.
- Goudie, A.S. & N.J. Middleton (2001): Saharan dust storms: nature and consequences. *Earth-Science Reviews* 56, 179-204.
- Grousset, F.E., Parra, M., Bory, A., Martinez, P., Bertrand, P., Shimmield, G. & R.M. Ellam (1998): Saharan wind regimes traced by the Sr-Nd isotopic composition of subtropical Atlantic sediments: Last glacial maximum versus today. *Quaternary Science Reviews* 17, 395-409.

## 8. References

---

- Goudie, A.S. & N.J. Middleton (2001): Saharan dust storms: nature and consequences. *Earth-Science Reviews* 56, 179-204.
- Guieu, C., Loye-Pilot, M.-D., Ridame, C. & C. Thomas (2002): Chemical characterization of the Saharan dust end-member: Some biogeochemical implications for the western Mediterranean Sea. *Journal of Geophysical Research* 107, 2002, d15, ACH5.1-ACH5.11.
- Hambach, U. Rolf, C. & E. Schnepf (2008): Magnetic dating of Quaternary sediments, volcanites and archaeological materials: an overview. *Eiszeitalter und Gegenwart. Quaternary Science Journal* 57, 25-51.
- Haslett, S.K. & C. Davis (2006): Late Quaternary climate-ocean changes in western North Africa: offshore geochemical evidence. *Transactions of the Institute of British Geographers* 31, 19-33.
- Hatté, C, Antoine, P., Fontugne, M., Lang, A., Rousseau, D.-D. & L. Zöller (2001):  $\delta^{13}\text{C}$  of loess organic matter as a potential proxy for palaeoprecipitation. *Quaternary Research* 55, 33-38.
- Heinkele, T. (1990): Bodengeographische und paläopedologische Untersuchungen im zentralen Lössplateau von China - ein Beitrag zur quartären Klima- und Landschaftsgeschichte. *Schriftenreihe des Instituts für Pflanzenernährung und Bodenkunde der Universität Kiel* 9, 120 pp.
- Helgeson, H.C., Murphy, W.M. & P. Aargaard (1984): Thermodynamic and kinetic constraints on reaction rates among minerals and aqueous solutions. II. Rate constants, effective surface area, and the hydrolysis of feldspar. *Geochimica et Cosmochimica Acta* 48, 2405-2432.
- Heller, F. & T.S. Liu (1986): Palaeoclimate and sedimentary history from magnetic susceptibility of loess in China, *Geophysical Research Letters* 13, 1169-1172.
- Herrmann, L., Jahn, R. & K. Stahr (1996): Identification and quantification of dust additions in perisaharan soils. In: Guerzoni, S. & R. Chester (Eds.): *The impact of desert dust across the Mediterranean*. Kluwer Academic Publishers, Netherlands, pp. 33–151.
- Hilgers, A., Murray, A.S., Schlaak, N. & U. Radtke (2001). Comparison of quartz OSL protocols using Lateglacial and Holocene dune sands from Brandenburg, Germany. *Quaternary Science Reviews* 20, 731–736.
- Hillaire-Marcel, C., Ghaleb, B., Gariépy, C., Zazo, C., Hoyos, M. & J.-L. Goy (1995): U-Series dating by the TIMS technique of land snails from palaeosols in the Canary Islands. *Quaternary Research* 44, 276-282.
- Hoelzmann, P., Gasse, F., Dupont, L., Salzmann, U., Staubwasser, M., Leuschner, D.C. & F. Sirocko (2004): Palaeoenvironmental changes in the arid and subarid belt (Sahara-Sahel-Arabian Peninsula) from 150 kyr to present. In: Battarbee, R.W., Gasse, F. & C.E. Stickley (eds.): *Past climate variability through Europe and Africa*. Springer, Dordrecht, 219-256.
- Höllermann, P. (2006): Zur geomorphologischen Wasserwirkung in den arid-semiariden Subtropen – Fallstudie Fuerteventura (Kanarische Inseln, Spanien). *Bayreuther Geographische Arbeiten* 27, 55-103.

## 8. References

---

- Hölting, B. (1996): Hydrogeologie. Einführung in die Allgemeine und Angewandte Hydrogeologie, 5th edition. Edition Enke, Stuttgart, 439 pp.
- Holz, C., Stuut, J.B. & R. Henrich (2004): Variability in terrigenous sedimentation processes off NW Africa and its relation to climate changes: inferences from grain-size distributions of a Holocene marine sediment record. *Sedimentology* 51/5, 1145-1154.
- Holz, C., Stuut, J.B., Henrich, R. & H. Meggers (2007): Variability in terrigenous sedimentation processes off NW Africa and its relation to climate changes: inferences from grain-size distributions of a Holocene marine sediment record. *Sedimentary Geology* 202, 499-508.
- Hooghiemstra, H., Stalling, H., Agwu, C.O.C. & L.M. Dupont (1992): Vegetational and climatic changes at the northern fringe of the Sahara 250.000-5.000 years BP: Evidence from 4 marine pollen records located between Portugal and the Canary Islands. *Review of Palaeobotany and Palynology* 74, 1-53.
- Hurrell, J.W. (1995): Decadal trends in the North Atlantic Oscillation: Regional temperatures and precipitation. *Science* 269, 676-679.
- Hurst, V. J. & A. C. Kunkle (1985): Dehydroxylation, rehydroxylation, and stability of kaolinite. *Clays and Clay Minerals* 33(1), 1–14.
- Instituto Tecnológico y Geominero de España (2005): Mapa geológico de España, Escala 1 : 100.000, Memoria de la hoja geológica de la Isla de Lanzarote. Madrid. ISBN: 84-7840-606-9
- Intergovernmental Panel on Climate Change (2007): Climate Change 2007, the Fourth Assessment Report. The Core Writing Team, Pachauri, R.K. & A. Reisinger (Eds.), IPCC, Geneva, Switzerland. pp 104.
- Issar, A.S. & H.J. Bruins (1983): Special climatological conditions in the deserts of Sinai and the Negev during the Latest Pleistocene. *Palaeogeography, Palaeoclimatology, Palaeoecology* 43, 63-72.
- Jacobs, Z., Duller, G.A.T. & A.G. Wintle (2006): Interpretation of single grain De-distributions and calculation of De distributions and calculation of De. *Radiation Measurements* 41, 264-277.
- Jahn, R. (1988): Böden Lanzarotes. PhD-thesis, Stuttgart-Hohenheim, 175 pp.
- Jahn, R. (1995): Ausmaß äolischer Einträge in circumsaharischen Böden und ihre Auswirkungen auf Bodenentwicklung und Standortseigenschaften. Habilitation, Stuttgart-Hohenheim, pp. 175.
- Jain, M., Murray, A.S. & L. Botter-Jensen (2004): Optically stimulated luminescence dating: How significant is incomplete light exposure in fluvial environments? *Quaternaire* 15/1-2, 143-157.
- Junfeng, J., Jun, C. & L. Huayu (1999): Origin of illite in the loess from the Luochuan area, Loess Plateau, central China. *Clay Minerals* 34/4, 525-532.
- Juyal, N., Chamyal, L.S., Bhandari, S., Bhushan, R. & A.K. Singhvi (2006): Continental record of the southwest monsoon during the last 130 ka: evidence from the southern margin of the Thar desert, India. *Quaternary Science Reviews*, 25, 2632-2650.

## 8. References

---

- Kageyama, M., Valdes, P.J., Ramstein, G., Hewitt, C. & U. Wyputta (1999): Northern Hemisphere storm tracks in present day and Last Glacial Maximum climate simulations: A comparison of the European PMIP Models. *Journal of Climate* 12, 742-760.
- Kallel, N., Duplessy, J.-C., Labeyrie, L, Fontugne, M., Paterne, M. & M. Montacer (2000): Mediterranean pluvial periods and sapropel formation over the last 200.000 years. *Palaeogeography, Palaeoclimatology, Palaeoecology* 157, 45-58.
- Kämmer, F. (1974): Klima und Vegetation auf Tenerife, besonders im Hinblick auf den Nebelniederschlag. *Scripta Geobotanica* 7, Göttingen, 78 pp.
- Kemp, R.A. (1999): Micromorphology of loess-palaeosol sequences: a record of palaeoenvironmental change. *Catena* 35/2, 179-196.
- Kim, J.-H., Meggers, H., Rimbu, N., Lohmann, G., Freudenthal, T., Müller, P.J. & R.R. Schneider (2007): Impacts of the North Atlantic gyre circulation on Holocene climate off northwest Africa. *Geology* 35/5, 387-390.
- Knippertz, P., Christoph, M. & P. Speth (2003): Long-term precipitation variability in Morocco and the link to the large-scale circulation in recent and future climates. *Meteorology and Atmosphere Physics* 83, 67-88.
- Konert, M. & J. Vandenberghe (1997): Comparison of laser grain size analysis with pipette and sieve analysis: a solution for the underestimation of the clay fraction. In: *Sedimentology* 44, 523 - 535.
- Koopmann, B. (1981): Sedimentation von Saharastaub im subtropischen Nordatlantik während der letzten 25 000 Jahre. *Meteor Forschungsergebnisse C/35*, 23-59.
- Kovda, I., Lynn, W., Williams, D. & O. Chichagova (2001): Radiocarbon age of Vertisols and its interpretation using data on gilgai complex in the North Caucasus. *Radiocarbon* 43, 603-609.
- Krbetschek, M.R., T. Trautmann, T., Dietrich, A. & W. Stolz (2000): Radioluminescence dating of sediments: methodological aspects. *Radiation Measurements* 32, 493-498.
- Krischner, H. (1990): Einführung in die Röntgenfeinstrukturanalyse. Edition Vieweg, Braunschweig. 193 pp.
- Kuhlmann, H. (2003): Reconstruction of the sedimentary history offshore NW Africa: Application of core-logging tools. PhD-thesis, University of Bremen, 99 pp.
- Kuhlmann, J., Freudenthal, T., Helmke, P. & H. Meggers (2004): Reconstruction of palaeoceanography off NW Africa during the last 40 000 years: influence of local and regional factors on sediment accumulation. *Marine Geology* 207, 209-224.
- Kühn, P., Billwitz, K., Bauriegel, A., Kühn, D. & W. Eckelmann (2006): Distribution and Genesis of Fahlerden (Albeluvisols) in Germany. *Journal of Plant Nutrition and Soil Science* 169, 420-433.
- Kukla, G. & Z.S. An (1989): Loess stratigraphy in central China. *Palaeogeography, Palaeoclimatology, Palaeoecology* 72, 203-225.

## 8. References

---

- Kunkel, G. (1993) : Die Kanarischen Inseln und ihre Pflanzenwelt. Edition Fischer, Stuttgart, Jena, 230 pp.
- Lai, Z.P., Wintle, A.G. & D.S.G. Thomas (2007): Rates of dust deposition between 50 ka and 20 ka revealed by OSL dating at Yuanbao on the Chinese Loess Plateau. *Palaeogeography, Palaeoclimatology, Palaeoecology* 248/ 3-4, 431-439.
- Lancaster, N., G. Kocurek, A. Singhvi, V. Pandey, M. Deynoux, J. F. Ghienne & K. Lo (2002): Late Pleistocene and Holocene dune activity and wind regimes in the western Sahara desert of Mauritania. *Geology* 30(11), 991–994.
- Lang, A. (1996): Die Infrarot-Stimulierte Lumineszenz als Datierungsmethode für holozäne Lössderivate. *Heidelberger Geographische Arbeiten* 101, 137 pp.
- Lang, A., Lindauer, S., Kuhn, R. & G.A. Wagner (1996): Procedures used for optically and infrared stimulated luminescence dating of sediments in Heidelberg. *Ancient TL* 14/3, 7-11.
- Lang, A. (2003): Phases of soil erosion-derived colluviation in the loess hills of South Germany. *Catena* 51, 209–221.
- Langbein, W.B. & S.A. Schumm (1958): Yield of sediment in relation to mean annual precipitation. *Transactions of the American Geophysical Union* 39/6, 1076–1084.
- Lepper, K., Larsen, N.A. & S. W. S. McKeever (2000): Equivalent dose distribution analysis of Holocene aeolian and fluvial quartz sands from Central Oklahoma. *Radiation Measurements* 32, 603–608.
- Lepper, K. & S.W.S. McKeever (2002): An objective methodology for dose distribution analysis. *Radiation Protection Dosimetry* 101/1-4, 349-352.
- Lian, O.B. & D.J. Huntley (1999): Optical dating studies of postglacial aeolian deposits from the south-central interior of British Columbia, Canada. *Quaternary Science Reviews* 18, 1453-1466.
- Lioubimtseva, E. (2004): Climate change in arid environments: revisiting the past to understand the future. *Progress in Physical Geography* 28/4, 1–29.
- Liu, Q., Banerjee, S.K., Jackson, M.J., Chen, F., Pan, Y. & R. Zhu (1998): An integrated study of the grain-size-dependent magnetic mineralogy of the Chinese loess/palaeosol and its environmental significance. *Journal of Geophysical Research* 108, doi:10.1029/2002JB002264
- Liu, Q., Barrón, V., Torrent, J. Eeckhout, S.G. & C. Deng (2008) : Magnetism of intermediate hydromaghemite in the transformation of 2-line ferrihydrite into hematite and its palaeoenvironmental implications. *Journal of Geophysical Research* 113, B01103, doi: 10.1029/2007JB005207.
- Mabbutt, J.A. (1989): Impacts of carbon dioxide warming on climate and man in the semi-arid tropics. *Climate Change* 15/1-2, 191-221.
- Maher, B.A. (1998): Magnetic properties of modern soils and Quaternary loessic paleosols: paleoclimatic implications. *Palaeogeography, Palaeoclimatology, Palaeoecology* 137, 25-54.

## 8. References

---

- Maher, B.A. & R. Thompson (1992): Palaeoclimatic significance of the mineral magnetic record of the Chinese loess and palaeosols. *Quaternary Research* 37, 155-170.
- Maher, B., Alekseev, A. & T. Alekseeva (2002): Variation of soil magnetism across the Russian steppe: its significance for use of soil magnetism as a palaeorainfall proxy. *Quaternary Science Reviews* 21, 1571-1576.
- Maley, J. (2000): Last glacial maximum lacustrine and fluvial formations in the Tibesti and other Saharan mountains, and large-scale climatic teleconnections linked to the activity of the Subtropical Jet Stream. *Global and Planetary Change* 26, 121-136.
- Marković, S.B., Oches, E., Sümeği, P., Jovanović, M. & T. Gaudenyi (2006): An introduction to the Upper and Middle Pleistocene loess-palaeosol sequences of Ruma section (Vojvodina, Yugoslavia). *Quaternary International* 149, 80-86.
- Markovic, S.B. Hambach, U., Catto, N., Jovanovic, M., Buggle, B., Machalet, B., Zöller, L., Glaser, B. & M. Frechen (2008): Middle and Late Pleistocene loess sequences at Batajnica, Vojvodina, Serbia. *Quaternary International* 198, 255-266.
- Martinson, D.G., Pisias, N.G., Hays, J.D., Imbrie, J., Moore, T.C. & N.J. Shackleton (1987): Age dating and the orbital theory of the Ice Ages: Development of a high-resolution 0 to 300,000-year chronostratigraphy. *Quaternary Research*, 27, 1-29.
- Mason, J.A., Jacobs, P.M., Greene, R.S.B. & W.D. Nettleton (2003): Sedimentary aggregates in the Peoria loess of Nebraska, USA. *Catena* 53, 377-397.
- Mason, J.A., Joeckel, R.M. & E.A. Bettis III (2007): Middle to Late Pleistocene loess record in eastern Nebraska, USA, and implications for the unique nature of Oxygen Isotope Stage 2. *Quaternary Science Reviews* 26, 773-792.
- Matasova, G., Petrovsky, E., Jordanova, N., Zykina, V. & A. Kapicka (2001): Magnetic study of Late Pleistocene loess/palaeosol sections from Siberia: Palaeoenvironmental implications. *Geophysical Journal International* 147, 367-380.
- McCave, I.N. & J.P.M. Syvitsky (1991): Principles and methods of geological particle size analysis. In: Syvitsky, J.P.M. (ed.): Principles, methods, and application of particle size analysis. Cambridge University Press, 3 - 21.
- Meco, J. & R. Pomel (1985): Les formations marines et continentales intervolcaniques des Iles Canaries orientales (Grande Canarie, Fuerteventura et Lanzarote): Stratigraphie et signification paléoclimatique. *Estudios Geológicos* 41, 223-227.
- Meco, J., Petit-Maire, N., Fontugne, M., Shimmiel, G. & A.J. Ramos (1997): The Quaternary deposits in Lanzarote and Fuerteventura (Eastern Canary Islands, Spain): an overview. In: J. Meco & N. Petit-Maire (Eds.): *Climates of the past. Proceedings of the CLIP meeting held in June 2-7, 1995 - Lanzarote und Fuerteventura (Canary Islands, Spain)*, IUGS-UNESCO, Las Palmas de Gran Canaria, 123-136.

## 8. References

---

- Meco, J., Ballester-Santos, J., Perera-Betancort, M.A., Marrero-Romero, R., Niz-Guadalupe, G. & A. Pallarés-Padilla (2002): Palaeoclimatología de Lanzarote y La Graciosa (yacimientos palaeontológicos). Servicio del Patrimonio Histórico del Cabildo de Lanzarote, 83 pp.
- Meco, J., Guillou, H., Carracedo, J.-C., Lomoschitz, A., Ramos, A.-J., G. & J.-J. Rodríguez-Yáñez (2002): The maximum warmings of the Pleistocene world climate recorded in the Canary Islands. *Paleogeography, Paleoclimatology, Paleoecology* 185, 197–210.
- Menéndez, I., Diaz-Hernandez, J.L., Mangas, J., Alonso, I. & P.-J. Sanchez-Soto (2007): Airborne dust accumulation and soil development in the North-East sector of Gran Canaria (Canary Islands, Spain), *Journal of Arid Environments* 71, 57-81.
- Menéndez, I., Cabrera, L., Sánchez-Pérez, I., Mangas, J. & I. Alonso (2009): Characterisation of two fluvio-lacustrine loessoid deposits on the island of Gran Canaria, Canary Islands. *Quaternary International* 196, 36-43.
- deMenocal, P.B., Ruddiman, W.F. & E.M. Pokras (1993): Influences of high- and low-latitude processes on African terrestrial climate: Pleistocene aeolian records from Equatorial Atlantic Ocean Drilling Program site 663. *Palaeoceanography* 8/2, 209-242.
- deMenocal, P., Ortiz, J., Guilderson, T. & M. Sarinthein (2000): Coherent high- and low-latitude climate variability during the Holocene warm period. *Science* 288, 2198–2202.
- Michalet, R., Guillet, B. & B. Souchier (1993): Hematite identification in pseudoparticles of Moroccan rubified soils. *Clay Minerals* 28, 233-242.
- Mizota, C. & Y. Matsuhisa (1995): Isotopic evidence for the aeolian origin of quartz and mica in soils developed on volcanic materials in the Canary Archipelago. *Geoderma* 66, 313-320.
- Moreno, A., Taragona, J., Henderiks, J., Canals, M., Freudenthal, T. & H. Meggers (2001): Orbital forcing of dust supply to the North Canary Basin over the last 250 kyr. *Quaternary Science Reviews* 20, 1327-1339.
- Moreno, A., Cacho, I., Canals, M., Prins, M.A., Sanchez-Goni, M.-F., Grimalt, J.O. & G.J. Weltje (2002a): Saharan dust transport and high-latitude glacial climatic variability: The Alboran Sea record. *Quaternary Research* 58, 318-328.
- Moreno, A., Nave, S., Kuhlmann, H., Canals, M., Targarona, J., Freudenthal, T. & F. Abrantes (2002b): Productivity response in the North Canary Basin to climate changes during the last 250.000 years: a multi-proxy approach. *Earth and Planetary Science Letters* 196, 147-159.
- Moreno, A. & M. Canals (2004): The role of dust in abrupt climate change: insights from offshore Northwest Africa and Alboran Sea sediment records. *Contributions to Science* 2/4, 485–498.
- Mountney, N.P. (2003): Modelling the Response of aeolian Desert Systems to Climate Change. British Sedimentological Research Group Annual General Meeting, Leeds, 20th-22<sup>nd</sup> of December 2003.

## 8. References

---

- Muhs, D.R., Bush, C.A., Stewart, K.C., Rowland, T.R. & R.C. Crittenden (1990): Geochemical evidence of Saharan dust parent material for soils developed on Quaternary limestones of Caribbean and Western Atlantic islands. *Quaternary Research* 33, 157-177.
- Murray, A.S. & A.G. Wintle (2000): Luminescence dating of quartz using an improved single-aliquot regenerative-dose protocol. *Radiation Measurements* 32, 57-73.
- Narcisi, B., Anselmi, B., Catalano, F., Dai Pra, G. & G. Magri (1992): Lithostratigraphy of the 250 000 year record of lacustrine sediments from the Valle di Castiglione Crater, Roma. *Quaternary Science Reviews* 11, 353-362.
- Narcisi, B. (2001): Palaeoenvironmental and palaeoclimatic implications on the Late-Quaternary sediment record of Vico volcanic lake (central Italy). *Journal of Quaternary Science* 16/3, 245-255.
- Nave, S., Salgueiro, E. & F. Abrantes (2003): Siliceous sedimentary record of the last 280 ka in the Canary basin (NW Africa). *Marine Geology* 196, 21-35.
- Nordt, L.C., Wilding, L.P., Lynn, W.C. & C.C. Crawford (2004): Vertisol genesis in a humid climate of the coastal plain of Texas, U.S.A. *Geoderma* 122, 83-102.
- Olley, J., Caitcheon, G. & A. Murray (1998): The distribution of apparent dose as determined by optically stimulated luminescence in small aliquots of fluvial quartz: Implications for dating young sediments. *Quaternary Geochronology* 17, 1033–1040.
- Olley, J.M., Pietsch, T. & R.G. Roberts (2004): Optical dating of Holocene sediments from a variety of geomorphic settings using single grains of quartz. *Geomorphology* 60, 337-358.
- Olson, C.G. & W.D. Nettleton (1998): Palaeosols and the effects of alteration. *Quaternary International* 51/52, 185-194.
- Ortiz, J.E., Torres, T., Yanes, Y., Castillo, C., de la Nuez, J., Ibanez, M. & M.R. Alonso (2006): Climatic cycles inferred from the aminostratigraphy and aminostratigraphy of Quaternary dunes and palaeosols from the eastern islands of the Canary Archipelago. *Journal of Quaternary Science* 21/3, 287-306.
- Petit-Maire, N., Delibrias, G., Meco, J., Pomel, S. & J.-C. Rosso (1986): Paléoclimatologie des Canaries orientales (Fuerteventura). *C. R. Académie des Sciences Série II*, 303(13), 1241–1246.
- Petschick, R. (2000): MacDiff 4.2.5. Bedienungsanleitung. [http://www.geologie.uni-frankfurt.de/Staff/Homepages/Petschick/PDFs/MacDiff\\_Manual\\_D.pdf](http://www.geologie.uni-frankfurt.de/Staff/Homepages/Petschick/PDFs/MacDiff_Manual_D.pdf).
- Petit-Maire, N., Delibrias, G., Meco, J., Pomel, S. & J.-C. Rosso (1986): Paléoclimatologie des Canaries orientales (Fuerteventura). *Comptes Rendues de l'Académie des Sciences* 303, Série II/13, 1241-1246.
- Pflaumann, U., Sarnthein, N., Ficken, K., Grothmann, A. & A. Winkler (1998): Variations in aeolian and carbonate sedimentation, seasurface temperature, and productivity over the last 3 Ma at site 958 off Northwest Africa. In: Firth, J.V. (Ed.), *Proceedings of the Ocean Drilling Program, Scientific Results 159T*, 3–16.

## 8. References

---

- Pomel, R.-S., Miallier, D., Fain, J. & S. Sanzelle (1985): Datation d'un sol brun-rouge calcifère par une coulée volcanique d'âge Würm ancien (51.000 ans) à Fuerteventura (Iles Canaries). *Méditerranée* 4, 59-68.
- Pons, A. & M. Reille (1988) : The Holocene- and Upper Pleistocene pollen record from Padul (Granada, Spain): A new study. *Palaeogeography, Palaeoclimatology, Palaeoecology* 66, 243-263.
- Porat, N., Zilberman, E., Amit, R. & Y. Enzel (2001): Residual ages of modern sediments in an hyperarid region, Israel. *Quaternary Science Reviews* 20, 795–798.
- Prescott, J.R. & J.T. Hutton (1994): Cosmic ray contributions to dose rates for luminescence and ESR dating : large depths and long-term time variations. *Radiation Measurements* 23, 497-500.
- Prospero, J.M. (1996): Saharan dust transport over the North Atlantic Ocean and Mediterranean: an overview. In: Guerzoni, S., Chester, R. (Eds.), *The impact of desert dust across the Mediterranean*. Kluwer Academic Publishers, Netherlands, 133–151.
- Prospero, J.M. & P.J. Lamb (2003): African Droughts and dust transport to the Caribbean: Climate change implications. *Science* 302, 1024-1027.
- Rognon, P. & G. Coudé-Gaussen (1987): Reconstruction paléoclimatique à partir des sédiments du Pleistocène Supérieur et de l'Holocène du nord de Fuerteventura (Canaries). *Zeitschrift für Geomorphologie N.F.* 31/1, 1-19.
- Rognon, P., Coudé-Gaussen, G., Le Coustumer, M.-N., Balouet, J. C. & S. Occhietti (1989): Le massif dunaire de Jandía (Fuerteventura, Canaries): Évolution des paléoenvironnements de 20.000 BP à l'actuel. *Bulletin de l'Association française pour l'étude du Quaternaire* 1989/1, 31-37.
- Rognon, P. & G. Coudé-Gaussen (1996): Changements dans les circulations atmosphérique et océanique à la latitude des Canaries et du Maroc entre les stades isotopiques 2 et 1. *Quaternaire* 7, 197-206.
- Rohdenburg, H. (1977): Neue 14-C-Daten aus Marokko und Spanien und ihre Aussagen für die Relief- und Bodenentwicklung im Holozän und Jungpleistozän. *Catena* 4, 215-228.
- Romero, C. (2003): *El relieve de Lanzarote*. Rubicón, Cabildo de Lanzarote, 242 pp.
- Rommens, T., Verstraeten, G., Bogman, P., Peeters, I., Poesen, J., Govers, G., van Rompaey, A. & A. Lang (2006): Holocene alluvial sediment storage in a small river catchment in the loess area of central Belgium. *Geomorphology* 77, 187–201.
- Rothe, P. (1996): *Kanarische Inseln*. Edition Gebrüder Bornträger Berlin, Stuttgart, 307 pp.
- Rousseau, D.-D., Zöller, L. & J.-P. Valet (1998): Late Pleistocene climatic variations at Achenheim, France, based on magnetic susceptibility and TL chronology of loess. *Quaternary Research* 49, 255–263.
- Ruddiman, W.F. & A. McIntyre (1981): The North Atlantic during the last deglaciation. *Palaeogeography, Palaeoclimatology, Palaeoecology* 35, 145-214.

## 8. References

---

- Sanchez-Goni, M.F., Turon, J.-L., Eynaud, F. & S. Gendreau (2000): European climatic response to millennial-scale changes in the atmosphere-ocean system during the last glacial period. *Quaternary Research* 54, 394-403.
- Santana-Santana, A. (2003): Consideraciones en torno al medio natural canario anterior a la conquista. *Eres (Arqueología/Antropología)* 11, 61–75.
- Sauer, D. & L. Zöller (2006): Mikromorphologie der Paläoböden der Profile Femés und Guatiza, Lanzarote. *Bayreuther Geowissenschaftliche Arbeiten* 27, 105–130.
- Schäfer, D. & L. Zöller (1996): Zur Charakterisierung des weichselzeitlichen Freilandfundplatzes vom Gamsenberg bei Oppurg/Thüringen. *Tübinger Monographien der Urgeschichte* 11, 235–246.
- Schellenberger, A. & H. Veit (2006): Pedostratigraphy and pedological and geochemical characterization of Las Carreras loess-palaeosol sequence, Valle de Tafi, NW-Argentina. *Quaternary Science Reviews* 25, 811-831.
- Schlichting, E., Blume, H.-P. & K. Stahr (1995): *Bodenkundliches Praktikum. Pareys Studentexte* 81, Edition Blackwell Wissenschaft, Berlin. 295 pp.
- Schmitt, J., Glaser, B. & W. Zech (2003): Amount-dependent isotopic fractionation during compound-specific isotope analysis. *Rapid Communications in Mass Spectrometry* 17, 970-977.
- Schubert, W.H., Ciesielski, P.E., Lu, C. & R.H. Johnson (1995): Dynamical adjustment of the trade wind inversion layer. *Journal of the Atmospheric Sciences* 52/16, 2941-2952.
- Schüle, J., Stahr, K., Zarei, M. & R. Jahn (1989): Basaltverwitterung und Bodenentwicklung seit dem mittleren Tertiär auf Lanzarote, Kanarische Inseln (Profil Malaya Chica). *Zeitschrift für Pflanzenernährung und Bodenkunde* 152, 105-113.
- Schwertmann, U., Murad, E. & D.G. Schulze (1982): Is there Holocene reddening (hematite formation) in soils of axeric temperate areas? *Geoderma* 27, 209-223.
- Sedov, S., Solleiro-Rebolledo, E., Morales-Puente, P., Arias-Herreia, A., Vallejo-Gómez, E. & C. Jasso-Castaneda (2003): Mineral and organic components of the buried palaeosols of the Nevado de Toluca, Central Mexico as indicators of palaeoenvironments and soil evolution. *Quaternary International* 106-107, 169-184.
- Solleiro-Rebolledo, E., Sedov, S., Gama-Castro, J., Flores-Román, D. & G. Escamilla-Sarabia (2003): Paleosol-sedimentary sequences of the Glacis de Buenavista, Central Mexico: Interaction of Late Quaternary pedogenesis and volcanic sedimentation. *Quaternary International* 106/107, 185-201.
- Siegert, M.J. & I. Marsiat (2001): Numerical reconstructions of LGM climate across the Eurasian Arctic. *Quaternary Science Reviews* 20, 1595–1605.
- Singhvi, A.K., Deraniyagala, S.U. & D. Sengupta (1986): Thermoluminescence dating of Quaternary red-sand beds: a case study of coastal dunes in Sri Lanka. *Earth and Planetary Science Letters* 80, 139-144.

## 8. References

---

- Singhvi, A. K. & M. R. Krbetschek (1996): Luminescence dating: A review and a perspective for arid zone sediments. *Annals of the Arid Zone* 35, 249–279.
- Spassov, S., Heller, F. Kretzschmar, R., Evans, M.E., Yue, L.P. & D.K. Nourgaliev (2003): Detrital and pedogenic magnetic mineral phases in the loess/palaeosol sequence at Lingtai (Central Chinese Loess Plateau). *Physics of the Earth and Planetary Interiors* 140, 255–275.
- Springer, M.E. (1958): Desert pavement and vesicular layer of some desert soils in the desert of the Lahontan Basin, Nevada. *Soil Science Society of America Proceedings* 22, 63–66.
- Stephan, S. (2000): Bt-Horizonte als Interglazial-Zeiger in den humiden Mittelbreiten: Bildung, Mikromorphologie, Kriterien. *Eiszeitalter und Gegenwart* 50, 95-106.
- Stoops, G. (2003): Guidelines for analysis and description of soil and regolith thin sections. Soil Science Society of America, Madison, WI, 184 pp.
- Suchodoletz, H. von, Fuchs, M. & L. Zöller (2008): Dating Saharan dust deposits on Lanzarote (Canary Islands) by luminescence dating techniques and their implication for palaeoclimate reconstruction of NW Africa. *Geophysics, Geochemistry, and Geosystems* 9. doi:10.1029/2007GC001658.
- Suchodoletz, H. von, Faust, D. & L. Zöller (2009a): Geomorphological investigations of sediment traps on Lanzarote (Canary Islands) as a key for the interpretation of a palaeoclimate archive off NW Africa. *Quaternary International* 196, 44-56.
- Suchodoletz, H. von, Kühn, P., Hambach, U., Dietze, M., Zöller, L. & D. Faust (2009b): Loess-like and palaeosol sediments from Lanzarote (Canary Islands/Spain) – indicators of palaeoenvironmental change during the Late Quaternary. *Palaeogeography, Palaeoclimatology, Palaeoecology* (accepted). doi:10.1016/j.palaeo.2009.03.019.
- Suchodoletz, H. von, Fuchs, M., Zöller, L. & I. Menéndez (submitted): Luminescence bleaching characteristics of Saharan dust – A case study from Lanzarote, Canary Islands (Spain). *Quaternary Geochronology*.
- Suchodoletz, H. von, Radtke, U., Blanchard, H. & L. Zöller (in preparation): Dating a Middle Pleistocene volcanic phase in Lanzarote (Canary Islands) using red thermoluminescence from baked soil and electron spin resonance from mollusc shells.
- Tipple, B.J. & M. Pagani (2007): The early origins of terrestrial C<sub>4</sub> photosynthesis. *Annual Review of Earth and Planetary Science* 35, 435-461.
- Torrent, J., Barrón, V. & Q. Liu (2006): Magnetic enhancement is linked to and precedes hematite formation in aerobic soils. *Geophysical Research Letters* 33, L02401. doi: 10.1029/2005GL024818.
- Trautmann, T., Krbetschek, M.R., Dietrich, A. & W. Stolz (2000): The basic principle of radioluminescence dating and a localized transition model. *Radiation Measurements* 32, 487-492.

## 8. References

---

- Turon, J.-L., Lézine, A.-M. & M. Denèfle (2003): Land-sea correlations for the last glaciation inferred from a pollen and dinocyst record from the Portuguese margin. *Quaternary Research* 59, 88-96.
- Tzedakis, P.C., McManus, J.F., Hooghiemstra, H., Oppo, D.W. & T.A. Wijmstra (2003): Comparison of changes in vegetation in northeast Greece with records of climate variability on orbital and suborbital frequencies over the last 450 000 years. *Earth and Planetary Science Letters* 212, 197-212.
- Vandenberghe, J., Zisheng, A., Nugteren, G., Huayu, L. & K.V. Huissteden (1997): New absolute time scale for the Quaternary climate in the Chinese loess region by grain-size analyses. *Geology* 25, 35 - 38.
- van Velzen, A.J. & M.J. Dekkers (1999): Low-temperature oxidation of magnetite in loess-paleosol sequences: A correction of rock magnetic parameters. *Studia Geophysica et Geodaetica* 43/4, 357-375.
- Verschuren, D., Briffa, K.R., Hoelzmann, P., Barber, K., Barker, P., Scott, L., Snowball, I., Roberts, N. & R.W. Battarbee (2004): Climate variability in Europe and Africa: A PAGES-PEP III time stream I synthesis. In: Battarbee, R.W., Gasse, F. & C.E. Stickley (eds.): *Past climate variability through Europe and Africa*. Springer, Dordrecht, 567-582.
- Walden, J., Oldfield, F. & J.P. Smith (1999): *Environmental magnetism: a practical guide*. Technical Guide Series 6, Quaternary Research Association, 250 pp.
- Wallinga, J. (2002): Optically stimulated luminescence dating of fluvial deposits: a review. *Boreas* 31/4, 303-322.
- Wan, Y., Kwong, J., Brandes, H.G. & R.C. Jones (2002): Influence of amorphous clay-size materials on soil plasticity and shrink-swell behaviour. *Journal of Geotechnical and Geoenvironmental Engineering* 128/12, 1026-1031.
- Williamson, D., Jackson, M., Banerjee, S.K. & N. Petit-Maire (2004): The magnetism of a glacial aeolianite sequence from Lanzarote (Canary Islands): coupling between luvic calcisol formation and Saharan dust trapping processes during wet deposition events off northwestern Sahara. *Geophysical Journal International* 157, 1090-1104.
- Wintle, A. G. (1973): Anomalous fading of thermoluminescence in mineral samples. *Nature* 245, 143-144.
- Wintle, A. G. (1998): Luminescence dating: Laboratory procedures and protocols. *Radiation Measurements* 27, 769-817.
- Wright, J.S. (2001): "Desert" loess versus "glacial" loess: quartz silt formation, source areas and sediment pathways in the formation of loess deposits. *Geomorphology* 36, 231-256.
- Xie, J. & M. J. Aitken (1991): The hypothesis of mid-term fading and its trial on Chinese loess. *Ancient TL* 9, 21-25.

## 8. References

---

- Yaalon, D. & H.J. Bruins (1977): Sediments and palaeosols as indicators of climatic fluctuations in the loessial desert fringe of the Negev, Israel. Proc. X INQUA Cong., Birmingham, 507.
- Yan, Z. & N. Petit-Maire (1994): The last 140 ka in the Afro-Asian arid/semiarid transitional zone. *Palaeogeography, Palaeoclimatology, Palaeoecology* 110, 217-233.
- Zarei, M. (1989): Verwitterung und Mineralneubildung in Böden aus Vulkaniten auf Lanzarote (Kanarische Inseln). Edition B. Schulz Berlin, 255 p.
- Zech, W. & G. Hintermaier-Erhard (2002): Böden der Welt. Edition Spektrum Akademischer Verlag Heidelberg, Berlin, 113 pp.
- Zech, M. (2006): Evidence for Late Pleistocene climate changes from buried soils on the southern slopes of Mt. Kilimanjaro, Tanzania. *Palaeogeography, Palaeoclimatology, Palaeoecology* 242, 303-312.
- Zhao, M., Beveridge, N.A.S., Shackleton, N.J., Sarnthein, N. & G. Eglinton (1995): Molecular stratigraphy of cores off northwest Africa: Sea surface temperature history over the last 80 ka. *Palaeoceanography* 10/3, 661-675.
- Zöller, L. (2000): Datation par thermoluminescence des loess. In: Aubry D., Guélat M., Detrey J. & Othenin-Girard, B. (eds.): *Dernier cycle glaciaire et occupations paléolithiques à Alle, Noir Bois*. Cahier d'Archéologie Jurassienne 10, 89-91.
- Zöller, L., Suchodoletz, H. von & N. Küster (2003): Ge archaeological and chronometrical evidence of early human occupation on Lanzarote (Canary Islands). *Quaternary Science Reviews* 22, 1299-1307.
- Zöller, L., Rousseau, D.-D., Jäger, K.D. & G. Kukla (2004): Last interglacial, Lower and Middle Weichselian - A comparative study from the Upper Rhine and Thuringian loess areas, *Zeitschrift für Geomorphologie* 48, 1-24.
- Zöller, L., von Suchodoletz, H., Blanchard, H., Faust, D. & U. Hambach (2004): Reply to the comment by J.C. Carracedo et al., on 'Ge archaeological and chronometrical evidence'. *Quaternary Science Reviews* 23, 2049-2052.
- Zöller, L., Faust, D. & H. von Suchodoletz (2006): *Pedostratigraphie des Quartärs auf Lanzarote*. Bayreuther Geowissenschaftliche Arbeiten 27, 1-21.

### 9. Contributions to included manuscripts

In this cumulative dissertation, four studies are included (chapters 4.2., 4.3., 4.4. and 4.5.). I am the author of all manuscripts, including preparation and drawing the figures. Grain size and XRD analyses of bulk samples, investigations of carbonate contents as well as luminescence datings were done by me, occasionally supported by technicians or student assistants.

The authors listed on the different studies contributed approximately as follows:

#### ***Chapter 4.2.***

|                    |   |
|--------------------|---|
| H. von Suchodoletz | 70 % (sampling, luminescence dating, discussion of results, manuscript preparation) |
| M. Fuchs           | 20 % (sampling, discussion of results, comments to improve the manuscript)          |
| L. Zöllner         | 10 % (discussion of results, comments to improve the manuscript)                    |

#### ***Chapter 4.3.***

|                    |   |
|--------------------|---|
| H. von Suchodoletz | 70 % (sampling, luminescence dating, discussion of results, manuscript preparation) |
| M. Fuchs           | 15 % (discussion of results, comments to improve the manuscript)                    |
| L. Zöllner         | 10 % (discussion of results, comments to improve the manuscript)                    |
| I. Menéndez        | 5 % (sampling, comments to improve the manuscript)                                  |

#### ***Chapter 4.4.***

|                     |   |
|---------------------|---|
| H. von Suchodoletz  | 70 % (field work incl. geomorphologic mapping, XRD- and grain size analyses, discussion of results, manuscript preparation) |
| D. Faust            | 15 % (field work, discussion of results, comments to improve the manuscript)  |
| L. Zöllner          | 10 % (discussion of results, comments to improve the manuscript)  |
| <i>Acknowledged</i> | 5 %: <i>M. Kappes and J. Schuman (GIS-calculations)</i>   |

#### ***Chapter 4.5.***

|                    |   |
|--------------------|---|
| H. von Suchodoletz | 57 % (sampling, grain size and XRD analyses of bulk samples, carbonate determinations, discussion of results, manuscript preparation) |
|--------------------|---|

## 9. Contributions to included manuscripts

---

|               |  |
|---------------|--|
| P. Kühn       | 12 % (micromorphological investigations, discussion of results, comments to improve the manuscript)                              |
| U. Hambach    | 8 % (rock magnetic analyses, discussion of results, comments to improve the manuscript)  |
| M. Dietze     | 5 % (XRD analyses of clay samples, discussion of results, comments to improve the manuscript)                                    |
| L. Zöller     | 4 % (discussion of results, comments to improve the manuscript)  |
| D. Faust      | 12 % (analyses of pH values, electric conductivity and Na-saturation, discussion of results, comments to improve the manuscript) |
| Acknowledged: | 2%: P. Felix-Henningsen (analyses of amorphous clay)   |

### 10. Acknowledgements/Danksagung

I thank everybody who supported me during the time of my PhD work.

Ganz besonders möchte ich meinem Doktorvater Herrn Prof. Dr. Ludwig Zöller danken, welcher mir durch Einwerbung eines Graduiertenstipendiums des Freistaats Bayern (Az. A 4550-I/3) und eines DFG-Projektes (Zo51/26-1) die Möglichkeit gab am Lehrstuhl für Geomorphologie der Universität Bayreuth zu promovieren, mich in guten wie in schlechten Zeiten immer unterstützte und mir jederzeit den für meine Arbeiten nötigen Freiraum bot.

Ebenso gilt mein ganz besonderer Dank Frau Dr. Hedwig Oberhänsli, welche völlig selbstverständlich die Zweitbetreuung meiner Arbeit übernahm, mir im GFZ Potsdam ein zweites wissenschaftliches und räumliches Standbein bot und mich jederzeit mit vollstem Einsatz unterstützte.

Ganz besonders möchte ich ebenfalls Herrn Prof. Dr. Dominik Faust (TU Dresden) danken, welcher mir während meiner gesamten Promotionszeit, vor allem aber auch in den schwierigsten Zeiten, immer tatkräftig zur Seite stand und das Vorankommen der Arbeit mit größtem Einsatz unterstützte.

Mein besonderer Dank gilt natürlich auch meinen Kollegen und Freunden vom Lehrstuhl für Geomorphologie in Bayreuth Dr. Markus Fuchs, Dr. Ulrich Hambach, Manfred Fischer und Björn Buggle, welche mir vorbehaltlos und jederzeit auch in schwierigen Zeiten mit Rat und Tat zur Seite standen, eine angenehme, anregende, ja sogar mitreißende Arbeitsatmosphäre schufen und auch nach Feierabend einem Norddeutschen Landschaft, Kultur und Leute Oberfrankens auf angenehmste Weise näher bringen konnten.

Ebenso gilt mein besonderer Dank natürlich auch meinen Kollegen, Mitdoktoranden und Freunden der Sektion 3.3. des GFZ Potsdam Susanne Blumberg, Sebastian Breitenbach, Iris Kristen, Olga Kwiecien, Stefan Lauterbach, Clara Mangili, Philippe Sorrel und Christian Wolff, mit welchen mich viele anregende Diskussionen, tatkräftige Hilfe sowie angenehm verbrachte Zeit verbinden. Ebenso möchte ich meinen Bürokollegen im GFZ Potsdam Dorothea Eue, Alexandra Wille, Dr. Birgit Heim und Matthias Zopperitsch für die angenehme Zeit danken.

Many colleagues from different institutes and countries accompanied and supported my work in several fields. Thus, I would like to thank Dr. B. Plessen, Dr. A. Brauer, D. S. Wulf und Dr. G. Schettler from GFZ Potsdam, Prof. Dr. R. Oberhänsli, Dr. B. Mocek and Dr. M. Wilke from the University of Potsdam, Dr. P. Kühn from the University of Tübingen, Prof. Dr. P. Felix-Henningsen from the University of Gießen, Prof. Dr. U. Radtke from the University of Cologne, Dr. J.-B. Stuu from the University of Bremen, Dr. R. Donner, Dr. F. Haubold und

## **10. Acknowledgements/Danksagung**

---

M. Dietze from the Technical University of Dresden, Dr. M. Krbetschek from the Technical University Bergakademie Freiberg, Dr. D. Muhs from the USGS Boulder/USA, Dr. I. Menéndez from the Universidad de Las Palmas de Gran Canaria/Spain, Dr. C. Criado from the Universidad de La Laguna de Tenerife/Spain as well as Prof. P. Höllermann from the University of Bonn.

Ohne die engagierte Arbeit der Laborantinnen des GFZ Potsdam und der TU Dresden wären viele Analysen nicht so schnell vorangeschritten. So sei an dieser Stelle Frau Petra Meier, Frau Juliane Herwig und Frau Beate Winkler ganz herzlich gedankt. In diesem Zusammenhang möchte ich auch den Hiwis des Lehrstuhls für Geomorphologie der Universität Bayreuth Melanie Kappes, Eva Kunert, Matthias Will, Katrin Poglitsch, René Müller, Michael Hark und Björn Reddersen sowie den ehemaligen Zivis des GFZ Potsdam Gert Herold und David Sonnabend für ihre Hilfe, teilweise auch über den Feierabend hinaus, ganz herzlich danken.

Yo deseo expresar el más sincero agradecimiento a Hans-Martin Sommer, así que al doctor Alquilino Miguélez-López y a Elena Mateo del Cabildo de Lanzarote por el ayuda fuerte y fructoso para los trabajos de campo en Lanzarote.

Und natürlich wäre, last but not least, ohne meine Freunde und Familie die Zeit der Promotion doch sehr einseitig gewesen. Vielen Dank Euch noch einmal an dieser Stelle! Ganz besonders möchte ich an dieser Stelle Henrik Blanchard, Jens Schumann, Peter Sinjukow und Niklas Nilius danken, welche mir nicht nur moralisch, sondern auch ganz praktisch für diese Arbeit zu Hilfe standen.

### **Declaration/Erklärung**

Hiermit erkläre ich, dass ich diese Arbeit selbständig verfasst und keine anderen als die angegebenen Quellen und Hilfsmittel verwendet habe. Ich erkläre ferner, dass ich an keiner anderen Hochschule als der Universität Bayreuth ein Promotionsverfahren begonnen habe.

Bayreuth, August 2007